Characterisation of the Zinc Transporter ZnT10 and its role in cellular homeostasis in healthy and Alzheimer's disease brain

Helen Bosomworth MRes BSc (Hons)

Thesis submitted for the degree of Doctor of Philosophy

Institute for Cell and Molecular Biosciences and Human Nutrition Research Centre

Newcastle University, UK

October 2012

Acknowledgements

Throughout the course of my PhD there have been many people without whom I would not have reached this point. First and foremost I would like to acknowledge the brilliant help, support and friendship given to me by Dr Ruth Valentine. I extend this thanks and gratitude to Prof. Dianne Ford for her continued assistance and encouragement. I would like to thank my Oral Biology lab colleagues, past and present; in particular Dr Jared Thornton for his meticulous attention to detail and direction to relevant scientific documentaries. Also to Lesley Old for her patience, Rob Shields for his entertainment, Timothy Bates for all those useful insights, Tarana Singh-Dang for her friendship and advice and to Karin Jaedicke for her faith in my abilities. Additionally I would like to thank those PI's and admin staff on Level 7 who have also been available to assist. This would not be complete without the great friendship and IT knowledge of Mark Vernon. Thank you to Dr Alison Howard and Dr Paul Adlard who both have been instrumental in this research.

Many times I have been brought back down to Earth and sanity with the amazing emotional support of my friends and family. Especially with the unfaltering love and encouragement of my parents, The Bosomworth style reassurance offered by my siblings and latterly, the perseverance of Richard, thank you. Finally, I would like to thank those who are no longer with us but I hope I was able to make proud.

Abstract

Zinc is essential to the structure and function of numerous proteins and enzymes so requires tight homeostatic control at both the systemic and cellular level. Two families of zinc transporters – ZIP (SLC39) and ZnT (SLC30) – contribute to zinc homeostasis. There are at least 10 members of the human ZnT family, and the expression profile and regulation of each varies depending on tissue type. Little is known about the role and expression pattern of ZnT10; however *in silico* data predict restricted expression to foetal tissue. In this thesis I show a differential expression profile for ZnT10 in adult human tissue by RT-qPCR and detect highest levels of expression in small intestine, liver and brain tissues. I present data revealing the functional activity of ZnT10 to be in the efflux direction. Using a plasmid construct to express ZnT10 with an N-terminal FLAG-epitope tag, subcellular localisation in a neuroblastoma cell line (SH-SY5Y) is shown to be at the Golgi apparatus under standard conditions of culture, with trafficking to the plasma membrane observed at higher extracellular zinc concentrations of 100 μM. I demonstrate using RT-qPCR down-regulation of ZnT10 mRNA levels in cultured intestinal and neuroblastoma cell lines in response to extracellular zinc, a response which is mirrored at the protein level. Furthermore, I demonstrate reduced transcription from the putative ZnT10 promoter at an elevated extracellular zinc concentration.

Reduction in ZnT10 mRNA expression in response to increased extracellular cobalt and conversely, an up-regulation of ZnT10 mRNA levels in response to increased extracellular nickel has also been observed by RT-qPCR in both SH-SY5Y and Caco-2 cells. Neither of these responses were reflected at the level of transcription using the ZnT10 promoter construct. In transiently transfected SH-SY5Y cells Western blotting reveals a reduction in p3xFLAG-ZnT10 protein levels in response to extracellular zinc; however both extracellular cobalt and nickel caused an increase in the level of

p3xFLAG-ZnT10 protein measured. Trafficking was observed with both cobalt and nickel treatments. Movement from the Golgi apparatus to a more diffuse localisation pattern was observed with cobalt treatment, whereas nickel elicited a response similar to zinc, with trafficking toward the plasma membrane. Extracellular copper did not induce a change at any level of investigation.

These features of ZnT10 localisation, regulation and function, together with the discovery that ZnT10 is expressed at high levels in brain tissue, indicate that ZnT10 has a role in regulating zinc homeostasis in the brain. Further investigation highlighted a down-regulation of ZnT10 in human Alzheimer's disease brain tissue and in the APP/PS1 transgenic mouse brain. Zinc was also shown to influence splicing events of β-secretase enzyme, known to be involved in Alzheimer's disease pathology. Zinc promoted an increase in the most active isoform at the mRNA level and thus the measured dysregulation of ZnT10 and therefore potential changes in levels of zinc may have relevance to the development of neurodegenerative disease.

Relevant Publications

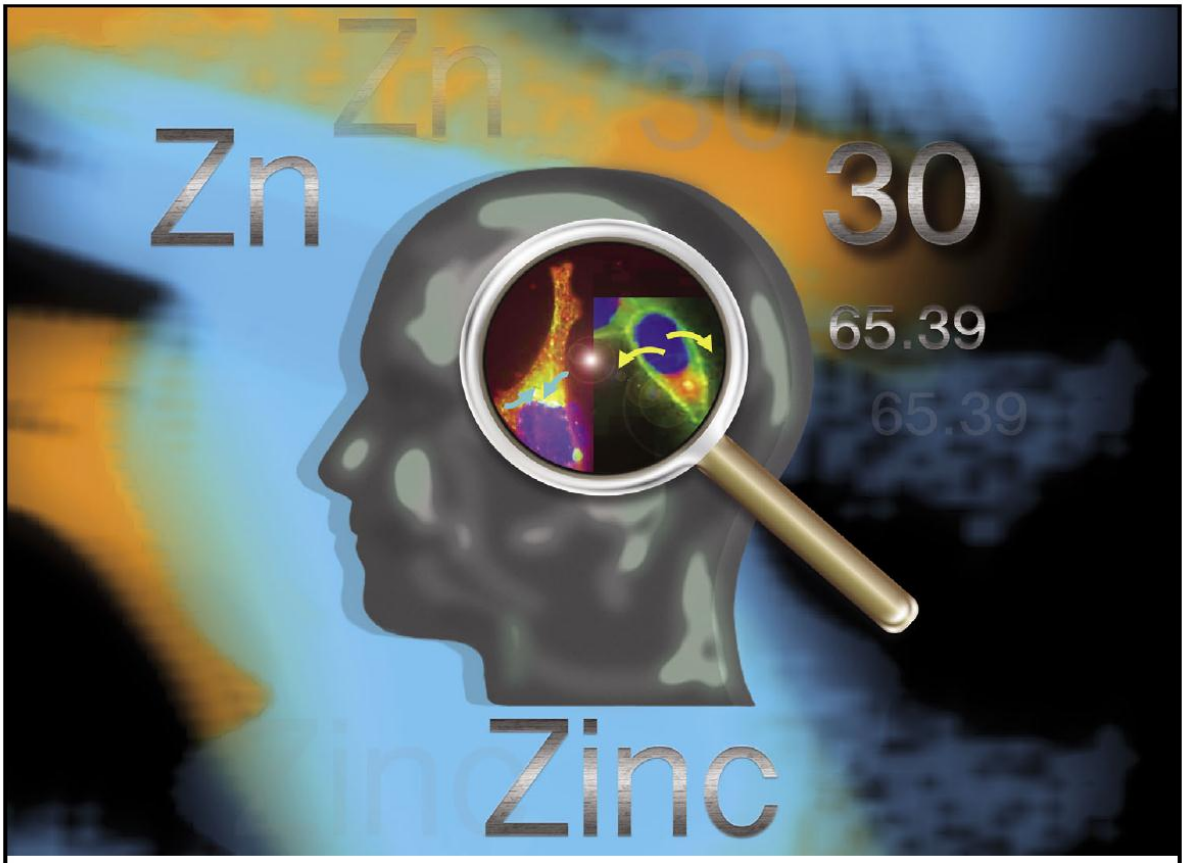

Showcasing research into zinc homeostasis by Dr Ruth Valentine and colleagues at the Human Nutrition Research Centre, the Institute for Cell and Molecular Biosciences, Newcastle University, UK

Efflux function, tissue-specific expression and intracellular trafficking of the Zn transporter ZnT10 indicate roles in adult Zn homeostasis

We report the differential expression profile of ZnT10 in adult human tissues. The localisation, regulation and function of ZnT10 suggests a role in regulation of Zn homeostasis in the brain, so may have relevance to the development of neurodegenerative disease.

As featured in:

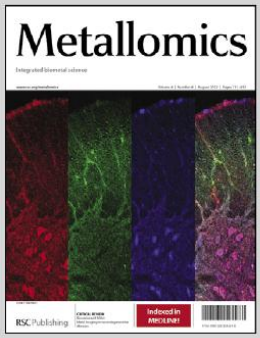

See Ruth Valentine *et al.*, *Metallomics*, 2012, **4**, 771–779

RSC Publishing

www.rsc.org/metallomics

Registered Charity Number 207890

Peer reviewed publications:

H. J. Bosomworth, J. K. Thornton, L. J. Coneyworth, D. Ford, R. A. Valentine, (2012). Efflux function, tissue-specific expression and intracellular trafficking of the Zn transporter ZnT10 indicate roles in adult Zn homeostasis. *Metallomics: integrated biometal science.*

L. J. Coneyworth, K.A. Jackson, J. Tyson, **H. J. Bosomworth**, E. Van der Hagen, G. M. Hann, O. A. Ogo, D. C. Swann, J. C. Mathers, R. A. Valentine, D. Ford, (2012). Identification of the human ZTRE (zinc transcriptional regulatory element) - a palindromic protein-binding DNA sequence responsible for zinc-induced transcriptional repression. *The Journal of biological chemistry*.

Peer reviewed abstract publications:

H. J. Bosomworth, G. M. Hann, D. Ford, R. A. Valentine. Identification and Characterisation of ZnT10. *Epithelia & Membrane Transport Themed Meeting, Proceedings of the Physiological Society,* (2011), 24, **C03 and PC03**

H. J. Bosomworth, D. Ford, R. A. Valentine. ZnT10 is expressed in adult human tissues. *70th Anniversary: From plough through practice to policy meeting, Proceedings of the Nutrition Society,* (2011), *70, OCE4, E127*

Conference presentations:

'Regulation of ZnT10 by Zinc in Adults' – International Society for Zinc Biologists, Melbourne Australia, 14th-19th Jan 2012 (Highly Commended Poster)

'Identification and Characterisation of ZnT10' - Epithelia & Membrane Transport Themed Meeting, Proc Physoc University College London 1st-3rd Sept 2011 (Oral communication and poster)

'Identification and Characterisation of ZnT10' - Young Physiologists Symposium Royal Veterinary College, London 31st Aug 2011 (Poster)

'ZnT10 is expressed in adult human tissues' - 70th Anniversary: From plough through practice to policy meeting, Proc Nut University of Reading 4th-6th July 2011 (Oral communication)

'ZnT10 is expressed in adult human tissues' - NorthEast Postgraduate Research Conference, Newcastle University 5th Nov 2010 (Poster)

'ZnT10 is expressed in adult human tissues' - The 60th Fujihara Seminar: Zinc signalling and cellular functions, Osaka, Japan 29th -31st Oct 2010 (Poster)

'ZnT10 is expressed in adult human tissues' - HNRC (Human Nutrition Research Centre) Research Day, Newcastle University 13th Oct 2010 (Oral Presentation)

'ZnT10 is expressed in adult human tissues' - IBDG (Inorganic Biochemistry Discussion Group) Meeting, Institute for Cell and Molecular Biosciences, Newcastle University 15th Sept 2010 (Poster)

Beacon NorthEast Your View Poster Session March 2010 (Public Engagement Poster)

Abbreviations

µM	Micromolar
Aβ	Amyloid-beta
ACE	Angiotensin converting enzyme
AD	Alzheimer's Disease
ADAM	A disintegrin and metalloprotease
AE	Acrodermatitis Enteropathica
AMPA	α-amino-3-hydroxy-5-methyl-4-isoxazole propionic acid/kainite
Ang	Angiotensin
ANOVA	Analysis of variance
APH-1	Anterior pharynx-defective 1
APOE	Apolipoprotein E
APP	Amyloid precursor protein
APPI	Amyloid precursor protein protease inhibitor
APPs	Amyloid precursor protein secretory fragment
APPsw	Swedish mutated amyloid precursor protein
ARB	Angiotensin type receptor blocker
AT	Angiotensin type
ATP	Adenosine triphosphate
BACE	Beta-site APP cleaving enzyme; β-secretase
BDNF	Brain derived neurotrophic factor
BLAST	Basic local alignment section tool
bp	Base pair
BSA	Bovine serum albumin
cAMP	Cyclic adenosine monophosphate
CDF	Cation diffusion facilitator
cDNA	Complementary deoxyribonucleic acid
CHO	Chinese Hamster Ovary
CMV	Cytomegalovirus
Co	Cobalt
$CoCl_2$	Cobalt chloride
COX	Cytochrome oxidase
CPRG	Chlorophenol red-β-D-galactopyranoside
CREB	cAMP response element binding protein
C_t	Threshold cycle
CTFγ	C-terminal fragment p7

Cu	Copper
CuBD	Copper binding domain
CuRE	Copper Responsive Element
$CuSO_4$	Copper sulphate
CQ	Clioquinol
DMEM	Dulbecco's modified Eagles medium
DNA	Deoxyribonucleic acid
dNTP	Deoxyribonucleotide triphosphate
dsDNA	Double stranded deoxyribonucleic acid
DTT	Dithiothreitol
E. coli	Escherichia Coli
EDTA	Ethylenediamine tetraacetic acid
eIF2	Eukaryotic translation initiation factor-2
EMSA	Electrophoretic mobility shift assay
ER	Endoplasmic Reticulum
EST	Expressed sequence tag
FACS	Fluorescence activated cell sorting
FBS	Foetal Bovine Serum
$GABA_A$	γ-aminobutyric acid type A
GAPDH	Glycerol-3-phosphate dehydrogenase
GSK3	Glycogen-synthase kinase-3
HA	Haemagglutinin
IEC	Intestinal epithelial cell
IL	Interleukin
Irt	Iron-regulated transporter
Kb	Kilobase
KLF4	Krüppel-like factor 4
KPI	Kunitz-type protease inhibitor
LB	Luria Bertani
LPS	Lipopolysaccharide
LTP	Long-term potentiation
M	Molar
MAP	Microtubule associated protein
MCI	Mild cognitive impairment
Mg	Magnesium
MHC	Major histocompatibility complex
mM	Millimolar

MMC	Mitochondrial metabolic competence
MMLV	Moloney murine leukaemia virus
MMP	Matrix metalloproteinase
MMSE	Mini-Mental State Examination
Mn	Manganese
MNK	Menkes copper transporting protein
MRE	Metal Responsive Element
mRNA	Messenger ribonucleic acid
MT	Metallothionein
MTF1	Metal-Responsive transcription factor-1
MTP	Metal tolerance protein
NADPH	Nicotinamide adenine dinucleotide phosphate
N-APP	N-terminal growth factor domain of APP
NCBI	National Centre for Biotechnology Information
ND	Negative dominant
NF-κB	Nuclear factor-κB
NFT	Neurofibrillary tangle
Ni	Nickel
$NiCl_2$	Nickel Chloride
NMDA	N-methyl-D-aspartate
nNOS	Neuronal nitric oxide synthase
NO	Nitric oxide
NSAID	Non-steroid anti-inflammatory drugs
ORF	Open reading frame
PBS	Phosphate-buffered saline
PCR	Polymerase Chain Reaction
PCAD	Preclinical Alzheimer's disease
PEN-2	Presenilin enhancer 2
PKC	Protein kinase C
PKR	Double stranded RNA dependant protein kinase
PMD	Post-mortem delay
PS1	Presenilin
RA	Retinoic acid
RAS	Renin-Angiotensin System
RIN	RNA integrity number
RNA	Ribonucleic acid
RNI	Reference Nutrient Intake

ROS	Reactive oxygen species
Rpm	Revolutions per minute
RT-PCR	Reverse-transcription polymerase chain reaction
RT-qPCR	Real-time reverse-transcription polymerase chain reaction
SD	Standard deviation
SDS	Sodium dodecyl sulphate
SDS-PAGE	Sodium dodecyl sulphate polyacrylamide gel electrophoresis
SEM	Standard error of the mean
siRNA	Small interfering RNA
SOD	Superoxide dismutase
SP	Senile plaques
Sv2	Synaptic vesicle protein
TBE	Tris-Boric Acid EDTA
TEMED	Tetramethylethylenediamine
Tg	Transgenic
TGN	*Trans*-Golgi Network
TLR3	Toll-like receptor 3
TMD	Transmembrane domain
TNAP	Tissue non-specific ALP
TNF-α	Tumour necrosis factor-α
TOPI	DNA topoisomerase I
UTR	Untranslated region
VSMC	Vascular smooth muscle cell
WGA	Wheat germ agglutinin
WT	Wild-type
ZIP	Zrt-Irt-like protein
Zn	Zinc
$ZnCl_2$	Zinc Chloride
ZnT	Zinc Transporter
ZRE	Zinc responsive element
Zrt	Zinc regulated transporter
ZTRE	Zinc transcriptional regulated element

Contents

List of Figures

List of Tables

Chapter 1: Introduction

1.1 Biological importance of zinc

Zinc is the most widely utilised divalent cation in biology despite not being the most abundant metal in this group. Biochemically zinc is essential for the function of many enzymes from all six enzyme classes (oxidoreductases, ligases, transferases, hydrolyases, isomerases, lyases) as established by the International Union of Biochemistry (Vallee and Falchuk, 1993). In fact, more recently knowledge of zinc has increased exponentially with bioinformatic estimates of approximately 2800 human proteins which are potentially zinc-binding *in vivo*, corresponding to 10 % of the human proteome (Andreini et al., 2006). However, this is a substantial increase from lower organisms as the zinc proteome represents about 5 % to 6 % in prokaryotes (Andreini et al., 2009). It can act in various ways in order to maintain the function of proteins and enzymes (Table 1.1). Firstly, zinc can act as a catalyst for many different enzymes. These enzymes are classified as zinc metalloenzymes if the removal of zinc decreases enzymatic activity without affecting the protein as a whole and adding zinc back into the system restores activity, for example, this is the case for carbonic anhydrase (reviewed by Liljas et al., 1994). Secondly, zinc can act as an integral structural element to various proteins. For example in zinc finger motifs where four cysteines or histidines coordinate a zinc ion so that it forms a tetrahedral complex. Proteins with this structure are involved in a number of cellular processes such as differentiation, proliferation, signal transduction, adhesion and transcription (Vallee and Falchuk, 1981). Furthermore, it has been established that in addition to its catalytic effect, zinc is also required to maintain structural elements of enzymes. One example of such is copper/zinc superoxide dismutase, where the divalent cation copper acts as the catalyst, zinc is vital for the configuration (Bannister et al., 1987). Other examples include zinc

as a cofactor for DNA polymerase, RNA polymerase and reverse transcriptase (Truong-Tran et al., 2001a). The third biochemical function of zinc is in the regulation of gene expression. The most characterised of these is for metal response element (MRE)-binding transcription factor-1 (MTF-1), this contains a zinc-finger DNA-binding domain which requires coordination of zinc ions so that it maintains its structure in order to bind to MREs in promoter regions of genes to regulate downstream expression (Heuchel et al., 1994, Langmade et al., 2000, Lichtlen et al., 2001, Wang et al., 2004c) (this will be discussed further in Section 1.5). Zinc appears to be particularly important in the central nervous system where it is found in presynaptic vesicles of certain glutamatergic neurones and, along with glutamate, is released during neurotransmission (Frederickson and Bush, 2001). Zinc can also act as an intracellular signalling molecule with the ability to influence cellular machinery at several levels (Glover et al., 2003). Known effectors of zinc signalling include protein tyrosine kinases (Hogstrand et al., 2009), protein kinase CK2 (Taylor et al., 2012), plasma membrane calcium ATPase (PMCA) (Hogstrand et al., 1999) and tight junction proteins (Finamore et al., 2008).

The ability of zinc to act in these ways can be attributed to its properties as an early transition metal. The transition metals have high melting points, mechanical strength and high density properties because of their relatively small atomic radius. The versatility afforded by a variable coordination sphere and being redox inert are distinct features of zinc within this chemical group that are likely to account for its widespread use in biology. In serum the majority of zinc is found bound to albumin (70 %), α-macroglobulin (18 %) and the remainder is bound to proteins such as transferrin therefore relatively little free zinc is available in solution within biological systems (Gibson et al., 2008), with free zinc estimates of 1.70×10^{-12} mol/l (Powell et al., 1999). In most cases zinc carries out its biochemical functions as a bound divalent cation.

Intracellular zinc is found predominantly bound to metallothioneins (MTs). This is a group of cysteine rich proteins, of which there are four major isoforms: MTI and MTII found ubiquitously, MTIII found mainly in the brain and MTIV, which is predominant in stratified tissues (Bell and Vallee, 2009). Due to their cysteine rich nature, MTs can bind up to 7 zinc atoms and the concentration of the MTs respond readily to changes in dietary zinc, implying a role in zinc homeostasis. At high intracellular zinc concentrations, MT levels increase therefore sequestering zinc. At low zinc concentrations, MT is able to release its bound zinc ions before being degraded. This zinc buffering property maintains a constant level of available zinc to carry out its numerous biological functions, despite fluctuations in total levels. The buffering capacity of MT is demonstrated in inflammation whereby, in the liver, MT can increase as much as 100-fold within 2 to 4 hours when in an inflammatory state. This subsequently increases hepatic uptake of plasma zinc (Coyle et al., 2002, Mocchegiani et al., 2006a). In addition to its role in inflammation, zinc has a role in reducing oxidative damage within cells, by both stimulating the activity of several antioxidants and stabilising lipids and/or proteins in order to protect cellular membranes (Frazzini et al., 2006). Furthermore, a role for zinc in adequate immune system response is evident in the zinc deficiency disease acrodermatitis enteropathica (AE), where symptoms include reduced immune function and increased susceptibility to infections from fungi, bacteria and viruses (Neldner and Hambidge, 1975, Haase and Rink, 2009, Prasad, 2000).

It has been demonstrated that zinc has a role in apoptosis, although its function remains ambiguous. Evidence suggests that high levels of zinc (300 μM) induce apoptosis in cultured cortical neurones (Sensi et al., 1999). *In vitro* studies using the fluorescent zinc marker, Zinquin, have shown there is a major redistribution of intracellular zinc during

the early stages of apoptosis. These studies are without the addition of extracellular zinc so imply a release of zinc from intracellular stores or metalloproteins (Zalewski et al., 1994). In addition it is proposed that there are two anti-apoptotic mechanisms of zinc. In the first instance zinc has a direct influence over regulators of apoptosis. For example, in the human acute lymphoblastic leukaemia cell line (Molt4) 10 µM $ZnCl_2$ inhibited the apoptopic protease, caspase-3 therefore suppressing apoptosis (Perry et al., 1997). Secondly, zinc plays a role in oxidative stress. For example, in 3T3 cells (mouse fibroblast) addition of 0.5 µM and 5 µM zinc led to elevated levels of oxidative stress markers such as antioxidant enzymes copper/zinc (CuZnSOD) and manganese (MnSOD) superoxide dismutases and activated AP-1 as compared to both control cells and those with the addition of 50 µM zinc (Oteiza et al., 2000). Indeed a link between these two pathways can be hypothesised as a deficiency in intracellular zinc can both lead to oxidative stress and therefore caspase activation as well as directly influencing caspase activation pathways (reviewed by Truong-Tran et al., 2001b).

The role for zinc in the regulation of intracellular processes is not limited to apoptosis. It has been highlighted as an important signalling molecule involved in transcriptional regulation (Section 1.6). Zinc has also been implicated in bone metabolism where it is involved in stimulating osteoblast formation (Yamaguchi and Hashizume, 1994) and inhibiting osteoclast formation (Kishi and Yamaguchi, 1994). Zinc deficiency is known to retard bone growth (Oner et al., 1984) and interestingly, osteoporotic women have been shown to excrete higher concentrations of urinary zinc (Herzberg et al., 1990). Additionally, neurotransmission in glutamatergic neurones also involves zinc release from intracellular synaptic vesicles into the extracellular space which is then thought to interact with membrane transporters on the post-synaptic membrane (Frederickson and

Bush, 2001) (see Section 1.7). These emphasise only a few of the numerous roles of zinc throughout biological systems (Table 1.1).

1.2 Zinc as a nutrient

In utero zinc is imperative for normal foetal development. However, its role is not limited to the developing embryo and the importance of zinc carries on throughout the lifespan of humans. Cells that are most sensitive to zinc deprivation are foetal and juvenile cells with high turnover opposed to those cells from tissues that are more stationary. Processes such as, but not limited to, growth and mental development in childhood require zinc. In adolescence zinc is important for the development of the reproductive system and through into adulthood zinc is required to maintain a healthy appetite and immune function. The total body content of zinc is only estimated to be about 2 g, distributed as approximately 60 % in skeletal muscle and 30 % in bone with lower levels throughout the organs (skin > liver > brain > kidneys > heart > hair > plasma) (Table 1.2) (Wastney et al., 1986, King et al., 2000, Jackson, 1989). Due to its low levels in plasma (< 0.1% of total body zinc, 12-16 μM) zinc is referred to as a trace element (Brown et al., 2001, King et al., 2000). There is no mechanism to enhance release of zinc from either bone or muscle and therefore neither can function as a zinc store, because of this it is essential to maintain an adequate supply of dietary zinc. These requirements are described in the UK as reference nutrient intakes (RNI) and are currently set as 9.5 and 7.0 mg/day for men and women respectively (age 18-50) (Table 1.3) (Henderson et al., 2003a). Due to the nature of zinc it is found bound to proteins, for example foods rich in this nutrient are red meats and some shellfish with lesser amounts in white meat, fish, cheese, cereals and legumes. In the case of cereals and pulses it is found bound to the endosperm.

1.2.1 *Zinc deficiency*

The essential role of zinc was first established by Raulin in 1869 when it was shown that the nutrient is required by *Aspergillus niger* in order to grow. Since then the importance has been established in animals and in humans. The first animal studies were in 1934 in rats (O'Dell and Reeves, 1989) and subsequently, in 1961 Prasad et al., first described a zinc deficiency syndrome in humans (Prasad et al., 1961). Prasad observed that a 21 year old male from Iran had symptoms of anaemia, hypogonadism, skin alterations and growth and mental retardation. In altering his diet from that of negligible levels of zinc to sources of increased zinc the clinical features of the patient were corrected. Severe zinc deficiency is evident in the human autosomal recessive disorder Acrodermatitis Enteropathica (AE). The clinical symptoms of this disease include circumoral and acral dermatitis, diarrhoea, alopecia as well as neuropsychiatric manifestations. AE is caused by an inborn error in zinc metabolism attributed to mutations in the intestinal zinc transporter ZIP4 (Section 1.4.1) (reviewed by Andrews, 2008). Investigation of AE and other milder nutritional zinc deficiencies have advanced knowledge into the physiological role of zinc. Extensive research has shown that insufficient zinc during pregnancy leads to congenital malformations and compromises immune functions, neurobehaviour, and overall neonatal survival. A dramatic example of the devastating effects of severe maternal zinc deficiency can be found in mothers with AE. In such cases low birth weight, spontaneous abortion, ancephalic foetus or dwarfism occurred in five out of seven cases (King et al., 2000). Milder zinc deficiencies during pregnancy have also been identified, with intraurine growth retardation, low birth weights and complications during labour being described in the literature (Shah and Sachdev, 2006). Deficiency can also contribute to certain states in adult humans, such as infertility and neurosensory disorders. For example, in men with

Crohn's disease (an autoimmune inflammatory disease of the alimentary tract, usually affecting the intestines) it has been hypothesised that zinc deficiency causes poor sperm function and therefore male infertility (El-Tawil, 2003). In relation to neurosensory disorders, it has been shown that zinc deficiency triggers abnormal glucocorticoid secretion inducing changes in functions of certain areas of the brain such as the hippocampus (Takeda and Tamano, 2009). The hippocampus is involved in learning and memory therefore this is one function of the brain that can be affected by zinc status throughout life. Studies in rats have shown that treatment with the zinc chelator; Clioquinol (CQ) impaired memory function of adult rats (Takeda et al., 2010) and indeed zinc ion availability has been implicated in the decline of function in the aged human brain (Mocchegiani et al., 2005).

The difficulty diagnosing zinc deficiency is the pleiotropic nature of such symptoms, i.e. it does not just affect one metabolic pathway as is the case for iron; zinc is involved in numerous pathways. Also mild zinc deficiency may not have clinical symptoms.. Homeostasis of zinc is tightly controlled and therefore markers such as blood plasma or serum zinc concentration can take long periods of deficiency in order to alter. This was evident when over a 6 month period on a zinc deficient diet (2.6 mg zinc/d), no significant changes were found in plasma zinc levels or in the activity of zinc-containing enzymes in a cohort of five postmenopausal women, age 50-63 years (Milne et al., 1987). A further complication with the use of plasma zinc concentrations as a measure of zinc adequacy, is that the levels naturally fluctuate daily with ever changing inflammatory and immune status, as well as with the use of oral contraceptives (Fairweather-Tait et al., 2008). Other biomarkers that may prove more useful are differential erythrocyte zinc transporter or metallothionein gene or protein expression which seem to rapidly respond to zinc treatments where plasma zinc does not however,

these may not be sensitive enough in order to measure marginal zinc deficiency (Ryu et al., 2008, Wood, 2000).

The risk of zinc deficiency in world populations is increased in regions where diets are predominantly high in plant-based foods and low in animal protein. This is not only due to the lower intake of zinc itself but also to the high concentrations of phytates found in cereals and pulses. Phytate chelates zinc therefore reducing dietary absorption. There are other groups that are at risk of zinc deficiency, despite living in regions with readily available sources of zinc. These include lactating women and growing infants which require an increase in their dietary intake of zinc due to a higher demand (Table 1.3). In addition, there are groups that have abnormalities that lead to malabsorption of nutrients, such as individuals with Crohn's disease, which may require supplementation in order to meet their daily requirements.

1.2.2 *Zinc toxicity*

Due to the tight regulation of zinc homeostasis ingestion of zinc is essentially non-toxic in humans. Intriguingly, however, adverse reactions to zinc have been reported in rare incidences when there is inhalation of zinc fumes or ingestion of unusually large amounts of zinc from food and beverages stored in galvanized containers (Vallee, 1988). In these cases excess zinc can causes nausea, fever and diarrhoea. There is a certain relationship between other divalent cations and zinc, therefore metabolism of other trace elements can be affected by long-term high zinc intake. This interaction is especially profound in the case of copper. A defect in copper metabolism is found in the autosomal recessive condition, termed Wilson's disease, such that there is an excessive hepatic copper accumulation. This can be fatal if the disease is not treated. High levels of zinc have been shown to be therapeutic in the condition, in that supplementation with

zinc (up to 150 mg/d) stimulates intestinal MT, which in turn chelates copper in the intestine, reducing accumulation and increases excretion in patient stools (Marcellini et al., 2005). Whilst this study assessed the zinc supplementation after 10 years, the efficacy of using longer term zinc supplements has not been investigated.

1.3 Systemic zinc homeostasis

Errors in homeostatic mechanisms, whether genetic and/ or environmental cause disease states and these highlight the importance of controlling such processes. Zinc is no exception, with both the side effects of toxicity and deficiency leading to health risks, so it is imperative that internal zinc concentration remains tightly regulated. This is achieved through the co-ordination of many proteins involved in absorption, movement, storage, trafficking and excretion of zinc. Zinc absorption is related to the amount of dietary zinc consumed, this correlation is negative, meaning that reduced intake of zinc will consequently increase the rate of absorption of zinc from the diet. This has been shown experimentally, where a low dietary intake of zinc (12 μmol/d) in adult males over a 15 day period, resulted in an increase in zinc absorption from 38 % to 93 % as compared to normal intake (85 μmol/d) (Taylor et al., 1991). In addition it is important to note that zinc absorption also appears to plateau at >308 μmol/d (King, 2011).

Two families of proteins are known to play a role in zinc homeostasis, these are the zinc transporters, ZIPs; that act to increase cytosolic zinc and the ZnTs, that are thought to efflux zinc, reducing cytosolic zinc concentrations. These can be differentially regulated in response to changing zinc status (see section 1.5), disease state and cases of infection. In addition there are binding proteins such as MT that enable storage of small reserves of zinc when the levels are adequate and conversely are able to release zinc when it is required for its many processes. Furthermore, regulation of MT by zinc enables this

protein to be up-regulated to chelate zinc in times of excess and be degraded when zinc levels are low. Impressively, studies have shown a constant whole body zinc content when dietary zinc differs by a 10-fold range (Kirchgessner, 1993). It is hypothesised that it is the response of the zinc transporters and MT to changes in local zinc status that allow whole body zinc content to be maintained (King et al., 2000).

Very early studies established that excess zinc is mainly excreted in faeces. It was shown that the level of excretion was equal to dietary intake except where injected levels were above 6 mg/day. In these cases excreted zinc levels were higher (McCance and Widdowson, 1942). Zinc for excretion in this manner is released into the gastrointestinal tract, the potential sources of such zinc is in pancreatic and biliary secretions, gastroduodenal secretions and transepithelial flux from the enterocytes (Krebs, 2000). In addition, McCance et al., (1942) noted that the kidneys play little part in zinc excretion with a constant level of zinc ions being excreted in the urine despite increased dietary intakes and/ or intravenous injections. However, more recent research has shown that zinc excretion in the urine is 6-fold higher in infants than adults, when normalised to body weight. This is perhaps a reflection of the maturation state of the kidney in infants (Wastney et al., 1999). The state of maturity has also been investigated in terms of zinc absorption using adult human intestinal Caco-2 cells against human foetal FHs 74 Int cells. The conclusion from this study was that developmental state plays an important role in zinc absorption in the intestine through intestinal zinc efflux and sequestration and import mechanisms (Jou et al., 2010). Other minor routes of zinc excretion include semen, sloughed skin, nails and hair (King et al., 2000).

Important alterations are made to homeostatic mechanisms during times of increased zinc requirements. For example during pregnancy and lactation there is an increased

demand for zinc due to the processes of embryogenesis, foetal growth and milk secretion (Donangelo et al., 2005). Zinc absorption during these times increases significantly to meet these demands. In times of foetal growth the demands are higher. In addition, in early lactation increased absorption allows maintenance of zinc levels whilst zinc is excreted from the mammary glands into the colostrum. As secretion decreases so too does zinc absorption. Even in cases of low dietary zinc, homeostatic mechanisms act to maintain adequate levels in breast milk (Kelleher and Lonnerdal, 2005).

1.4 Mammalian zinc transporters

As described in Section 1.2, there is no specific storage mechanism for zinc within the body and therefore zinc must be ingested daily to maintain recommended levels (Table 1.3). In order to carry out its vital roles within the body, zinc needs to be absorbed from the diet, transported around the body and enter and exit a wide range of organs and more specifically cells. The absorption and homeostasis of zinc from the diet and within the body is undertaken by zinc transporters of which there are two known families; ZIP (Zinc-regulated and iron-regulated transporter protein, SLC39 family) and ZnT (members of the cation diffusion facilitator, SLC30, family) (Lichten and Cousins, 2009). Homolgues in species other than humans are referred to as Zip (Slc39) and Znt (Slc30). The families have contrasting roles within the cell. ZIPs are concerned with increasing cytosolic zinc concentrations, whereas ZnTs are thought to be predominantly involved in the efflux of zinc from the cytoplasm either out of the cell or sequestering it into intracellular compartments therefore reducing cytosolic zinc concentration. To date, there are 10 identified ZnTs in humans and 14 known ZIPs, however the expression of each varies depending upon the tissue. In order to play the opposing functions there are

distinct structural differences between the two as described in the proceeding sections (1.4.1 and 1.4.2).

1.4.1 *ZIP family*

The ZIP family of zinc transporters are named after the yeast Zrt1 protein (Zinc-regulated transporter 1) and the *Arabidopsis* Irt1 protein (Iron-regulation transporter 1) giving the full title of Zinc-regulated and iron-regulated transporter protein. Most of these proteins have a predicted topology of eight transmembrane spanning domains (TMD) with extracellular N- and C- termini (Figure 1.1A) (Kambe et al., 2004, Palmiter and Huang, 2004). In addition, in most of these transporters there is long loop region between TMD III and IV, which predominantly contains histidine-rich domains of 3-5 histidine residues. Due to the potential of these residues to bind metal it is thought that this region may be important in zinc transport or its regulation however this has not been shown experimentally in the mammalian transporters (Eide, 2006). Interestingly however, the mutation of this region in the yeast Zrt1 seems to affect subcellular localisation of the protein rather than the transporter's function (Gitan et al., 2003). The sequences of TMD IV and V are highly conserved and due to their amphipathic nature, it is hypothesised that it is this region that forms a pore through which zinc can pass. The role described in the literature for ZIP transporters is to increase cytosolic zinc concentrations by either importing zinc across a plasma membrane from the extracellular space or transporting it from the lumens of organelles into the cytoplasm. The ZIP family can be split into a further 4 families depending on their degree of sequence conservation. These are subfamilies I, II LIV-1 or gufA (Figure 1.1B) (Gaither and Eide, 2001a).

The first identified member of the ZIP family, ZIP1 (SLC39A1), is expressed in a wide variety of cell types. ZIP1 is an interesting transporter due to its cell-type dependent localisation pattern. For example, in the human erthyromyeloblastoid leukaemia cell line K562, over-expression of hZIP1 showed a pattern consistent with the plasma membrane localisation. This data was obtained by indirect immunofluorescence by stably transfecting the hZIP1 construct that contained a haemagglutinin (HA) antigen epitope tag (Gaither and Eide, 2001b). However in COS-7 (monkey kidney fibroblast) and PC3 (human prostate cancer) cell lines localisation was shown to the endoplasmic reticulum (ER). The technique in this case differed slightly from Gaither et al., (2001) in that this hZIP1 construct had a FLAG-tag and the cells were transiently transfected (Milon et al., 2001). Furthermore, in human embryonic kidney (HEK293) cells stably transfected with a construct expressing the mouse homologue of human ZIP1; mZip1, with a haemagglutinin (HA) antigen epitope tag, post-translational modification has been proposed due to the translocation of mZip1 depending on the zinc status of the cell. In cases of zinc deficiency mZip1 is modified such that endocytosis of the transporter is decreased, with an observed higher expression at the plasma membrane, which in turn is correlated with an increase in zinc uptake into the cell (Wang et al., 2004a). In addition, site directed-mutagenesis was used to replace the loop histidines between TMD III and IV with alanines to ascertain the function of these highly conserved residues. Upon transfection into the PC3 cells, results indicated that these histidines are important in zinc transport function but are not involved in the plasma membrane localisation (Milon et al., 2006). One example of the importance of human ZIP1 in health and disease is in the development of prostate cancer. Down-regulation of hZIP1 has been proposed as a critical event in the progression of the disease. hZIP1 is found in the normal peripheral zone glandular epithelium and has been identified as

important in the uptake of circulating zinc at the basolateral membrane of prostate cells. Under normal conditions the prostate tissue has a high level of zinc accumulated however in adenocarinomatous glands, hZIP1 gene and protein expression is decreased, thus causing subsequent zinc depletion (Franklin et al., 2005). In support of this hypothesis is a study which investigated ZIP1 levels in African Americans, which found that incidence rates are highest in this racial group (Rishi et al., 2003). The researchers revealed that ZIP1 levels in normal prostate tissues from African American men are decreased when compared with age-matched white men. Therefore Franklin et al., (2007) have proposed ZIP1 as a tumour suppressor gene (Franklin and Costello, 2007, Costello and Franklin, 2006).

In contrast to ZIP1, the second member of this family of zinc transporters, ZIP2 (SLC39A2) appears to have a restricted expression pattern in human tissues. It is thought to be present at low levels in prostate, uterus, cervical epithelium, optic nerve and monocytes (Eide, 2004). Interestingly, this expression pattern is different in mouse with higher levels of mZip2 in skin, liver, ovary and visceral yolk sac (Dufner-Beattie et al., 2003a). Although both hZIP2 (Gaither and Eide, 2000) and mZip2 (Dufner-Beattie et al., 2003a) exhibit the characteristic uptake function in transfected cells when expressing ZIP2 from a CMV promoter, their mechanism of regulation appears to be different. Human ZIP2 expression was investigated in the monocytic cell line, THP-1, and human peripheral blood mononuclear cells and upon depletion of zinc with the intracellular zinc chelator TPEN [N,N,N*,N*-tetrakis(2-pyridylmethyl) ethylenediamine] hZIP2 mRNA expression increased (Cao et al., 2001). However, when pregnant mice underwent dietary restriction of zinc mRNA levels of mZip2 in the embryonic visceral endoderm remained unchanged when analysed by semi-quantitative reverse-transcriptase (RT)-PCR (Dufner-Beattie et al., 2003a). In line with hZIP1,

hZIP2 also shows down-regulation in prostate cancer cells. Intriguingly however, hZIP2 is expressed at the apical cell membrane and therefore is thought to be involved in retaining levels of zinc in the cellular compartments by 're-uptaking' zinc from prostatic fluid (Desouki et al., 2007).

ZIP3 research focuses mainly on the mouse isoform and it is found at low levels in numerous tissues however it is most abundant in the testes. Consistent with mZip2, when pregnant mice are on a zinc restricted diet mZip3 levels do not change in the embryonic visceral endoderm of the intestine (Dufner-Beattie et al., 2003a). The localisation pattern of mZip3 appears to be consistent with that of mZip1 whereby in stably transfected HEK293 cells under zinc replete conditions the localisation of mZip3 was to the intracellular organelles with rapid transit between these and the plasma membrane. However, in the same cell line model, zinc depletion has been found to increase the trans-localisation of mZip3 to the plasma membrane (Wang et al., 2004a). Importantly, the function of mZip3 was assessed in transiently transfected HEK293 cells using ^{65}Zn and competitor metal assays. The predicted uptake function was observed and was strongly inhibited by excess zinc thereby indicating a carrier mediated process. Zinc uptake by mZip3 was also inhibited by other metals (copper, cadmium, manganese, cobalt, magnesium and nickel) therefore indicating some promiscuity with respect to substrate specificity this transporter (Dufner-Beattie et al., 2003a). The research into human ZIP3 is mainly based around the fact that it is also implicated in prostate cancer, again exhibiting a down-regulatory effect in diseased cells (Franklin et al., 2005). It appears to act in the same way as hZIP2 in that it is localised to the apical cell membrane and is involved in 're-uptaking' zinc from the prostatic fluid in order to retain zinc levels (Desouki et al., 2007). It is proposed that this down-regulation of hZIP1-3 in the development of prostate cancer is due to the epigenetic silencing of gene

expression, though this has not been tested experimentally. Due to this role in the development of prostate cancer, these genes have been highlighted as potential tumour-suppressor genes (Franklin and Costello, 2007, Costello and Franklin, 2006).

ZIP4 (SLC39A4) and ZIP5 (SLC39A5) were both discovered due to their involvement in the development of the zinc deficiency disease *Acrodermatitis enteropathica* (AE). This is an autosomal recessive disorder, in which mis-sense mutations, splicing defects or transcriptional-inactivation by upstream deletions in the hZIP4 transporter render it either inactive or mis-localised, so that it is retained in the ER. hZIP4 is abundant in tissues that are important for zinc absorption such as the intestine, colon, stomach and the kidneys and in these tissues it is localised to the apical membrane (Wang et al., 2002). Therefore, inactivation/ mis-localisation limits the body's ability to absorb adequate dietary zinc. Wang et al., (2001) discovered that not all of the mutations that cause AE were mapped to the ZIP4 locus (~3.5-cM region on 8q24), and indeed the condition in humans can be overcome by dietary supplementation implying a compensatory mechanism for intestinal zinc uptake. Thus they highlighted a putative zinc-uptake protein, named 'hORF1', as a candidate. Wang and colleagues discovered that this gene is expressed primarily in the epithelium of the colon and in adenocarcinoma cells by SAGE (Serial Analysis of Gene Expression) data, allowing speculation that mutation of this gene could be responsible for cases of AE where the locus 8q24.3 is not mutated (Wang et al., 2001, Wang et al., 2002). This ORF1 gene is now known as hZIP5. ZIP4 and ZIP5 are 30 % homologous and they display a similar pattern of tissue expression, although their roles are somewhat contrasting. Investigations in mouse have elucidated the roles of these two transporters. In localisation experiments mice were fed a zinc adequate or a zinc deficient diet before immunohistochemical analysis of the proximal small intestine (duodenum) and

pancreas. The results showed that mZip5 is located on the basolateral membrane when cells are zinc replete, but the same state causes internalisation of mZip4 from the apical membrane through endocytosis. Furthermore, Western blot analysis of membrane proteins from the visceral yolk sacs, showed that in cases of zinc deficiency mZip5 is internalised, whereas mZip4 mRNA is stabilised and the protein is translocated to the apical membrane. It is mZip5 translation, not transcription, that is zinc responsive with mRNA remaining bound to polysomes under zinc deplete states. However, transcription run-on assays were performed that indicated there was no difference in transcriptional rate of mZip4 between zinc adequate and zinc deficient diets implying post-transcriptional regulation (Weaver et al., 2007). In contrast to this, Liuzzi et al., (2009) have argued that the transcriptional factor Krüppel-like factor 4 (KLF4) is able to bind to the mZip4 promoter in zinc deficient conditions in MODE-K cells. This binding is hypothesised to be important for the up-regulation of mZip4 (Liuzzi et al., 2009). The discrepancies indicated here highlight the importance of validation of the cell line models used as it should be noted that low levels of mZip4 can only be detected by RT-qPCR, and not RT-PCR, in MODE-K cells (Huang et al., 2006).

ZIP6 (SLC39A6) and ZIP7 (SLC39A7) have been identified as having a role in certain breast cancers supporting the hypothesis that transporter dysregulation can lead to uncontrolled cell proliferation. Both transporters have widespread expression however they have a number of differences. ZIP6 has become a reliable marker of oestrogen-receptor-positive cancers as it is regulated by oestrogen and has been found to be increased in these cases (Tozlu et al., 2006, Schneider et al., 2006). Using FACS (Fluorescence activated cell sorting) analysis of transiently transfected Chinese hamster ovary (CHO) cells the uptake function of ZIP6 has been confirmed. In addition, CHO cells were transiently transfected with ZIP6 with a V5 epitope tag allowing use of an

anti-V5 antibody to assess immunostaining and localisation patterns. This gave a pattern of localisation consistent with plasma membrane staining (Taylor et al., 2003). Conversely, ZIP7 has been shown to be localised to the ER and Golgi apparatus. In human lung fibroblasts (WI-38), human prostate epithelial cells (RWPE1), human erythroleukemia cells (K-562), and human mammary gland epithelial cells (MCF-7) an anti-ZIP7 antibody was used to show a pattern of staining consistent with the Golgi apparatus (Huang et al., 2005). In addition, localisation studies in CHO cells transiently transfected with ZIP7 with a V5 epitope tag (as with ZIP6) enabled visualisation of an ER pattern of localisation using an anti-V5 antibody (Taylor et al., 2004). Both studies established the zinc transport ability of ZIP7. Huang et al., (2005) used ZnT7/ZIP7-co-expressing CHO cells and the fluorescent zinc tracer dye, Zinquin, to show that ZIP7 negates the zinc accumulation seen in the Golgi apparatus that is found in cells expressing ZnT7 alone. Taylor et al., (2004) used FACS analysis of transiently transfected CHO cells, as for ZIP6, to confirm transport of zinc concluding that ZIP7 has the ability to transport intracellular zinc across the membrane on which it is positioned. The role for ZIP7 in breast cancer has become apparent in that elevated ZIP7 is associated with breast cancer in tamoxifen resistant (TamR) cell lines thus leading to elevated zinc levels and increased growth factor activation. The impact of this is an increase in cell growth and invasion, this can be reversed by ZIP7 knock-down using small interfering RNA (siRNA) thus reducing intracellular zinc levels and growth factor activation (Taylor et al., 2008). Further investigation into this mechanism has led to ZIP7 being proposed to be important in zinc-mediated tyrosine kinase signalling therefore suggesting ZIP7 as a potential therapeutic target in cancer (Hogstrand et al., 2009).

ZIP8 (SLC39A8, originally BIGM103) expression is in the lung, kidney, testis, liver, brain, small intestine and the membrane fraction of mature red blood cells (Wang et al., 2007, Ryu et al., 2008). In four stably transfected human cell lines (HEK-293, RK-13, COS-7, and MCF-7) hZIP8 was localised to the lysosomes (Begum et al., 2002), however in adult murine erythrocytes anti-mZip8 antibody staining was consistent with plasma membrane localisation (Ryu et al., 2008). Zinc transport by ZIP8 has been elucidated to as transfected CHO cells accumulated more zinc than their mock-transfected counterparts (Begum et al., 2002). In addition to its role in zinc transport mZip8 has been shown to be responsible for the accumulation and >10-fold increase in the rate of intracellular cadmium influx in a mouse fibroblast cell line (Dalton et al., 2005). In primary human lung epithelia and BEAS-2B cell cultures the inflammatory mediator, tumour necrosis factor-α (TNF-α), was shown to induce ZIP8 mRNA expression, furthermore the expression of ZIP8 meant an increase in intracellular zinc content which coincided with cell survival when stimulated with TNF-α implying a role in immune activation of inflammation through cytoprotection (Besecker et al., 2008). ZIP8 has also been found to be elevated in breast cancer and more specifically Fulvestrant-resistant cell lines. It has been proposed that the elevation of these zinc transporters has a role in the development of the Fulvestrant-resistance of the cancers (Taylor et al., 2007).

ZIP9 (SLC39A9) is a less well characterised transporter in the ZIP family. Transient transfection of hZIP9 with an HA epitope tag has shown it to localise to the *trans*-Golgi network (TGN) irrespective of zinc status. It is the only known member of the subfamily I in mammals and a role in mobilising zinc as part of the secretory pathway has been implied because stable expression of hZIP9-HA decreases alkaline

phosphatase activity, a marker of zinc homeostasis in this pathway, in DT40 cell lines (Matsuura et al., 2009).

In zebrafish gills, an area studied due to its functional similarities to mammalian intestines, excess zinc down-regulates ZIP10 (Slc39a10) mRNA expression as shown by real-time RT-PCR (RT-qPCR). Conversely, a decrease in zinc increases ZIP10 mRNA levels (Zheng et al., 2008). This has led to the discovery of metal regulatory elements (MREs) in the zebrafish *Zip10* gene. In addition, Zheng et al., (2008) show Zip10 functions as an importer using the *Xenopus* oocyte expression system whereby uptake of ^{65}Zn into oocytes injected with Zip10 mRNA was compared to water-injected controls. Consistent with other members of the ZIP family, ZIP10 is dysregulated in breast cancer shown in clinical samples where ZIP10 mRNA expression correlated significantly with the metastasis of breast cancer to the lymph node. Furthermore, in breast cancer cell line studies the more invasive and metastatic cell lines (MDA-MB-231 and MDA-MB-435S) have an increased ZIP10 mRNA expression as compared with the less metastatic breast cancer cell lines (MCF7, T47D, ZR75-1 and ZR75-30). Intriguingly, knockdown experiments using siRNA to assess the involvement of ZIP10 in cell migration in MDA-MB-231 and MDA-MB-435S cells have revealed that a decrease in ZIP10 expression subsequently decreases zinc concentrations and inhibits the migratory properties of these cancer cells (Kagara et al., 2007).

There is little information in the literature relating to ZIP11 (SLC39A11) however, it is note-worthy that it is the only ZIP to be a member of the gufA subfamily. Using an anti-Zip11 antibody it has been shown in mouse mammary epithelial cells (MECs) that Zip11 showed a localisation pattern consistent with the Golgi apparatus as it co-localised with the marker p58. This is thought to be important for zinc export from the

Golgi and into milk. Also Zip11 has been postulated to be a key player in the 're-uptake' of zinc from milk during lactation as protein expression of Zip11 can increase more than two-fold during lactation in mice (Kelleher et al., 2012). Despite this more research is required to understand the zinc transporting system in mammary glands.

In neurobiology ZIP12 (SLC39A12) is an interesting candidate for further investigation. Although research is severely lacking into this transporter, missense mutations in the ORF of ZIP12 occur about twice as regularly in post-mortem brain tissue DNA samples from a small number of patients with schizophrenia as compared to controls (62 unrelated Caucasian schizophrenics versus 35 unrelated and unaffected Caucasians) (Bly, 2006). This observation is more compelling when it is coupled with the knowledge that zinc concentration in the schizophrenic brain is low compared with controls (Kimura and Kumura, 1965).

Zip13 (Slc39a13) has been found to be located to the Golgi apparatus in mouse osteoblasts, chondrocytes, pulpal cells, and fibroblasts with use of an anti-Zip13 antibody. In addition, in primary dermal fibroblasts from $Zip13^{-/-}$ knockout mice, the zinc levels in the Golgi apparatus were increased as compared to wild-type cells as measured by electron probe X-ray micro analysis ((EPMA) a technique that is able to detect zinc levels in a restricted area of a single cell) implying Zip13 acts to increase the zinc concentration of the cytosol by transporting zinc out of the Golgi apparatus (Fukada et al., 2008). A 9 bp deletion in exon 4 of ZIP13 leads to the spondylocheiro dysplastic form of Ehlers-Danlos syndrome (SDF-EDS) (Giunta et al., 2008). Patient phenotype includes the features of EDS: progressive kyphoscoliosis, hypermobility of joints, and hyperelasticity of skin combined with severe hypotonia of skeletal muscles,

coupled with short stature (Beighton et al., 1998). These phenotypic observations implicate a role for ZIP13 in bone and connective tissue development.

ZIP14 (SLC39A14) is most closely linked to ZIP8 with almost 50 % homology between the two transporters. Similar to ZIP8 the transport function of ZIP14 has been identified by transfection of CHO cells with a ZIP14 construct, this gave a cellular accumulation of zinc (Taylor et al., 2005). Subsequent investigations using the *Xenopus* oocyte expression system have revealed the ability of ZIP14 to transport zinc, cadmium, iron and manganese (Pinilla-Tenas et al., 2011). ZIP14 mRNA expression is thought to be widespread with highest levels in the liver, pancreas, heart, thyroid gland, and small intestine. Localisation studies were completed in CHO cells using a ZIP14 construct with a V5 epitope tag. Using an anti-V5 antibody the cells displayed a plasma membrane localisation pattern (Taylor et al., 2005). There are 2 splice variants of mZip14 that have been identified in mouse: mZip14A and mZip14B. Both variants are most highly expressed at the mRNA level in the liver and duodenum however, following this, mZip14A abundance is higher in kidney and then testis opposed to mZip14B being greater in the brain and then the testis. Researchers showed that both mZip14 variant transporters are located on the apical membrane in transiently transfected Madin-Darby canine kidney (MDCK) polarised epithelial cells (Girijashanker et al., 2008). In experiments that do not distinguish between these transcripts, it has been shown that inflammation and lipopolysaccharide (LPS) up-regulate mZip14 mRNA levels in the mouse liver thereby playing an interesting role in inflammation. It is thought that interleukin-6 is the cytokine that mediates this increase mZip14 expression because in interleukin-$6^{-/-}$ mice LPS did not induce mZip14 expression and in primary hepatocyte cell cultures interleukin-6 treatment induced an increase in mZip14 mRNA and protein expression with an increase in localisation of the

protein to the plasma membrane. This led the investigators to hypothesise that mZip14 is an acute-phase gene enabling it to contribute to the hypozincaemia of the inflammation and infection response (Liuzzi et al., 2005).

1.4.2 *CDF family*

Members of the cation diffusion facilitator (CDF) family are broadly thought to be involved in the sequestration of both essential and toxic metals. In bacteria this family of transporters have been shown to be involved in transport of many cations however, the homologous proteins in mammals all have known or assumed zinc transport function and are therefore known as the ZnT family of zinc transporters. They are thought to have an involvement in mammalian zinc homeostasis (reviewed by Montanini et al., 2007). Confirmation of this zinc transporter activity has been performed for ZnT 1, 2, 4-8, either indirectly by survival of zinc susceptible cells in medium with a high zinc content, or by directly measuring uptake or accumulation of zinc (using zinc fluorescent probes or radioactive zinc) in transfected or mutated mammalian cells, zinc-sensitive yeast strains and *Xenopus* oocytes (Palmiter and Findley, 1995, Palmiter et al., 1996a, Huang and Gitschier, 1997, Kambe et al., 2002, Huang et al., 2002, Kirschke and Huang, 2003, Chimienti et al., 2004, Cragg et al., 2002). An additional method measured zinc transport indirectly in support of the *Xenopus* oocytes experiments for ZnT5vB, this utilised a reporter construct system to show movement of zinc (Valentine et al., 2007). This system is based on the β-galactosidase reporter system used in zinc-sensitive baby hamster kidney (BHK) cell lines to measure ZnT1 and ZnT2 function (Palmiter and Findley, 1995, Palmiter et al., 1996a, Palmiter, 1994). It is likely that these transporters act as secondary active transporters or antiporters due to their movement of zinc against a concentration gradient (Guffanti et al., 2002). All known members of the human ZnT family of

transporters contain a conserved CDF motif in their amino acid sequence. In comparison to ZIPs, ZnT family members primarily have six TMD with a basic region between TMD IV and V. Conversely to ZIPs however, the topology is such that the N- and C- terminals are thought to be intracellular (Figure 1.2), an orientation only proven for ZnT1 residing in the plasma membrane (Palmiter and Findley, 1995). Hydropathy plots indicate that four of the amphipathic TMDs act to form a channel for the translocation of zinc however this has not been validated experimentally. Furthermore, motifs have been found that may allow for protein-protein interaction and it is evident that some ZnTs act as hetero- or homo-dimers. There are three subfamilies of ZnTs: Subfamily I contains only ZnT9, subfamily II contains ZnT 1, 5, 6, 7 and 8 and subfamily III contain ZnT 2, 3 and 4 (reviewed by Palmiter and Huang, 2004). Data on the subfamily of ZnT10 is not available.

The sequence that codes for ZnT1 is found on chromosome 1. It is a simple gene structure that consists of 2 exons. Much investigation has been carried out into the rodent forms of Znt1. It has ubiquitous tissue expression, however is more abundant in tissues involved in zinc acquisition such as the small intestine, liver and kidney (McMahon and Cousins, 1998, Cousins and McMahon, 2000). In BHK cell lines, Znt1 is localised to the plasma membrane when visualised using a fluorescently tagged Znt1 construct (Cousins and McMahon, 2000). In addition, direct investigation of the small intestine of mice using a Znt1 specific antibody yielded a localisation pattern to the basolateral membrane of enterocytes (McMahon and Cousins, 1998). It is hypothesised that this localisation ideally places this transporter to transfer zinc from the enterocyte into the circulation and indeed Palimter et al., (1995) demonstrated this efflux activity experimentally using an indirect method. In zinc sensitive BHK cells that stably express the MRE-βGeo (a construct involving 5 MRE sequences and a β-galactosidase-

neomycin phosphotransferase (lacZ-neo) fusion gene) β-galactosidase activity measured such that these cells showed increased zinc efflux with transient transfection of Znt1 (Palmiter and Findley, 1995). Other functions postulated include, recovery of zinc in the kidney, from its position on the basolateral membrane of nephron tubules; protection against zinc-induced neuronal damage in the brain and maternal to foetus regulation of zinc levels in the villous yolk sac membrane (McMahon and Cousins, 1998, Liuzzi et al., 2001, Tsuda et al., 1997). Znt1 knock-out mice are embryonic lethal which emphasises the importance of Znt1 and, incidentally, zinc in development of the foetus. Furthermore, Znt1 has been shown to be expressed in the rat placenta from at least day 8 of gestation in addition to being found in the villus yolk sac of a day 18 rat placenta (Cousins and McMahon, 2000). Interestingly, Znt1 mRNA expression levels are increased in both the small intestine and kidney of mice fed a supplemented zinc diet (180 mg Zn/kg). This confers resistance to zinc by increasing efflux of zinc out of the cell (Liuzzi et al., 2001). There are two MRE (Metal Responsive Element) sequences found in the promoter of *Znt1* and *in vitro* DNA-binding assays demonstrated that Metal Transcription Factor-1 (MTF1) is able to bind to these to regulate Znt1 expression (see section 1.6) (Langmade et al., 2000). Furthermore, Langmade et al., (2000) showed that MTF1 is essential for basal levels of Znt1 expression in mouse embryo fibroblasts using homozygous deletions of the *MTF1* gene.

ZnT2 has a differential expression pattern with mRNA expression detected in the small intestine, kidney, placenta, pancreas, testis, seminal vesicles and the mammary gland (Kelleher and Lonnerdal, 2002, Liuzzi et al., 2003, Liuzzi et al., 2001, Clifford and MacDonald, 2000, Palmiter et al., 1996b). This transporter is involved in the accumulation of zinc into intracellular vesicles, revealed by transient transfection of Znt2 into zinc resistant BHK cells. In this system, when extracellular zinc was added

(100-200 μM) and the cells were stained with Zinquin, the fluorescence of the dye was restricted to the cytoplasm and was punctate therefore implying vesicular localisation (Palmiter et al., 1996a). More specifically, it has been hypothesised that these vesicles are late endosomes. Due to its vesicular localisation it has been suggested that ZnT2 acts through an exocytotic pathway, allowing zinc to be incorporated into secreted proteins to control endogenous losses. Znt2 is up-regulated at the mRNA level in response to increased dietary zinc concentrations in rats. For example, dietary zinc (180 mg Zn/kg) up-regulates Znt2 in the small intestine and kidney of rats (Liuzzi et al., 2001) and semi-quantitative RT-PCR techniques were used to show high levels of zinc in the lateral lobes of rat prostate tissue correlate with the high levels of Znt2 expression (Iguchi et al., 2002). Late stage gestation and early lactation induces an increase in Znt2 mRNA and protein expression in both maternal and foetal tissues (Liuzzi et al., 2003). The role of ZnT2 in mammary gland zinc homeostasis is a little more ambiguous however. A mis-sense mutation in the *ZnT2* gene substitutes a conserved histidine at amino acid 54 with arginine (H54R) in the ZnT2 transporter in affected mothers. This mutation has been linked to a reduction in zinc secretion from mammary epithelial cells resulting in transient zinc deficiency in breast-fed infants (Chowanadisai et al., 2006). Under normal zinc conditions the observations are that whilst basolateral membrane abundance remains constant, apical membrane Znt2 protein expression decreases throughout lactation in rat (Kelleher and Lonnerdal, 2003). It is thought that this is due to the compartmentalisation of the transporter in order to sequester the physiologically high concentrations of zinc.

The original characterisation of mouse Znt3 demonstrated a restricted mRNA expression profile in the brain and testis by Northern blot and RT-PCR (Palmiter et al., 1996b). In this study Palmiter et al., (1996b) also used an anti-Znt3 antibody to show

that staining of Znt3 coronal sections of mouse brain is similar to the Timm's staining (identifying histochemically reactive zinc) of glutamatergic neurones therefore leading to the hypothesis that Znt3 functions to package zinc into vesicles in these cells. More recent studies have identified a more widespread expression of ZnT3 however. Immunohistochemical techniques have detected Znt3 protein in the mouse retina (Redenti and Chappell, 2004) and both mRNA and protein, detected by RT-qPCR and immunohistochemical techniques respectively, have identified Znt3 present in mouse pancreatic islets and beta cells (Smidt et al., 2009). In the rat mRNA has been detected by microarray in the duodenal epithelium (Wongdee et al., 2009) and by PCR techniques in humans ZnT3 mRNA has been found in the airway epithelium (Ackland et al., 2007), adipose epithelium (Smidt et al., 2007) and in the androgen-sensitive human prostate adenocarcinoma cell line (LNCaP) (Iguchi et al., 2004). The expression in the mouse pancreas has led to speculation of an involvement of ZnT3 in diabetes aetiology. Indeed, Smidt et al., (2009) have shown that under conditions of severe beta-cell stress, Znt3 knock-out mice have impaired glucose metabolism with respect to control mice. Furthermore, there was an increased level of apoptosis in rat INS-1E cells, a pancreatic β-cell model, coupled with a reduction in insulin secretion with knock-down of Znt3 using siRNA (Petersen et al., 2011). As mentioned above, in areas of the mouse brain Znt3 sequesters zinc into synaptic vesicles of glutamatergic neurones (Palmiter et al., 1996b). Levels of Znt3 mRNA are detectable only a matter of days before birth but are at adult levels by 3 weeks post-partum. Interestingly, the amount of zinc in the synaptic vesicles correlates with the protein levels of Znt3 and studies have shown that homozygous disruption of mouse *Znt3* gives a marked reduction in the amount of detectable zinc in regions of the brain known to express Znt3 and upon further investigation there was no trace of zinc in synaptic vesicles (Cole et al., 1999). It

is intriguing however, that the Znt3 knockout mouse appeared normal. This normal phenotype implies that the lack of zinc in synaptic vesicles can be compensated for by another mechanism or indeed is not important in normal physiological conditions. Transcriptional regulation of ZnT3 by zinc has not been investigated.

Znt4 was first discovered in the mouse model of mutant zinc metabolism; lethal milk (*lm*). In this model pups that suckle on *lm/lm* dams exhibit zinc deficiency symptoms and die before weaning. Further investigation showed that the milk was deficient in zinc and this inborn mutation was mapped to chromosome 2 and, more specifically, the *Znt4* gene where there is non-sense mutation (C to T substitution) at 934 bp resulting in premature termination of translation at codon 297 (Huang and Gitschier, 1997). The major side-effect of the mutation is the production of zinc deficient milk. The milk being deficient of zinc and not void indicates that other transporters, such as ZnT2, are acting to try and maintain zinc levels. Huang et al., (1997) also carried out Northern blot analysis to establish that Znt4 is expressed in liver, lung, kidney, spleen, heart and brain as well as in both normal mouse mammary gland and mammary gland tumour. Northern blot analysis of a broader range of rodent tissues has shown Znt4 to be abundantly expressed in rat brain, testes, lung, kidney and intestinal epithelial cells. A ZnT4 construct with a *myc*-epitope tag was transiently transfected into Caco-2 cells in order to give localisation data. The pattern of staining is consistent with intracellular vesicles, such as endosomes, and the Golgi apparatus with translocation from the Golgi apparatus to the intracellular vesicles (Murgia et al., 1999). It is thought that the main function of ZnT4 is to facilitate zinc entry into secretory vesicles of particular glands therefore allowing for zinc secretion of these exocrine glands. In mouse fed zinc deficient (<1 mg Zn/kg) or zinc supplemented (180 mg Zn/kg) diets there was no difference in Znt4

mRNA expression levels in the small intestine or kidney as compared with those mice on a zinc adequate (30 mg Zn/kg) diet (Liuzzi et al., 2001).

ZnT5 is unusual because it has two isoforms which have different localisation patterns. ZnT5 variant A (ZnT5vA) is localised to the Golgi apparatus (Kambe et al., 2002) whereas ZnT5 variant B (ZnT5vB) has been shown to localise to the ER and in human intestinal Caco-2 cells localise to the apical enterocyte membrane (Cragg et al., 2002, Valentine et al., 2007). The sequences of the isoforms vary at the N- and C-terminal regions but the differing subcellular localisations have been attributed to their alternative C-terminal sequences (Thornton et al., 2011). In addition, it has been established that zinc does not induce translocation of either of the variants (Jackson et al., 2007). Another difference between the variants is in their functional activity. Over-expression of a ZnT5vA construct in HeLa cells enabled ^{65}Zn uptake into Golgi-enriched vesicles from HeLa cells thereby decreasing cytosolic zinc implying that ZnT5vA acts as an effluxer (Kambe et al., 2002). In addition, ZnT5vA has been hypothesised to also act as a heterodimer with ZnT6. Transfection of both constructs into model yeast systems that exhibit a zinc-suppressible large cell phenotype (*msc2*, *zrg17*, *msc2* and *zrg17* mutants) suppressed the growth defect of the mutants even before the addition of zinc implying that these two transporters form a complex that functions to deliver zinc into the secretory pathway (Ellis et al., 2005). Uniquely, by using direct measurement of ^{65}Zn into *Xenopus laevis* oocytes expressing the ZnT5vB construct and indirectly using a promoter reporter gene assay in transiently transfected Caco-2 cells ZnT5vB has been found to transport zinc bi-directionally (Cragg et al., 2002, Valentine et al., 2007). Both ZnT5vA and ZnT5vB are ubiquitously expressed. Most studies into this transporter are indiscriminate using cross-reactive experiments and therefore report on ZnT5 as a whole. An attempt to distinguish between the two

variants and their expression at the mRNA showed a decrease in ZnT5vA mRNA expression in response to 150 µM zinc in Caco-2 cells. This study was unsuccessful in making a specific ZnT5vB probe but RT-qPCR analysis of total ZnT5 levels also displayed this down-regulation in response to 150 µM zinc. Down-regulation in response to zinc of a transporter that has been shown to efflux zinc is opposite to what would be expected, whether this is due to the bi-directional actions of ZnT5 is unknown. Further investigation of this response used actinomycin D, to block gene transcription, showed that increasing zinc concentrations had an effect on stabilising ZnT5 mRNA (Jackson et al., 2007).

Northern blot analysis shows presence of two transcripts of mouse Znt6 (1.7 kb and 2.4 kb in size) that differ in their 3'-untranslated regions corresponding to alternative polyadenylation signals. The expression pattern of both transcripts appears to be restricted whereby the Northern blot shows the mRNA is present in the liver, brain, kidney and small intestine with the 1.7 kb transcript displaying higher levels of expression. Western blot analysis shows Znt6 protein to be present in the mouse brain with very low levels in the small intestine and kidney. Interestingly, it is thought that Znt6 undergoes post-translational modification in the lung as a band of slightly larger size (55 kD opposed to 51 kD) was observed in this tissue (Huang et al., 2002). Znt6 expression in yeast mutants led Huang et al., (2002) to conclude that Znt6 transports zinc out of the cytoplasm into either an intracellular pool or out of the cell as over-expression in yeast displayed the ability of the transporter to diminish the cytoplasmic zinc. Moreover, endogenous Znt6 was detected in normal rat kidney (NRK) cells with localisation to the *trans*-Golgi Network (TGN), interestingly though this localisation pattern is altered when the cells are treated with medium containing 200 µM zinc. The researchers showed that the antibody signal was distributed toward the periphery of the

cells with the addition of extracellular zinc therefore indicating zinc-induced translocation of the protein. Alkaline phosphatases (ALPs) have been shown to require the action of zinc transporters, such as ZnT5, in the DT40 cell line (a chicken B lymphocyte-derived cell line) as they are able to transport zinc into the Golgi apparatus and ALPs require this zinc for their activation. Therefore, tissue non-specific ALP (TNAP) activity has been proposed as a marker to measure zinc supply to the zinc-requiring enzymes in the secretory pathway (Suzuki et al., 2005a). Given the localisation of ZnT6, further investigation into the action of this transporter were explored in relation to the TNAP activity. Investigators found that, in DT40 cells where ZnT6 was knocked out ($ZnT6^{-/-}$), TNAP activity was reduced by 20 % implying that ZnT6 is important in the secretory pathway. Independently, $ZnT5^{-/-}$ cells were also found to reduce TNAP activity by a similar amount to the $ZnT6^{-/-}$ mutant and in a double mutant ($ZnT5^{-}ZnT6^{-/-}$) this reduction in activity was at a similar level still implying that ZnT5 and ZnT6 work in the same pathway. In support of this theory, co-transfection of ZnT5 and ZnT6 constructs restored TNAP activity whereas transfection of ZnT5 or ZnT6 independently failed to change TNAP activity. Moreover, co-immunoprecipitation studies revealed that ZnT6 forms a hetero-dimer with ZnT5 adding further weight to this hypothesis (Suzuki et al., 2005b).

Northern blot analysis for Znt7 showed abundant expression of mRNA in the liver, spleen, and small intestine with lower levels in the kidney, lung, and brain of mouse tissues. The mRNA was barely detectable in the heart. Post-transcriptional and/or post-translational modification of Znt7 is postulated due to the results of the Western blot analysis using an anti-Znt7 antibody. Firstly, protein was not detected in the mouse brain, liver, kidney, and heart despite the mRNA being detected in these tissues by the Northern blot. Secondly, whilst the protein was detected in the lung and small intestine

the apparent molecular mass on the Western blot of Znt7 was higher than the calculated 42.5 kD thereby implying post-translational modification (Kirschke and Huang, 2003). Using the same anti-Znt7 antibody, Kirchke et al., (2003) also stained endogenous Znt7 in rat small intestinal epithelial cells (hERIE 380) and human lung fibroblasts (WI-38) and saw a localisation pattern consistent with the Golgi apparatus. In addition the same pattern of staining was found in the NRK cells when cells were transfected with a Znt7-*myc* construct and detected using an anti-*myc* antibody. Furthermore, these researchers also looked at the function of Znt7. In transfected CHO cells the zinc probe, Zinquin, was found to accumulate in the Golgi apparatus with the addition of 75 μM of extracellular zinc, this implies that Znt7 acts to transport zinc into this subcellular compartment. Further elucidation of the role of ZnT7 has been achieved by using the ALP system mentioned above. ZnT7 has been shown to be required for ALP activity in the DT40 cell model thereby suggesting a role in delivering zinc into the secretory pathway, similar to ZnT5 and ZnT6 (Suzuki et al., 2005a). However, ZnT7 does not require the actions of another transporter as it acts alone, but the co-immunoprecipation experiments show it forms homo-oligomer complexes (Suzuki et al., 2005b). Knock-out studies in mice, have given zinc-deficient phenotypes; strikingly with a decreased body-fat composition thus implying that Znt7 plays a role in this process. Such mice are irresponsive to dietary zinc supplementation. In addition, the expression of Znt7 in the small intestine has been shown to be important in the absorption of zinc as a radioactive zinc feeding study displayed lower serum and tissue-associated zinc that were as a result of reduced zinc absorption in the gut (Huang et al., 2007). Given the localisation pattern of ZnT7 in the Golgi apparatus it is unlikely that ZnT7 is directly involved in zinc efflux into the circulation but the evidence suggested that ZnT7 is enterocytes acts to traffic zinc across these cells (Wang and Zhou, 2010).

ZnT8 research is particularly interesting in the context of diabetes. The *ZnT8* gene locus has been found to be associated with an increased risk of type II diabetes. A single nucleotide polymorphism (SNP) rs13266634 in the *SLC30A8* gene was shown to be associated with reduced insulin secretion by genotyping of 921 metabolically characterised German subjects (Staiger et al., 2007). Using RT-PCR on human tissue RNA samples ZnT8 expression was found to be restricted to only the islets of Langerhans in the pancreatic β-cells (Chimienti et al., 2004). Further characterisation by Chimienti et al., (2004) revealed that in insulin-secreting INS-1 cells (the rat insulinoma pancreatic β-cell model) over-expressing a ZnT8-EGFP construct the transporter gave a localisation pattern consistent with that of insulin therefore it was concluded that ZnT8 is associated with the insulin granule secretory pathway. In addition, with the use of Zinquin, over-expression of ZnT8-EGFP in HeLa cells showed an accumulation of zinc in the cells when 75 μM of extracellular zinc was added to the system. Its role in the pancreas is thought to be two-fold. Firstly, it has been shown to transport zinc from the cytoplasm so that it accumulates in vesicles. Secondly, the co-localisation with insulin-secretory granules implies that ZnT8 provides zinc for the insulin maturation process and/ or the storage of insulin in these pancreatic β-cells. A theory strengthened by the knowledge that zinc is needed for the storage of insulin as it forms a hexamer with two zinc ions bound. Therefore, upon release of insulin, zinc is also released into circulation. Indeed, ZnT8 knockdown studies using siRNA not only increased the level of apoptosis in these cells but also give an increased intracellular content of insulin coupled with a lower insulin secretion in INS-1 cells proving that ZnT8 is imperative to this pathway (Petersen et al., 2011).

Little is known about ZnT9. However Northern blot analysis of four human foetal tissues (brain, lung, liver, and kidney) showed mRNA expression in all these tissues.

RT-PCR showed presence of mRNA in all tested tissues and cells (16 human adult tissues and 14 cancer cell lines) therefore displaying widespread expression. Western blot analysis using an anti-ZnT9 antibody in the foetal cell line (MRC-5) revealed localisation to the cytosolic and nuclear fractions but not membrane fractions (Sim and Chow, 1999). Furthermore, Sim et al., (1999) showed that in normal embryonic lung cells the anti-ZnT9 antibody displayed a localisation pattern that implied association with the cytoskeleton however in liver carcinoma cells the staining was to the nuclei of smaller or dividing cells, but giving staining of the peri-nuclear ring in the cytoplasm of larger, more mature cells. The importance of this differing localisation remains unknown.

Prior to 2012 knowledge on ZnT10 was limited to a single article. Seve at al., (2004) reported bioinformatic data which found the human *SLC30A10* gene is localised to human chromosome 1 at the position q41. The gene spans 15 kb with an arrangement of 4 exons, and was predicted to code for a 52.7 kDa protein. When compared to other family members ZnT10 is predicted to contain the conserved 6 TMDs and a basic region between TMD IV and V. Using ClustalW alignment of amino acid sequences ZnT10 was found to be most homologous with ZnT1 with a score of 48.3. An *in silico* method was used to assess the tissue expression pattern. This was performed by using an expressed sequence tag (EST) data mining strategy whereby the programme BLASTN was used to run the predicted ZnT10 transcript (ORF, 5' and 3' UTRs) against the human EST database. This gave a predicted ZnT10 expression profile. Interestingly, using this method ZnT10 was predicted to be restricted to foetal tissue and more specifically foetal liver and brain (Seve et al., 2004).

1.5 Zinc absorption

Zinc is absorbed across the intestinal enterocyte along the entire gastrointestinal tract. Although primarily absorbed in the proximal small intestine (with a proximal to distal absorption gradient), the colon has the ability to absorb zinc throughout and evidence of up-regulation of absorption from sites within the colon has been observed when small intestine absorption is impaired (Seal and Mathers, 1989, Hara et al., 2000). It is known that enterocytes contain zinc transporter proteins expressed in their membranes and more specifically ZIP4 has been implicated in the uptake of zinc from the gastrointestinal lumen across the apical membrane. Furthermore, immunohistochemical localisation studies in mice revealed that in cases of zinc restriction Zip4, found on the apical membrane of enterocytes is up-regulated along the length of the gastrointestinal tract. However, when the body is zinc replete Zip4 is internalised and degraded (Dufner-Beattie et al., 2003b). Conversely, Zip5 has been found to be localised to the basolateral membrane of enterocytes and therefore is internalised during zinc deficiency. Thus it is hypothesised that, in zinc replete conditions, ZIP5 functions to influx zinc from the blood stream into enterocytes, ultimately for excretion into the intestinal lumen (Dufner-Beattie et al., 2004). Once in the cell one hypothesis for the intracellular trafficking of zinc implicates a member of the CDF family, ZnT7, in the movement of zinc across the enterocyte. In fact *Znt7* null mice exhibited poor appetite and reduced body weight gain symptoms that were not alleviated by zinc supplementation. In addition these mice were unable to accumulate ^{65}Zn in the small intestine, in particular the Golgi apparatus of enterocytes, a process required for successful dietary zinc absorption (Huang et al., 2007). It is possible that ZnT5vA carries out an overlapping role in the enterocytes as it too is localised to the Golgi apparatus in the small intestine (Kambe et al., 2002, Yu et al., 2007). It has been shown

that ZnT5vB localises to the apical membrane of enterocytes, the alteration in localisation is attributed to the C-terminal domain (Thornton et al., 2011). This variant exhibiting bi-directional transport across the plasma membrane and is involved in zinc uptake in human intestinal Caco-2 cells (Valentine et al., 2007). It is evident that metallothionein (MT), an intracellular metal buffer, and ZnT1, a zinc effluxer, regulate levels of zinc across the basolateral membrane, out of enterocytes and into the systemic circulation (McMahon and Cousins, 1998, Bell and Vallee, 2009). It is not these transporters that are exclusively expressed within enterocytes and other members of these families play a role in zinc absorption (see section 1.4) (reviewed by Wang and Zhou, 2010). Free zinc is toxic therefore zinc is circulated chelated by binding proteins such as albumin, α-macroglobulin and transferrin. Zinc is distributed throughout the body to all organs.

Zinc absorption is different to that of other nutrients such as iron because it is the dietary zinc intake that reflects the amount of zinc absorbed not the zinc status of the individual (King, 2011). The efficiency of the absorption of zinc can also be influenced by the presence of phytate as discussed above (section 1.2.1).

1.6 Molecular mechanisms of gene regulation by zinc

There are numerous molecular mechanisms of transcriptional control that are sensitive to zinc in a wide range of organisms. There are four fundamental mechanisms of zinc-sensitive transcriptional regulation. Firstly, in conditions of low zinc availability a positive regulatory factor binds in order to stimulate transcription. This is evident in the yeast *Saccharomyces cerevisiase* where the DNA motif responsible for this activation of the equivalent transporters (ZRT1, 2 and 3) has been identified. It is hypothesised that in low zinc conditions a transcriptional regulator; Zap1, is induced and binds to the 11

bp Zinc Response Element (ZRE) in the promoter regions of the transporters subsequently increasing their transcription so that they can increase cytosolic zinc concentrations (Lyons et al., 2000). Secondly, again under conditions of low zinc availability, a negative regulatory factor can bind. In bacteria the ArsR-SmtB family transcriptional de-repressors act to repress the expression of certain operons at stress-inducing concentrations of divalent metal ions including zinc. Direct binding of such metal ions results in de-repression (reviewed by Busenlehner et al., 2003, Waldron and Robinson, 2009). Third is under conditions of high zinc availability a negative regulatory factor can bind. For example, the transcriptional repressor Zur binds two zinc ions in order to bind to DNA and repress the transcription of a zinc importer in the *znuABC* gene cluster (Patzer and Hantke, 2000) therefore reducing zinc intake. The final mode of transcriptional regulation is in conditions of high-zinc availability through binding of a positive regulatory factor. This is evident in the case of the transcription factor MTF1. MTF1 has 6 zinc fingers and these bind DNA at a specific consensus sequence within promoter regions. The DNA motif is a MRE and is characterised by the 7 bp sequence TGCRCNC (Heuchel et al., 1994). Binding of MTF1 to MREs is known to increase expression of genes such as MTI and II and ZnT1 in order to protect cells from high zinc concentrations (Langmade et al., 2000, Wimmer et al., 2005). MTF1 can also act in a repressive role. Zip10 expression is increased in the conditional MTF1 knockout mouse (Wimmer et al., 2005). Further research has shown that Zip10 includes MREs downstream of the transcriptional start site and binding of MTF1 to these MREs mediates transcriptional repression (Lichten et al., 2011). In addition, the zebrafish Zip10 has two distinct transcriptional start sites and experimentation reveals that Zip10 is regulated by alternative promoters that are oppositely-regulated by zinc. Both promoters contain MRE clusters and thus, this shows that MREs can function as both

repressor and activation elements (Zheng et al., 2008). It is possible that MTF1 requires accessory proteins in order to form co-activator complexes in order to fulfil these contrasting roles. Indeed, activation of the MTI promoter requires transcription factor Sp1 and the histone acetyltransferase p300/CPB in complex with MTF1 and this activation was reduced by siRNA knockdown of p300/CBP. However the accessory proteins evidently differ between complexes as p300/CBP knockdown did not affect MTF1-mediated activation of the mouse *Znt1* gene (Li et al., 2008). Interestingly, there must be mechanisms in addition to MTF1 that are able to influence zinc induced repression as mutation of the consensus MRE sequence in ZnT5 was unable to abolish the zinc-induced repression ordinarily observed in transfected Caco-2 cells (Jackson et al., 2007).

Another particularly important mammalian transcription factor that is zinc dependent is Nuclear Factor-κB (NF-κB) (Bao et al., 2007). There are many processes where NF-κB modulates transcriptional activity of genes such as immunoreceptors and cytokines. In fact reactive oxygen species (ROS) can induce a redox-dependent signal transduction pathway that leads to NF-κB activation and therefore stimulation of the inflammatory immune response. This has been implicated in disease as inflammation causes extensive damage in the brain of Alzheimer's disease (AD) patients (Zimmerman et al., 2004). Under normal conditions, NF-κB is maintained in its inactive state in the cytoplasm by association with the inhibitory protein, IκB. Zinc has been found to induce phosphorylation of IκB thereby stimulating its degradation and activating NF-κB, increasing the translocation of NF-κB from the cytosol to the nucleus in HUT-78 cells (a T helper 0 cell line) (Bao et al., 2007, Prasad et al., 2001). Conversely, in zinc deficiency states NF-κB activation is reduced meaning decreased stimulation of genes involved in the inflammatory immune response such as interleukin-2 and its receptor

(interleukin-2Rα) in the HUT-78 cell line thus providing evidence for a role of zinc in the immune system and implications for human health (Prasad, 2008).

Zinc fingers are common structures in transcription factors that enable binding of the proteins to DNA sequences. The transcription factor Sp1 contains three such domains and is able to both repress and activate transcription (Li and Davie, 2010). The interaction between MTF-1 and Sp1 is intriguing. In cells where MTF1 is present it has been found that a complex containing Sp1 and p300 forms when extracellular zinc increased (Li et al., 2008). Furthermore, Sp1 may be implicated in dysregulation of genes in AD. For example, β-secretase 1 (BACE1) contains a functional Sp1 response element and increased expression of Sp1 causes an increase in BACE1 transcription ultimately resulting in an increase in the formation of neurotoxic amyloid-β (Aβ) peptides (Christensen et al., 2004).

Zinc transporters are essential for zinc regulation and they are imperative for both efflux and influx of zinc across membranes in order to maintain zinc homeostasis. It follows therefore that these genes have been shown to be regulated by mechanisms that alter in response to the zinc state of the cell. More specifically, studies into the regulation of mZip4 identified the transcription factor Krüppel-like factor 4 (KLF4) in the activation of *mZip4*. In the murine intestinal epithelial cell (IEC) line MODE-K both KLF4 and mZip4 were up-regulated in zinc deficient conditions but siRNA knockdown studies of KLF4 reduced the activation of mZip4 (Liuzzi et al., 2009). Moreover, Liuzzi et al., (2009) used electrophoretic mobility shift assays (EMSAs) with the nuclear extracts of this MODE-K cells to show that KLF4 binds to the mZip4 promoter, a phenomenon that is increased when zinc is limited. Further investigation with reporter constructs involving the wild-type and mutated mZip4 promoter led the authors to conclude that

regulation of mZip4 is through a KLF4 response element. However, as highlighted in section 1.4.1, there are discrepancies in the literature with regards transcriptional regulation of mZip4 with Weaver et al., (2007) attributing regulation to post-transcriptional mechanisms.

In the ZnT family ZnT1 is known to be regulated by MTF1, mentioned above (Langmade et al., 2000). In addition, the regulation of ZnT5 highlights the complexities of zinc related transcriptional regulation given that transcription of both variants is driven by a single promoter. Five core MREs identified in the putative promoter region of the ZnT5 transcript led to speculation that the mode of regulation was via the binding of MTF1. However, mutation of the consensus MRE sequence in ZnT5 was unable to abolish the zinc-induced repression ordinarily observed in transfected Caco-2 cells (Jackson et al., 2007). Furthermore, Jackson et al., (2007) identified a 204 bp region comprising -154 bp prior to transcriptional start codon and +50 bp into the ORF of ZnT5 that is required for the zinc-induced transcriptional repression of ZnT5. More recently, EMSAs have revealed that there is a protein factor that binds to the ZnT5 promoter in a zinc-dependent manner. Through this Coneyworth et al., (2012) identified the binding site in the ZnT5 promoter responsible for zinc-induced transcriptional repression, namely the ZTRE (for Zinc Transcriptional Regulatory Element) (Coneyworth et al., 2012). Analysis of this sequence, using a promoter reporter assay in Caco-2 cells, confirmed that this region is essential for repression of transcription in response to zinc. Further research is required to establish whether such sequences are more widespread in biology enabling elucidation of further roles for zinc.

1.7 Zinc in the brain

In the context of my research, the brain is the organ that is particularly relevant. It is known that zinc is required in the brain and, as in every organ, it is under strict regulation. The brain is no exception in terms of zinc moving through membrane channels of cells enabling it to modulate the function of many proteins. Importantly, neurological zinc is found in presynaptic vesicles of certain glutamatergic neurones with stores of up to 300 μM zinc in nerve terminals and, along with glutamate, zinc is released during neurotransmission (Frederickson, 1989, Frederickson et al., 1983). The concentration of this release of 'free' zinc into the extracellular space is the topic of much debate. However, electrical stimulation has led to estimates of between 10 μM and 100 μM (Li et al., 2001) with observations of up to 100 nM of 'free' zinc under conditions when ischaemia and reperfusion were initiated by excitotoxic stimulation (Frederickson et al., 2006). However, there are developmental differences, zinc release from the immature hippocampus is much more modest than that from the adult due to the neurons responsible for such release being developed postnatally (Kay, 2003). The cell bodies of these so called 'gluzinergic' neurons are predominantly in the cerebral cortex or the limbic structures. The limbic system is often referred to as the 'emotional brain' and includes structures such as the thalamus, hypothalamus, amygdala, and hippocampus. The cerebral cortex consists of four lobes; temporal, occipital, parietal and frontal which can be attributed to the following functions respectively; language and speech, vision, sensory areas (e.g. pressure, touch and pain) and complex brain processes such as personality (Kandel et al., 2000).

The gluzinergic neurones are essential in order to control many physiological and pathophysiological brain functions. However the role of zinc in brain function at a

cognitive level remains ambiguous despite the importance of the micronutrient for learning and memory being repeatedly reported (reviewed by Sindreu and Storm, 2011). Postsynaptically, gated channels such as the NMDA (N-methyl-D-aspartate) channels, voltage gated calcium channels and AMPA (α-amino-3-hydroxy-5-methyl-4-isoxazole propionic acid/kainite) channels seem to be sensitive to extracellular zinc (Paoletti et al., 2009). Such channels are opened by both glutamate and depolarization of the neuronal membrane caused by neuronal activity therefore allowing maximal translocation of zinc from the presynaptic neuron into the postsynaptic neuron with intense neuronal activity. Translocation means that zinc is able to exhibit downstream effects on synaptic transmission thereby triggering synaptic potentiation and initiate signal cascades in the postsynaptic neuron, thus modulating processes such as transcription in these cells (Sensi et al., 2009).

Zinc interacts with NMDA and $GABA_A$ (γ-aminobutyric acid type A) receptors thereby affecting their activity. The actions of these receptors are opposing; NMDA is an excitatory receptor and $GABA_A$ is an inhibitory receptor. It is through interaction with these receptors that zinc is able to influence both excitatory and inhibitory synaptic transmission although it is thought, under normal conditions, that the dominant effect of zinc is to reduce excitability (Frederickson et al., 2005). The main hypothesis for the mode of action of zinc for learning and memory is through the interaction with the $GABA_A$ receptors on the synapses. It is thought that zinc is required by the inhibitory $GABA_A$ receptors in order to mediate long-term potentiation (LTP), a process integral to memory formation (Kodirov et al., 2006). LTP is inhibited by administration of extracellular zinc chelators implying a role for zinc and confirmation of the role of said $GABA_A$ receptors has been established by the use of a receptor antagonist that subsequently restored LTP (Smart et al., 1994).

Whilst the processes described above are important physiologically it is also evident that zinc can have a detrimental effect on neurons. For example, excitotoxicity is the phenomenon whereby excessive glutamate release causes over-activation of glutamate receptors. As glutamate is released so too is zinc, the increased translocation of which causes zinc-induced cell injury. Moreover, zinc can promote oxidative stress by activating reactive oxygen species (ROS)-generating enzymes such as nicotinamide adenine dinucleotide phosphate (NADPH) oxidase and neuronal nitric oxide (NO) synthase (nNOS) (Sensi et al., 2009). Ischaemic neuronal death follows the same process; studies investigating such pathways have highlighted the prominence of zinc. Ischaemic injury was initially attributed to Ca^{2+} however upon further investigation the chelators used in the original studies were found to have a higher affinity for zinc (Smith, 2009). During excitotoxic and ischaemic injury there are many mechanisms at play. For example, under conditions of oxidative stress and/ or acidosis MTs release their intracellular store of zinc thereby activating neuronal apoptosis by the p38 MAPK pathway (Pal et al., 2003). Furthermore, under compromised conditions the mitochondria play an important role in reducing cytosolic zinc concentrations by activation of mitochondrial membrane cation-permeable channels. However, the proceeding zinc accumulation within the mitochondria can lead to a loss of mitochondrial membrane potential, increased production of ROS and ultimately cell death via apoptosis (reviewed by Dineley et al., 2003). Cell death by zinc is not limited to apoptosis, zinc can also promote necrosis by inhibiting glycolysis and therefore depleting ATP production. In addition, autophagy can be induced by zinc whereby increased zinc concentrations in the lysosomes ultimately result in permeabilisation of the lysosomal membrane releasing cathepsin D (reviewed by Hoyer-Hansen and Jaattela, 2007, Sensi et al., 2009).

1.7.1 *Role of ZIPs in brain zinc homeostasis*

Nutrients that enter the brain must cross the blood-brain barrier. It is thought that ZIPs are expressed in the cells forming the blood-brain barrier and therefore function in the uptake of zinc into the brain. However, research is limited into the role of ZIPs in the brain. As expected though, in the Zip1 and Zip3 double knockout mouse there was a 50 % reduction in post-synaptic zinc uptake (Qian et al., 2011), thus indicating that ZIPs in the brain, as in other organs, are involved in cellular zinc uptake enabling an increase in cytosolic zinc where necessary. Furthermore, in the rat brain Zip1 was found in all brain regions tested. Conversely, Zip4 was only found in the choroid plexus and brain capillaries (Belloni-Olivi et al., 2009). In addition, Zip1, Zip7, Zip8, Zip9, Zip10 and Zip13 were found to be expressed in the mouse brain under conditions of zinc deficiency with a 3-fold increase in Zip10 mRNA under dietary restriction (Lichten et al., 2011). This is particularly interesting given the blood-brain barrier system means that zinc homeostasis in the brain is very tightly regulated. Therefore brain zinc levels are not easily disrupted by dietary zinc deficiency. However, zinc deficiency can reduce the zinc concentration in the hippocampus (Takeda and Tamano, 2009). Further implication of a ZIP family member in brain homeostasis is evident for ZIP12 where missense mutations in the ORF of ZIP12 occur about twice as regularly in post-mortem brain tissue DNA samples from a small number of patients with schizophrenia as compared to controls (62 unrelated Caucasian schizophrenics versus 35 unrelated and unaffected Caucasians) (Bly, 2006). The work by Bly et al., (2006) furthers an earlier study identifying changes in zinc concentration s in the schizophrenic brain (Kimura and Kumura, 1965) and thereby indicates a role for ZIP12 in brain zinc homeostasis. To elucidate the mechanisms of the ZIPs in the brain fully, requires further investigation.

1.7.2 *Role of ZnTs in brain zinc homeostasis*

As with other organs the homeostasis of zinc in the neurons has a number of pathways of regulation and zinc homeostasis in the neurons cannot be attributed to one transporter. In line with other tissues the ZnT family predominantly act to decrease cytosolic zinc in their various locations throughout the cell body e.g. ZnT1 on the surface membrane. Studies have revealed a neuroprotective role for Znt1 mediating an increase in zinc efflux against toxic zinc surges in seizures and/ or ischaemia (Tsuda et al., 1997). It is thought that it is nitric oxide that triggers release of zinc in these cases and the zinc, in turn, causes an up-regulation of Znt1 expression although the mechanism has not been fully elucidated (Aguilar-Alonso et al., 2008). In addition, Znt2 and Znt4 were also found to be up-regulated in the rat brain presumably to decrease cytosolic zinc concentrations initiated by nitric oxide production. ZnT5, ZnT6 and ZnT7 have also been found to be expressed in several regions of the brain with increased mRNA levels of the transporters tested (ZnT1, ZnT4 and ZnT6) in human AD brains (Beyer et al., 2012) and in mouse models of AD (Znt1, Znt4, Znt6 and Znt7) (Zhang et al., 2008).

However, the main body of research in ZnTs in the brain is into ZnT3. In the presynaptic neuron the sequestering of zinc into presynaptic vesicles is under the control of ZnT3 (section 1.4.2). The process begins in the Golgi apparatus where ZnT3 is inserted into the membranes of the vesicles and subsequently these vesicles are transported down the axon to the presynaptic terminal. It is evident that in this location the vesicles contain both zinc and glutamate ready for release via exocytosis when the neuron is stimulated (Frederickson et al., 2005). Znt3 knockout mice were used to demonstrate that Znt3 is required for zinc transport into these synaptic vesicles. With the disruption of the *Znt3* gene histochemically reactive zinc was undetectable in these

mouse brains (Cole et al., 1999). There is much still to be learnt about the ZnT family and their roles in homeostasis of zinc in the brain.

1.7.3 *Role of MTs and the mitochondria in brain zinc homeostasis*

Also in line with whole body zinc homeostasis, another important aspect of brain zinc homeostasis is MT. MTI, MTII and MTIII isoforms are all found in the brain. Consistent with the other MT's (Section 0), MTIII can sequester zinc by forming a complex coordinated by its cysteine residues. In addition, these cysteine residues can be oxidised resulting in the release of zinc ions and so MT act as both a zinc sink and a zinc source (reviewed by Palmiter, 1998). This is evident in MTIII knockout mice where in certain areas of the hippocampus and the thalamus cell injury is reduced. This could imply that MTIII would, under normal physiological conditions, release zinc and contribute to this insult (Lee et al., 2003). Conversely, in the CA3 area of the hippocampus cell death increases suggesting that MTIII normally chelates zinc in order to prevent such toxicity (Ueno et al., 2002).

A less well characterised component of zinc homeostasis in neurons is in the mitochondria. It is known that zinc is sequestered into the mitochondria through both the Ca^{2+} uniporter (Saris and Niva, 1994) and a Ca^{2+} uniporter-independent mechanism (Sensi et al., 1999). It has been hypothesised that this elevates the oxidative stress and buffering burden of the neurons however the mechanism of this under normal conditions has not been elucidated (Sensi et al., 2009). In summary, the homeostasis of zinc ions within the neurons is reliant upon the coordination and balance of the three systems; coordination of uptake and efflux by ZIPs and ZnTs, MT buffering capacity and sequestering of zinc by the mitochondria. The dual personality of this micronutrient

and its repeated implication in neurodegenerative diseases only emphasises the importance of maintaining the regulation of its actions in the brain.

1.8 Ageing, zinc and the brain

The World's population is ageing at a rapid rate, the UK is no exception (Figure 1.3), and so the need to understand the ageing process is becoming increasingly important.

There are many economic implications for this shifting demographic, with the impact on public services and the families involved in the care of individuals being great (Dening and Barapatre, 2004). It is well established that an investment in health throughout the life course improves prospects for healthy ageing; however there are still major limitations to our knowledge of the process of ageing. One major area of concern in the elderly is the dramatic decrease in nutritional status due to both physiological and pathological changes that induce a loss of taste, smell and appetite and increase satiating effects to give end states including age related anorexia (Volkert et al., 2010). Adequate nutrition is a factor that affects health at all stages throughout life and in this age group, undernutrition reduces the ability of the individual to remain healthy in older years. Whilst it is recognised that these changes occur, research at the molecular level to determine the underlying causes are incomplete and in particular research into the role of zinc is limited. It is evident that zinc status decreases with age with various theories as to why (Mocchegiani et al., 2006b, Mocchegiani et al., 2006a). It could be related to inadequate diet (such as consumption of less zinc-rich red meat) (Wong and Ho, 2012)or a reduced ability of the body to maintain homeostasis of this micronutrient (Mocchegiani et al., 2006a). It is also evident that taste acuity declines with age and zinc status has been linked with both loss of appetite and ability to taste, both of which rely heavily on zinc status (Stewart-Knox et al., 2005, Suzuki et al., 2011). A link with a

reduced appetite has been attributed to a relationship between the hormone leptin and zinc (Ott and Shay, 2001). In the case of taste acuity it has been shown that the hormone gustin is affected by the amount of dietary zinc present (Shatzman and Henkin, 1981). It is important to note if appetite is decreased intake of zinc rich foods will be reduced therefore exacerbating the other symptoms of zinc deficiency. The cellular mechanisms for the influence of zinc on both leptin and gustin are unknown. In addition there are tissue specific changes in zinc metabolism. For example, in age-related macular degeneration there is an accumulation of zinc in the sub-retinal pigment epithelial deposits of eyes implying a dyshomeostasis in these patients (Lengyel et al., 2007). However, zinc supplementation can influence immune status of elderly individuals (Mocchegiani et al., 2012b) thus displaying the varying roles of the cation.

Zinc is also important for immune function with zinc deficiency causing defects in both innate and adaptive immune responses (reviewed by Prasad, 2008). Furthermore, alterations in zinc transporters have been observed with lipopolysaccharide (LPS) stimulation ultimately decreasing intracellular zinc concentrations (Kitamura et al., 2006). Chronic inflammation is a well-documented feature of ageing (Chung et al., 2006). The pathway towards this disease state is thought to be induced by the cytokine interleukin-6. This is known to up-regulate ZIP14 in the liver thereby increasing zinc uptake in these cells (Liuzzi et al., 2005). The consequence of this is that zinc is redistributed into the liver where it is sequestered and bound to MT (Andrews, 2000). As a result plasma zinc concentration decreases significantly, a phenomenon that has been repeatedly observed with older age (Fairweather-Tait et al., 2008).

Physiological ageing of the brain is not fully understood. However it is widely recognised that brain ageing can be characterised by a significant reduction in brain

weight by approximately 10 % at 80 years of age. These reductions are attributed to atrophy of the neurons and their connections (Bertoni-Freddari et al., 2006). Synapses are undergoing constant remodelling in order to change in response to events throughout an individual's lifespan. The parameters that alter are the synaptic density, the average size of the junctional zones and the overall contact area of the synapses. Old age induces a change such that there is an inverse correlation between synaptic density and the average size of the junctional zones. In other words, in physiological ageing (compared with adulthood) there is a decrease in the synaptic density that is paired to an increase in average size of junctional zones. In addition there is a significant reduction in the overall contact area of the synapses in old patients (reviewed by Bertoni-Freddari et al., 2008). Whilst the increase in the average size of junctional zones presumably indicates a compensatory mechanism for the reduction in synaptic density this, coupled with the reduction in overall contact area, explains the progressive impairment in cell-to-cell communication in the elderly. Cognitively this presents as a decline of brain functions such as impairment in learning and memory functions.

Changes to mitochondria also occur in the aged brain. Synaptic mitochondria have a greater burden of oxidative stress and buffering than those at other positions in the neurons (see section 1.7.3). With age, mitochondria decrease in number, but so to compensate, there is an increase in mitochondrial size meaning that ultimately there is no change in mitochondrial volume density (Bertoni-Freddari et al., 1993). Despite this, there is a significant decrease in the cytochrome oxidase (COX) activity on the inner mitochondrial membrane in the older cohort (Bertoni-Freddari et al., 2003). COX is a key component of the mitochondrial electron transport chain and therefore its activity is thought to be a reliable marker of neuronal metabolism and, indeed, mitochondrial metabolic competence (MMC) (Wong-Riley, 1989). This MMC decline is hypothesised

to be a major contributor to the development of the synaptic pathology described above. Furthermore, if mitochondria are compromised and are unable to sequester zinc released during neurotransmission, then the high intracellular zinc concentrations will persist longer than ordinarily needed for its physiological function. The resultant downstream effect of this excess zinc is that it is toxic for the neurons (Bertoni-Freddari et al., 2008).

It is clear that altered zinc homeostasis is implicated in the physiological effects of ageing. An important mediator of zinc homeostasis is the ZnT zinc transporters, however there is a lack of definitive evidence on whether there are significant alterations in transporter expression and function in the aged population (Fairweather-Tait et al., 2008).

1.9 Alzheimer's disease

Alzheimer's disease (AD) is the world's most common form of dementia affecting approximately 24 million people worldwide and with the increase in the ageing population this incidence is predicted to grow (Mayeux and Stern, 2012). AD is a neurodegenerative disease that manifests as progressive global cognitive decline, most noticeably there is a deficit in memory functions. Remarkably defects in episodic memory (memory of autobiographical events) have been found up to seven years before clinical diagnosis (Grober et al., 2008). At a morphological level there is a distinct change in neuronal volume, and indeed neuronal survival, in many types of dementia (Gemmell et al., 2012). Compared with the elderly population (described above, section 1.8) AD patients have the same average size of junctional zones but with further decreases in synaptic density and overall contact area (Bertoni-Freddari et al., 2008). Moreover, the atrophy seen in AD correlates significantly with memory impairment. Major contributors to this atrophy are the pathological hallmarks of the disease; senile

plaques (SP) composed of aggregated amyloid-β (Aβ) peptide and neurofibrillary tangles (NFTs) of the cytoskeletal protein tau (Figure 1.4).

Although many cognitive tests such as the Mini-Mental State Examination (MMSE) are routinely used to predict the incidence of AD in life, the disease can only be diagnosed definitively at post-mortem and it is the SP and NFTs that contribute to this diagnosis through Thal and Braak staging respectively (Thal et al., 1997, Braak and Braak, 1991). Both markers have the same pattern of progression with stages 1 and 2 referring to presence in the entorhinal cortex and hippocampus (areas associated with memory formation). Stages 3 and 4 indicate progression to the temporal association cortex and amygdala (areas associated with emotions and personality). The most advanced stages, 5 and 6, include progression to most neocortical areas encompassing the four lobes of the cerebral cortex and therefore correlate with the devastating decline in a patient's ability to function in routine day-to-day tasks.

In order to understand the process of SP production it is important to investigate the cleavage of amyloid precursor protein (APP) (Figure 1.5). The function of APP is unknown. It is a type I membrane protein found on chromosome 21 (Goldgaber et al., 1987).Interestingly, the implications of up-regulated APP are seen in Down's syndrome patients where, due to the trisomy of chromosome 21 there is an increase of APP present. This cohort have a high prevalence of AD at a very early age (Tokuda et al., 1997). Additionally, studies into familial AD (accounting for approximately 5-10 % of AD) have highlighted the importance of correct processing of APP. For example, in a Swedish family a double mutation in the APP gene (APPsw) means that there is a shift in processing of APP towards the amyloidogenic pathway (see below) and therefore neurotoxicity (Citron et al., 1992). There are 3 major isoforms of APP; APP695,

APP751, and APP770 (the number corresponding to the number of amino acid residues). These arise from alternative splicing events. All three isoforms are expressed in both neuronal and non-neuronal cells however there is a high abundance of APP695 in neurones compared with APP751 and APP770 (Haass et al., 1991). The structure of APP is such that it has a large extracellular region, a transmembrane helix and a short cytoplasmic tail. At the N-terminal region APP contains an N-terminal growth factor domain (N-APP), a copper binding domain (CuBD) and APP protease inhibitor domain (APPI). In addition exon 7 includes a Kunitz-type protease inhibitor (KPI) consensus sequence. Full-length APP is 770 amino acid residues however the major neuronal form is only 695 residues and lacks the Kunitz protease inhibitor (KPI) domain. Intriguingly, the level of expression of APP including the KPI domain (KPI-APP) correlates with the number of SP found in AD and the expression of APP695 is reduced in these cases (Zhan et al., 1995).

APP is cleaved in the ectodomain, near the transmembrane domain, by either of the proteases α-secretase or β-secretase (reviewed by Selkoe, 2001). The zinc metalloproteinase, α-secretase, is a member of the disintegrin and metalloprotease (ADAM) family and proteolysis via this enzyme follows the non-neurotoxic non-amyloidogenic pathway. α-secretase cleavage results in release of secretory APP (APPsα) and a C-terminal membrane bound fragment, C83 (α-stub). Intramembrane proteolysis of C83 is carried out by the integral membrane aspartyl protease γ-secretase. γ-secretase is less well characterised but it is known that it consists of the proteins presenilin, nicastrin, APH-1 (anterior pharynx-defective 1), and PEN-2 (presenilin enhancer 2) and it depends on the presence of all four of these proteins to be active. Cleavage of C83 by γ-secretase yields a secretory N-terminal peptide fragment p3 and a short lived C-terminal fragment p7 (CTFγ) which is thought to act as a transcriptional

regulator. There are two iosforms of p3 ($p3_{40}$ and $p3_{42}$) due to the two cleavage sites recognised by γ-secretase. Importantly, the resultant products in the non-amyloidogenic pathway do not contribute to SP formation in AD (Figure 1.5).

Conversely however, β-secretase is the first enzyme in the amyloidogenic pathway which results in formation of Aβ peptide which ultimately aggregate in extracellular SPs (Blennow et al., 2006). β-secretase (beta-site APP cleaving enzyme; BACE) is a novel aspartyl protease. Cleavage of APP by BACE is at a different position to α-secretase and therefore yields an alternative secretory fragment (APPsβ) and a fractionally larger membrane anchored C-terminal segment, C99 (β-stub). Subsequently γ-secretase (as described above) cleaves C99 in the transmembrane domain at either of the two cleavage sites producing Aβ fragments either $Aβ_{40}$ or $Aβ_{42}$ and CTFγ. Both $Aβ_{40}$ and $Aβ_{42}$ are soluble peptides that are secreted from the cells (Figure 1.5). The physiological function of Aβ is thought to be the homeostatic control of neuronal activity, whereby Aβ is secreted in response to neuronal activity to depress excitatory synaptic transmission via AMPA and NMDA receptors (Snyder et al., 2005). $Aβ_{42}$ is a pathogenic peptide that readily forms oligomers. $Aβ_{40}$ does not aggregate alone however it is able to form oligomers with $Aβ_{42}$. In certain disease states Aβ production increases with a shift in $Aβ_{40}$:$Aβ_{42}$ ratio towards increased levels $Aβ_{42}$. The accumulation and oligomerisation of Aβ in the neurons has subsequent, yet subtle, effects on synaptic efficacy. Snyder et al., (2005) investigated the regulation of NMDA receptors and found that Aβ promotes endocytosis, decreasing the phosphorylation of the transcription factor cAMP response element binding protein (CREB) and ultimately decreasing the transcription of target genes promoting neuronal survival (Snyder et al., 2005). As accumulation of Aβ increases, there is gradual extracellular deposition of these oligomers such that aggregates form giving a pattern of diffuse SP. Aggregates of Aβ

are variable, partly helical structures. Aggregation is dependent upon membrane binding, peptide interaction and metal chelation. Furthermore, cations such as copper, iron and zinc are coordinated by 3 histidines and a tyrosine in Aβ inducing a β-sheet-like conformational change and enabling enhanced aggregation (Talmard et al., 2009, Faller, 2009). Downstream effects of such peptide oligomers and depositions are via initiation of pathways such as microglial and astrocytic activation thus causing neuronal injury. It is noteworthy that the toxicity of Aβ is attributed mainly to the Aβ oligomers rather than the more advanced SP depositions. Subsequent effects of Aβ complexes are altered neuronal ionic homeostasis causing oxidative stress, neurotransmitter deficits and triggering the inflammatory response ultimately inducing neuronal dysfunction and atrophy (Selkoe, 2001). The involvement of Aβ in the decline of neuronal function in AD (the amyloid cascade hypothesis) is the leading argument for pathogenesis of this dementia.

The second pathological hallmark of AD is NFTs. These are aggregations of the hyperphosphorylated form of the protein tau. Under normal conditions the physiological role of tau is involvement in the stabilisation of microtubules (Kosik, 1990). Therefore as a consequence, hyperphosphorylation of tau and subsequent aggregation causes disruption of the cytoskeleton of the cell. This contributes to the alteration in cell volume and atrophy. NFTs are thought to be secondary to the increased Aβ production described above. It is hypothesised that the accumulation of Aβ peptide promotes microglial and astrocytic activation which causes neuronal injury and subsequent altering of both kinase and phosphatase activity. The increase in the activity of these enzymes means that the tau protein is uncharacteristically hyperphosphorylated. In this state tau has a gain-of-function that enables it to sequester normal tau in addition to other microtubule associated proteins (MAPs). Ordinarily it is the MAPs that would

compensate for the loss of functional tau, however once these essential proteins are sequestered the microtubule network is destabilised therefore promoting tangle formation (Crouch et al., 2008). One kinase that is particularly prominent in this process is glycogen-synthase kinase-3 (GSK3). GSK3 is active in its non-phosphorylated form and active GSK3 contributes to tau hyperphosphorylation (Ferrer et al., 2002). In addition there is an age related factor regulating GSK3, in that its level of phosphorylation is decreased with age, resulting in an increase in kinase activity (Tomobe et al., 2012). Therefore an increase in age means an increase in the activity of GSK3, thus allowing a larger proportion of tau to be hyperphosphorylated. Furthermore, a link between oxidative stress and hyperphosphorylation of tau has been postulated (Lovell et al., 2004). In AD there are alterations in protein kinase signalling pathways that are known to be sensitive to oxidative stress. These kinases lead to further tau hyperphosphorylation and therefore increase NFT burden. NFT formation enables a feedback loop in that, with the changes described, results in neuronal injury exacerbating the condition.

A link between zinc and AD was eluded to when it was discovered that zinc is a key component of amyloid plaques (Bush et al., 1993). It has also been shown that zinc is implicated in the regulation of APP transcription and enzymes involved in both of its processing pathways (Grilli et al., 1995, Izumi et al., 1992). Furthermore, ZnT dysregulation is evident for more than one transporter in AD pathology (Zhang et al., 2008). These findings imply an important role for dyshomeostasis of zinc in AD.

1.9.1 *APP, Aβ, NFTs and the role of zinc*

The transcription of APP is regulated by the zinc-dependent transcription factors Sp1 and NF-κB (Grilli et al., 1995, Izumi et al., 1992). The promoter of APP contains two

NF-κB binding sites in its regulatory region (Quitschke, 1994). When activated, NF-κB binding significantly up-regulates APP transcription (Grilli et al., 1995). Similarly, Sp1 is able to bind to the positive regulatory region of the APP promoter and up-regulate transcription of the gene (Izumi et al., 1992). It is also noteworthy that Aβ itself can trigger downstream activation of NF-κB, in turn increasing APP transcription and ultimately increasing Aβ accumulation (Kaltschmidt et al., 1997).

As discussed in section 1.9, APP is processed via either the non-amyloidogenic or the amyloidogenic pathway (producing fragment p3 or Aβ, respectively). Zinc has a detrimental effect on both of these pathways. APP has a zinc binding site and when zinc is bound it subsequently inhibits proteolytic cleavage by α-secretase (non-amyloidogenic pathway) as well as inhibiting APP degradation, thus further APP is available for conversion to Aβ by BACE (amyloidogenic pathway) (Bush et al., 1993). In addition, soluble forms of Aβ peptides are degraded by the matrix metalloproteinase-2 (MMP-2) under normal conditions. MMPs depend on the presence of zinc at their catalytic site in order to be active therefore alteration in zinc status could further exacerbate the condition by the reduction of Aβ degradation (Baramova and Foidart, 1995).

Zinc is able to promote formation of Aβ oligomers and aggregates at physiological concentrations available in the brain by binding Aβ at 3 N-terminal histidine residues. It is evident that these intermediate Aβ oligomers are the most toxic form of Aβ and indeed that it is these oligomers that are required for the Aβ mediated inhibition of synaptic transmission. Interestingly, rodents do not present with AD pathology under physiological conditions (Bush et al., 1994). One explanation for this is that in rodent Aβ there are three amino acid substitutions that alter one of the crucial bridging

histidines. Logically, the disruption of zinc binding to Aβ has been explored as a therapeutic target. Initially the chelating agent EDTA showed a disruption of the Aβ-metal interaction, therefore reducing aggregation. Subsequently, CQ, a moderate metal chelating agent capable of crossing the blood-brain barrier, was administered initially to an AD transgenic (Tg) mouse model. These mice showed a decrease in SP burden by 49 % (Cherny et al., 2001). Furthermore, it is hypothesised that the beneficial effects of CQ on Aβ are two-fold. In addition to preventing zinc-Aβ aggregates ZnCQ complexes were found to activate Aβ-degrading MMPs. The proposed mode of action is that CQ delivers bound zinc to the cell which activates the phosphoinositol-3 kinase pathway resulting in the up-regulation of MMPs (Cherny et al., 2001, Crouch et al., 2008).

Aside from its effects on Aβ, CQ was used to demonstrate the effect of zinc on GSK3 and therefore NFT formation. In agreement with the positive effects seen for the ZnCQ complex on Aβ burden, in this instance ZnCQ complexes were found to increase phosphorylation of GSK3, therefore decreasing tau phosphorylation and NFT formation (White et al., 2006).

In humans the results for CQ were positive where it reached Phase 2 clinical trials. However due to the controversy over the efficacy of the drug, more recently a CQ derivative, PBT2 is being tested for its therapeutic uses in AD (Lannfelt et al., 2008).

1.9.2 *ZnT dysregulation in AD*

The research into ZnT expression in AD is of particular importance given the possible role of zinc in AD pathology. Zhang et al., (2008) found that at the protein level Znt1, Znt3, Znt4, Znt6 and Znt7 showed a significant increase in the hippocampus and neocortex of APP/PS1 transgenic mice. The largest increase in expression was for Znt3, particularly relevant due to its role in neurotransmission. Znt5 showed an increase that

was not significant. Furthermore, the SPs from these mouse models were tested by immunoreactions to ascertain whether there is expression of Znts within these aggregates. Intriguingly there was a distinct expression pattern evident with Znt1 and Znt4 found throughout the SPs whereas Znt3, Znt5 and Znt6 were in peripheral regions and Znt7 predominantly in the core (Zhang et al., 2008).

Human studies of ZnT dysregulation in AD have corroborated the mouse model results, however they have also highlighted an important factor in disease progression. The decline in multiple cognitive functions in the progression of AD is thought to begin with an interim stage labelled mild cognitive impairment (MCI) with only 5 % of these patients remaining stable i.e. not developing dementia. In addition, there is a condition which is described as preclinical AD (PCAD). In this case the patient does not have any overt clinical manifestations of AD but does have significant AD pathology at post-mortem (Galvin et al., 2005). There are differences in ZnT expression profiles between AD and the precursor states in the ZnTs tested. For example in both MCI and PCAD ZnT1 expression is significantly lower than controls (Lovell et al., 2005, Lyubartseva et al., 2009) however ZnT1 has been found to be up-regulated in the human AD brain (Beyer et al., 2012). It is hypothesised that down-regulation in MCI and PCAD leads to an increase in intracellular zinc. The effect of this is thought to be two-fold in that an increase in intracellular zinc means more available zinc to bind to both APP and Aβ in order to exacerbate disease progression as well as the presence of zinc itself being able to up-regulate ZnT1 transporter expression as a compensatory mechanism. The increase of ZnT1 evident in AD brain tissue is thought to cause an increase in zinc ions available in the extracellular space for initiation of Aβ deposition and SP formation. Interestingly, in terms of the nutritional status of the elderly which is known to be deficient in zinc (Fairweather-Tait et al., 2008), it is perhaps note-worthy that mice fed a zinc deficient

diet had a decrease in Znt1 expression (Dong et al., 2008). These are important aspects of research that have not been fully explored.

Research into ZnT4 and ZnT6 has also emphasised the need for more understanding of ZnT regulation in the disease state. ZnT4 and ZnT6 have also been implicated in AD progression, with elevated protein levels of both transporters in the hippocampus of AD patients (Smith et al., 2006). ZnT6 is located in the Golgi apparatus and therefore it has been hypothesised that the increase in levels of this transporter in AD results in an increase in zinc in this organelle. The importance of this is related to the localisation of both APP and the enzymes that metabolise APP, which are found in the Golgi apparatus. Therefore, the accumulation of zinc could subsequently promote Aβ formation by binding to APP and inhibiting α-secretase (Lyubartseva et al., 2009). ZnT4 is found in the lysosomal and endosomal compartments in hippocampal tissue and similarly an increase in ZnT4 transporter expression would be expected to enable the sequestration of zinc into these compartments. This is evident further by reports of Aβ accumulation in this system in the post-mortem AD brain (Takahashi et al., 2002). Interestingly, researchers have found that there is a positive correlation between Braak score (NFT pathology) and ZnT1 levels that is significant such that ZnT1 increases with an increase in Braak score. A trend towards significance was also revealed for ZnT6 (Lovell et al., 2005, Lyubartseva et al., 2009).

For research into the implications of zinc in AD it is intriguing that ZnT3 has been found to be localised predominantly in the membranes of zinc-rich synaptic vesicles in the hippocampus (Palmiter and Huang, 2004). As discussed above, synaptic zinc has been shown to facilitate the precipitation of Aβ. Furthermore, Znt3 knockout mice are devoid of zinc in these zinc-enriched terminals. In the transgenic mouse model of AD,

tg2576, there is an over-expression of the Swedish mutated human form of APP. It is interesting to note that there is an age-dependent hyperactivity of the Znt3 protein in the female Tg2576 mouse model when compared to the male Tg2576 mice which is abolished in the Znt3 knockout mouse (Lee et al., 2002). This is particularly relevant with AD being more prevalent in the female population. Indeed, in the AD Tg2576 mouse model, ablation of Znt3 inhibits the production of Aβ pathology. The translation of research into ZnT3 in humans however, reveals some discrepancies between species. The expression of ZnT3 appears to be decreased in the cortical regions of human AD patients (Beyer et al., 2009, Adlard et al., 2010) which is in contrast to the increase found in mouse models (Zhang et al., 2008).

It follows that further understanding of the ZnT family and their interactions may elucidate a role for ZnTs and zinc in the progression and pathology of AD.

1.9.3 *Genes in AD*

Familial AD accounts for approximately 5-10 % of AD. Studies of these cases have highlighted a few genes that are implicated in the disease. For example, chromosome 19 hosts a coding sequence (Apolipoprotein E, APOE) which can be linked to familial AD (Strittmatter et al., 1993). In this instance the frequency of the specific allele ε4 is increased in AD sufferers and for those people who are homozygous for the ε4 allele the age of onset is earlier than those with either ε2 or ε3 alleles (Corder et al., 1993). There are many hypotheses for these observations however there are no conclusive data for the association. In addition, Presenilin 1 (PS1) is located on chromosome 14 (Sherrington et al., 1995) and this gene has a homologue on chromosome 1 known as Presenilin 2 (PS2). Presenilin is part of the larger γ-secretase complex that is known to cleave APP in the transmembrane domain (Brown et al., 2000). The presence of either PS1 or PS2 is

essential for γ-secretase activity (Figure 1.5) and mutations give an increase in $A\beta_{42}$ production (Citron et al., 1997). Mutations at the N-terminal of this gene have been implicated in familial AD (Berezovska et al., 2005).

Interestingly, it has been shown that there are different splice variants that are more prevalent in sporadic AD. Alternative splicing of the N-terminal region of PS1 results in either the presence or absence of four amino-acids. It is thought that the addition of these amino acids means the addition of a potential phosphorylation site and thus functional differences between the isoforms. It is hypothesised that these may play a role in the pathogenesis of AD (Scheper et al., 2004). Moreover, Presenilin 2 has a truncated variant (PS2V) and the protein levels of this variant are significantly increased in the cortex of AD patients (Smith et al., 2004) which supports previous work that found that this splice variant was generated in hypoxic neuroblastoma cells (Sato et al., 1999). Also it has been shown that aluminium accelerates and enhances production of this isoform (Matsuzaki et al., 2004) and it follows that other metals could have an effect in disease aetiology.

Another gene of interest encodes the enzyme β-secretase (BACE). This is known to be involved in the amyloidogenic pathway (Figure 1.5). BACE1 is a type I transmembrane aspartic proteinase found on chromosome 11 and it has a homolog BACE2 on chromosome 21; however, BACE2 is only expressed at low levels in neurones and does not have the same cleavage activity as BACE1 with regards to APP (Vassar et al., 2009). Moreover, Aβ production correlates positively with BACE1 activity and both protein expression and activity of BACE1 are increased in the frontal cortex of human post mortem AD brain tissue. In contrast BACE2 activity was not altered in AD and there was no correlation with its activity to Aβ production (Ahmed et al., 2010). In

BACE1 knockout mice there is an absence of Aβ production and, although these mice appear healthy, there is evidence that there is a reduced myelination and some cognitive deficits. BACE1 does have four known splice variants and, similarly to PS, the enzymatic activity of the alternative splice variants differs (Mowrer and Wolfe, 2008). There are nine exons in the BACE1 gene and normal processing results in the full-length active protein of 501 amino acids (BACE 501) from the normal 5' splice site of exon 3 in combination with the normal 3' splice site of exon 4 (Figure 1.6). There is an alternative 5' splice site within exon 3 as well as an alternative 3' splice site within exon 4. Combinations of the use of these yield the various isoforms. The next largest isoform contains 476 amino acids (BACE 476), this results from use of the normal 5' splice site in exon 3 with the use of alternative 3' splice site in exon 4 giving rise to the in-frame deletion of 75 base pairs. Similarly, an in-frame deletion of 132 base pairs is evident for the isoform BACE 457 (457 amino acids). In this case the alternative splice site is the 5' splice site of exon 3 in combination with the normal 3' splice site in exon 4. It follows that the final splice variant results from the use of both alternative splice sites (5' alternative splice site of exon 3 in combination with the 3' alternative splice site of exon 4) yielding the isoform that is an in-frame deletion of 207 base pairs, BACE 432. BACE 501 is the isoform that is expressed at the highest levels in AD and the other isoforms are expressed at relatively low levels with a decrease in expression correlating to size (i.e. BACE 476 > BACE 457 > BACE 432). Investigations into the expression profiles have found that there is no significant difference in the splicing pattern between the cerebellum, frontal lobe and hippocampus. Importantly however, the activity of the alternatively spliced isoforms is considerably reduced compared with BACE 501. The difference in activity is attributed to the conformational change and its effect on the catalytic site. The important active aspartates site lie within exons 2 and 6 and therefore

the alternative splicing between these residues will alter the final folding of the protein and presumably, the access of substrates to the active site. Furthermore, influencing the splicing events in favour of the alternatively spliced isoforms (i.e. decreasing BACE 501 but increasing BACE 476, 457 and 432 to varying degrees) reduces the production of Aβ in cell line models without having an overall effect on total BACE1 expression thereby supporting the argument that BACE 501 is the main contributor to Aβ production (Mowrer and Wolfe, 2008). In the tg2576 mouse model of AD it has been shown that there is no change in the mRNA level of BACE1 within the brain. Despite this, there is increase enzymatic activity of BACE1 within these brains. The rise in activity is attributed to an increase in expression of the largest isoform BACE 501 (Zohar et al., 2005). This has led to the proposal that BACE1 protein expression and activity increases in AD brains despite the mRNA levels remaining the same in both transgenic mice models (Zohar et al., 2005) and AD patients (Holsinger et al., 2002, Fukumoto et al., 2002).

Metals have been implicated in expression and activity of BACE1. The focus of much research has been on copper, due to the presence of a 24-residue peptide in BACE1 C-terminal that contains cysteine residues able to bind single copper atom with high affinity. In addition, BACE1 interacts with the copper chaperone for superoxide dismutase-1 (SOD-1) such that when BACE1 is over-expressed in CHO cells SOD-1 activity is reduced (Angeletti et al., 2005, Dingwall, 2007). Furthermore, copper and manganese increase the expression of BACE1 in rat adrenal medulla cells (PC12), conversely, zinc, iron and aluminium do not (Lin et al., 2008). It is note-worthy that there are discrepancies in the literature for BACE1 expression levels but that the majority of work focuses predominantly on total BACE1 rather than extrapolating for the isoform differences. Investigation into the splicing events of these isoforms is

incomplete and further studies of this and the potential role of metals within these may elucidate pathways implicated in AD pathogenesis.

Overall zinc seems to be implicated in the AD disease process - whether it is metal dyshomeostasis that causes these irregularities or vice versa remains to be determined. This research is important in order to increase our knowledge and work towards finding a solution to this devastating disease.

1.10 Human intestinal epithelial cell line Caco-2

Caco-2 cells were originally isolated from a primary colonic tumour in a 72-year-old Caucasian male. These cells are widely used as an intestinal epithelial cell line model following the observations of Hidalgo IJ et al., (1989). It was found that when Caco-2 cells are grown on plastic dishes or nitrocellulose filters they develop the characteristics of normal enterocytes. For example the cell layers are morphologically polar and have well-developed brush borders at their apical surface. Furthermore, this differentiation to form a monolayer with microvilli and tight junction formation is evident when grown on Transwell polycarbonate membranes enabling many subsequent studies to exploit the transport functionality to use them as a model system for intestinal epithelial transport (Hidalgo et al., 1989). In addition, the formation of these relevant layers means that proteins, such as transporters, are distributed in their physiologically appropriate positions (reviewed by Ho et al., 2002, Raffaniello et al., 1992).

Limitations are evident for this cell line and inherent variability between batches of Caco-2 cells must be monitored. Therefore culture conditions must be regulated and careful observation of characteristics and passage number is required. Caco-2 cells have some subtle differences to native enterocytes in that there are alternations in the synthesis and expression levels of certain transporters found *in vivo*. For example, the

glycoprotein apoB-100 is found in the cell line opposed to the shorter apo-48 version evident in the intestine and there are lower levels of intestinal fatty acid binding protein than in the human body (Ho et al., 2002). Despite these differences they do however provide a simple cell model that enable collection of data on transporter studies without the use of animal models and without interspecies correlation because they are of human origin. Thus they enable studies of specific genes in terms of absorption, metabolism and gene and protein regulation in order to provide detailed information on nutrient interactions (Ho et al., 2002).

1.11 Human neuroblastoma cell line SH-SY5Y

In 1970 the SN-K-SH cell line was cloned from a metastatic neuroblastoma cell in a four-year old female. SH-SY5Y cells are thrice cloned derivative of these SN-K-SH cells that are genetically female and since the early 1980's have been used as a neuronal cell line model. SH-SY5Y cells possess a number of both biochemical and functional properties of neurons that enable them to carry out this role (Biedler et al., 1973). For example, SH-SY5Y cells act like neuronal cells in that they can convert glutamate to the neurotransmitter GABA, they express neurofilament proteins and nerve growth factor receptors. Importantly, SH-SY5Y cells are capable of proliferating under standard cell culture conditions (Ciccarone et al., 1989). Interestingly, they are also able to differentiate like stem cells when induced with retinoic acid (RA) and brain derived neurotrophic factor (BDNF) (Singh and Kaur, 2007, Cernaianu et al., 2008).

As with all cell line models, there are limitations to this cell model in that there are inherent variability between batches of SH-SY5Y cells that must be monitored. Therefore culture conditions must be regulated and careful observation of characteristics and passage number is required. Again, there are differences between SH-SY5Y as a

neuronal cell line and native neurons. For example the expression levels and distribution of markers used for mature neurons namely, but not exclusively, β-III tubulin; a marker for differentiation and decreased proliferation (Katsetos et al., 2003) and synaptic vesicle protein (Sv2); a marker for synapses different in SH-SY5Y cells to native neurons (Vautrin, 2009). Although SH-SY5Y cells are widely used to investigate AD (Agholme et al., 2010), the tau protein differs in expression in the cell line opposed to the adult human brain. In the cell line only the foetal isoform of tau is present (Uberti et al., 1997). Not only do expression levels and localisation of this isoform differ between the adult human brain and the cultured cells but it also doesn't form NFTs despite being heavily phosphorylated (Alonso et al., 2001). With these limitations taken into account however, numerous neurological studies have used the SH-SY5Y cell line effectively to study neuronal processes such as differentiation and metabolism in addition to pathways involved in neurodegenerative diseases.

1.12 Aims and Objectives

Prior to 2012 the only information regarding the zinc transporter ZnT10 was *in silico* data that predicted its expression to be restricted to foetal tissue only (Seve et al., 2004) Therefore the primary aim of the work described herein was to characterise ZnT10. The objectives for this were to:

1. Study the expression profile and subcellular localisation of ZnT10

   Both semi-quantitative RT-PCR and quantitative real-time PCR (RT-qPCR) were used to establish the expression pattern of ZnT10 in adult human tissues. Immunohistochemical detection of a FLAG-tagged construct was carried out to establish the subcellular localisation patterns in SH-SY5Y cells.

2. Characterise the functional and regulatory properties of ZnT10 in response to metals

   To indirectly determine the transport activity of the transporter using a reporter gene assay experiment. To determine the expression of ZnT10 in response to extracellular metal treatments using both semi-quantitative RT-PCR and RT-qPCR in SH-SY5Y and Caco-2 cell lines.

3. To investigate the ZnT10 putative promoter response to zinc

   The Caco-2 cell line was used as a model system for reporter gene assays to examine the regulation of the *ZnT10* gene at the promoter level.

4. To further research the area of ZnT dysregulation and the role of zinc in AD

   RT-qPCR was used to explore possible involvement of ZnT10 in AD in both human and transgenic (Tg) mouse tissue. In addition to investigate the influence of extracellular zinc on the BACE1 splice variants in the SH-SY5Y cell model.

Biological Process	Function of Zinc	Reference
DNA and protein synthesis	Zinc is a cofactor for many enzymes including, DNA polymerase, RNA polymerase and reverse transcriptase. DNA-binding zinc finger proteins promote gene transcription by enhancing DNA-protein binding.	(Truong-Tran et al., 2001; Vallee et al., 1981)
Gene Expression	A variety of mechanisms for the zinc sensitive transcriptional regulation of genes have been characterised in a number of different organisms. In mammals the best characterised mechanism is the up-regulation of genes in response to elevated zinc-often mediated by the transcriptional factor MTF-1 to an MRE within a gene regulatory region.	(Heuchel et al., 1994; Langmade et al., 2000; Lichtlen et al., 2001; Wang et al., 2004)
Bone Metabolism	Zinc stimulates osteoblast formation and inhibits osteoclast formation. Zinc deficiency retards bone growth. Osteoporotic women excrete higher concentrations of urinary zinc.	(Herzberg et al., 1990; Kishi and Yamaguchi, 1994; Oner et al., 1984; Yamaguchi and Hashizume, 1994)
Inflammation	Metallothioneins release zinc in response to inflammatory exposure to stimulate the activity of a number of antioxidants therefore reducing oxidative damage.	(Frazzini et al., 2006; Mocchegiani et al., 2006)
Immunity	Zinc deficiency is associated with impaired immune response. AE is characterised by a decrease in immune function and increased susceptibility to fungal, bacterial and viral infections.	(Hasse and Rink, 2009; Prasad, 2000)
Enzymes	Over 300 enzymes including members from all six enzyme classes have been identified with require zinc for their function.	(Vallee and Falchuk, 1993)
Signalling	Release of zinc during neurotransmisson along with glutamate. Influence cellular machinery such as protein tyrosine kinases, protein kinases CK2 and tight junction proteins.	(Frederickson and Bush, 2001; Hogstrand et al., 2003; Hogstrand et al., 2009; Taylor et al., 2012; Finamore et al., 2008)

Table 1.1 Examples of the biological functions of zinc. AE – acrodermatitis enteropathica, MRE – Metal Responsive Element, MTF-1 - Metal Responsive Element binding transcription factor. (adapted from Coneyworth; PhD thesis, 2009)

Tissue	Zinc Concentrate (µg/g wet weight)	Percent of total body zinc
Skeletal Muscle	51	57
Bone	100	29
Skin	32	6
Liver	58	5
Brain	11	1.5
Kidneys	55	0.7
Heart	23	0.4
Hair	150	-0.1
Blood Plasma	1	-0.1

Table 1.2 Distribution of zinc within the body Example is for a normal adult man (70 kg) (adapted from King et al., 2000)

Age	LRNI	EAR	RNI
0-3 months	2.6	3.3	4.0
4-6 months	2.6	3.3	4.0
7-12 months	3.0	3.8	5.0
1-3 years	3.0	3.8	5.0
4-6 years	4.0	5.0	6.5
7-10 years	4.0	5.4	7.0
Males			
11-14 years	5.3	7.0	9.0
15-18 years	5.5	7.3	9.5
19-50+ years	5.5	7.3	9.5
Females			
11-14 years	5.3	7.0	9.0
15-18 years	4.0	5.5	7.0
19-50+ years	4.0	5.5	7.0
Pregnancy	*	*	*
Lactation			
0-4 months			+6.0
4+ months			+2.5

Table 1.3 UK Dietary reference values for zinc (mg/kg). * No increment. (The National Diet and Nutrition Survey, 2003)

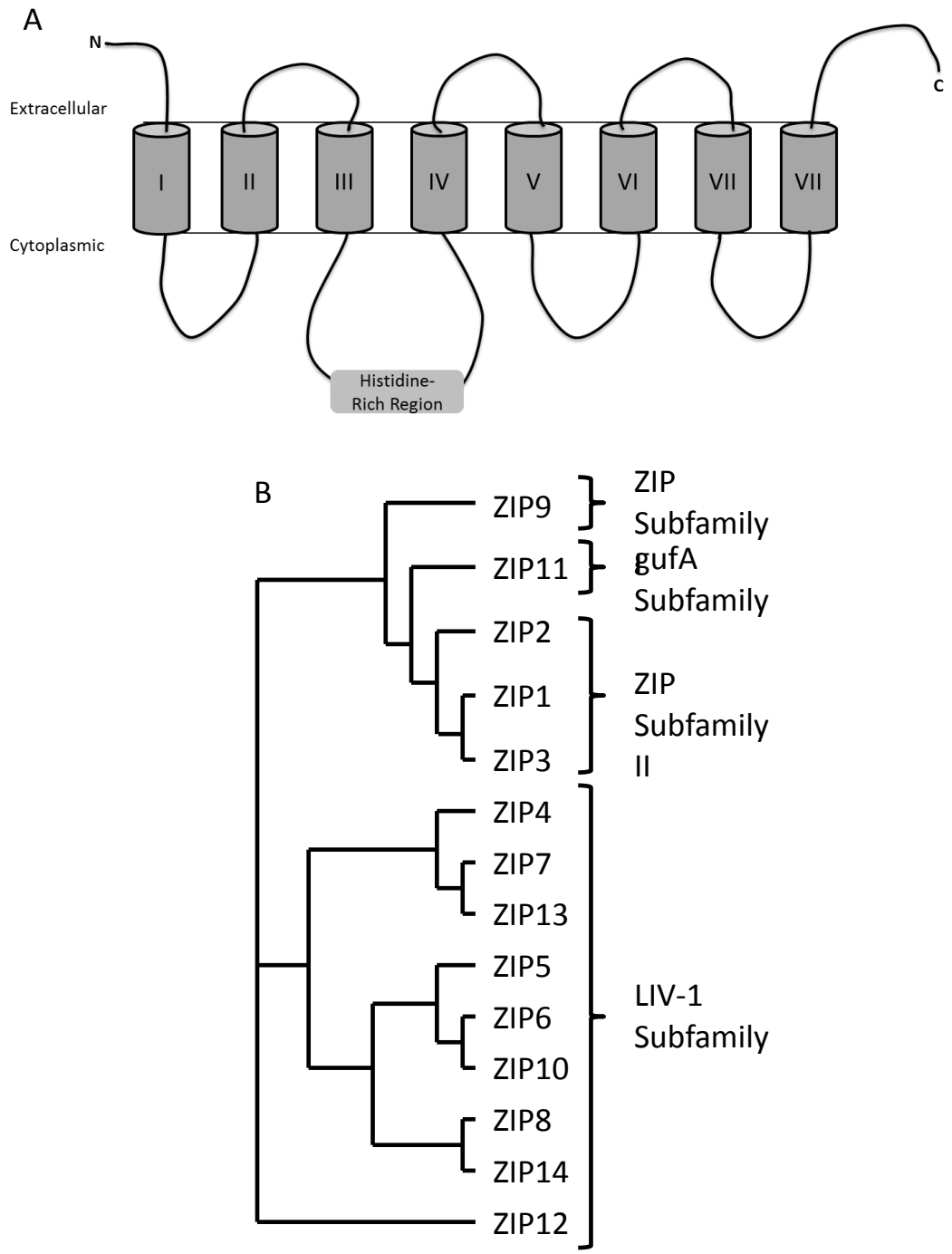

Figure 1.1 Predicted topology and arrangement of the ZIP family members. **A**. The conserved structure of ZIP proteins is eight transmembrane domains (TMD) with extracellular N- and C- termini. The histidine rich region is thought to reside in the cytoplasm between TMD III and IV. **B.** Phylogenetic tree of the human members of the ZIP transporter family, with sub-classes of the ZIP transporters highlighted (adapted from Taylor et al., 2007).

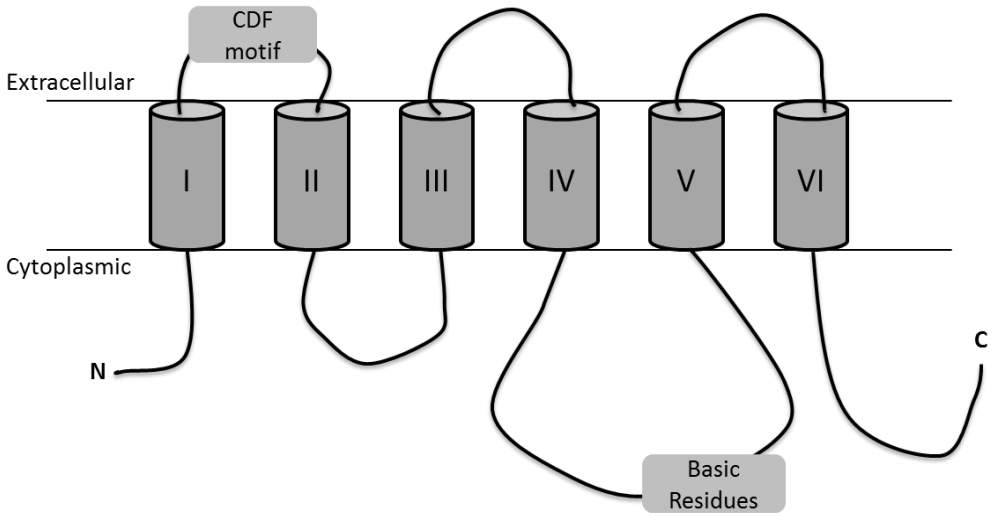

Figure 1.2 Predicted topology of the ZnT family members. Most family members contain 6 TMD with an intracellular N- and C-termini. The conserved CDF motif is extracellular and between TMD I and II. There is a conserved cytoplasmic basic residue region between TMD IV and V.

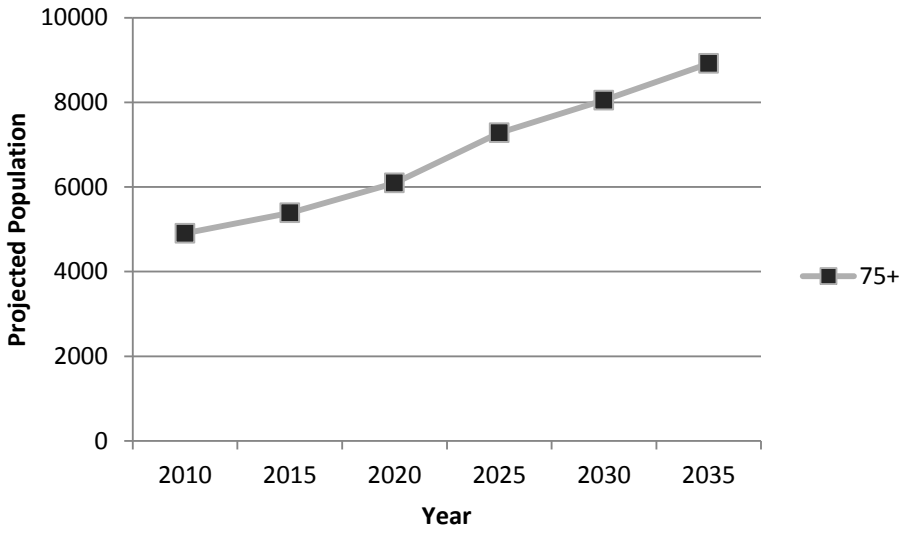

Figure 1.3 Projected UK population demographics for people over 75. Data sourced from Office of National Statistics, National Population projections 2010-based (http://www.ons.gov.uk/ons/publications/re-reference-tables.html?edition=tcm%3A77-229866)

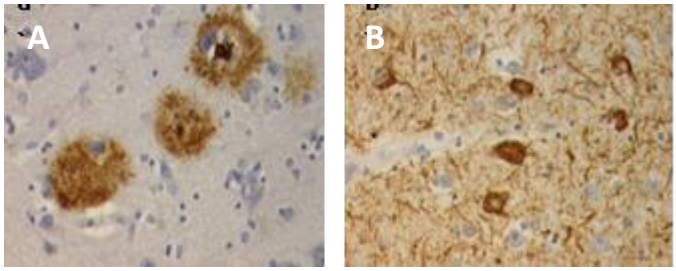

Figure 1.4 Pathological hallmarks of AD. Section of brain tissue stained with: **A.** anti-amyloid beta antibody; SP, aggregates of Aβ peptides shown in brown **B.** Anti-tau antibody; NFTs, tangles of the microtubule protein tau, shown in brown. Brain sections from the Newcastle Brain Tissue Resource (Newcastle, UK).

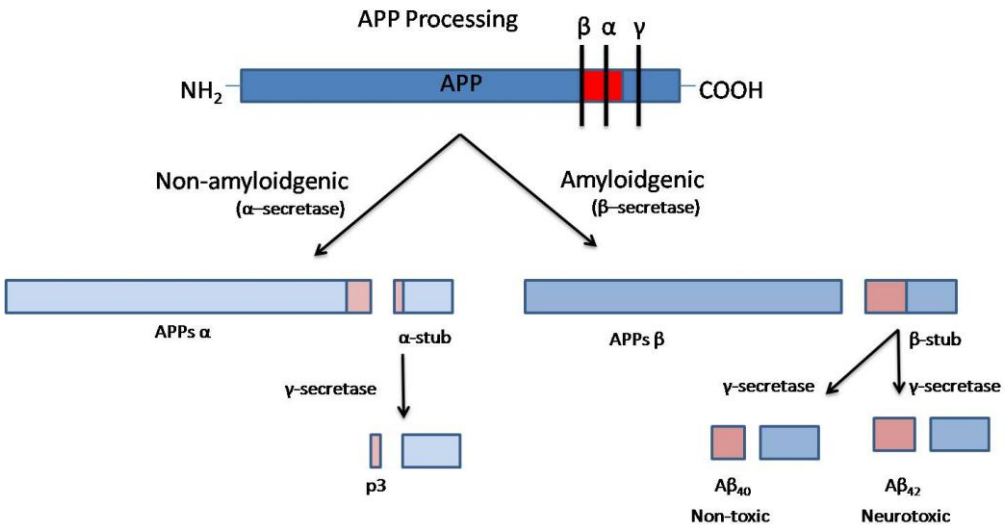

Figure 1.5 Processing of APP; amyloidgenic and non-amyloidgenic pathways. APP is cleaved in the ectodomain, near the TMD. Proteolysis via α-secretase follows the non-neurotoxic non-amyloidogenic pathway. α-secretase cleavage results in release of secretory APP (APPsα) and a C-terminal membrane bound fragment, C83 (α-stub). Intramembrane proteolysis of C83 is carried out by the integral membrane aspartyl protease γ-secretase, yielding a secretory N-terminal peptide fragment p3. The resultant products in the non-amyloidogenic pathway do not contribute to SP formation in AD. Cleavage of APP by β-secretase (BACE) is the first step in the amyloidogenic pathway yielding the secretory fragment APPsβ, and membrane anchored C-terminal segment, C99 (β-stub). Subsequently γ-secretase cleaves C99 in the TMD at either of the two cleavage sites producing Aβ fragments either $A\beta_{40}$ or $A\beta_{42}$ which aggregate in extracellular SPs.

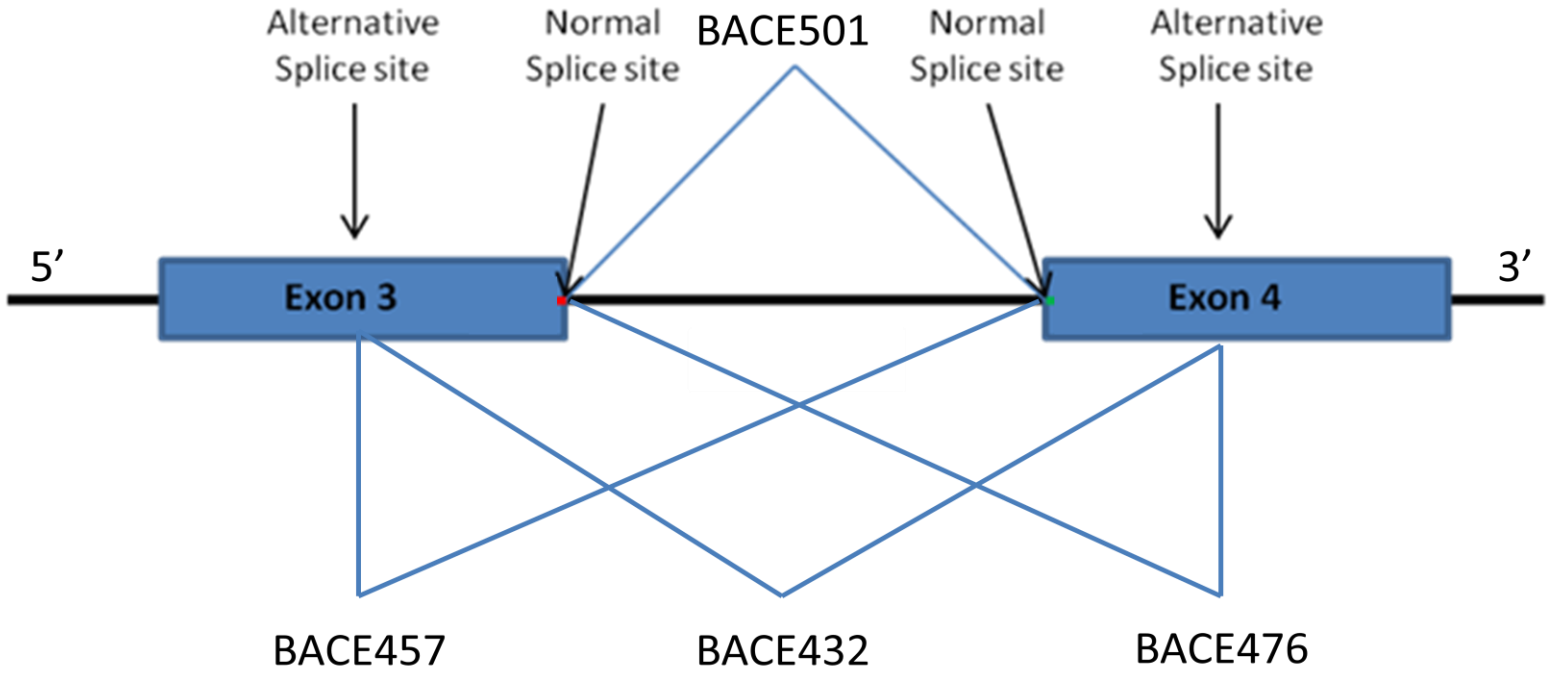

Figure 1.6 Schematic of the BACE1 splice variants. The full-length active protein of 501 amino acids (BACE 501) from the normal 5' splice site of exon 3 in combination with the normal 3' splice site of exon 4. The next largest isoform is 476 amino acids (BACE 476), this results from use of the normal 5' splice site in exon 3 but the alternative 3' splice site in exon 4 giving rise to the in-frame deletion of 75 base pairs. An in-frame deletion of 132 base pairs is evident for the isoform BACE 457 (457 amino acids). In this case the alternative splice site is the 5' splice site of exon 3 in combination with the normal 3' splice site in exon 4. The final splice variant results from the use of both alternative splice sites (5' alternative splice site of exon 3 in combination with the 3' alternative splice site of exon 4) yielding the isoform that is an in-frame deletion of 207 base pairs, BACE 432 (adapted from Mowrer and Wolfe, 2008).

Chapter 2: Materials and Methods

2.1 Tissue culture techniques

2.1.1 *Culture of mammalian cells*

Aseptic techniques were used to culture all mammalian cells used. Procedures were carried out in a class II laminar flow hood and all reagents were purchased sterile. A high temperature and pressure autoclave was used to ensure that reusable consumables were sterile. Routinely cells were cultured in basal media (Sigma) in 75 cm^3 flasks (Greiner) in an environment of 5 % CO_2/ 95 % air at 37 °C unless otherwise stated. All reagents were purchased from Sigma unless otherwise stated.

2.1.2 *Growth and maintenance of cultured cells*

Caco-2 and SH-SY5Y cells were propagated in basal media; Dulbecco-Modified Eagles Medium (DMEM) with 4.5 g/L glucose, 0.11 g/L sodium pyruvate and 0.11 g/L L-glutamine supplemented with 10 % (v/v) foetal calf serum. Cells were assessed using light microscopy and once confluent were passaged (usually every 4-5 days) in an appropriate ratio (Caco-2 cells; 1:4, SH-SY5Y cells; 1:9). In order to passage growth media was discarded and the cells were washed in sterile phosphate buffered saline (PBS: 137 mM $NaCl_2$, 2.7 mM KCl, 4.3 mM $Na_2HPO_4.7H_2O$, 1.4 mM KH_2PO_4, pH 7.3). To detach cells from the flask, cells were incubated in 3 mL x 90 trypsin-EDTA at 37 °C for 5-10 minutes. The trypsin was neutralized by adding 7 mL of the above culture medium. Cells were then reseeded into sterile flasks (Caco-2 cells; 1:5, SH-SY5Y cells; 1:10).

2.1.3 *Transient transfection of cultured cells*

Cultured cells were seeded into well plates at the relevant density (24 well plate; 175,000 cells per well in 0.5 mL culture medium, 12 well plate; 350,000 cells per well in 1 mL culture medium and 6 well plate; 700,000 cells per well in 2 mL culture medium). Transfection mixes were prepared by incubating Opti-MEM® I Reduced-Serum Medium (Invitrogen) and the transfection reagent GeneJammer (Stratagene Europe, Netherlands; Caco-2 cells) or Lipofectamine 2000 (Invitrogen; SH-SY5Y cells) at room temperature for 3-5 min. The volumes were well plate dependent: 24 well plate; 25 µL Optimem and 1 µL transfection reagent, 12 well plate; 50 µL Optimem and 2.5 µL transfection reagent and 6 well plate; 125 µL Optimem and 2.5 µL transfection reagent. Appropriate plasmid DNA was then added to the mix in the appropriate proportions: 24 well plate; 0.5 µg DNA, 12 well plate; 1 µg DNA and 6 well plate; 2.5 µg DNA and mixes were incubated for 30-45 min at room temperature. Culture medium was removed from the cells and replaced with half the well volume of DMEM without FBS (24 well plate; 0.25 mL medium, 12 well plate; 0.5 mL medium and 6 well plate; 1 mL medium). Transfection mixes were added drop-wise to each well and cells were incubated at 37 °C (5 % CO_2 in air) for 3 hours before the addition of the DMEM with 20 % FBS to reach the final well volume. Cells were incubated for 24 hours at 37 °C (5 % CO_2 in air) before treatments.

2.1.4 *Treatment of cultured cells*

Twenty four hours post-transfection, seeding medium was replaced with culture medium containing the appropriate treatment. Cells were incubated with treatment medium in the presence of 10 % FBS for a further 24 hours unless otherwise stated. RNA, DNA and protein were extracted as described in sections 2.4. Reporter gene assays were carried out as per section 2.7.1.

2.1.4.1 Metal Treatments

For zinc treatments of cultured cells, $ZnCl_2$ was added to the medium at concentrations of 50 µM, 100 µM and 150 µM. The concentration of basal culture medium containing 10 % FBS is 3 µM Zn^{2+} (Cragg et al., 2002). For cobalt and nickel 100 µM of the relevant chloride was added to the medium. For copper 100 µM $CuSO_4$ was added to the medium.

2.1.4.2 Angiotensin II, Lipopolysaccharide and tert-Butyl hydroperoxide

Human angiotensin II (Ang II) (Sigma; A9525) and *E. coli* Lipopolysaccharide (LPS) (Sigma; L 2630) were added to the medium in the absence of FBS at final concentrations of 0.1 µM and 100 ng/ mL respectively. Tert-Butyl hydroperoxide (tBHP) (Aldrich; 19997) was added to the medium in the presence of 10 % FBS for 40 min at a final concentration of 0.025 mM and then this was replaced with medium containing 10 % FBS for the remainder of the incubation period.

2.1.5 *Cell viability assay*

To assess the viability of the cells alamarBlue® (Invitrogen) was used according to the manufacturer's instructions: briefly, alamarBlue® measures the amount of reduction of resazurin to resorufin by respiring, viable cells. AlamarBlue® was added to the cell medium at a volume of 10 % of the total well volume 3 hours prior to reading. Absorbance values were taken at 570 and 600 nm. Calculated as a percentage, viability was assessed as a ratio of oxidised:reduced alamarBlue®.

2.2 Transgenic mouse brain samples

Frontal cortex brain tissue samples were obtained from 12 month old female wild-type (WT) (n = 5) and APP/PS1 mice (n = 11) (supplied by Dr Paul Adlard, The University of Melbourne). Brain samples were removed and snap frozen before being stored in

RNA Later at -80 °C. Samples were shipped in RNA Later on dry ice and on receipt brain samples were ground using liquid nitrogen. RNA was extracted using Trizol as described in section 2.4.

2.3 Human brain bank samples

Frontal cortex RNA samples from human Alzheimer's disease pathology cases (n = 13; female n = 8, male n = 5) and age-matched controls (n = 10; female n = 3, male n = 7) (Appendix I) were supplied by the Newcastle Brain Tissue Resource (Newcastle, UK).

2.4 RNA, DNA and protein extraction

2.4.1 *Simultaneous RNA/DNA and Protein Extraction from cells and tissues*

RNA, genomic DNA and protein were all extracted from cell and/or tissues using TRIzol® Reagent (Invitrogen). Tissues were homogenised in 1 mL TRIzol® reagent per 50-100 mg tissue and incubated for 5 min at room temperature. Subsequent volumes are relative to 1 mL TRIzol® reagent. A volume of 0.2 mL of chloroform was added and samples were shaken by hand for 15 seconds. Samples were incubated at room temperature for 2-3 min before centrifugation at 12,000 x g for 15 min at 2-8 °C in order to complete phase separation.

2.4.1.1 RNA Extraction

The top aqueous phase was transferred to a fresh tube and the RNA was precipitated by adding 0.5 mL of isopropyl alcohol. Samples were incubated at room temperature for 10 min and centrifuged at 12,000 x g for 10 min at 2-8 °C. Supernatant was discarded and the pellet washed in 1 mL 75 % ethanol and centrifuged at 7500 x g for 5 min at 2-8 °C. Supernatant was discarded and the RNA pellet was air dried for approximately 5 min and re-dissolved in RNase-free water (approximately 20 µL). Concentration of RNA

was determined by measuring the absorbance on a Nano drop, A260/ A280 ratios were taken and samples were stored at -80 °C.

2.4.1.2 DNA Extraction

The DNA was precipitated from the interphase and organic phase with 0.3 mL 100 % ethanol and mixing by inversion. Samples are incubated for 2-3 min at room temperature before sedimenting the DNA by centrifugation at 2000 x g for 5 min at 2-8 °C. The phenol-ethanol supernatant was removed (saved for Protein Isolation, section 2.4.1.3). The pellet was washed twice in 1 mL 0.1 M sodium citrate in 10 % ethanol by incubating at room temperature for 30 min with periodic mixing and centrifuging at 2000 x g for 5 min at 2-8 °C. The supernatant was discarded and the DNA pellet suspended in 1.5 mL of 75 % ethanol. Samples were stored at 2-8 °C.

2.4.1.3 Protein Isolation from brain tissues

Protein was precipitated from the phenol-ethanol supernatant by the addition of 1.5 mL isopropanol and incubation for 10 min at room temperature. Protein was sedimented at 12,000 x g for 10 min at 2-8 °C. The supernatant was discarded and protein pellet washed 3 times in 2 mL 0.3 M guanidine hydrochloride in 95 % ethanol by incubation for 20 min at room temperature and centrifugation at 7500 x g for 5 min at 2-8 °C. The supernatant was discarded and the pellet was washed in 2 mL 100 % ethanol for 20 min at room temperature. The samples were centrifuged at 7500 x g for 5 min at 2-8 °C before discarding the supernatant and air drying the pellet for 5-10 min. The protein was re-dissolved 50 µL 2 x sample buffer (2 % sodium dodecyl sulphate (SDS), 10 % glycerol, 125 mM Tris (pH 6.8), 5 % β-mercaptoethanol). Concentration of protein was determined by measuring the absorbance at 280 nm on a Nano drop before the samples were stored at -20 °C. Dilutions for loading onto SDS-PAGE were into 2 x sample

buffer containing bromophenol blue (2 % sodium dodecyl sulphate (SDS), 10 % glycerol, 125 mM Tris (pH 6.8), 0.002 % bromophenol blue, 5% β-mercaptoethanol). Samples were sonicated and/ or heated to 70 °C for 5 min before being subjected to SDS-PAGE (section 2.7.2).

2.4.2 *Protein extraction from cells*

Protein was extracted from cultured cells by first trypsinising the cells then the neutralized suspension (plus media) was placed in a 15 mL universal tube and centrifuged at 1000 g for 5 min at 4 °C. The supernatant was decanted off and the cells were washed in 1 mL PBS and transferred to an 1.5 mL eppendorf tube. Samples were centrifuged at 10000 g for 5 min at 4-8 °C before discarding the supernatant and resuspending the samples in 50 µL 2 x sample buffer (2 % sodium dodecyl sulphate (SDS), 10 % glycerol, 125 mM Tris (pH 6.8), 5 % β-mercaptoethanol). Concentration of protein was determined by measuring the absorbance at 280 nm on a Nano drop before the samples were stored at -20 °C. Dilutions for loading onto SDS-PAGE were into 2 x sample buffer containing bromophenol blue (2 % sodium dodecyl sulphate (SDS), 10 % glycerol, 125 mM Tris (pH 6.8), 0.002 % bromophenol blue, 5 % β-mercaptoethanol). Samples were sonicated and/ or heated to 70 °C for 5 min before being subjected to SDS-PAGE (section 2.7.2).

2.5 RNA procedures

2.5.1 *First strand cDNA synthesis using Superscript III reverse transcriptase*

Superscript III reverse transcriptase was the enzyme of choice for semi-quantitative RT-PCR. Synthesis of RNA into cDNA was carried out typically with reactions containing 1 µg of RNA, 1 µL oligo (dT) (VH Bio Ltd, 50 µM), 1 µL dNTP (New England Biolabs, 10 mM) into a final volume of 13 µL with RNase free water. The samples were

then incubated at 65 °C for 5 min, followed by incubation on ice for 1 min. Subsequently, 4 µL 5x First Stand Buffer (Invitrogen, 250 mM Tris-HCl [pH 8.3], 375 mM KCl, 15 mM $MgCl_2$), 1 µL 0.1 M DTT (Invitrogen), 1 µL Superscript III reverse transcriptase (Invitrogen) and RNase free water was added to a total volume of 20 µL. Samples were incubated at 50 °C for 60 min before inactivating the enzyme at 70 °C for 15 min. For negative control reactions water was added instead of the enzyme.

2.5.2 *First strand cDNA synthesis using Moloney Murine Leukaemia Virus Reverse Transcriptase (M-MLV RT)*

M-MLV RT was the enzyme of choice for quantitative RT-qPCR. Synthesis of RNA into cDNA was carried out typically with reactions containing 1 µg of RNA, 1 µL oligo (dT) (VH Bio Ltd, 0.625 mM), into a final volume of 12.5 µL with RNase free water. The samples were then incubated at 70 °C for 5 min, followed by incubation on ice for 1 min. Subsequently, 5 µL 5x First Stand Buffer (Promega, 250 mM Tris-HCl (pH 8.3 at 25 °C), 375 mM KCl, 15 mM $MgCl_2$ and 50 mM DTT), 2 µL dNTP (New England Biolabs, 10 mM), 1 µL M-MLV RT (Promega) and RNase free water was added to a total volume of 25 µL. Samples were incubated at 37 °C for 60 min before inactivating the enzyme at 70 °C for 15 min. For negative control reactions water was added instead of the enzyme.

2.5.3 *Design of PCR Primers*

All primers were synthesised by Integrated DNA Technologies (IDT), Inc. Oligonucleotide primers were designed, by hand, to be typically 20-24 base pairs long. Where possible, primers were designed such that they had a G or C nucleotide at the 3' and 5' end. The GC content was ideally approximately 50 % and the melting temperature was between 50-60 °C. Additional parameters for RT-qPCR were that they

yielded a 100-150 bp product and where possible, either forward or reverse primer was over an exon-intron boundary.

2.5.4 *Polymerase Chain Reaction (PCR)*

Amplification of cDNA regions was typically completed in 50 µL reactions containing 25 µL 2x *Taq* mastermix (New England Biolabs, UK), 1 µL sense primer (0.2 µM), 1 µL antisense primer (0.2 µM) and 1 µL template cDNA. Generally denaturation was at 94 °C for 30 sec, extension was at 72 °C for 60 sec over the course of 35 cycles. Individual annealing temperatures were optimised for each PCR product and are given alongside primers as detailed in Chapters 3, 4, 5, 6 and 7.

2.5.4.1 Agarose Gel Electrophoresis

PCR products were analysed on 2.5 % agarose gels. Agarose was dissolved in 1x TBE buffer (89 mM Tris base, 89 mM Boric Acid, 2 mM EDTA) by boiling. Ethidium bromide (2 µg/mL) was then added. The cooled solution was poured into gel trays and allowed to set. In gel tanks, set gels were immersed in 1x TBE buffer. Samples were added to a 0.2 x volume of Orange G loading dye. Samples were compared against 10 µL of either a 1 kb or a 100 bp DNA ladder (New England Biolabs, UK) to assess the size of bands. Gels were run for 40 min at 120 V. Where required, band intensities were quantified by densitometry using GeneTools (SynGene).

2.5.4.2 Purification of PCR products from agarose gel or PCR reactions

If multiple bands were observed on agarose gels the band of interest was excised from the gel so that products could then be subsequently ligated into vectors. This process was initiated by cutting the band from an agarose gel using a sterile scalpel blade under UV light. The QIAquick gel extraction kit (Qiagen,UK) was used according to the manufacturer's protocol. Briefly, gel slices were weighed and the appropriate amount of

high-salt solubilisation buffer (provided in the kit) was used to dissolve the remaining gel at 50 °C. The solution was applied to a QIAquick spin column and binding of the nucleic acids to the membrane was allowed by centrifugation. Subsequent wash steps allowed removal of impurities such as enzymes and salts before the pure DNA was eluted into a low salt buffer. DNA extracted was stored at -20 °C.

PCR products that gave a single band on an agarose gel were purified directly from the PCR reaction using QIAquick PCR purification kit according to the manufacturer's protocol. Directly to the PCR reaction a high salt buffer was added and then as above the PCR product was bound to a QIAgen spin column by centrifugation before purification and elution.

2.5.4.3 Digestion of PCR products with restriction endonuclease

Restriction endonucleases were used to digest PCR products in order to be able to ligate them together (section 2.6.6). Typically, digest reactions contained the appropriate reaction buffer (NEB biolabs) and 5 – 10 Units of specific restriction endonuclease in a final volume of 10 µL. Digest reactions were incubated in a water bath at 37 °C for 1-2 hours.

2.5.5 *Real-time PCR (RT-qPCR)*

RT-qPCR was performed using the DNA engine opticon 2 (MJ Research). Typical reactions contained 7.5 µL Power SYBR Green PCR Master Mix (Applied Biosystems), 1.5 µL sense primer (0.25 µM), 1.5 µL antisense primer (0.25 µM) and 1 µL template cDNA made to 15 µL with RNase free water. Amplification was carried out in ABgene 96 well plates under the following conditions; denaturation at 95 °C for 10 min followed by 40 cycles of 95 °C for 15 sec and an annealing/extension stage of 60 °C for

10 sec before the plate was read. A melt curve was subsequently completed over 55-90 °C with 1 °C increments over 1 sec. Each sample was measured in duplicate.

2.5.5.1 Standard curves

Standard curves were generated for all RNA analysed by RT-qPCR and the relevant controls in order to determine the relative concentrations of samples. The primers designed for RT-qPCR were used to carry out conventional PCR to amplify templates to be used for standard curves. These products where ligated into pCR®-TOPO vector (Invitrogen, UK, Appendix A) (section 2.6.1) and transformed into chemically competent *E. coli* cells (Top10; Invitrogen) (section 2.6.2). Once the plasmid DNA was extracted, serial dilutions were performed on each construct in RNase free water, each of these was assigned an arbitrary concentration. A standard curve was created by plotting the log of arbitrary concentration against cycle threshold (C_t) value. Analysis was performed in duplicate and each RT-qPCR analysis contained the standard curve.

2.5.5.2 Data analysis

Expression of the RNA of interest was calculated by taking the C_t value, averaging the duplicates, and then reading from the standard curve the arbitrary concentration of the samples. These were run alongside a control RNA in order to normalise the results and were finally expressed as a ratio of RNA of interest:control RNA. Efficiency values were calculated using the equation E = (10(-1/slope) - 1)*100 and were required to fall within the range of 80-115 %.

2.6 Generation of plasmid constructs

2.6.1 *Cloning into TOPO™ TA vector*

In a final volume of 6 µL the PCR products to be cloned, sterile water, 1 µL salt solution and 1 µL pCR®-TOPO vector (Invitrogen; Appendix A) were added. The

reactions were mixed gently and incubated at room temperature for 5 min. The tubes were placed on ice before carrying out the One Shot™ Transformation reaction (section 2.6.3) or transformation into electrocompetent *E. coli* cells (section 2.6.6).

2.6.2 *Cloning into TOPO™ pBlue vector*

The –891 to +51 bp region of the ZnT10 promoter was generated by PCR from genomic DNA from SH-SY5Y cells with primers and thermal cycling parameters as stated in Table 4.2 and subcloned into the vector pBlue-TOPO® (Invitrogen; Appendix B), upstream of the β-galactosidase reporter gene. In a final volume of 6 µL the PCR products to be cloned, sterile water, 1 µL salt solution and 1 µL pBlue-TOPO® vector (Invitrogen) were added. The reactions were mixed gently and incubated at room temperature for 5 min. The tubes were placed on ice before carrying out the One Shot™ Transformation reaction (section 2.6.5) or transformation into electrocompetent *E. coli* cells (section 2.6.7).

2.6.3 *Digestion of plasmids with restriction endonuclease*

Restriction endonucleases were used to digest plasmids to confirm that the plasmid contained the correct insert in the correct orientation. Typically, digest reactions contained the appropriate reaction buffer (NEB Biolabs) and 5 – 10 Units restriction endonuclease in a final volume of 10 µL. Digest reactions were incubated in a water bath at 37 °C for 1-2 hours. Analysis was by agarose gel electrophoresis (section 2.5.4.1)

2.6.4 *Overnight ligations*

After digestion of both the vector and DNA insert by specific restriction endonucleases (section 2.6.3) the concentration of the vector and insert was measured using a Nano drop. Appropriate vector:insert molar ratios (typically 1:1 or 1:3) were determined

where the reaction contained 50 ng vector, 50-200 ng insert, 1 µL 10 x T4 DNA ligase buffer (NEB Biolabs, 500 mM Tris-HCl,100 mM $MgCl_2$,10 mM ATP, 100 mM Dithiothreitol, pH 7.5), T4 DNA ligase (NEB Biolabs, 1 U/µL) and nuclease free water to a volume of 10 µL. Reactions were incubated overnight at 16 °C. Ligation reactions were then precipitated with ethanol.

2.6.5 *One Shot™ Transformation reaction*

2 µL of the cloning reaction was added to chemically competent Top10 *E. coli* cells (Invitrogen). They were mixed gently and incubated on ice for 5-30 min. Cells were then heat shocked in a water bath at 42 °C for 30 sec. Tubes were transferred to ice and 250 µL of room temperature LB medium was added. Tightly capped tubes were shaken horizontally in an orbital shaker at 37 °C, 200 rpm for 1 h. Transformed cells were propagated on LB plates containing 50 µg/ml ampicillin.

2.6.6 *Production of competent cells*

Electrocompetent DH5α cells were generated by initially growing a colony in LB (orbital shaker; 37 °C, 200 rpm) until an optical density of 0.5 was reached. All centrifuges were pre-cooled and all water and glycerol was cold. Cells were kept on ice when not in the centrifuge. The centrifuge steps were: 6000xg for 15 min at 4 °C and resuspend in 800 mls water, 6000 x g for 15 min at 4 °C and resuspend in 400 mls water, 6000 x g for 15 min at 4 °C and resuspend in 16 mL 10 % glycerol, 6000 x g for 15 min at 4 °C and resuspend in 3.2 mls 10 % glycerol. Cells were aliquotted on dry ice to snap-freeze and stored at -80 °C.

2.6.7 *Transformation into electrocompetent E. coli cells*

1 µL of the cloning reaction was added to electrically competent *E. coli* cells (section 2.6.6). This mixture was transferred into a cool cuvette and placed into an electroporator

at 25 µFD, 200 OHMS (Ω), 1.5 kV. Room temperature LB medium, 500 µL, was added and the mixture transferred to an eppendorf tube containing a further 500 µL of room temperature LB medium. Capped tubes were incubated in a water bath at 37 °C for 1 h. Transformed cells were propagated on LB plates containing 50 µg/ml ampicillin.

2.6.8 *Generation of full length FLAG-ZnT10 plasmid DNA construct*

Full length cDNA corresponding to ZnT10 was generated by RT-PCR from SH-SY5Y RNA and subsequent nested PCR using Velocity Polymerase (Bioline) with primers and thermal cycling parameters as stated in Table 3.5. The product was gel purified using the QIAquick Gel Extraction Kit according to manufacturer's instructions (Qiagen) (section 2.5.4.2) and subcloned into the vector pCR2.1-TOPO (Invitrogen Appendix A) (section 2.6.1). The identity of the pCR2.1-ZnT10 product was confirmed by sequencing (MWG Biotech). A large scale plasmid preparation (Plasmid Maxi kit, Qiagen) was digested with *Eco*RI and *Bam*HI (New England Biolabs) (section 2.6.3), and the DNA purified from the band resolved by agarose gel electrophoresis using the QIAquick Gel Extraction Kit (Qiagen) (section 2.5.4.2). This DNA was subcloned in-frame into the vector p3xFLAG-CMV-10 (Sigma, Appendix D) to give plasmid p3xFLAG–ZnT10, prior to transformation into electrocompetent *E. coli* cells (section 2.6.7). The identity of the product was confirmed by sequencing (MWG Biotech) (Appendix F).

2.7 Protein Procedures

2.7.1 *Reporter gene assays*

2.7.1.1 Transient transfection of Caco-2 cells for measurement of reporter gene activity

Caco-2 cells were seeded into 12-well plates at a density of 3.5 x 10^5 cells per well for co-transfection and for individual transfections. Twenty-four hours post-seeding cells

were transfected either with pBlue-ZnT10 (section 2.6.2) construct alone or co-transfected with p3xFLAG-ZnT10 (section 2.6.8) or p3xFLAG-BAP (Sigma-Aldrich; Appendix E) plus the reporter gene construct pBlue-MT2a (Helston et al., 2007) using GeneJammer transfection reagent (Stratagene), with a ratio of DNA to GeneJammer of 1.5 µg:2.5 µl. Transfection medium was removed after twenty-four hours and replaced with basal medium with or without either 100 µM $ZnCl_2$, 100 µM $CoCl_2$, 100 µM $NiCl_2$, 100 µM $CuSO_4$. Twenty-four hours post-treatment cell lysates were prepared.

2.7.1.2 Whole cell lysate preparation

Reporter gene assays were completed on cells in 12 well plates. Cells were washed with 1 mL PBS before addition of 100 µL lysis buffer (0.25 M Tris pH 7.4, 0.25 % (v/v) NP-40, 2.5 mM EDTA) and freezing at -20°C for 30 min. Cells were defrosted at room temperature to complete lysis. Sterile cell scrapers (Greiner) were used to harvest cells before transfer to 1.5 mL eppendorf tubes. Cell debris was pelleted by centrifugation of the cell lysates at 12,000 g for 5 min at 4-8 °C. The supernatant was transferred to a new tube for subsequent analysis.

2.7.1.3 β-Galactosidase reporter assay

The High Sensitivity β-Galacosidase Assay Kit (Stratagene) was used for reporter gene assays. When the β-galactosidase enzyme is expressed by the plasmid it is able to catalyse a reaction using the substrate chlorophenol red-β-D-galactopyranoside (CPRG) so to induce a colour change from yellow to orange/ red depending on expression levels. In a 96 well plate, 130 µL of 1.2 mg/mL CPRG (in buffer containing 100 mM NaCl, 25 mM MOPS and 10 mM $MgCl_2$, pH 7.5) was added to 20 µL of cell lysate (from section 2.7.1.2) to give a final volume of 150 µL. Well plates were shielded from light and incubated at 37 °C until the colour change occurred. Reactions were stopped by the

addition of 80 µL 0.5 M Na_2CO_3 when the colour change was observed. Incubation time was recorded and absorbance was measured at 560 nm using a BioTek Synergy HT plate reader.

2.7.1.4 Determination of protein concentration

Bradford assays were used to determine cell lysate protein concentrations. The colour of Coomassie Brilliant Blue G-250 dye (Bradford reagent; Bio-Rad) changes in response to various concentrations of protein due to binding of the dye to primarily basic (especially arginine) and aromatic amino acid residues (Bradford, 1976). Bovine Serum Albumin (BSA) was used to generate a standard curve 0-100 µg/mL in a volume of 50 µL, eight replicates were analysed in a 96 well plate. Dilutions of the cell lysates (1:50) in a total volume of 50 µL were added to the plate and 200 µL Bradford reagent (Bio-Rad, UK) diluted 1 in 5 with H_2O was added to all reactions. Absorbance was measured at 560 nm using a BioTek Synergy HT plate reader and protein concentrations were calculated from the standard curve.

2.7.1.5 Data analysis

Specific activity of β-galactosidase (U) was calculated by first calculating the nmoles of chlorophenol red (CR) formed per mL (optical density at 560 nm x 55). This is then converted to nmoles of CR formed (CR x total assay volume (0.23 mL)). The activity of β-galactosidase per minute (U x 10^3) was calculated using the assay time (CR/ length of time at 37 °C (min)). Values were corrected for protein concentration measured in each sample (U/ (protein concentration of lysate (mg/mL)/ volume of lysate in assay (20 µL)) U x 10^3/mg). Results are shown as mean ± standard error of the mean (SEM) for all experiments. Statistical comparisons were made by Student's paired *t*-test (Excel). Differences between means were considered significant at $p < 0.05$.

2.7.2 *Western blotting procedure*

Proteins (40 µg) were separated on 10 % SDS polyacrylamide gels (SDS-PAGE). A 10 % acrylamide resolving gel solution was prepared (in 15 mL; 5.1 mL 30 % acrylamide mix (29:1 acrylamide:bisacrylamide), 3.9 mL 1.5 M Tris-HCl pH 8.8, 0.15 mL 10 % SDS (w/v), 6 mL water) to which 150 µL of 10 % freshly prepared ammonium persulphate and 6 µL TEMED polymerisation agent was added. The mixed solution was poured between two glass plates (BioRad) to within approximately 3 cm from the top. The gel was overlaid with 150 µL water and allowed to set for 15-20 minutes. After the gel had set the water was removed with paper tissues. A 5 % stacking gel was prepared (in 15 mL; 1.5 mL 30 % acrylamide mix (29:1 acrylamide:bisacrylamide), 1.14 mL 1.5 M Tris-HCl pH 6.8, 0.09 mL 10 % SDS (w/v), 6.3 mL water) to which 90 µL of 10 % freshly prepared ammonium persulphate and 9 µL TEMED polymerisation agent was added. The mixed solution was poured on top of the resolving gel and allowed to set for 20 minutes. Gels were run at 180 V for 1-1.5 hours before being transferred by semi-wet blotting onto PVDF membranes at 100 V for 90 min. Blocking of the membranes was carried out in 5 % non-fat milk powder in 1x PBS containing 0.1 % (w/v) Tween-20 for 1 h before membranes were incubated in 1x PBS, pH 7.4, containing 0.01% Tween-20 and 5 % non-fat milk powder with primary antibody at the appropriate concentration, overnight at 4 ºC followed by incubation for 1 h at room temperature with a horseradish peroxidise – conjugated IgG secondary antibody (1:5000 dilution) (Sigma). Primary antibodies were monoclonal mouse anti-FLAG M2 (1:1000, Sigma-aldrich) and rabbit polyclonal anti-alpha tubulin (1:5000, Abcam). Bound secondary antibodies were visualised using a luminol-based enhanced chemiluminescence kit (Thermo Scientific). Band intensities were quantified by densitometry using GeneTools (SynGene).

2.7.3 *Subcellular localisation of FLAG-tagged construct*

SH-SY5Y cells were seeded in 24-well plates on glass cover slips at a density of 1.75 x 10^5 cells per well in 0.5 mL culture medium. Twenty-four hours post-seeding cells were transfected transiently with p3xFLAG-ZnT10 (section 2.6.8) or BAP-FLAG (Sigma, Appendix E) using Lipofectamine 2000 reagent (Invitrogen), with a ratio of DNA to Lipofectamine 2000 of 0.5 µg:0.5 µl. In some experiments cells were treated with 100 µM extracellular $ZnCl_2$ for 24 h post-transfection and incubated for 24 h prior to fixation. Twenty-four hours post-transfection, cells were fixed in 4 % paraformaldehyde (in 1x PBS) for 15 min at room temperature, and then washed three times with 1x PBS. Cells were permeabilised by treatment with 0.1 % Triton X-100 for 10 min followed by washing in 0.1% Tween-20 in 1x PBS. Cells were incubated with monoclonal anti-FLAG M2-FITC antibody (1:1000, Sigma-Aldrich) for 1 h at 4 ºC then washed three times with 0.1 % Tween-20 in 1x PBS. Cells were co-stained with 2 µg/mL rhodamine-labelled wheat germ agglutinin (WGA) for 5 min at room temperature before washing twice with 0.1 % Tween-20 in 1x PBS and visualising using fluorescence microscopy (Olympus BX61 Fluorescent microscope).

2.8 Bioinformatics tools

2.8.1 *Protein topology prediction*

The database TMpred was used to predict the putative membrane topology of ZnT10. This uses an algorithm derived from the statistical analysis of the TMbase database of naturally occurring transmembrane protein segments (Hofmann and Stoffel, 1993). The web site used to access this software was http://www.ch.embnet.org/software/TMPRED_form.html. This pattern was confirmed by TMHMM, an algorithm model for TransMembrane prediction using Hidden Markov Models which was accessed through the use of InterProScan

(http://www.ebi.ac.uk/Tools/pfa/iprscan/). This database enabled simultaneous searches for conserved signal peptides and the cation diffusion facilitator (CDF) motif using SignalP and TIGRFAM respectively. The presence of a CDF motif was confirmed using ScanProsite (http://expasy.org/tools/scanprosite/). *N*-glycosylated sites, *O*-glycosylated sites, phosphorylation sites and sequence alignments were completed using NetNGlyc, NetOGlyc, NetPhos and ClustalW respectively. The software was accessed via the websites:

http://www.cbs.dtu.dk/services/NetNGlyc/

http://www.cbs.dtu.dk/services/NetOGlyc/

http://www.cbs.dtu.dk/services/NetPhos/

http://www.genome.jp/tools/clustalw/

2.8.2 *Nucleotide consensus sequences*

The database fuzznuc was used to search for appropriate nucleotide consensus sequence patterns such as Metal Response Elements (MREs) and the putative Zinc Transcriptional Regulatory Element (ZTRE). This was accessed via the website http://emboss.bioinformatics.nl/cgi-bin/emboss/fuzznuc.

2.9 Statistical Analysis

Experiments were performed routinely in triplicate and each experiment was repeated at least twice. Results are expressed as means ± SEM throughout. Statistical comparisons were made using one-way ANOVA followed be Bonferroni's multiple comparisons *post hoc* test (Microsoft SPSS) or by Student's paired *t*-test (Excel). Differences between means were considered significant at $p < 0.05$.

Chapter 3: Characterisation of ZnT10

3.1 Outline

The work presented in this chapter is concerned with characterising the putative zinc transporter, ZnT10 bioinformatically as well as determining its expression pattern and establishing its functional response to zinc. Previous bioinformatics research into ZnT10 has been published (Seve et al., 2004) and this chapter aims to both confirm and extend these findings. Seve et al., (2004) provided only *in silico* data relating to all ten members of the ZnTs, but also developed this analysis further for ZnT10. As discussed previously in Chapter 1, members of the ZIP transporter family generally function to increase cytosolic zinc concentrations, whereas ZnT family members are usually involved in lowering cytosolic zinc concentration by effluxing out of the cell or into intracellular compartments. Distinct structural differences between the two families may relate to their opposing roles. In general, members of the ZIP family have eight transmembrane domains (TMDs), compared with six in members of the ZnT family and the predicted topology is such that the N- and C- termini in ZnT family members are intra-cytosolic, but in ZIP family members are extra-cytosolic (Kambe et al., 2004). This tenth family member would be predicted, in line with other family members, to contain a cation diffusion facilitator (CDF) motif, six TMDs and intracellular N- and C-termini although this orientation is only confirmed for ZnT1 (Palmiter and Findley, 1995). In addition, most ZnT transporters also contain a histidine-rich region, between TMDs IV and V. Such regions are predicted to be cytoplasmic and could function as potential metal binding domains. In the previously published article, Seve et al., (2004) used the programmes BLASTN and TBLASTN, which use nucleotide or protein sequences respectively, to identify ZnT10 by analysing genomic DNA and translated

sequences of ZnT1 (human, mouse and rat), Znt2 (rat), ZnT3 (human and mouse), ZnT4 (human, mouse and rat), ZnT5 (human), ZnT6 (human) and ZnT7 (human) for homologous sequences. Previous bioinformatics data predicts, using the internet programme TMPred that ZnT10 also contains six transmembrane domains with intracellular N- and C- termini (Seve et al., 2004). Furthermore, this work highlighted that there is a basic region between TMD IV and V in ZnT10 that is serine rich. The expectation according to central dogma is that this region should be histidine rich but this basic serine rich region is in concurrence with other zinc transporters, namely ZnT6. It was previously found that ZnT6 did not have the characteristic histidine rich region but retained serine residues in the same region that were hypothesised to have been retained from the prokaryotic ancestors of this family (Huang et al., 2002). It is noteworthy that, Seve et al., (2004) found conservation between aspartate at position 247 in TMD V and position 276 in TMD VI for ZnT10 with aspartate residues in ZnT5 at position 599 and 621, respectively. Using HEK-293 cells and a construct expressing ZnT5 has revealed the importance of Asp599 in zinc binding. In these experiments Zinpyr-1, the zinc sensing cell-permeable fluorescent probe, showed that when this aspartate was mutated (D599A) zinc was no longer sequestered into the Golgi apparatus (Ohana et al., 2009).

The *in silico* expressed sequence tag (EST) technique used to look at the expression profile of ZnT10 predicted that ZnT10 expression would be restricted to foetal tissue, more specifically foetal liver and foetal brain (Seve et al., 2004). This was intriguing in that this was the only known zinc transporter to be restricted in this way.

In order to increase knowledge of this transporter the preliminary aim of the work reported in this chapter was to characterise ZnT10 using both *in silico* and *in vitro*

techniques. This chapter reports novel bioinformatic findings relating to ZnT10 and confirms the presence of ZnT10 in foetal tissue but in addition, presents novel findings that indicate ZnT10 is also expressed in adult mouse and human tissue.

Studies to date have revealed that there are at least 10 members of the human ZnT family with the mRNA expression of each varying depending upon the tissue type. ZnT1 is expressed ubiquitously and is more abundant in tissues involved in zinc acquisition such as the small intestine (McMahon and Cousins, 1998, Cousins and McMahon, 2000). ZnT2 has a differential expression pattern with mRNA expression detected in the small intestine, kidney, placenta, pancreas, testis, seminal vesicles and the mammary gland (Kelleher and Lonnerdal, 2002, Liuzzi et al., 2001, Liuzzi et al., 2003, Clifford and MacDonald, 2000, Palmiter et al., 1996a). Until recently it was thought that ZnT3 expression was restricted to the brain and the testis. However, it has been reported that ZnT3 exists in the retina, pancreatic cells and some areas of the epithelium (Smidt and Rungby, 2012). ZnT4 has been found to be abundantly expressed in mammary gland, brain and intestinal epithelial cells (Huang and Gitschier, 1997). In contrast, both variants of ZnT5 (A and B) have ubiquitous expression patterns (Kambe et al., 2002, Cragg et al., 2002). ZnT6 appears to have a restricted expression profile whereby the mRNA is present in the liver, brain, kidney and small intestine (Huang et al., 2002). ZnT7 mRNA is more widespread than that of ZnT6, with the mRNA being found in liver, kidney, spleen, heart, brain, small intestine and lung (Kirschke and Huang, 2003). ZnT8 is expressed only in the islets of Langerhans in pancreatic β-cells (Chimienti et al., 2004). Analysis of four human foetal tissues (brain, lung, liver, and kidney) showed ZnT9 mRNA expression in all these tissues and in addition RT-PCR showed presence of mRNA in all tested tissues and cells (16 human adult tissues and 14 cancer cell lines) therefore displaying widespread expression. (Sim and Chow, 1999).

The majority of above research used both Northern blot and RT-PCR techniques in order to determine the expression profile of the ZnTs. The last known member of this family has not yet been characterised in this way. Seve et al., (2004) were able to elucidate a restricted expression profile using an *in silico* technique. The EST data mining technique uses a sub-sequence from a cDNA sequence in order to search the EST database using a search programme such as BLASTN (a programme that enables searching of nucleotides) in order to assess whether the cDNA is expected to be found in particular tissues. BLASTN was used in the case of ZnT10 to search the human EST database using the query sequences of the ORF 5' and 3' UTR. As stated above, this gave the prediction that ZnT10 would be expressed in foetal tissue only and more specifically, it would be restricted to foetal liver and foetal brain. This is unusual as no other ZnTs are restricted to foetal tissue alone. ZnT1 levels at birth are extremely low and Seve et al., (2004) used ZnT10's homology to ZnT1 to hypothesise that ZnT10 may play a similar role to ZnT1 in the developing foetus.

The ZnT family of transporters are predominantly thought to be effluxers, reducing cytosolic zinc concentrations. Previous measurements for the ZnTs have been indirect for all experiments except those for ZnT5 (Valentine et al., 2007, Cragg et al., 2002). Such experiments generally use transfected cell lines to assess 'rescue' in response to zinc treatment. ZnT5vB is the only transporter that has been reported to be bi-directional thereby able to act to both increase and decrease cytosolic zinc (Valentine et al., 2007). These experiments are two-fold, the researchers use radioactive ^{65}Zn to directly assess transport in *Xenopus laevis* oocytes. In addition, Valentine et al., (2007) used an indirect promoter reporter assay to further characterise ZnT5vB function. Indirect measurements are commonplace in measuring ZnT function and similar promoter reporter assays have also been used to characterise Znt1 and Znt2. These

systems are based on the β-galactosidase reporter system whereby a zinc sensitive promoter drives expression of the β-galactosidase gene at differing levels depending on the zinc concentration of the cell. For Znt1 and Znt2 in BHK cells that stably express the MRE-βGeo (a construct involving 5 MRE sequences and a β-galactosidase-neomycin phosphotransferase (lacZ-neo) fusion gene), β-galactosidase activity was measured with transient transfection of either Znt1 or Znt2 the results showing an increased zinc efflux (Palmiter, 1994, Palmiter et al., 1996a, Palmiter and Findley, 1995). By comparison, for ZnT5 the effect of increased ZnT5vB transporter expression on the intracellular zinc status was analysed by measuring the response of a β-galactosidase reporter gene to zinc driven by a zinc responsive MT2a construct (Valentine et al., 2007, Helston et al., 2007). No functional characterisation of ZnT10 has been carried out therefore it is important to establish the functional activity of ZnT10 especially given its restricted expression profile in adult human tissue. Here I report that indirect measurements, as used for functional characterisation of ZnT5vB, indicate that ZnT10 follows suit with other family members and effluxes zinc such that cytosolic zinc concentrations are reduced.

3.2 Bioinformatic screening of ZnT10

There are a number of features present in the sequence of ZnTs, discussed in section 1.4.2, which are both conserved and/or allow predictions to be made about characteristics of the protein. This section confirms those already found in the literature as well as identifying novel features.

3.2.1 *Topology modelling*

The ZnT family members have certain conserved structures in their topology. It is assumed, although not proven, that the structure is important for zinc binding and

transport. One conservation throughout most family members is six TMD which Seve et al., (2004) predicted to be present in ZnT10 using the freely available TMPred package. This package is based on the protein sequence database SwissProt and it uses an algorithm combining several weight-matrices for scoring in order to predict membrane-spanning regions and their orientation (Hofmann and Stoffel, 1993). Confirmation of this topology was established with both TMPred and TMHMM using InterProScan. TMHMM is based on a hidden Markov model and whilst the programme agreed with TMPred in the number of TMD there were minor differences in the positions of all TMD except TMD I (Table 3.1). In line with the other ZnT members, both programmes strongly preferred the model with a predicted intracellular N- and C- termini. In addition to the above observations, partial sequence alignment with ClustalW highlighted that ZnT10 does not contain the histidine rich region of most the other family members however, similarly to ZnT6, a serine rich region between TMD IV and V with a high predominance of the basic residues lysine and arginine has been identified (Seve et al., 2004) (Figure 3.1A). Furthermore, using the partial sequence alignment of TMD V and VI there are conservation of two asparagine residues (Asp 247 and Asp 276) in ZnT10 with Asp 599 and Asp 621 of ZnT5 that are thought to be important for zinc binding (Figure 3.1B). A summary diagram of the predicted topology of ZnT10 is shown in Figure 3.2A.

3.2.2 *CDF sequence identification*

ZnTs are members of the CDF family and are therefore expected to have a CDF motif near their N-terminal region, which generally lie between TMD I and II (as represented in Figure 3.2A). The consensus sequence for the CDF motif is given in Figure 3.2B. A CDF consensus sequence has been identified in ZnT10, using the freely available programme ScanProsite (ExPASy). ScanProsite allows input of a sequence motif and

subsequently scans the given protein (or the Prosite database) for the presence of that motif. The results identified a CDF motif at amino acids 34-50 (SiALLSDSFNmlsDLiS) in ZnT10 (Figure 3.2C). This furthers the existing knowledge and both the extent to which it matches and its presence at the N-terminus between TMD I and II (despite extending into TMD II) implies that ZnT10 is a true member of the ZnT, and indeed, the CDF family.

3.2.3 *Identification of sites for post-translational modification*

Proteins contain many sites and/ or sequences that can be modified to create the mature protein in order to alter the structure, function or localisation of the protein. One such sequence is a signal peptide sequence which enables proteins to be targeted to the correct position within the cell (Stryer et al., 2002). One such example of signal peptide usage is for the enzyme elastase. This protein needs to pass through channels in the ER membrane and into the ER lumen and in order for this translocation to occur the 29 amino acid signal peptide is required. Protein synthesis begins at the ribosomes of the ER and it is during this translation that the signal peptide directs the growing peptide through the ER channels. On completion of the translocation the signal peptide is cleaved and subsequently degraded (Stryer et al., 2002). The SignalP programme uses several artificial neural networks and hidden Markov models in combination in order to predict the probability of a signal peptide within a given sequence (Petersen et al., 2011). Scores > 0.45 result in a positive prediction of a signal peptide. The ZnT10 amino acid sequence was submitted into this database and the results gave a maximum cleavage site probability 0.465 between amino acid position 29 and 30 (G and Y) predicting that there is a potential signal peptide present in the N-terminal of the protein (Figure 3.2C).

A modification commonly involved in the conformation of proteins is *N*-glycosylation. This process is where N-linked glycans are attached to the nitrogen of side chains of asparagine or arginine, an important process occurring in the ER that is essential for correct protein folding. NetNGlyc (http://www.cbs.dtu.dk/services/NetNGlyc/) examines the sequence context of Asn-Xaa-Ser/Thr sequons using artificial neural networks in order to predict *N*-glycosylation sites within an amino acid sequence. Scores that are > 0.5 indicate a predicted glycosylation site. Within ZnT10 three *N*-glycosylation sites are predicted at amino acids Asp 377, 471 and 481 with scores of 0.7864, 0.6268 and 0.5148 respectively (Figure 3.2C, Table 3.2).

Similarly NetOGlyc (http://www.cbs.dtu.dk/services/NetOGlyc/) uses neural networks to predict *O*-glycosylation sites within an amino acid sequence. *O*-glycosylation is a functional modification occurring in the Golgi apparatus. In this process *O*-linked glycans are attached to an hydroxyl oxygen of serine, threonine, tyrosine, hydrolysine or hydroxyproline side chains. Again, scores that are > 0.5 indicate a predicted glycosylation site. Within ZnT10 one *O*-glycosylation site is predicted at amino acid Thr 183 with a score of 0.595 (Figure 3.2C, Table 3.2).

Another functional modification within mature proteins is phosphorylation, this activates or deactivates many proteins or enzymes. Most commonly the amino acid site for phosphorylation is a serine however phosphate can also be added to the side chains of threonine and tyrosine. NetPhos (http://www.cbs.dtu.dk/services/NetPhos/) uses neural network predictions for the three possible phosphorylation sites; serine, threonine and tyrosine. Scores that are > 0.5 indicate a predicted phosphorylation site. Results yielded 15 predicted phosphorylation sites within ZnT10; seven serine sites at amino acids 5, 69, 149, 197, 233, 363, 446, (scores of 0.955, 0.852, 0.609, 0.998, 0.754, 0.862

and 0.998 respectively) four threonine sites at amino acids 8, 192, 196, 219 (scores of 0.732, 0.974, 0.928 and 0.839 respectively) and four tyrosine at amino acids 278, 359, 440, 479 (scores of 0.631, 0.836, 0.885 and 0.957 respectively) (Figure 3.2C, Table 3.2).

3.3 Adult mouse tissue expression

All known members of the ZnT family have homologues in mouse. Prior to 2012, all data on ZnT10 was *in silico* therefore, mouse tissue was assessed for the expression of Znt10 at the mRNA level.

3.3.1 *ZnT expression in adult mouse brain*

RNA was extracted from mouse brain tissue (section 2.4.1) and, using appropriate primers (Table 3.3), a gradient RT-PCR was performed in order to establish the Znts present in the mouse brain. Kidney tissue RNA was used as a positive control in all cases, as all Znts previously studied are expressed in kidney, except for Znt8 in which pancreatic RNA was used because this is the only area where Znt8 is known to be expressed (Chimienti et al., 2004). Mt1 and 18S rRNA were used as PCR controls to establish the integrity of the RNA and whether the PCR's had been successful. In all cases Mt1 and 18S rRNA were found in mouse brain, kidney and pancreas. All Znts except Znt8 were found in the mouse brain (Figure 3.3). Znt8 was amplified in the mouse pancreas, confirming Znt8 is absent from this tissue and not inadequate primer design (Figure 3.3B). As expected Znt3 was found in the mouse brain however it was absent from mouse kidney (Figure 3.3A). There was difficultly confirming the presence of Znt1 initially, however this was attributed to the fact that in the first brain that was analysed the cerebellum RNA was lost in the extraction process. The cerebellum has been shown to have a high level of Znt1 expression (Sekler et al., 2002). The most

surprising of these results was the novel finding that a faint ZnT10 band was present in mouse brain, given that this was RNA extracted from an adult mouse brain tissue, an area where Znt10 had not been predicted to be expressed (Seve et al., 2004) (Figure 3.3C).

3.3.2 *Confirmation that Znt10 is expressed in adult mouse tissues*

Using *in silico* methodologies Znt10 has only been predicted to be found in foetal tissue (Seve et al., 2004) specifically foetal liver and brain, therefore it was important to establish the specificity of the band found in adult mouse brain. In order to do this, RNA extracted from mouse foetal liver alongside adult mouse brain and kidney samples (Section 2.4.1) were used in a standard RT-PCR (Section 2.5.4), using primers specific to mouse Znt10 (Table 3.3). Gel electrophoresis identified distinct bands at the size corresponding to Znt10 in mouse foetal liver as well as mouse adult brain. Bands were not observed in the mouse adult kidney sample (Figure 3.4). Positive PCR products were sequenced by MWG and confirmed identity with mouse Znt10 (NM_001033286.2). This provides the first evidence that Znt10 expression is not restricted to foetal tissue, however appears to have a restricted pattern of expression in the adult mouse as it is not present in the adult mouse kidney.

3.4 Adult human tissue expression

Due to the presence of Znt10 in adult mouse brain research was expanded into the expression profile of ZnT10 at the mRNA level in adult human tissues.

3.4.1 *Semi-quantitative analysis*

To assess further the pattern of ZnT10 expression, human ZnT10 primers (Table 3.4) were designed. Initially, the ZnT10 primers were used to assess the expression profile of ZnT10 in 19 human tissues (Ambion RNA tissue panel) by RT-PCR (see section 2.5.4),

using GAPDH as the normalisation control (Table 3.4). The tissue panel RNA was reverse transcribed into cDNA using the reverse transcriptase Superscript III (section 2.5.1). RT-PCR was carried out over 30 cycles and did not reached saturation. Of the 19 tissues sampled, seven were shown to express ZnT10 at the mRNA level. The ratio to GAPDH of RT-PCR products were calculated using densitometry techniques (GeneTools) giving a profile of levels of expression being liver > brain > testes > small intestine > colon > ovary > cervix (Figure 3.5). It is important to bear in mind that this RT-PCR can only be used semi-quantitatively and therefore can only give an indication of relative expression levels as it is impossible to know the position on the curve as to whether the PCR reaction has gone to completion.

3.4.2 *Confirmation of relative expression levels of ZnT10 using RT-qPCR*

In order to further quantify the presence of ZnT10 in adult human tissues quantitative RT-qPCR (RT-qPCR) was used to investigate the relative expression levels of ZnT10 in the tissues. Standards for GAPDH and ZnT10 products were generated by amplifying the region between the primers shown in Table 3.4, and subcloned into the vector pCR2.1-TOPO TA (Appendix A, Invitrogen) following methods shown in section 2.6.1, to give the standards pCR2.1-ZnT10 and pCR2.1-GAPDH. The identity of the products was confirmed by sequencing (MWG Biotech). Ten-fold serial dilutions of each of pCR2.1-ZnT10 and pCR2.1-GAPDH were used to generate standard curves (see section 2.5.5.1). For RT-qPCR, a second reference gene was used; DNA topoisomerase I (TOPI) in accordance with the MIQE guidelines (Bustin et al., 2009). TOPI primers were purchased from PrimerDesign. A TOPI PCR product was produced and subcloned into the pGEM-T-easy vector to give the standard TOPI-pGEM. To confirm the identity of the product it was amplified in end-point PCR, cloned and sequenced (generated by Dr Alison Howard). A standard curve was created by performing ten-fold

serial dilutions of this standard. All standard curves passed acceptance criteria (Figure 3.6). The Ambion tissue panel was reverse transcribed into cDNA using the reverse transcriptase MMLV (RNase H positive, Promega), as described in section 2.5.2. Subsequently, this was used as the template for RT-qPCR giving an expression profile in 20 adult human tissues relative to both GAPDH (Figure 3.7) and TOPI (Figure 3.8). For RT-qPCR, using GAPDH as the reference gene, there were relatively high levels of ZnT10 found in small intestine > liver > testes > brain and lower transcript levels in the ovary > colon > cervix > prostate > placenta. In addition low levels of mRNA are shown to be in prostate tissue which was not included in the initial semi-quantitative analysis (Figure 3.7). Using the TOPI analysis expression levels appeared to differ slightly, however higher mRNA levels are found in the liver > brain > testes > small intestine and lower mRNA levels found in the ovary > colon > cervix > prostate > placenta (Figure 3.8).

3.5 Functional analysis of ZnT10

The majority of ZnTs and indeed members of the CDF family have been shown to act as effluxers and therefore decrease cation concentrations in the cytoplasm. With the exception of ZnT5, which has been shown to have bi-directional capabilities directly (Valentine et al., 2007) measurements of ZnT functional abilities have been researched using a range of indirect techniques. In this chapter, we report an indirect measurement technique which involves the measurement of activity of the zinc-responsive metallothionein 2a (MT2a) promoter when co-expressed with ZnT10 in human intestinal Caco-2 cells (see section 2.7.1). This method has previously been used to demonstrate functional activity of ZnT5 (Valentine et al., 2007). RNA extracted from SH-SY5Y cells was used as a template to clone full-length ZnT10 (see section 2.6.8). A

nested PCR was used in order to generate the appropriate product. Initially the Full-length ZnT10 primers from Table 3.5 were used to generate a 1727 bp product. This PCR mix was subsequently used as the template in a further PCR with the Full-length ZnT10 primers (Table 3.5) to produce a 1455 bp product with *Eco*RI and *Bam*HI restriction sites (Figure 3.9A). The band was excised from a 1 % agarose gel, purified using QIAgen gel purification kit. NEBcutter was used to establish that *Pst*I and *Eco*RV both have one digest site within ZnT10. Restriction digests using these enzymes was carried out to confirm the identity of the PCR product. Incubation of the ZnT10 PCR product with these enzymes yielded fragments of the appropriate sizes (*Pst*I, yielding products of 998 bp and 459 bp, and *Eco*RV, yielding products of 1076 bp and 381 bp; Figure 3.9B). This PCR product was subcloned into a number of vectors including pEGFP-C1 vector (BD Biosciences Clontech; Appendix C) and FLAG-10 (Appendix D) using standard methodology. None of the restriction digests with *Eco*RI and *Bam*HI gave a 1455 bp drop out indicating that the cloning reactions were unsuccessful. An alternative method was employed and the full-length ZnT10 PCR product generated using *Taq* polymerase, was subcloned using TA cloning into TOPO TA pCR2.1 vector (Appendix A). Restriction digests with *Eco*RI and *Bam*HI gave the expected 1455 bp drop out (Figure 3.10Ai). To further confirm the correct insert the TOPO TA-ZnT10 construct was used as a template for PCR using ZnT10 primers from Table 3.4 (Figure 3.10Aii) Identity was confirmed by sequencing and no mutations were observed (MWG Biotech). This enabled us to produce an increased concentration of the construct which was subsequently cloned into the p3xFLAG-CMV-10 (Sigma) vector. Restriction digests of the p3xFLAG-ZnT10 construct with *Eco*RI and *Bam*HI confirmed the presence of the correct size drop out product (Figure 3.10B). Sequencing (MWG

Biotech) was used to confirm the presence of the correct insert, without mutation and in-frame with the N-terminal FLAG epitope tag (Appendix F).

This p3xFLAG-ZnT10 construct was used in a promoter reporter assay to indirectly assess functional activity of full-length ZnT10. To determine the effect of increased ZnT10 expression on intracellular zinc concentration the effect of heterologous over-expression of ZnT10 in the p3xFLAG vector on the activity of a zinc-activated reporter gene, comprising the *E. coli* β-galactosidase coding sequence downstream of the zinc-activated human MT2a promoter (pBlue-MT2a) in Caco-2 cells was measured (Helston et al., 2007). This method has been used previously to examine activity of ZnT5vB in this cell line with the same reporter construct (pBlue-MT2a model) (Valentine et al., 2007). Co-expression of ZnT10 (from plasmid p3xFLAG) decreased β-galactosidase activity driven by the MT2a promoter significantly, (approximately two-fold) in standard culture medium compared with cells co-transfected with pBlue-MT2a plus p3xFLAG-BAP vector (no ZnT10 insert). This two-fold decrease was also observed with the addition of 100 μM extracellular zinc when compared with cells co-transfected with pBlue-MT2a plus p3xFLAG-BAP vector (no ZnT10 insert). These results indicate a decrease transcription from the zinc-responsive MT2a promoter and so indicate a decrease in intracellular zinc concentration (Figure 3.11). Therefore, we would speculate that ZnT10 is acting to efflux zinc either out of the cell or into intracellular organelles in line with the majority of other family members.

3.6 Discussion

ZnT10 is thought to be a member of the CDF family, a ubiquitous family of heavy metal transporters first discovered by Nies and Silver (1995). Members of the CDF family are found in all three phylogenetic domains; archaea, bacteria, and eukaryote.

Across kingdoms all CDF family members are broadly involved in the sequestration of both essential and toxic metals. Indeed members of the prokaryotic CDF family are implicated in transport and homeostasis of the cations zinc, cobalt, manganese, iron, cadmium and nickel (Gaither and Eide, 2001a). Plant CDF members are usually referred to as Metal Tolerance Proteins (MTP) whereas their vertebrate equivalents are known as ZnTs or Solute Carrier Family 30 (SLC30). The eukaryotic counterparts have predominantly been investigated for their zinc transporter role and therefore are thought to be involved in homeostasis of the zinc cation (reviewed by Montanini et al., 2007). Furthermore, throughout the phylogeny kingdoms, there is evidence that the majority of proteins that possess the highly conserved CDF motif (Figure 3.6B) act to efflux cations out of the cytoplasm to either outside the cell or into subcellular organelles. Moreover, the structure of this family of transporters has also been conserved in that the majority of CDF proteins possess six putative TMDs, with cytoplasmic N- and C- termini. Such structures have been experimentally demonstrated for bacterial members (Anton et al., 1999, Wei and Fu, 2005), with predictions only for the eukaryotic counterparts. The exception to this is for ZnT1 (Palmiter and Findley, 1995). Importantly, in the context of this research, the two splice variants of ZnT5 (ZnT5vA and ZnT5vB) are exceptions to this common structural rule, having a predicted 15 and 12 TMD, respectively (Kambe et al., 2002, Cragg et al., 2002). The CDF signature sequence is normally found between TMDs I and II (Paulsen and Saier, 1997). Both my investigations and those of Seve et al., (2004) show that ZnT10 appears to follow this common pattern. It is evident, from this previous *in silico* work and confirmed here that ZnT10 has a predicted putative six TMD with the expected intracellular N- and C- termini (Figure 3.2A). I have also confirmed the presence of the CDF motif (SiALLSDSFNmlsDLiS;

Figure 3.2C) between amino acids 34 and 50 which, incidentally, is between TMD I and running into TMD II in line with the position of the motif in other family members.

One area in which ZnT10 does differ from the majority of its ZnT family members is the presence of a basic region consisting of predominantly serine and other basic residues (Arg and Lys) with the absence of histidine entirely from this area (Figure 3.1A). This is opposed to the conserved histidine-rich domain found in most eukaryotic ZnTs between TMD IV and V. However this is not without precedence as ZnT6 has a non-histidine basic region that, in agreement with ZnT10, is between TMD IV and V and therefore is thought to be cytoplasmic (Huang et al., 2002). It is worthy of note that the histidine-rich domains of other ZnT family members are also found between TMD IV and V and are cytoplasmic. The importance of this is thought to be in the metal binding process where these basic residues would be able to coordinate the metal ions for transport across membranes. The serine residues found in ZnT6 and ZnT10 may be retained from the prokaryotic ancestors of the transporters instead of a histidine-rich domain (Huang et al., 2002). Due to the basic nature of both serine and histidine the amino acids share many characteristics implying this area of the protein would have similar properties.

In terms of metal binding, the conservation of Asp 247 and Asp 276 in TMD V and VI of ZnT10 with Asp 599 and Asp 621 in the TMD equivalent to TMD V and VI in ZnT5 is of interest (Figure 3.1B). Both of these residues are thought to be important in coordination of the zinc ion and Asp 599 of ZnT5 has been shown experimentally to be involved in zinc binding (Ohana et al., 2009). Paulsen et al., (1997) hypothesised the importance of these residues in the context of the structure of the ZnTs. This group found that helices I, II, V and VI were amphipathic and that in these TMD the

hydrophobic residues were localised to one side of the helix whereas the semi-polar hydrophilic, and intriguingly more conserved, amino acids are positioned on the opposite side. In this case the arrangement of the TMD would form a central-water filled channel, allowing postulation that the conserved aspartyl residues in TMDs V and VI found on the hydrophilic side would face inwards allowing for cation binding to occur (Paulsen and Saier, 1997). It is reasonable therefore, to assume that ZnT10 could undergo post-translational modification to control its actions or ensure correct topology. There are many databases which allow predictions of such modifications relative to the amino acid sequence. A selection of these programmes have been used here, in order to predict the possibility of modifications.

The first prediction programme used was SignalP, this allows one to ascertain the probability of ZnT10 having a signal peptide which will ensure correct targeting within the cell before cleavage (under normal circumstances). The results of this *in silico* programme predicted that ZnT10 has a signal peptide of 29 amino acids with a cleavage site between G29 and Y30 (Figure 3.2C). Given that this predicted cleavage site is in the N-terminal region, if functional, would need to be taken into consideration when carrying out localisation studies with an N-terminal tagged vector (Chapter 4).

The Net series of databases uses neural networks to predict both glycosylation and phosphorylation sites within proteins. There are two forms of glycosylation; *N*-glycosylation and *O*-glycosylation that correspond to conformational or functional modifications respectively. *N*-glycosylation is the process where N-linked glycans are attached to the nitrogen of side chains of asparagine or arginine. It occurs in the ER ensuring correct protein folding. NetNGlyc predicted 3 *N*-glycoslyation sites at Asp 377, 471 and 481 amino acids in ZnT10. For the functional modification *O*-

glycosylation, *O*-linked glycans are attached to an hydroxyl oxygen of serine, threonine, tyrosine, hydrolysine or hydroxyproline side chains. One such site is predicted in ZnT10 at Thr 183 using NetOGlyc.

Phosphorylation is as a functional modification where a phosphate is added to the side chain of a serine or, less commonly, either threonine or tyrosine residue within mature proteins. This phosphorylation, acts to activate or deactivate many proteins or enzymes. Within ZnT10 there are 15 predicted sites with 7 serine residues and 4 of each threonine and tyrosine residues. These data are summarised in Table 3.2. One relatively unexplored avenue of research into ZnTs is experimental evidence of post-translational modifications. It is evident that a CDF family member found in yeast, Zrt1, is ubiquitinated and therefore internalised at high concentrations of zinc (Gitan et al., 2003) and similar mechanisms have been found for the ubiquitination of some mammalian plasma membrane proteins e.g. the growth hormone receptor undergoes endocytosis due to the ubiquitination machinery (Hicke, 1997). Of more relevance to this study, Western blot analysis of ZnT7 produced many bands on a gel (Kirschke and Huang, 2003). One hypothesis the authors drew from this was that ZnT7 could be modified e.g. glycosylated post-translationally. Furthermore the phosphorylation of both ZIPs and ZnTs is thought to be widespread throughout the families with ZnT1, ZnT3, ZnT6, ZIP3, ZIP6, ZIP7, ZIP8 and ZIP10 shown to be phosphorylated at more than one site (summarised in Hogstrand et al., 2009). In fact the authors hypothesise that the presence of multiple phosphorylation sites may play an important role in zinc transporter function, a theory that needs to be investigated experimentally. The prediction of post-translational modifications for ZnT10 has yielded a number of interesting findings. In particular the prediction of 15 phosphorylation sites supports the hypothesis that these are required for zinc transporter function.

Information published previously concerning ZnT10 expression is limited. An article reporting *in silico* analysis of the tissue expression profile of members of the SLC30 (ZnT) zinc transporter family based on data mining for ESTs reported in cDNA libraries has been published (Seve et al., 2004). This analysis indicated that ZnT10 expression was restricted to foetal liver and foetal brain and that foetal-specific expression was unique to ZnT10 within the family. I report here confirmation that ZnT10 is expressed in foetal tissues but also identify a pattern of differential expression in adult tissue, using a human RNA tissue panel analysed by both semi-quantitative RT-PCR and RT-qPCR. Expression in adult tissue was not restricted to human tissue and Znt10 expression was observed in adult mouse brain, but not adult mouse kidney, mirroring approximately the relative levels of expression of ZnT10 in the tissues in humans (Figure 3.4). The presence in adult tissue is in agreement with a very recent paper that has been published simultaneously with the completion of this PhD research that also establishes the presence of ZnT10 in adult tissue (Patrushev et al., 2012).

Although exact relative levels of ZnT10 mRNA expression differed slightly between the two methods and with the two reference genes, it was observed that ZnT10 expression levels were highest in liver, brain, small intestine and testes and lowest in ovary and cervix, by all three methods. The exception to this was expression in the colon, where I observed high levels of ZnT10 by semi-quantitative analysis but lower levels by RT-qPCR relative to both reference genes (GAPDH and TOPI). The real-time analysis also indicated very small amounts in the placenta and prostate (prostate tissue RNA was not present in the original RT-PCR analysis). These inconsistencies in relative levels highlight some of the limitations of the techniques and indeed the importance of appropriate use of reference genes. For example, semi-quantitative RT-PCR does not have the sensitivity of RT-qPCR therefore the placental expression was not evident

from this analysis. In addition semi-quantitative RT-PCR indicated high levels of ZnT10 transcript in the colon, a result disputed by the use of RT-qPCR compared with both TOPI and GAPDH. RT-PCR is an end-point reaction and whilst the PCR experiment did not reach saturation we cannot be sure that we are measuring the level of PCR product at the same point on the curve for all reactions thus we can only measure ZnT10 mRNA levels semi-quantitatively.

The RT-qPCR showed small discrepancies between results relative to GAPDH and TOPI. For both GAPDH and TOPI there are two groups of tissues – those with high expression and those with low expression. The differences lie in those tissues in the high expression group. Relative to GAPDH expression of ZnT10 was highest in the small intestine > liver > testes > brain tissue compared with highest levels of expression in liver > brain > testes > small intestine relative to TOPI. However there is agreement for both reference genes in the tissues with relatively low levels of tissue expression ovary > colon > cervix > prostate > placenta. Where possible, more than one reference gene should be used in analysis but here the apparent difference in the order of expression for RT-qPCR analysis can be attributed to the use of different reference genes. TOPI (DNA topoisomerase I) is involved in transcription, it is an enzyme that is important in the transient breaking and re-joining of a single strand of DNA to allow it to pass through one another thereby altering the topology of the DNA. It follows that during proliferation events, such as cell proliferation in cancer progression, TOPI is up-regulated (Romer et al., 2012, Nishioka et al., 2011). The tissue panel used is compiled from pooled RNA from tissues from at least three human post-mortem donors (Life Technologies). This is worth taking into consideration as the cause of death could be a factor in the alteration of transcript levels of TOPI, thereby altering relative ratios in the tissues tested. The other reference gene chosen, GAPDH has been shown to be

expressed at different levels dependent on tissue type (Barber et al., 2005). Further analysis indicates that these differences are small since when the top and bottom members of the 'high group' are compared as a ratio to GAPDH no significant difference between the highest level of expression (small intestine) compared with the lowest level of expression in this group (brain; $p = 0.2$ by Student's *t*-test) is observed. When I carried out the same analysis relative to TOPI there was no significant difference between the observed highest expression levels (liver) with lowest (small intestine; $p = 0.551$ by Student's *t*-test). Moreover, for both reference genes there are significant differences between the 'high group' and the 'low group'; brain versus ovary relative to GAPDH ($p = 0.007$ by Student's *t*-test) and small intestine versus ovary relative to TOPI ($p = 0.027$ by Student's *t*-test).

Importantly, throughout the three experiments the tissues in which there was expression are constant thus proving a differential expression pattern for ZnT10. The expression in small intestine, liver and brain perhaps reflects a role for ZnT10 in zinc systemic homeostasis through the regulation of intestinal and hepatic uptake/efflux and in brain where zinc plays a specific role in the modulation of synaptic transmission.

In terms of zinc transport function, efflux is a characteristic of the CDF family however, in the case of the ZnTs these measurements have predominantly been indirect observations of zinc transport i.e. the effect of transporter expression on cellular responses to zinc. One method of indirect measurement is in cell 'rescue' by transfection of a zinc transporter into a system which, under normal conditions, displays defective zinc transport. An example of this is the investigation of zinc transport for Znt4. Over-expression of a Znt4 construct in *Δzrc*, a yeast model that has a defective zinc vacuolar transporter (ZRC1) was able to rescue the growth of *Δzrc* in a high-zinc

medium (Huang and Gitschier, 1997). The same *Δzrc* yeast model was used to assess the zinc transport ability of Znt6, yet in this instance the growth was not rescued. However, the yeast models *Δzrt1*, *Δzrt3* and *Δmcs2* all have defects such that they exhibit a severe decrease in cytoplasmic zinc concentrations. For *Δzrt1* the defect is in the high affinity zinc uptake protein but for both *Δzrt3* and *Δmcs2* there are defects in the relocation of zinc from the vacuoles, ER and nucleus to the cytoplasm. With the over-expression of Znt6 and treatment with 1.0 mM $ZnCl_2$, the growth inhibition seen in these mutants was partially alleviated and thus Huang et al., 2002 conclude that Znt6 does transport zinc. Furthermore, the role of heterodimerisation between ZnT5 and ZnT6 has been studied more recently. TNAP activity has been proposed as a marker to measure zinc supply to the zinc-requiring enzymes in the secretory pathway (Suzuki et al., 2005a). Co-transfection of ZnT5 and ZnT6 constructs restored TNAP activity in DT40 $ZnT6^{-/-}$ cells whereas transfection of ZnT6 independently failed to change TNAP activity. Moreover, co-immunoprecipitation studies revealed that ZnT6 forms a hetero-dimer with ZnT5 indicating that ZnT6 is able to transport zinc when it is able to form a hetero-dimer with ZnT5 (Suzuki et al., 2005b).

Zinc sensitive fluorescent dyes and fluorescent probes have also been a useful tool in determining the function of ZnTs. Over-expression of the ZnTs is consistent throughout the ZnT functional experiments. The role of Znt7 in zinc transport has been investigated by using Znt7-*myc*-expressing CHO cells and the fluorescent zinc probe Zinquin. Results revealed increased extracellular zinc lead to accumulation of vesicular zinc in the perinuclear regions, implying an efflux role of Znt7 out of the cytoplasm and into these vesicles (Kirschke and Huang, 2003). The studies relating to ZnT8 are similar in methodology. A ZnT8 construct tagged with a GFP epitope was transfected into HeLa cells and assessed under different zinc conditions again, using the Zinquin probe.

Fluorescence microscopy results indicated that expression of ZnT8-EGFP leads to zinc accumulation in intracellular vesicles in the presence of extracellular zinc (Chimienti et al., 2004). However in β-cells (MIN6 cells), where ZnT8 is endogenously expressed, over-expression of ZnT8 and use of the fluorescent probes Zinquin, FluoZin-3 and RhodZin3-AM showed an influx of zinc at the plasma membrane in addition to the accumulation of zinc in the secretary granules eluded to above (Nicolson et al., 2009).

Promoter reporter assays have been used for numerous studies into the functional activity of ZnTs. Measurements for Znt1, Znt2 and Znt3 were taken in zinc sensitive baby hamster kidney (BHK) cells stably expressing the MRE-βGeo construct that were transfected with the appropriate construct and treated with high levels of extracellular zinc. Transfection of Znt1 or Znt2 into this cell line resulted in the reduction of basal β-galactosidase activity therefore implying a decrease in intracellular zinc concentration. This approach was validated by the fact that efflux of radioactive ^{65}Zn was increased in cells transfected with Znt1 (Palmiter and Findley, 1995). Znt1 efflux has also been implicated in neuronal zinc homeostasis with transfection of rat Znt1, wild-type and a mutated version, into the neuronal PC12 cells. The mutant was a negative dominant (ND) mutation lacking an 83 bp region. In support of previous research it was found that wild-type Znt1 was able to increase zinc efflux and therefore provide a zinc resistance system in the cells conversely, the mutant displayed the opposite effect (Kim et al., 2000). In comparison, investigation with the zinc fluorescent probe Zinquin showed Znt2 acts to accumulate zinc into intracellular vesicles (Palmiter et al., 1996a). Interestingly for Znt2 the construct was made with a fluorescent tag so it could be visualised and this transporter co-localised in the vesicles with Zinquin.

Use of both promoter reporter assays and zinc sensitive fluorescent probes were used to assess the function of Znt3. This Znt behaves slightly differently to Znt1 and Znt2 in that there is no change in the BHK cells with over-expression of the construct in response to zinc, or incidentally other heavy metals (copper, cobalt, or cadmium), with no evident Zinquin fluorescence (Palmiter et al., 1996b). The authors suggest that this is due to the absence of an unknown necessary chaperone protein(s) that would be expressed in an endogenous situation. No other functional experiments have been carried out for Znt3 however disruption of the *Znt3* in the *Znt3* null mouse model shows an absence of vesicular zinc in neurons indicating that Znt3 is important in zinc accumulation in the synapses (Cole et al., 1999).

A combination of the techniques described above has been used to assess ZnT5 functionality. However, ZnT5 is unique in the investigation of efflux as both direct and indirect measurements have been used. Interestingly, this is also the only ZnT thus far that has shown zinc transport to be bi-directional (Valentine et al., 2007). In 2002, ZnT5 was shown to act as an effluxer, by indirect measurements by over-expressing a ZnT5 construct in HeLa cells and assessing the uptake of ^{65}Zn. ZnT5 transfection enabled ^{65}Zn uptake into Golgi-enriched vesicles from HeLa cells thereby decreasing cytosolic zinc (Kambe et al., 2002). However, work carried out at the same time found differing results. Using functional expression of ZnT5 in *Xenopus laevis* oocytes it was reported that there is a progressive increase of ^{65}Zn across the plasma membrane and therefore it was concluded that ZnT5 has the ability to import zinc and increase cytoplasmic zinc concentration (Cragg et al., 2002). The differences between these two pieces of research may be explained by distinguishing between the two splice variants. Kambe et al., (2002) were looking at the function of ZnT5vA and Cragg et al., (2002) at ZnT5vB. Furthermore, subsequent direct investigation into ZnT5vB (i.e. the *Xenopus Laevis*

model (Valentine et al., 2007)) showed that this isoform has bi-directional properties. In addition, indirect measurement of ZnT5vB confirmed zinc transport in the influx direction in a physiologically relevant cell line, Caco-2 cells. In this model system the effect of increased ZnT5 transporter expression on the intracellular zinc status was analysed by measuring the response of a β-galactosidase gene to zinc driven by a zinc responsive MT2a construct (Valentine et al., 2007). Furthermore, this study used the zinc sensitive fluorescent probe Rhodzin-3 to demonstrate the accumulation of zinc in Caco-2 cells transiently transfected with the N-terminal GFP tagged ZnT5vB construct further confirming the uptake of zinc by this variant.

ZnT9 has been found to be implicated in the redistribution of mammary gland zinc pools and the secretion of zinc into milk but despite its implication in the "Zn-transporting network" functional studies on the proposed transporter have yet to be carried out (Kelleher et al., 2011). Similarly, the functional role of ZnT10 has not been investigated previously and thus I measured the functional ability of ZnT10 in a physiologically relevant cell type where I have shown ZnT10 to be endogenously expressed. The effect of over-expression of ZnT10 on the intracellular zinc status of the human intestinal cell line Caco-2 was determined by measuring the activity of a zinc-stimulated reporter gene. This has been described previously to demonstrate the zinc uptake function of ZnT5 (Valentine et al., 2007). Moreover, a comparative study by Palimter et al., (1995) goes some way to validate promoter reporter assays. Decreased activity of the zinc-responsive MT2a promoter when ZnT10 was co-expressed in Caco-2 cells indicated a decrease in total intracellular zinc content and so I predict that ZnT10 is a putative effluxer in accordance with the other ZnT family members (Figure 3.11). Whilst direct measurements would strengthen this result this would involve the use of radioactive zinc (^{65}Zn) and therefore would pose a number of health and safety risks. It

is also not known whether the use of the *Xenopus laevis* model system (as used for ZnT5) is optimal, for these zinc transporters as in this system bi-directional capacity can be shown, depending on the experimental conditions (Valentine et al., 2007). However, the indirect measurement used in this research has previously been reported to be suitable and consistent with direct measurements for ZnT5vB. In addition, the promoter reporter assays using a similar system have been used and reported for Znt1, Znt2 and Znt3 (Palmiter and Findley, 1995, Palmiter et al., 1996a, Palmiter et al., 1996b, Valentine et al., 2007). Therefore, I believe the results reported demonstrate ZnT10 activity as a putative effluxer of zinc, although limitations for all methods should be kept in mind.

Data presented in this chapter furthers our understanding of the characteristics of the CDF family member ZnT10. In summary I have found that ZnT10 contains the conserved CDF motif placing it in this family. In addition, predicted topology modelling indicate that ZnT10 has the conserved structure of six TMD with a basic cytoplasmic region between TMD IV and TMD V. In addition there are conserved residues in TMD V and VI that are hypothesised to be involved in the binding of zinc. ZnT10 is predicted to have a 29 amino acid signal peptide sequence at its N-terminal. Post-translationally ZnT10 is predicted to have 3 *N*-glycosylation sites, 1 *O*-glycosylation site and 15 possible sites for phosphorylation. I have found ZnT10 to be differentially expressed in adult human tissues with relatively high levels in small intestine, liver, brain and testes and lower levels in ovary, colon, cervix, placenta and prostate. Finally I provide evidence that ZnT10 is a functional zinc transporter and show indirectly that it reduces cytoplasmic zinc and therefore propose ZnT10 transports in the efflux direction.

	TMPred	TMHMM
TMD I	aa 12-22	aa 12-22
TMD II	aa 42-61	aa 42-60
TMD III	aa 82-102	aa 81-101
TMD IV	aa 115-133	aa 115-135
TMD V	aa 245-265	aa 241-263
TMD VI	aa 281-299	aa 277-299

Table 3.1 Predicted topology of ZnT10. The programmes used were TMPred and TMHMM

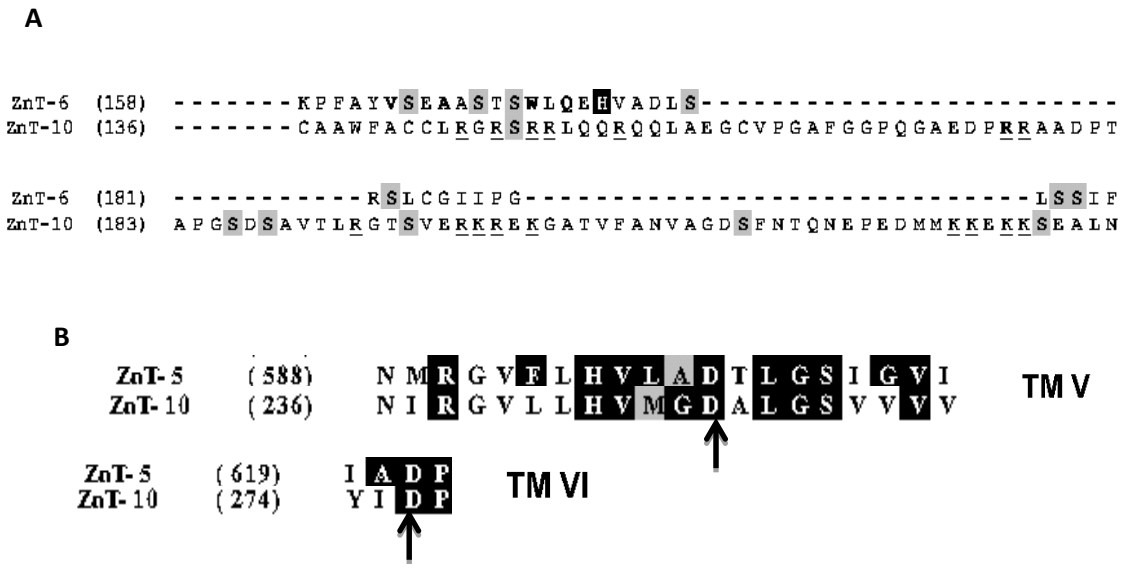

Figure 3.1 ZnT10 sequence alignments A. Partial sequence alignment of the basic region of ZnT6 and ZnT10 using the ClustalW programme. Histidine residues are highlighted in black, serine residues highlighted in grey and additional ZnT10 basic residues are underlined **B.** Partial sequence alignment of TMD V and VI of ZnT10 with the equivalent regions in ZnT5 using the ClustalW programme (adapted from Seve et al., 2004)

A

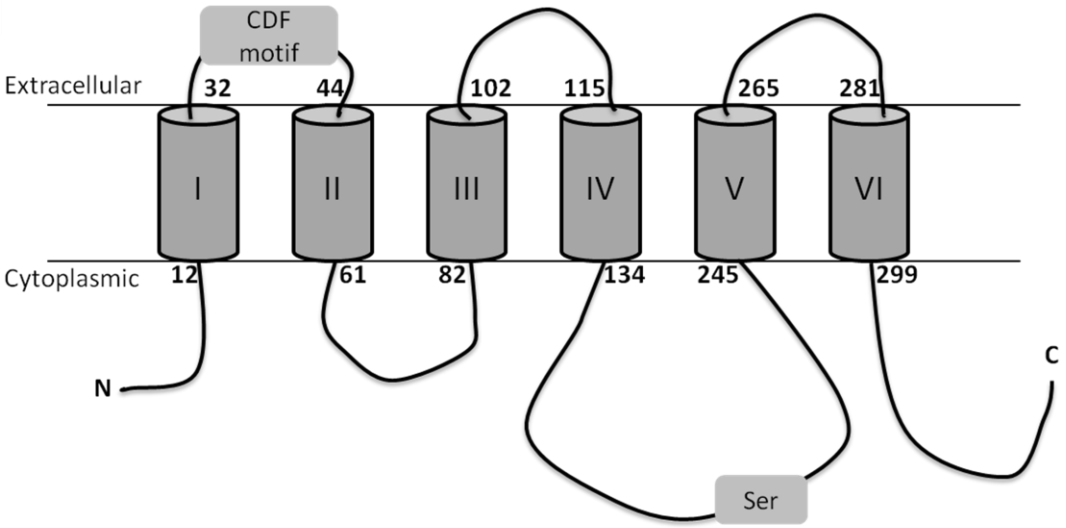

B

SX[ASG][LIVMT][LIVMT][SAT][DA][SGAL][LIVFYA][HDN]X(3)DX(2)[AS]

C

MGRYSGKTCRLLFMLVLTVAFFVAELVSGIYLGNSIALLSDSFNMLSDLISLCVGLSA

GYIARRPTRGFSATYGYARAEVVGALSNAVFLTALCFTIFVEAVLRLARPERIDDPEL

VLIVGVLGLLVNVVGLLIFQDCAAWFACCLRGRSRRLQQRQQLAEGCVPGAFGGPQ

GAEDPRRAADPTAPGSDSAVTLRGTSVERKREKGATVFANVAGDSFNTQNEPEDMM

KKEKKSEALNIRGVLLHVMGDALGSVVVVITAIIFYVLPLKSEDPCNWQCYIDPSLTV

LMVIIILSSAFPLIKETAAILLQMVPKGVNMEELMSKLSAVPGISSVHEVHIWELVSGKI

IATLHIKYPKDRGYQDASTKIREIFHHAGIHNVTIQFENVDLKEPLEQKDLLLLCNSPCI

SKGCAKQLCCPPGALPLAHVNGCAEHNGGPSLDTYGSDGLSRRDAREVAIEVSLDSC

LSDHGQSLNKTQEDQCYVNRTHF

Figure 3.2 A bioinformatic profile of ZnT10 A. Topology Model of ZnT10 using TMPred **B.** CDF motif consensus sequence where [] = can be a number of amino acid, X(n) a run of any amino acid, no brackets it must be that amino acid **C.** Predicted protein sequence. Highlighted in yellow; Position 34-50 CDF motif sequence SIALLSDSFNmlsDLiS; Underlined transmembrane domains according to TMPred; Highlighted in purple; Signal peptide cleavage site amino acid 29; Highlighted in green; N-glycosylation sites amino acid 377, 471 and 481; Highlighted in blue; O-glycosylation sites amino acid 183; Highlighted in red; phosphorylation sites,7 serine amino acid 5, 69, 149, 197, 233, 363, 446, 4 threonine amino acid 8, 192, 196, 219, 4 tyrosine amino acid 278, 359, 440, 479.

Modification	Amino Acid	Score
N-glycosylation	Asp 377	0.7864
	Asp 471	0.6268
	Asp 481	0.5148
O-glycosylation	Thr 183	0.595
Phosphorylation	Ser 5	0.955
	Ser 69	0.852
	Ser 149	0.609
	Ser 197	0.998
	Ser 233	0.754
	Ser 363	0.862
	Ser 446	0.998
	Thr 8	0.732
	Thr 192	0.974
	Thr 196	0.928
	Thr 219	0.839
	Tyr 278	0.631
	Tyr 359	0.836
	Tyr 440	0.885
	Tyr 479	0.957

Table 3.2 Predicted modification sites of ZnT10. The programme used were NetNGlyc, NetOGlyc and NetPhos respectively.

Name/ Accession Number	Primer Sequences	Amplicon Length (bp)	Annealing Temp (°C)
Znt1 NM_009579	5'-$_{1575}$CTG GGA AGG ATG CAG AGA AG$_{1594}$-3' 5'-$_{1731}$GAT GAT TCG GGC TGT TTG TT$_{1711}$-3'	157 bp	60
Znt2 NM_001039677	5'-$_{266}$CGG TCC TTC TTA GGA TCT CTG$_{286}$-3' 5'-$_{376}$CTT CTG GGC ATG GCA ATA ATG G$_{355}$-3'	111 bp	60
Znt3 NM_011773	5'-$_{736}$GTG CCA ATC TGC TAA TGG CC$_{755}$-3' 5'-$_{847}$GAC ATT GGG TAT CCA TGC CC$_{828}$-3'	112 bp	60
Znt4 NM_011774	5'-$_{627}$GCT TGT AGG TGG ATA CAT GGC$_{647}$-3' 5'-$_{749}$GTT GGT GAC TTT GAG GAC AG$_{730}$-3'	123 bp	60
Znt5 NM_022885	5'-$_{1513}$GTG CTT GAA TCT GCT TTT TAC C$_{1534}$-3' 5'-$_{1641}$GCA GCA AAC AGT CCC ATG AC$_{1622}$-3'	129 bp	60
Znt6 NM_144798	5'-$_{33}$CCA TGG GGA CGA TTC ATC TC$_{62}$-3' 5'-$_{166}$GCA CAG CAC GTT GAT TGC AC$_{145}$-3'	134 bp	60
Znt7* NM_023214	5'-$_{470}$GAG CAG AAG TCC TGG CTG GC$_{488}$-3' 5'-$_{579}$GTG GTG CAC ATC TGG AGG AGC$_{559}$-3'	110 bp	60
Znt8 NM_172816	5'-$_{397}$CTA GAC AGA GAA CTT CGA CAG$_{417}$-3' 5'-$_{532}$CTT GCT TGC TCG ACC TGT TC$_{513}$-3'	136 bp	60
Znt9 NM_178651	5'-$_{238}$CAG GGA TGG AAG AAT GTA ATG$_{258}$-3' 5'-$_{379}$CTT TTG GAG TCT GTG AGC CC$_{360}$-3'	142 bp	56
Znt10 NM_001033286	5'-$_{826}$GTA GCA GGT GAT TCC CTG AAC$_{846}$-3' 5'-$_{965}$GTG ATG ACC ACA ACC ACG GAC$_{945}$-3'	140 bp	60
Mt1 NM_013602	5'-$_{308}$GCA AGA AGA GCT GCT GCT CC$_{327}$-3' 5'-$_{448}$CCG ATA CTA TTT ACA CGT GGT G$_{427}$-3'	141 bp	60
18S rRNA NM_011296	5'-$_{117}$CAT TAA GGG CGT GGG GCG G$_{135}$-3' 5'-$_{247}$GTC GTG GGT TCT GCA TGA TG$_{228}$-3'	131 bp	60/56

Table 3.3 RT-PCR primers used on mouse brain RNA to generate Znts, Mt1 and 18S rRNA. The numbering on each of the oligonucleotides represents its position on the gene. *(Helston et al., 2007).

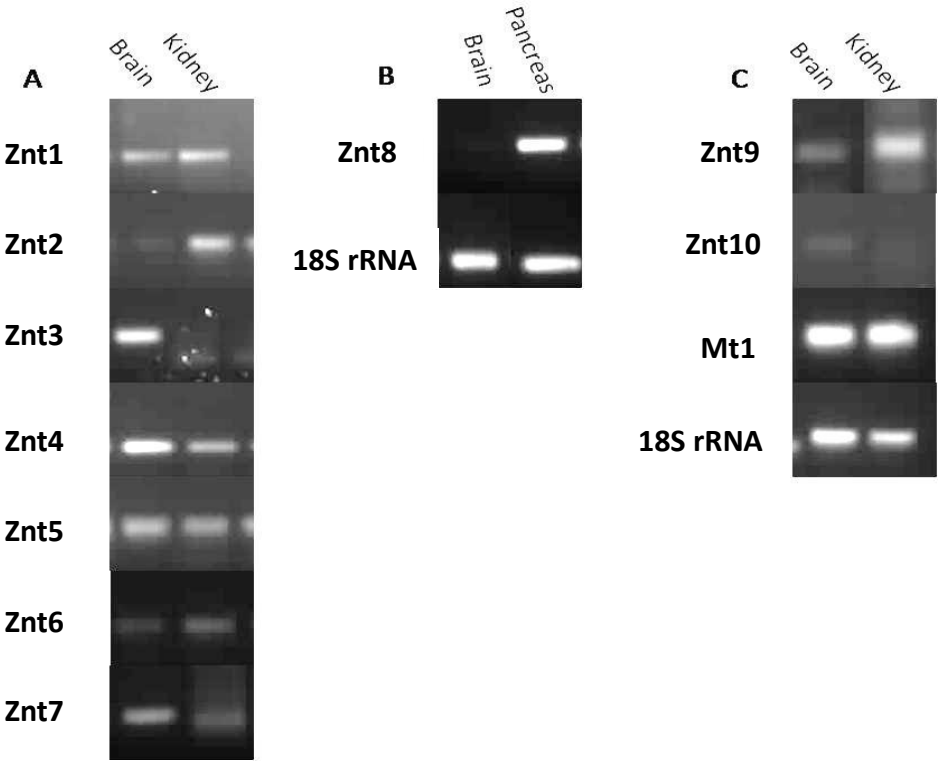

Figure 3.3 Expression of Znts and the positive controls (Mt1 and 18S rRNA). **A.** Znt1-7 expression in mouse brain and kidney. **B.** Expression of Znt8 and the reference gene 18S rRNA in the mouse brain and pancreas. **C.** Expression of Znt9, Znt10 and Mt1 (an additional positive control) and 18S rRNA in the mouse brain and kidney. Negative control RT-PCR reactions identical to those yielding the products shown except for the omission of Superscript III reverse transcriptase resulted in no products.

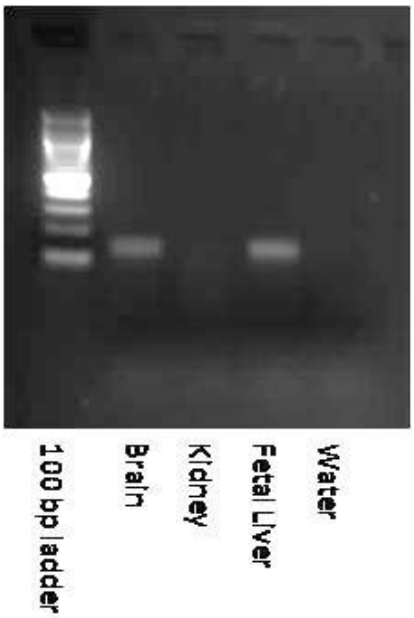

Figure 3.4 Confirmation of expression in adult mouse tissue. Znt10 is expressed in adult mouse brain, but not adult mouse kidney. Primers used given in Table 3.3. Bands were generated by RT-PCR from RNA samples extracted from mouse tissues indicated. Negative control RT-PCR reactions identical to those yielding the products shown except for the omission of Superscript III reverse transcriptase resulted in no products.

Name/ Accession Number	Primer Sequences	Amplicon Length (bp)	Annealing Temp (°C)
ZnT10 NM_018713.2	$5'_{-844}$CGT AGC AGG TGA TTC CTT CAA C_{865}-3' $5'_{-956}$CAT CTC CCA TCA CAT GCA AAA G_{935}-3'	113 bp	RT-PCR 56.2 qPCR 60
GAPDH* NM_002046.3	$5'_{-113}$TGAAGGTCGGAGTCAACGGCTTTG$_{136}$-3' $5'_{-240}$CATGTAAACCATGTAGTTGAGGTC$_{217}$-3'	128 bp	RT-PCR 56.2 qPCR 60

Table 3.4 Primer sequences for human ZnT10 and GAPDH RT-PCR and RT-qPCR analysis *(Valentine et al., 2007)

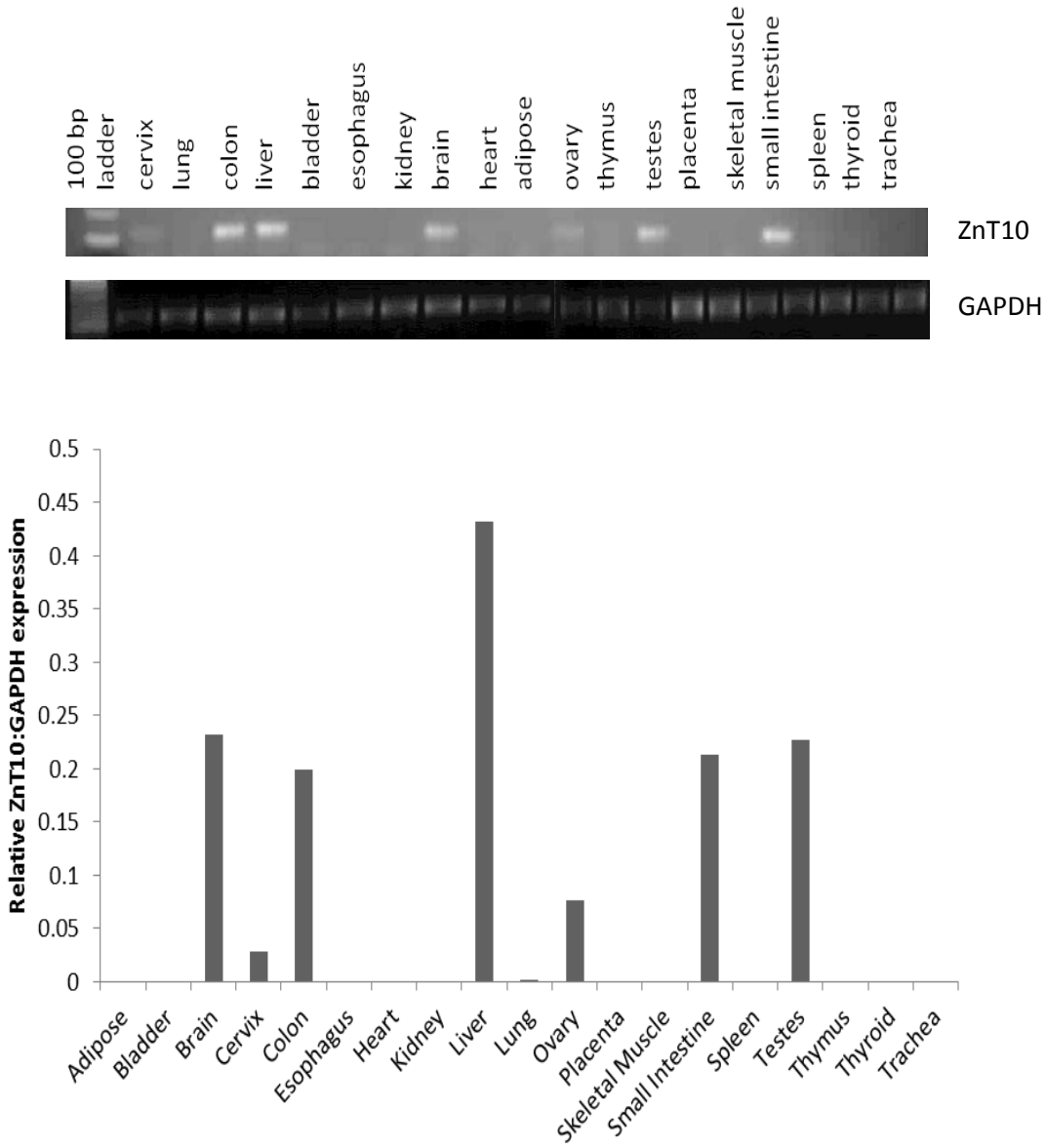

Figure 3.5 ZnT10 mRNA is expressed in adult tissues. Relative levels of ZnT10 mRNA in a range of adult human tissues (Ambion human tissue panel) measured by semi-quantitative RT-PCR, using *Taq* polymerase (New England Biolabs). Data are expressed relative to glyceraldehyde-3-phosphate dehydrogenase (GAPDH) mRNA levels measured in the same samples. Negative control RT-PCR reactions identical to those yielding the products shown except for the omission of Superscript III reverse transcriptase resulted in no products.

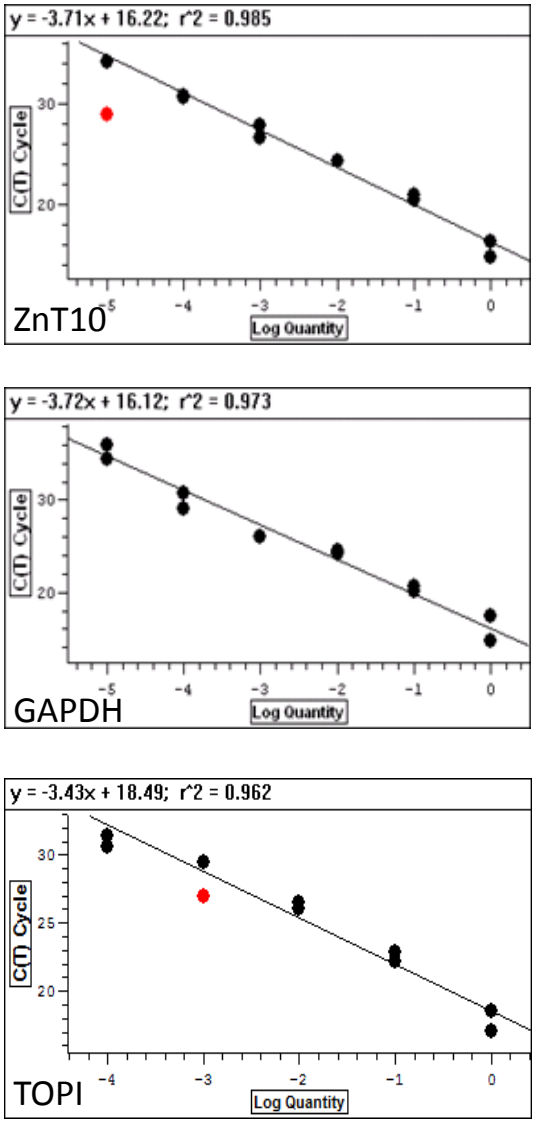

Figure 3.6 Standard curves generated to measure relative levels of ZnT10 by RT-qPCR, using SYBR green fluorescence and the DNA Engine Opticon 2 (MJ Research). Standards for GAPDH and ZnT10 products were generated by amplifying the region between the primers shown in Table 3.4, and subcloned into the vector pCR2.1-TOPO TA (Invitrogen). TOPI primers were purchased from PrimerDesign. A TOPI PCR product was produced and subcloned into the pGEM-T-easy vector to give the standard TOPI-pGEM (generated by Dr Alison Howard). The mean log concentration of each dilution was plotted against PCR cycle number at which the fluorescent threshold was crossed (C_T).Excluded data points are shown in red. These standard curves were used to calculate relative levels of ZnT10 transcripts.

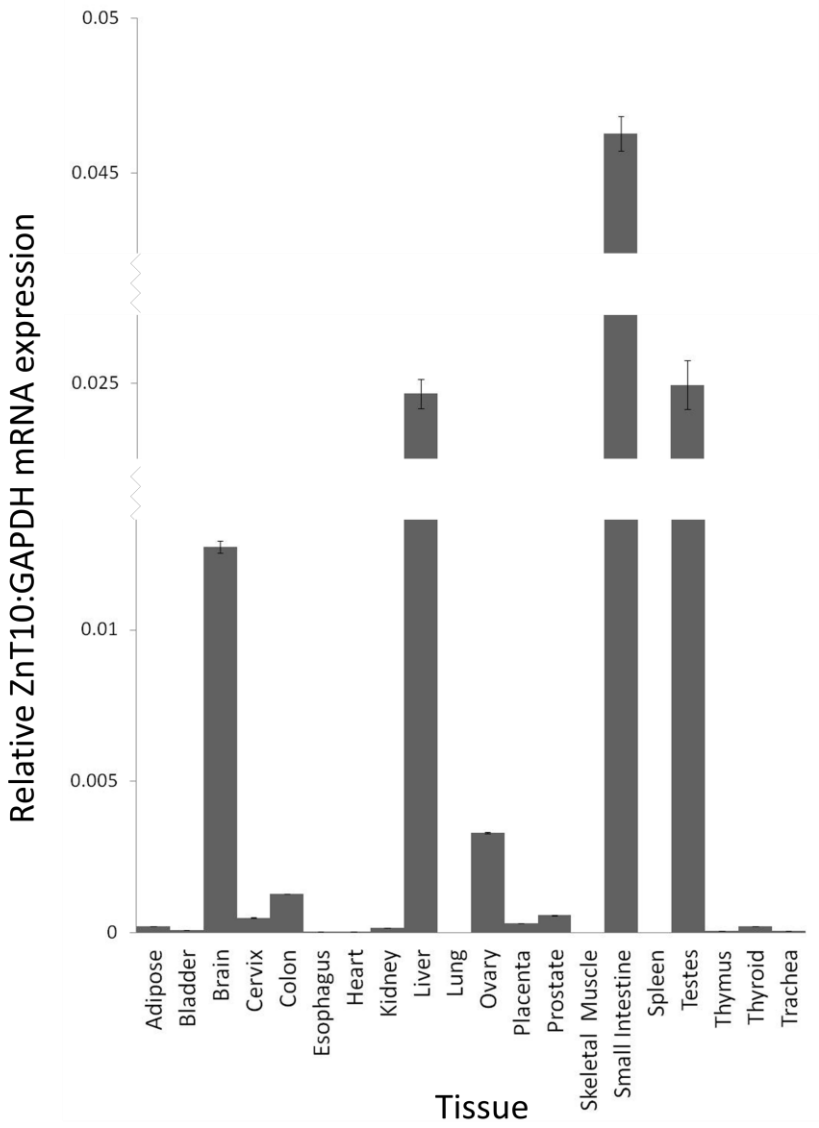

Figure 3.7 ZnT10 mRNA expression in adult tissues relative to GAPDH. Relative levels of ZnT10 mRNA in a range of adult human tissues (Ambion human tissue panel) measured by RT-qPCR, using SYBR green fluorescence and the DNA Engine Opticon 2 (MJ Research). Data are expressed relative to glyceraldehyde-3-phosphate dehydrogenase (GAPDH) mRNA levels measured in the same samples. Values are means (n = 3), with standard errors represented by vertical bars.

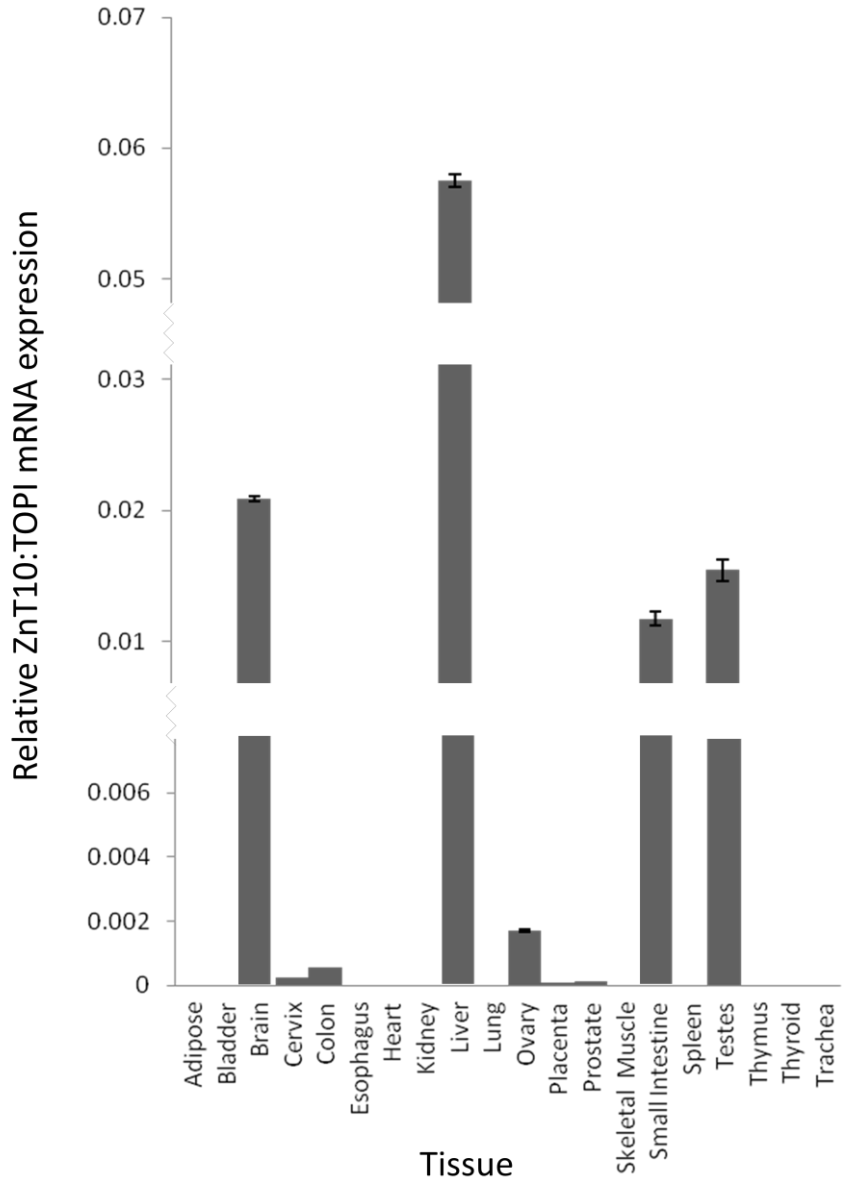

Figure 3.8 ZnT10 mRNA expression in adult tissues relative to TOPI. Relative levels of ZnT10 mRNA in a range of adult human tissues (Ambion human tissue panel) measured by RT-qPCR, using SYBR green fluorescence and the DNA Engine Opticon 2 (MJ Research). Data are expressed relative to topoisomerase I (TOPI) mRNA levels measured in the same samples. Values are means (n = 3), with standard errors represented by vertical bars.

Name/ Accession Number	Primer Sequences	Amplicon Length (bp)	Annealing Temp (°C)
Full ZnT10 NM_018713.2	$5'_{-212}$ATGGGC CGCTACTCTG$_{228}$-3′	1727 bp	58
	$5'_{-1726}$ GCCAAGCTTGTGGTTCCAAAGTG$_{1705}$-3′		
	$5'_{-1666}$AAAATGCGTTCTGTTGACATAACATTG$_{1640}$-3′	1455 bp	58

Table 3.5 RT-PCR primers used to generate full-length ZnT10 construct by nested RT-PCR. The numbering on each of the oligonucleotides represents its position on the gene.

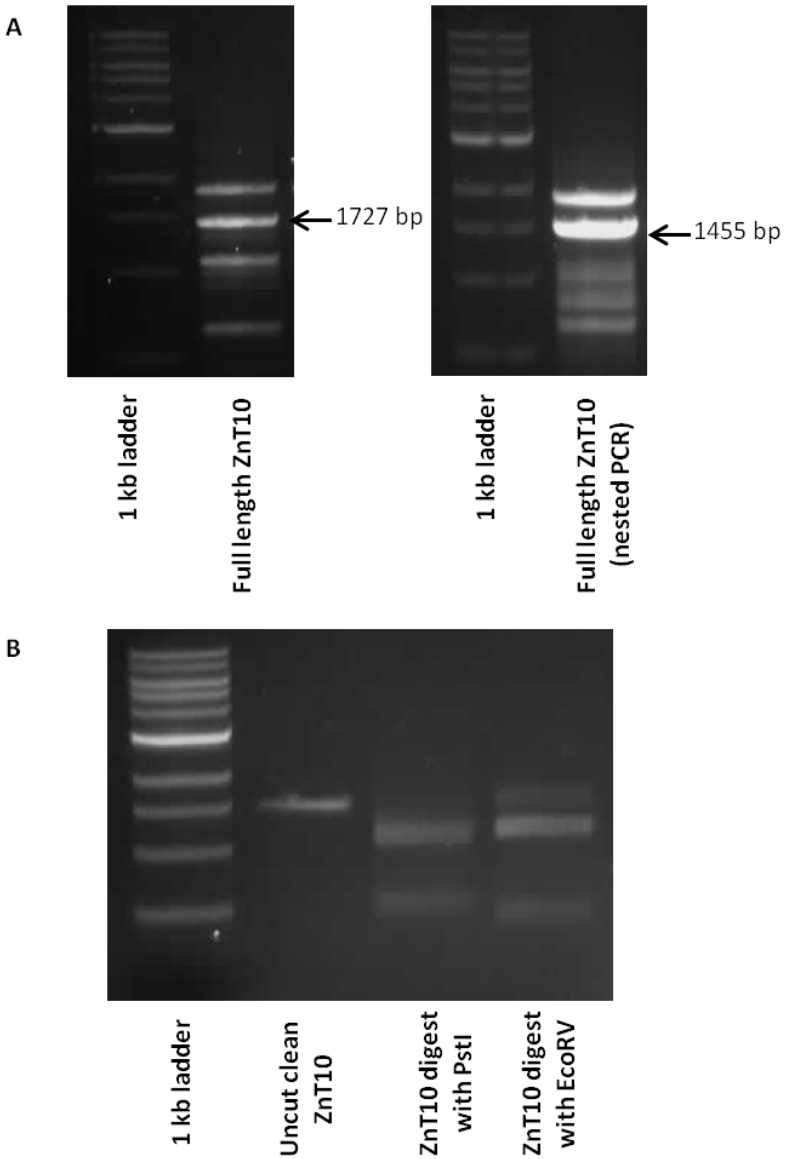

Figure 3.9 Generation of full-length ZnT10 PCR product A. Nested PCR products for full-length ZnT10 from SH-SY5Y RNA using primers in Table 3.5 **B.** Confirmation of PCR product after PCR clean-up (QIAgen) using restriction enzymes *Pst*I, yielding products of 998 bp and 459 bp, and *Eco*RV, yielding products of 1076 bp and 381 bp.

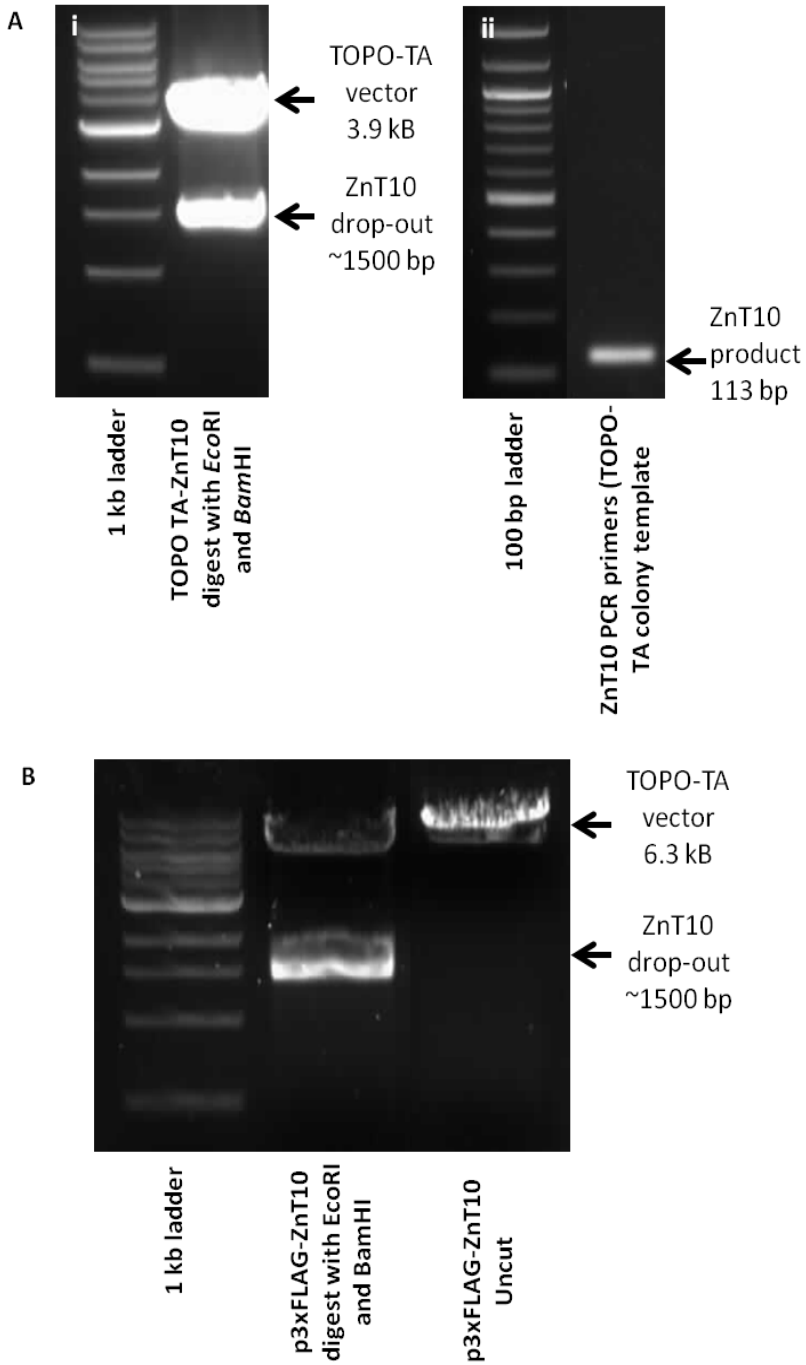

Figure 3.10 Analysis of full-length construct A. Confirmation of insert presence in TOPO-TA vector **(i)** using a restriction digest with enzymes *Eco*RI and *Bam*HI **(ii)** using ZnT10 RT-PCR primers (Table 3.4) and TOPO-TA-ZnT10 as a template **B.** Confirmation of insert presence in p3xFLAG vector using a restriction digest with enzymes *Eco*RI and *Bam*HI. Identity was confirmed by sequencing (MWG Biotech).

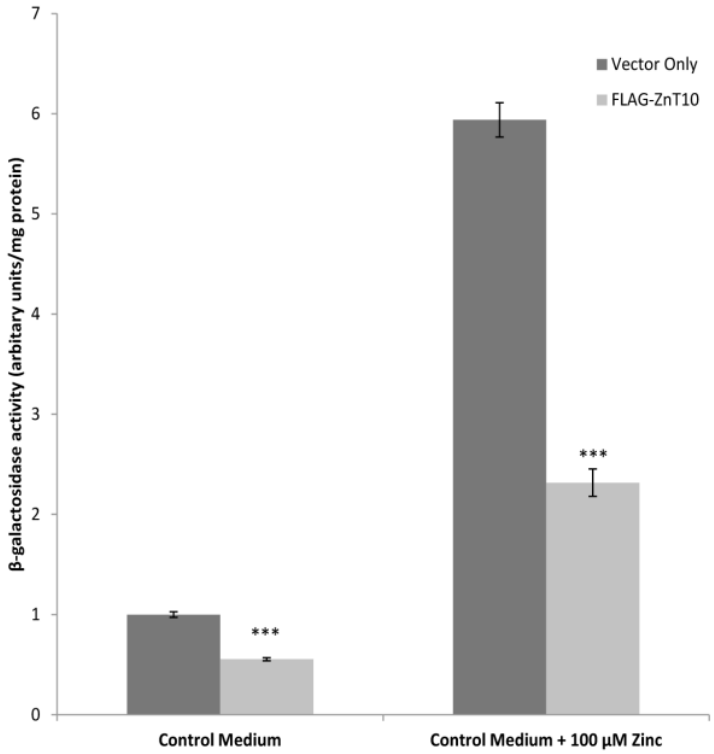

Figure 3.11 The effect of ZnT10 expression on the activity of the zinc-activated MT2a promoter. Data are β-galactosidase activity in lysates from Caco-2 cells co-transfected transiently with an MT2a-promoter-β-galactosidase-reporter construct (pBlue-MT2a) plus ZnT10 (p3xFLAG–ZnT10) or corresponding vector only (p3XFLAG-BAP vector), as indicated and maintained for 24 h in control medium with or without the addition of 100 µM $ZnCl_2$. Values are means (n=3-6), with standard errors represented by vertical bars. *** $p < 0.001$ by Student's *t* -test.

Chapter 4: Regulation of ZnT10 in response to zinc

4.1 Outline

In this chapter it is hypothesised that ZnT10 may be involved in zinc homeostasis due to its response to zinc treatments. Results presented here show ZnT10 mRNA expression is down-regulated in response to zinc using both semi-quantitative RT-PCR and RT-qPCR. In addition, Western blotting techniques indicate that this down-regulation is evident at the protein level; in p3xFLAG-ZnT10 transiently transfected SH-SY5Y cells. Using bioinformatics techniques I identify the presence of a putative Zinc Transcriptional Regulatory Element (ZTRE) which appears to be involved in this down-regulatory response at the transcriptional level. This response is lost when this ZTRE sequence is mutated. Furthermore, in SH-SY5Y cells transiently expressing p3xFLAG-ZnT10 there appears to be a translocation of ZnT10 within the cell in response to zinc treatment.

As discussed in Chapter 1, the body's ability to regulate homeostasis of nutrients is imperative to survival. Zinc is no exception to this. For example zinc deficiency through foetal development leads to growth retardation and in the adult human leads to immunodeficiency, hair loss and loss of appetite (Prasad et al., 1961). In excess zinc can cause nausea, diarrhoea and local neuronal deficits (Vallee, 1988). Zinc has also been implicated in disease states such as neurodegenerative diseases and diabetes (Frederickson, 1989, Chimienti et al., 2004). Homeostasis of zinc - biosystemically and at the cellular level - requires regulated expression and/or activity of zinc transporters such as the ZnTs. An example of this is ZnT1, found at the plasma membrane, where a major role is to efflux zinc out of the cell (Cousins and McMahon, 2000, Palmiter and Findley, 1995). ZnT1 mRNA expression is up-regulated in response to increased zinc

concentrations (Liuzzi et al., 2001), mediated through transcriptional regulation by metal response element transcription factor-1 (MTF-1) (Langmade et al., 2000).

Zinc is obtained through the diet as it is bound to proteins in foods such as shellfish, red meat and, to a lesser extent cereals and legumes. The absorption of zinc takes place in the gastrointestinal tract by the enterocytes and whilst this is important for zinc homeostasis the balance between absorption of exogenous zinc, gastrointestinal secretion and excretion of endogenous zinc are critical in order for the body to be able to balance this nutrient. Absorption by the enterocytes is mediated by the interplay of ZIPs and ZnTs (see section 1.5). For example, transporters found to be expressed in these cell types include ZnT1, ZnT2, ZnT4, ZnT5, ZnT6, ZnT7, ZIP4, and ZIP5 (reviewed by Wang and Zhou, 2010).

ZnTs have varying localisation patterns depending on their function. For example ZnT1 is implicated in regulating efflux of zinc across the basolateral membrane, out of enterocytes and into systemic circulation (McMahon and Cousins, 1998) whereas ZnT7 is involved in intracellular trafficking of zinc and is able to facilitate the accumulation of zinc in the Golgi apparatus (Huang et al., 2007). Indeed the two transcripts of ZnT5 give an insight into the importance of cellular localisation with ZnT5vA localising to the Golgi apparatus, presumably to fulfil a role in zinc accumulation (Kambe et al., 2002, Yu et al., 2007). Conversely, ZnT5vB is localised to the apical membrane of enterocytes with bi-directional properties important in the uptake of zinc in human intestinal Caco-2 cells and to the ER in unpolarised cells (Valentine et al., 2007, Thornton et al., 2011).

Levels of dietary zinc are able to influence expression levels of the ZIPs and ZnTs found along the length of the gastrointestinal tract. For instance, studies in mice have

revealed alternative processes for Zip4 and Zip5 depending on zinc status. In cases of zinc restriction Zip4, found on the apical membrane of enterocytes is up-regulated along the length of the gastrointestinal tract in order to maximise zinc absorption however Zip5 is internalised during zinc deficiency so that minimal zinc influx takes place from the blood stream therefore, ultimately, restricting gastrointestinal secretion (Dufner-Beattie et al., 2003b, Dufner-Beattie et al., 2004). The converse is also true, when mice are zinc replete Zip4 is internalised through endocytosis whereas Zip5 is up-regulated on the basolateral membrane (Weaver et al., 2007). In addition, it is evident that buffers such as MT, regulate levels of zinc within enterocytes. Regulation of MT by zinc enables this protein to be up-regulated to chelate zinc in times of excess and be degraded when zinc levels are low (Bell and Vallee, 2009). It is the response of the zinc transporters and MT to changes in local zinc status that allow whole body zinc content to be maintained (King et al., 2000).

Results presented in Chapter 3 reveal a differential pattern of expression of ZnT10 including the small intestine and, to a lesser extent, colon, therefore it too may play a role in zinc absorption at this site.

Zinc homeostasis is not only maintained through the absorption process. Free zinc is toxic therefore little or no free zinc is available in solution within biological systems and zinc is circulated within serum chelated by binding proteins such as albumin (70 %), α-macroglobulin (18 %) and bound to other proteins such as transferrin (Gibson et al., 2008). Zinc is distributed throughout the body to all organs. As in enterocytes, intracellular zinc may be bound to MT. MT plays a very important role in maintaining cellular zinc homeostasis. At high intracellular zinc concentrations, MT levels increase therefore sequestering zinc. At low zinc concentrations, MT is able to release its bound

zinc ions before being degraded. This allows a constant level of zinc in the serum to carry out its numerous biological functions (Coyle et al., 2002).

Significant in the context of this research, in addition to the expression of ZnT10 in the gastrointestinal tract, ZnT10 displayed a restricted expression profile that included relatively high levels of expression in the brain. In the brain zinc is packaged into pre-synaptic vesicles by ZnT3 and subsequently released during neurotransmission in neurones of the hippocampus (Palmiter et al., 1996b). Znt3 knockout mice have shown deficits in spatial memory and behaviour dependent on the hippocampus (Martel et al., 2011). The dyshomeostasis of zinc within the brain has been implicated in neurodegenerative diseases. For example, zinc has been shown to be present in aggregates in diseases such as Alzheimer's providing evidence to strengthen the hypothesis that zinc is implicated in neurodegeneration (Frederickson, 1989). Furthermore, it has been hypothesised, though not proven, that an observed up-regulation of ZnT1 expression in the brain contributes to the zinc dyshomeostasis identified in Alzheimer's disease (Zhang et al., 2008), the hypothesis is that the increase in ZnT1 expression causes an increase in zinc ions available in the extracellular space for the initiation of amyloid-β deposition. Given the relatively high expression levels of ZnT10 measured in brain tissue, it suggests a role for this transporter in the homeostasis of zinc in this organ.

Key transcription factors found in bacteria, yeast and higher metazoans have been identified through their ability to regulate sets of genes that contribute to the maintenance of zinc homeostasis and/or the ability to adapt to differences in the availability of zinc. In bacteria the ArsR-SmtB family of transcriptional de-repressors act to repress the expression of certain operons at stress-inducing concentrations of

divalent metal ions including zinc. Direct binding of such metal ions results in de-repression (reviewed by Busenlehner et al., 2003, Waldron and Robinson, 2009). Transcriptional activators include the MerR family of DNA-under-winding transcriptional activators that are able to bind metal and subsequently under-wind promoter regions such that RNA-polymerase recognition sequences are optimally aligned (reviewed by Waldron and Robinson, 2009). The less well defined Fur family is known to contain structural zinc sites. This family of transcriptional regulators bind DNA after binding metals and mainly function to repress transcription however, direct activation of transcription is evident for some promoters (reviewed by Waldron and Robinson, 2009). In *E. coli* the MerR family factor ZntR has been found to stimulate zinc-responsive expression of a zinc exporter ZntA (a cation-translocating ATPase) by binding to the DNA and distorting its alignment (Outten et al., 1999). In contrast the transcriptional repressor Zur, a member of the Fur family of transcription factors, binds two zinc ions in order to bind to DNA and repress the transcription of a zinc importer in the *znuABC* gene cluster (Patzer and Hantke, 2000).

In *S. cerevisiae* investigations have identified an 11 bp zinc-responsive element (ZRE) in the promoter regions of certain genes, for example; the high affinity zinc uptake transporter ZRT1 (Zhao and Eide, 1997) and the vacuolar zinc exporter ZRT3 (MacDiarmid et al., 2000), as well as many others (Wu et al., 2008). The transcription factor Zap1 is itself induced and binds to the ZRE in cases of zinc deficiency thereby inducing activation of these genes (Lyons et al., 2000). Conversely, transcriptional repression of zinc-dependent alcohol dehydrogenases is achieved by Zap1 under conditions of zinc limitation. Zap1 acts to induce an intergenic transcript that in turn is able to displace the transcriptional activator (Bird et al., 2006). For the uptake transporter ZRT2, transcriptional repression is achieved by the binding of Zap1 to a

non-consensus ZRE at a transcriptional start site (Bird et al., 2004). Transcriptional control of the expression of proteins including zinc transporters appears to play a major role in zinc homeostasis in plants (reviewed by Sinclair and Kramer, 2012, Palmer and Guerinot, 2009), and *Arabidopsis* transcription factors crucial to the response to zinc deficiency, with orthologs in other plant species, have been identified recently (Assuncao et al., 2010).

In higher animals, the increased transcription of genes at higher levels of zinc availability is mediated in some instances through binding of the transcription factor MRE-binding transcription factor 1 (MFT1). MTF1 has 6 zinc fingers and these bind DNA at a specific consensus sequence within promoter regions. The DNA motif is called a Metal Responsive Element (MRE) and is characterised by the 7 bp sequence TGCRCNC (Heuchel et al., 1994). In order to protect cells from levels of high zinc MTF1 mediates transcriptional up-regulation of genes such as mouse metallothoinein-1 and -2 genes (Mt1 and Mt2) and the gene for the zinc transporter Znt1 (Slc30a1), responsible for the efflux of zinc across the plasma membrane (Heuchel et al., 1994, Langmade et al., 2000). Like yeast Zap1, MTF1 can also act in a repressive role. Zip10 expression is increased in the conditional MTF1 knockout mouse (Wimmer et al., 2005). Further research has shown that Zip10 includes MREs downstream of the transcriptional start site and binding of MTF1 to these MREs mediates transcriptional repression (Lichten et al., 2011). In addition, the zebrafish Zip10 has two distinct transcriptional start sites and experimentation reveals that Zip10 is regulated by alternative promoters that are oppositely-regulated by zinc. Both promoters contain MRE clusters which shows that MREs can function as both repressor and activation elements (Zheng et al., 2008). It is possible that MTF1 requires accessory proteins in order to form co-activator complexes in order to fulfil these contrasting roles. Indeed,

activation of the Mt1 promoter requires transcription factor Sp1 and the histone acetyltransferase p300/CPB in complex with MTF1 and this activation was reduced by siRNA knockdown of p300/CBP. However the accessory proteins evidently differ between complexes as p300/CBP knockdown did not affect MTF1-mediated activation of the mouse *Znt1* gene (Li et al., 2008). Interestingly, there must be mechanisms in addition to MTF1 that are able to influence zinc induced repression as mutation of the consensus MRE sequence in ZnT5 was unable to abolish the zinc-induced repression ordinarily observed in transfected Caco-2 cells (Jackson et al., 2007). To understand zinc homeostasis it is thus essential to uncover additional mechanisms of zinc-regulated gene expression. One mode of regulation has been elucidated in the ZIP family of transporters, namely ZIP4. It is known that ZIP4 is essential for zinc absorption, as highlighted by the disease *Acrodermatitis enteropathica* (AE) (Wang et al., 2002). It is evident that Zip4 protein is stabilised and translocated to the apical membrane in zinc deficient conditions (Dufner-Beattie et al., 2004). Researchers have also hypothesised that at the level of transcription Zip4 mRNA is up-regulated when cells are zinc deplete. In fact, recent studies have identified the transcription factor Krüppel-like factor 4 (KLF4) in the activation of *Zip4*. In the murine intestinal epithelial cell (IEC) line MODE-K both KLF4 and Zip4 were up-regulated in zinc deficient conditions but siRNA knockdown studies of KLF4 reduced the activation of Zip4 (Liuzzi et al., 2009). Moreover, Liuzzi *et al.*, (2009) used EMSAs with the nuclear extracts of MODE-K cells, to show that KLF4 binds to the Zip4 promoter, a phenomenon that is increased when zinc is limited. Further investigation with reporter constructs involving the wild-type and mutated Zip4 promoter demonstrated that this regulation of Zip4 is through a KLF4 response element. These results should be interpreted with caution though given the low levels of Zip4 evident in the MODE-K cells (Huang et al., 2006). Data

produced by Weaver et al., (2007) indicates that regulation is at a post-transcriptional level.

Similarly, EMSAs have revealed that there is a protein factor that binds to the ZnT5 promoter in a zinc-dependent manner. Through this there has been identification of the binding site in the ZnT5 promoter responsible for zinc-induced transcriptional repression, namely the ZTRE (for Zinc Transcriptional Regulatory Element) (Coneyworth et al., 2012). Results presented here show the discovery of the presence of a ZTRE sequence in the human ZnT10 promoter. Thus, I present evidence for a down-regulatory response to zinc at both the mRNA and protein level and present a transcriptional regulatory process that operates in mammalian cells to repress transcription of ZnT10 in response to increased zinc availability. Abolition of the response was evident with mutation of this putative ZTRE region.

4.2 Regulation of ZnT10 by extracellular zinc at the mRNA level

4.2.1 *Semi-quantitative analysis*

In order to establish whether ZnT10 mRNA transcript levels were altered in response to extracellular zinc treatments, semi-quantitative RT-PCR was carried out on human neuroblastoma cells, SH-SY5Y. Cells were treated with either basal medium, or medium supplemented with 150 µM $ZnCl_2$ for 24 h. SH-SY5Y cell viability was established over the concentration range by counting using the Trypan blue exclusion method (83.1 % + 2.5 viable untreated cells compared with 80.4 % + 4.4 viable cells at 150 µM $ZnCl_2$) (Figure 4.1A). Cell viability was further confirmed by measuring the reduction of resazurin to resorufin (Alamar Blue, Invitrogen). No significant difference between treated (100 µM zinc) and untreated SH-SY5Y cells was observed ($p = 0.159$) (Figure 4.1B). RNA from SH-SY5Y cells was harvested (Section 2.4.1) and RT-PCR

performed using primers designed to anneal to human β-actin and MT1(A) and human ZnT10 (Table 4.1). When normalized to β-actin, ZnT10 mRNA expression was reduced in cells treated with 150 µM extracellular zinc compared with untreated cells (basal medium) (Figure 4.2). Levels of metallothionein mRNA, known to be up-regulated by zinc (Heuchel et al., 1994), were increased at 150 µM compared with basal media (3 µM zinc) indicating that the treatments were successful with a significant increase in expression (Figure 4.2).

4.2.2 *Real-time quantitative analysis (RT-qPCR)*

To confirm the semi-quantitative findings RT-qPCR was employed as described previously (section 2.5.5). Standard curves were generated as described (section 2.5.5.1) and for all RT-qPCR standard curves passed acceptance criteria (Figure 4.3). The effect of zinc availability on levels of expression of ZnT10 mRNA in both SH-SY5Y cells and Caco-2 cells was determined by culturing cells at increasing concentrations of zinc (up to 150 µM $ZnCl_2$) for 24 h. Three concentrations of extracellular zinc (50 µM, 100 µM and 150 µM $ZnCl_2$) were analysed in both SH-SY5Y cells and Caco-2 cells. In addition to the cell viability data shown in Figure 4.1, it has previously been reported that there is no effect on Caco-2 cell viability at this concentration of zinc (Jackson et al., 2007). Total RNA was extracted from cells and RT-qPCR was carried out using GAPDH as the reference gene. Cells treated with increasing levels of extracellular zinc showed a significant decrease in ZnT10 mRNA expression (Figure 4.4A and 4.4C). GAPDH showed a consistent level of expression independent of the zinc treatment and was therefore chosen as the reference gene and normalisation control. GAPDH has previously been used to normalise zinc response by RT-qPCR (Jackson et al., 2007, Hojyo et al., 2011). All levels were assessed as a ratio to GAPDH. Furthermore, using Caco-2 mRNA at an extracellular zinc concentration of 100 µM ZnT10 mRNA levels

were additionally assessed as a ratio to a further reference gene; TOPI. There was also a significant decrease in ZnT10 transcript abundance relative to TOPI in Caco-2 cells treated with 100 µM extracellular zinc (Figure 4.4E). A further control experiment, using MT1, revealed the expected increase in response to zinc in RNA from the same SH-SY5Y and Caco-2 cells (Figure 4.4B and 4.4D).

In addition, the removal of FBS from the media was investigated to see whether this in itself effects ZnT10 expression. The results above show that the addition of 100 µM extracellular zinc gives a decrease in ZnT10 expression. Here we also show that medium both with and without FBS elicits the same down-regulation in response to the extracellular zinc (p = 0.02 without FBS, p = 0.04 with 10 % FBS by Student's t-test) (Figure 4.5). Therefore all experiments herein were completed in the presence of 10 % FBS.

4.3 Identification of a putative ZTRE in the proximal promoter region of ZnT10

4.3.1 *Bioinformatic analysis to identify potential transcriptional element sequences*

To date research has focused on transcriptional up-regulation of zinc effluxers such as ZnT1 (Langmade et al., 2000). The increased transcription of genes at increased levels of zinc availability is mediated, in some instances through binding of the transcription factor MTF1 to copies of the MRE in the promoter region. In addition, it is known that MREs can mediate both positive and negative regulation in zebrafish Zip10 however this is under the control of alternative promoters (Zheng et al., 2008). Analysis using the bioinformatics programme, Fuzznuc (http://www.hpa-bioinfotools.org.uk/pise/fuzznuc.html), identified two putative MREs in the promoter region of ZnT10; TGCGCGC (-60 bp to -54 bp relative to the ATG start site) and

TGCGCTC (-44 bp to 38 bp relative to the ATG start site). The data above reveals a novel observation concerning the expression of ZnT10, such that there is a reduction in ZnT10 mRNA in SH-SY5Y and Caco-2 cells in response to increasing the extracellular zinc concentration from 3 μM to 150 μM. The indirect measurement of promoter-reporter activity shown in Chapter 3 leads to the prediction that this transporter acts as an effluxer and therefore I would expect an increase in response to extracellular zinc however the down-regulation described above is not without precedence. ZnT5, a ubiquitous transporter, also shows this down-regulatory response to extracellular zinc (Cragg et al., 2002, Jackson et al., 2007). Further investigation by our group showed that there is a region upstream of ZnT5's ATG start site (-154 to +50, relative to the end of the 5' UTR) responsible for this transcriptional repression (Jackson et al., 2007). Recent analysis of this region by EMSAs has enabled the identification of a specific sequence known as the **Z**inc **T**ranscriptional **R**egulatory **E**lement (ZTRE) found in this 204 bp promoter region (Coneyworth et al., 2012) (Figure 4.6A). As there is also a down-regulatory response of ZnT10 in response to extracellular zinc, the 5'-UTR of ZnT10 was investigated to see whether it contained a putative ZTRE sequence. Entrez Gene was used to establish that ZnT10 is present on Chromosome 1. A 3 kb upstream region from the ATG was screened for the presence of a ZTRE sequence, using the software package Fuzznuc. This search identified a putative ZTRE within the mRNA 72 bp upstream of the translational ATG start site (Figure 4.6B). The identified sequence CCCACCT(GTGGCTGCGCGCG)GGGTGGG spans nucleotides 140-166 of the ZnT10 transcript sequence NM_0187132. This sequence differs from the ZTRE in ZnT5 at two positions in the upstream half of the (imperfect) palindromic region and at one position in the downstream half; these differences are permissive according to the analysis of substitutions that retain binding of the protein factor identified by EMSA

(Coneyworth et al., 2012). I thus predicted that ZnT10 promoter activity would respond to zinc in a similar manner as ZnT5.

4.3.2 *Response of the putative promoter region of ZnT10 to zinc*

To study transcriptional regulation by zinc of the ZnT10 gene, I measured the response of the active promoter region to changes in the extracellular zinc concentration in Caco-2 and SH-SY5Y cells. I generated a ZnT10 promoter-reporter construct (Figure 4.6B, Table 4.2; -762 to +180, relative to the transcription start site, in pBlue-TOPO (Appendix B)) in which the candidate ZTRE (position +58 to +84) was retained (pBlueSLC30A10prom (Appendix G)) (Section 2.6.2). Cells were transfected transiently with the pBlueSLC30A10prom for 24 h in both basal medium or medium supplemented with 100 µM $ZnCl_2$. Reporter gene expression (β-galactosidase activity) driven by the ZnT10 promoter was reduced significantly at the higher zinc concentration in Caco-2 cells (Figure 4.7A). A similar, but non-significant down-regulatory trend was observed in SH-SY5Y cells transfected with the –762 to +180 bp ZnT10 promoter- reporter construct (Figure 4.7A). As a positive control, I carried out parallel experiments using the well characterized, zinc-responsive human MT2a promoter (Helston et al., 2007) as the insert in the promoter-reporter construct; as expected, reporter gene expression was increased at the elevated zinc concentrations (Figure 4.7B).

4.3.3 *Response of the putative promoter region of ZnT10 after mutation of the ZTRE*

In order to ascertain whether it is indeed the putative ZTRE within the 942 bp promoter reporter construct pBlueSLC30A10prom that is responsible for the transcriptional repression at elevated zinc concentrations an additional promoter-reporter construct was

made; pBlueSLC30A10prom$_{MUT}$ (Appendix H). Within the mutated construct, pBlueSLC30A10prom$_{MUT,}$ the primers shown in Table 4.2 were used to substitute the ZTRE of ZnT10, retaining the inter-palindrome linker region but mutating the palindromic sequences at either end as shown in Figure 4.8A. This gave an end-product of a 942 bp promoter reporter construct to compare with pBlueSLC30A10prom. The mutated construct was generated by Georgia Hann. In line with previous experiments, Caco-2 cells were transfected transiently with either the pBlueSLC30A10prom or pBlueSLC30A10prom$_{MUT}$ for 24 hour in both basal medium or medium supplemented with 100 µM $ZnCl_2$. Reporter gene expression (β-galactosidase activity) was reduced at the higher zinc concentration for pBlueSLC30A10prom however this response was abrogated by substitution of the candidate ZTRE (Figure 4.8B). Again, as a positive control, I carried out parallel experiments using the well characterized, zinc-responsive human MT2a promoter (Helston et al., 2007) as the insert in the promoter-reporter construct; as expected, reporter gene expression was increased at the elevated zinc concentrations (Figure 4.8C).

4.4 ZnT10 expression in response to zinc at the protein level

To examine the effect of zinc on ZnT10 protein expression, SH-SY5Y cells were transiently transfected with the plasmid p3xFLAG–ZnT10, a plasmid construct from which ZnT10 was expressed with an N-terminal FLAG epitope tag. Twenty-four hours post transfection cells were treated with basal medium or medium supplemented with 100 µM $ZnCl_2$ for a further 24 hours. Subsequently the cells were lysed using a buffer containing 4 % SDS, 125 mM Tris and 5 % β-mercaptoethanol in order to extract the protein (section 2.4.2). This protein was electrophoresed on a denaturing 10 % acrylamide gel and blotted onto a PVDF membrane (section 2.7.2). Quantities of protein

prepared from cells treated under both conditions, was determined spectrophotometrically (Nanodrop). 10 µg of sample was loaded onto gels. Equal loading of samples was confirmed by re-immunoprobing blots with an anti-α-tubulin antibody. Western blot analysis used an anti-FLAG antibody (Sigma; 1 in 1000 dilution) and subsequently an anti-mouse IgG-HRP secondary antibody (GE Healthcare; 1 in 20000 dilution). These were visualised by enhanced chemiluminescence (ECL) HRP substrate (Thermo Scientific). This revealed a protein band of approximately 56 kDa (the expected size for ZnT10 (53 kDa) plus 3 x FLAG (3 kDa)) in both samples, indicating that N-terminal cleavage had not taken place. Western blots were stripped and re-probed, using an anti-α-tubulin primary antibody (Abcam; 1 in 5000 dilution) and an anti-rabbit IgG -HRP secondary antibody (Abcam; 1 in 20000 dilution). Analysis of ZnT10 expression levels by densitometric quantification of band intensities, expressed as a ratio to α-tubulin, revealed a significant decrease in ZnT10 protein expression at 100 µM $ZnCl_2$ compared with the untreated cells (Figure 4.9).

The down-regulatory response at the protein level was not being driven by the strong CMV promoter upstream of the ZnT10 ORF in the FLAG vector (p3xFLAG-CMV-10 (Sigma)). A further promoter-reporter construct, created by cloning the CMV promoter region (Genbank accession number X03922.1) into a pBlueTOPO vector (Invitrogen), upstream of the β-galactosidase reporter gene was produced and transfected transiently into Caco-2 cells. Cells were exposed to basal medium or medium supplemented with 100 µM and 150 µM $ZnCl_2$ for 24 hours. Treatment with the higher zinc concentrations resulted in an unexpected significant increase in promoter activity compared with basal medium (Figure 4.10). This result indicates that the decrease in ZnT10 at the protein level is a true response of ZnT10 and does not reflect any effect of zinc on the CMV promoter (this experiment was carried out by Lisa Coneyworth).

Attempts to investigate endogenous ZnT10 levels were unsuccessful due to the lack of antibody specificity to ZnT10. The two commercially available ZnT10 antibodies (sc-160941, sc-160942; Santa Cruz) did not reveal specific bands for ZnT10 on an immunoblot using samples from the SH-SY5Y cells in which we have confirmed ZnT10 expression at the mRNA level by RT-PCR. Furthermore, SH-SY5Y cells transiently transfected with the plasmid p3xFLAG–ZnT10 which using an anti-FLAG antibody revealed a specific band (indicating that transfection was successful) also did not produce a signal using either commercial ZnT10 antibody. The specificity of the two antibodies was questioned. Contradictory data referring to ZnT10 expression enhancing insulin secretion, referred to in the available Santa Cruz data sheet informed the investigation into antibody specificity. An investigation was carried out by RT-PCR and Western blot analysis. Both ZnT10 commercial antibodies are described as being cross-reactive with mouse (Santa Cruz) therefore RT-PCR was carried out using primers specific to mouse Znt8 and mouse Znt10 (Table 4.3) on RNA prepared from mouse brain and pancreatic tissue. The results of this experiment as expected revealed expression of Znt8 in the pancreas and not in the brain (Chimienti et al., 2004), and conversely for Znt10 the opposite was found; Znt10 is present in the brain and not in the pancreas (Figure 4.11A), confirming our previous investigations (Chapter 3).

The Western blot was completed using protein extracted from the same mouse brain and pancreas tissue. This was probed with the Znt10 antibodies purchased from Santa Cruz. Figure 4.11B, shows cross reactive bands (of approximately 20 kDa and 50 kDa) are only visible in the lane loaded with protein from pancreatic tissues and not in the lane derived from brain. These results clearly show that this antibody is not specific for Znt10 (which is present in the brain and is not present in the pancreas) and indicate that the antibody is potentially picking up Znt8, although our experiments do not prove this.

4.5 Intracellular localisation of ZnT10 and its response to extracellular zinc treatment

To examine the intracellular localisation of ZnT10, SH-SY5Y cells were transiently transfected with the plasmid p3xFLAG–ZnT10, a plasmid construct from which ZnT10 was expressed with an N-terminal FLAG epitope tag. Forty eight hours post transfection cells were fixed using 4 % PFA and stained with the anti-FLAG-FITC antibody (1:1000, Sigma). Rhodamine conjugated wheat germ agglutinin (WGA), a lectin that selectively binds N-acetylglucosamine and N-acetylneuraminic acid, was used to stain the Golgi apparatus in cells permeabilised with 0.1 % Triton X-100 following PFA fixation (WGA; 1:500). ZnT10 showed co-localisation with WGA in permeabilised cells, consistent with localisation to the Golgi apparatus (Figure 4.12). Alteration in the pattern of localisation by changing the extracellular zinc concentration in basal medium with the addition of 100 µM extracellular zinc for a 24 hour period immediately prior to viewing the cells revealed a different pattern of localisation, which showed a reduced co-localisation with the wheat germ agglutinin in permeabilised cells and a more diffuse pattern of localisation including some expression towards the plasma membrane (Figure 4.12). Transfection experiments were carried out in triplicate on two separate occasions. All p3xFLAG-ZnT10 transfected cells revealed an identical pattern of localisation under the different zinc treatments. p3xFLAG-BAP (used as a negative control, Appendix E) showed a diffuse pattern of expression throughout the cell in all experiments, which was not altered by extracellular zinc treatment (Figure 4.13), confirming that localisation of the signal to specific subcellular regions was a function of the attached ZnT10 protein. The two commercially available ZnT10 antibodies (sc-160941, sc-160942; Santa Cruz) did not show any specific staining using this approach. The immunocytochemistry with these antibodies showed no difference from the

secondary or to the primary. The blocking peptide did not reduce the signal. I was unable to establish specific staining under other conditions tested with these antibodies but I believe they are not specific to ZnT10 (section 4.4).

4.6 Discussion

In this chapter I show, by both semi-quantitative and RT-qPCR, a decrease in endogenous ZnT10 mRNA expression in response to increased extracellular zinc concentration in both the Caco-2 and SH-SY5Y cell line models. This is a surprising but not unprecedented response for a zinc transporter which has been shown to act as an effluxer (section 3.5) but this response is not unique for mammalian zinc transporters. The most notable down-regulation of a mammalian zinc transporter is the decrease in mRNA expression levels of Zip4 in response to increased levels of zinc with internalisation of Zip4 from the apical membrane through endocytosis (Dufner-Beattie et al., 2004). Presumably, this is in fact an important way of regulating zinc intake in the enterocytes. In the context of this research however, perhaps of more relevance is the regulation of ZnT5. In the original paper describing ZnT5vB (referred to as hZLT1) the response to zinc at the mRNA level was very intriguing. In Caco-2 cells there was a significant increase in ZnT5vB mRNA but no change in ZnT5vB mRNA levels in the placental cell line JAR with increased extracellular zinc (Cragg et al., 2002). The tight regulation of maternal zinc concentrations through intestinal absorption and mobilisation of zinc stores were hypothesised to render placental regulation of zinc superfluous. I do not see a cell line dependent response for ZnT10 however both cell lines used (intestinal and brain) are from tissues that require very stringent levels of control of such nutrients.

Subsequently, a body of research has developed looking at the regulation of both splice variants of ZnT5. Interestingly, ZnT5vA has been shown to be an effluxer (Kambe et al., 2002) and ZnT5vB is capable of bi-directional transport of zinc (Valentine et al., 2007). It is particularly relevant that with increased levels of extracellular zinc ZnT5vA mRNA expression levels decrease significantly, moreover, in the same paper researchers show an overall decrease in mRNA levels in response to an increase in extracellular zinc (Jackson et al., 2007). All these results highlight a complex system of regulation for this transporter especially given that transcription of both variants is driven by a single promoter.

Five core MREs identified in the putative promoter region of the ZnT5 transcript leads to speculation that the mode of regulation is via the binding of MTF1. However, mutation of the consensus MRE sequence in ZnT5 was unable to abolish the zinc-induced repression ordinarily observed in transfected Caco-2 cells (Jackson et al., 2007). Furthermore, ZnT5 mRNA was found to be stabilised by increased extracellular zinc thus, the authors concluded that it is a complex interplay between the effect of zinc on both transcription of ZnT5 and mRNA stability of the transcript that act in opposition that balances mRNA abundance. It remains unclear as to why the efflux variant (ZnT5vA) decreases in response to zinc however similarities can be drawn to ZnT10 with localisation of both transporters to the Golgi apparatus (see section 4.5). Indeed these observations may be commensurate with a mode of transcriptional regulation through which expression is repressed at higher zinc levels if the primary function of ZnT10 is delivery of zinc to proteins in the Golgi apparatus, rather than homeostasis of cytosolic concentrations. The effect of mRNA stability, seen for ZnT5, would be an interesting avenue of research as RT-qPCR allows measurement of the level of mRNA expression in the cells at that time point however it is unable to

establish that the effect seen is at the level of transcription because mRNA level is a balance between synthesis and degradation. Therefore the mRNA level seen can be affected by mRNA stability and indeed has been shown to be an important factor in the regulation of ZnT5 where the first example of zinc mediating stability of mRNA was demonstrated (Jackson et al., 2007).

It is known that MREs can mediate both positive and negative regulation in zebrafish Zip10 however this is under the control of alternative promoters (Zheng et al., 2008). In contrast, there must be mechanisms in addition to those mediated through the MREs that are able to influence zinc induced repression as mutation of the consensus MRE sequence in ZnT5 was unable to abolish the zinc-induced repression ordinarily observed in transfected Caco-2 cells (Jackson et al., 2007). Furthermore, the authors identified a 204 bp region comprising -154 bp prior to transcriptional start codon and +50 bp into the ORF of ZnT5 that was required for the transcriptional repression seen at increased extracellular zinc concentrations (Jackson et al., 2007). Given the response of this region was indistinguishable from the promoter as a whole it suggests that this region contains the necessary regulatory elements. More recent EMSA analyses have revealed the binding site in the ZnT5 promoter responsible for the zinc-induced transcriptional repression, namely the ZTRE. Sequences that concur with the identified ZTRE sequence, established to be permissive for binding of a putative transcriptional regulatory protein(s) that acts at this site, occur in the 5'UTR of ZnT10. I have confirmed that this sequence functions in the same way as the ZTRE in ZnT5 to confer transcriptional repression in response to zinc, using a promoter-reporter construct assay. In addition, mutation of this ZTRE region truncates this response highlighting the importance of the sequence in transcriptional down-regulation. A zinc-dependent transcriptional regulatory mechanism based on this principle – zinc induced binding of a

transcriptional repressor – has not previously been described in a eukaryotic system but this mode of operation is, in principle, analogous to the regulation of the *E. coli* znuABC operon. This transcriptional repression is mediated by a member of the Fur family of transcription factors, namely Zur. In this case Zur binds two zinc ions in order to bind to DNA at the almost-perfect palindromic binding site sequence for Zur (TGTGATATTATAACA) and repress the transcription of a zinc importer in the *znuABC* gene cluster (Patzer and Hantke, 2000). This sequence does however show no similarity with the ZTREs identified in the ZnT family. The current findings do not exclude the possibility that a separate transcriptional regulatory mechanism operates in mammalian cells under conditions of zinc deficiency to increase the expression of genes involved in zinc scavenging, such as those involved in high affinity uptake across the plasma membrane. This is evident in the enterocytes and the up-regulation of Zip4 in response to zinc deficiency (Dufner-Beattie et al., 2004). This is mediated by KLF4 which is able to bind to a KLF4 responsive element in the promoter region of Zip4 so to activate transcription (Liuzzi et al., 2009). Although these results for Zip4 should be interpreted with caution though given the low levels of Zip4 evident in the MODE-K cells (Huang et al., 2006). Data produced by Weaver et al., (2007) indicates that regulation is at a post-transcriptional level.

Results presented here show a decrease in reporter gene activity driven by a region of the ZnT10 promoter (-762 to +180 bp, relative to the start of transcription) in response to increased extracellular zinc. Comparison of a 204 bp region of ZnT5 (Jackson et al., 2007) with the ZnT10 promoter sequence in this reporter construct reveals elements with a high level of similarity. A putative ZTRE has been identified in the 5' UTR of the ZnT10 gene and it has been shown that it is functional in a promoter-reporter construct. Inspection of other ZnT family members revealed sequences that concur with

what we identify thus far to be permissible as a ZTRE with respect to protein binding in the 5'UTR and 500 bp region immediately upstream of the start of transcription. These sequences are present in six out of ten ZnTs with ZnT2, ZnT6, ZnT8 and ZnT9 being the exception (Coneyworth et al., 2012). Coordinated regulation of multiple members of the gene family through this transcriptional regulatory mechanism is thus implicated. For the ZnT5 promoter region substitutions to the ZTRE sequence in the competitor oligonucleotide that abrogated protein binding to this region as detected by EMSA have been made in only one half of the palindromic sequence, thus it appears that both sections of sequence are necessary. It is feasible that two linearly-separated sequences in DNA come into proximity to allow binding to both of a single protein or protein complex by virtue of the folding of DNA into chromatin. This phenomenon has yet to be investigated for ZnT10 and indeed the analysis of other promoters that contain ZTREs would elucidate further genes in which zinc was involved in the regulation.

Cells transfected transiently to over-express ZnT10 fused to a FLAG epitope tag at the N-terminal region revealed a decrease in ZnT10 expression at the protein level with increasing levels of extracellular zinc. The presence of a band of approximately 56 kDa (the expected size for ZnT10 (53 kDa) plus 3 x FLAG (3 kDa)) in this N-terminal vector indicates that signal peptide cleavage does not occur contrary to the predictions of Chapter 3. This strategy to investigate the effects of extracellular zinc on levels of ZnT10 protein expression was employed as the commercially available antibodies to ZnT10 (Santa Cruz) were not effective in my hands and in fact experiments carried out proved non-specificity of these antibodies. I believe the decrease in protein expression in response to extracellular zinc to be a true representation of endogenous protein as results reflected effects seen at the mRNA level. Although the ZnT10 ORF was driven by the strong CMV promoter in the p3xFLAG-ZnT10 vectors I was able to exclude the

possibility that the down-regulatory observation was not a result of zinc activity through this CMV promoter used to drive expression. When the CMV promoter was used to drive β-galactosidase activity driven by zinc, there was an increased activity in response to zinc (experiments carried out by Lisa Coneyworth) and therefore it can be concluded that the down-regulatory response measured at the protein level is a true indication of ZnT10 response to zinc.

The subcellular localisation of ZnT10 in SH-SY5Y cells is at the Golgi apparatus in cells transfected transiently with an N-terminal FLAG-tagged construct of ZnT10 under conditions of 3 μM extracellular zinc (basal medium). At concentration of 100 μM extracellular zinc, ZnT10 was observed to re-localise towards the plasma membrane. Several zinc transporters have been shown to alter their localisation in response to metals, in particular for members of the ZIP family of zinc transporters, specifically ZIP1, 3, 4, 5 and 8 (Wang et al., 2004b, Desouki et al., 2007). Interestingly experimentation into Zip4 and Zip5 indicate that the transporters have antagonistic functions in the control of zinc homeostasis. In zinc replete states Zip5 is located on the basolateral membrane, but the same state causes internalisation of Zip4 from the apical membrane through endocytosis. Conversely, Western blot analysis of membrane proteins from the visceral yolk sacs, showed that in cases of zinc deficiency Zip5 is internalised, whereas Zip4 mRNA is stabilised and the protein is translocated to the apical membrane (Wang et al., 2004b). Furthermore, some of the AE mis-sense mutations cause retention of the protein at high levels in the plasma membrane, consistent with impaired zinc sensing to control Zip4 trafficking (Wang et al., 2002). The mechanisms underlying the responses of the mammalian ZIP family of zinc transporters to dietary zinc are still poorly understood however the mutations found in ZIP4 are clearly involved.

A better understanding of transporter trafficking comes from investigation of other metal transporters, more specifically the Menkes copper transporting protein (MNK). MNK was first identified due to the X-linked copper deficiency disorder, Menkes disease. MNK is normally localised on the *trans*-Golgi network (TGN) however, trafficking has been reported when cells are exposed to excessive copper such that MNK translocates to the plasma membrane presumably to increase efficiency of removal of excess copper from cells. Di-leucine motifs in the C-terminal portion of MNK have undergone mutation analysis with the conclusion that these motifs mediate the copper-induced exocytosis of MNK from the TGN to the plasma membrane, (Petris and Mercer, 1999). Similarly, these motifs also occur in ZnT6 and are predicted to be involved in re-localisation of ZnT6 from the TGN to the cytoplasm and plasma membrane (Huang et al., 2002).

Based on the assumption that di-leucine signals consist of an invariant leucine in the first position and a hydrophobic residue L, I, V or M in a more tolerant second position, di-leucine motifs occur in ZnT10 between amino acid positions 242 and 243 as well as 286 and 287 and 298 and 299, which are found within the predicted C-terminal cytosolic region. It is possible that the re-distribution of ZnT10 from the Golgi apparatus to the plasma membrane is dependent on one or more of these di-leucine motifs. The importance of these motifs in the intracellular distribution and zinc-induced redistribution of ZnT10 should be addressed in future experiments in which they are deleted by site-directed mutagenesis. It has recently been reported, using a similar ZnT10 over-expression approach, that ZnT10 localises to recycling endosomes, in vascular smooth muscle cells derived from rat thoracic aortas and HEK293 cells (Patrushev et al., 2012). Although I do not observe a similar pattern of localisation, it may be explained by the different cell types used in the two experiments. Here

physiological cell types are chosen, where endogenous ZnT10 mRNA expression was detected (intestine and brain). Chapter 3 shows I did not detect endogenous expression at the mRNA level of ZnT10 in heart, muscle or kidney tissue.

The translocation seen here coupled with the functional role of ZnT10 referred to in chapter 3, leads to speculation that ZnT10 may have two important cellular functions. Firstly, ZnT10 may be involved in transporting cytoplasmic zinc into the Golgi apparatus, where it may deliver zinc to nascent zinc-containing proteins. Secondly, ZnT10 may play a role in cellular zinc homeostasis through zinc export, based on its zinc-induced intracellular redistribution to the plasma membrane.

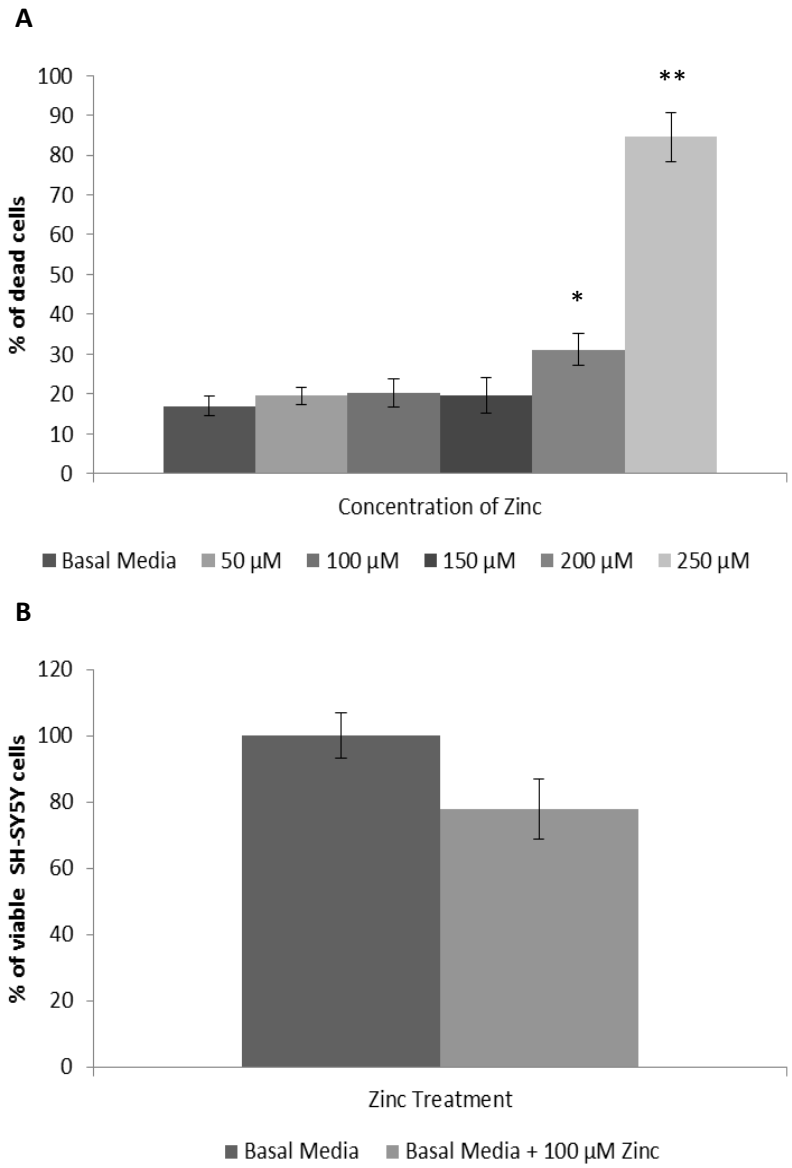

Figure 4.1 Response of SH-SY5Y cells to extracellular zinc treatment A. Estimated percentage cell death of SH-SY5Y cells after treatment with varying concentrations of $ZnCl_2$ for 24 hours using trypan blue. All values are shown as mean ± SEM, n = 3. (Hollie Ord, BSc Student) **B.** Cell viability measured by the conversion of resazurin to resorufin (Alamar Blue, Invitrogen) in the presence of 100 µM extracellular zinc concentration (indicated). All values are shown as mean ± SEM, n = 3.

Name/ Accession Number	Primer Sequences	Amplicon Length (bp)	Annealing Temp (°C)
ZnT10 NM_018713	$_{844}$CGT AGC AGG TGA TTC CTT CAA C$_{865}$ $_{956}$CAT CTC CCA TCA CAT GCA AAA G$_{935}$	113	RT-PCR 56.2 qPCR 60
β-actin* NM_001101.3	$_{905}$TCCACGAAACTACCTTCAAC $_{924}$ $_{1509}$TTTAGGATGGCAAGGGAC $_{1492}$	605	56.2
GAPDH** NM_002046.3	$_{113}$TGAAGGTCGGAGTCAACGGCTTTG$_{136}$ $_{240}$CATGTAAACCATGTAGTTGAGGTC$_{217}$	128	60
MT1* NM_005946	$_{71}$ATGGACCCCAACTGCTCC$_{88}$ $_{256}$TCAGGCACAGCAGCTGCAC$_{238}$	186	60

Table 4.1 Primer sequences for human ZnT10 analysis of extracellular zinc treatments by RT-PCR and RT-qPCR analysis. The numbering on each of the oligonucleotides represents its position on the gene. *(Cragg et al., 2005),**(Valentine et al., 2007)

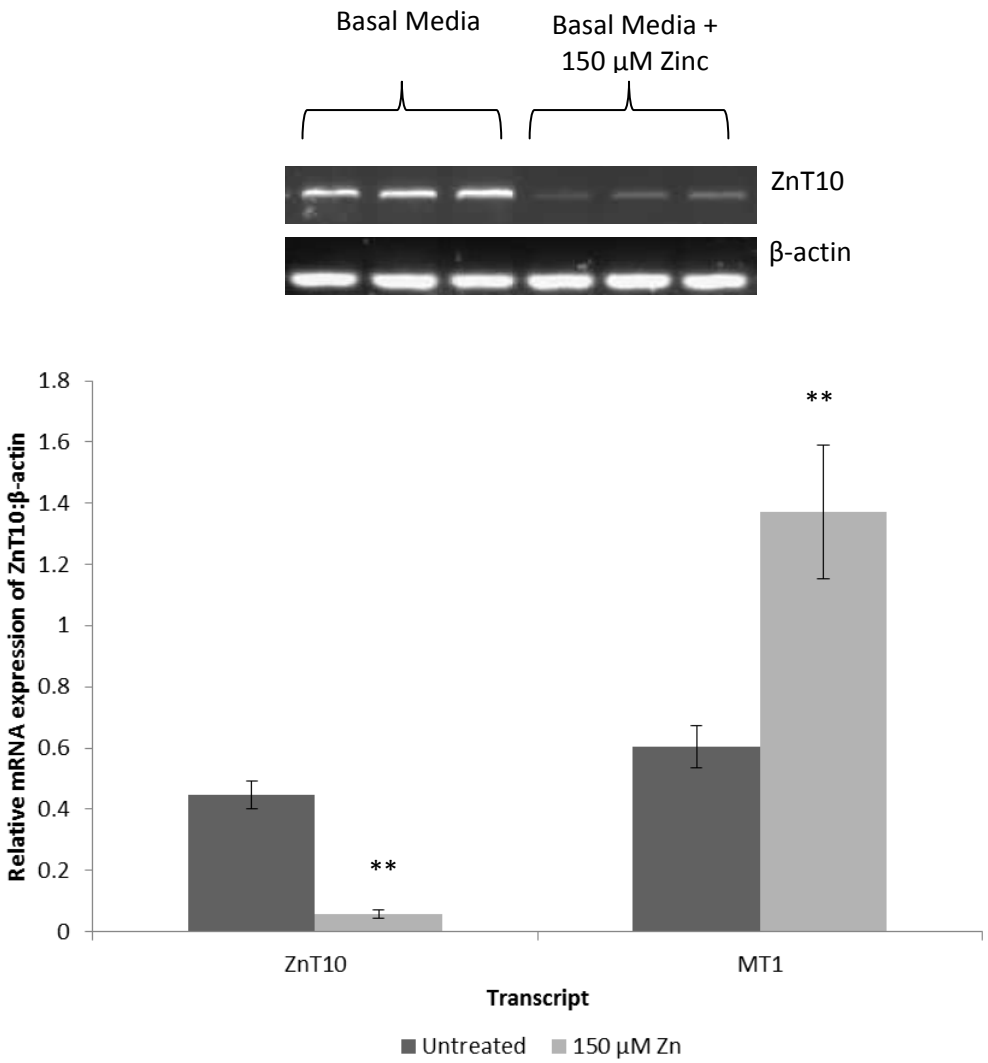

Figure 4.2 Analysis of relative ZnT10 mRNA levels in response to 150 µM extracellular zinc treatment in SH-SY5Y cells Histograms were obtained by densitometric measurement of band intensities from the ethidium bromide-stained agarose gels shown. Bands were generated by semi-quantitative RT-PCR from the RNA samples generated from SH-SY5Y cells using primers in Table 4.1. Analysis of relative ZnT10 mRNA levels and MT1 (as a positive control) are expressed as a ratio to β-actin. All values are shown as mean ± SEM, $n = 3$. *** $p < 0.001$, ** $p < 0.01$, by Students *t*-test.

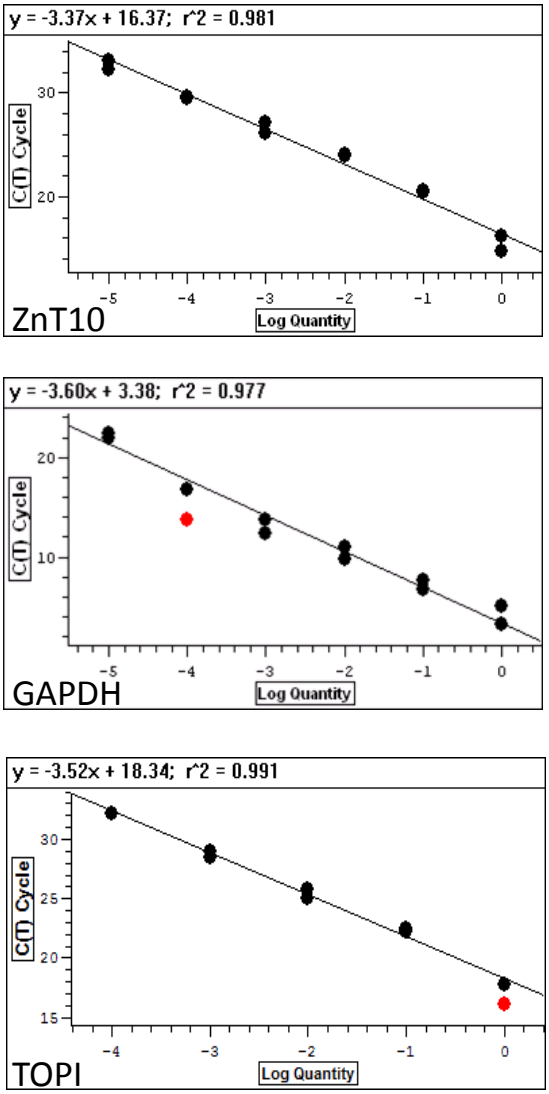

Figure 4.3 Standard curves generated to measure relative levels of ZnT10 by RT-qPCR, using SYBR green fluorescence and the DNA Engine Opticon 2 (MJ Research). Standards for GAPDH and ZnT10 products were generated by amplifying the region between the primers shown in Table 4.1, and subcloned into the vector pCR2.1-TOPO TA (Invitrogen). TOPI primers were purchased from PrimerDesign. A TOPI PCR product was produced and subcloned into the pGEM-T-easy vector to give the standard TOPI-pGEM (generated by Dr Alison Howard). The mean log concentration of each dilution was plotted against PCR cycle number at which the fluorescent threshold was crossed (C_T). Excluded data points are shown in red. These standard curves were used to calculate relative levels of ZnT10 transcripts.

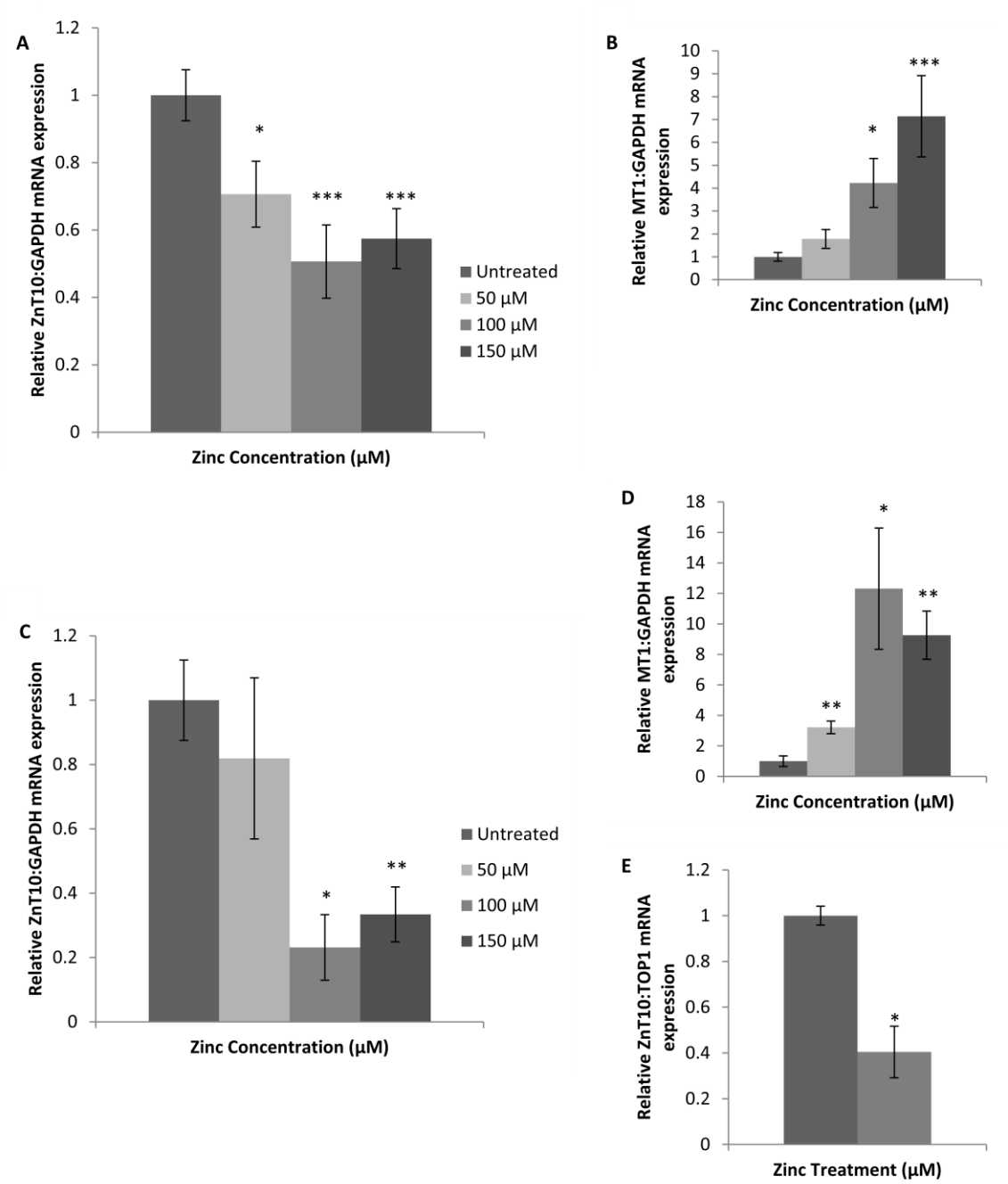

Figure 4.4 The effect of increased extracellular zinc on ZnT10 mRNA expression in SH-SY5Y and Caco-2 cells. Cells were cultured for 24 h in basal media (3 µM Zn) or at the zinc concentrations indicated (added as $ZnCl_2$) then total RNA was extracted. Levels of ZnT10 and MT-1 mRNA were measured by RT-qPCR, using SYBR green fluorescence and the DNA Engine Opticon 2 (MJ Research). (**A**) ZnT10 levels in SH-SY5Y cells (**B**) MT-1 levels in SH-SY5Y cells (**C**) ZnT10 levels in Caco-2 cells (**D**) MT-1 levels in Caco-2 cells Data are expressed relative to GAPDH mRNA levels measured in the same samples. All values are shown as mean ± SEM, $n = 6$. *** $p < 0.001$, ** $p < 0.01$, significantly different from 3 µM zinc (untreated) by one-way ANOVA followed by Bonferroni's multiple comparisons test. (**E**) ZnT10 levels for Caco-2 cell RNA expressed relative to TOPI mRNA levels, values are shown as mean ± SEM, $n = 3$. *$p < 0.05$ by Students *t*-test.

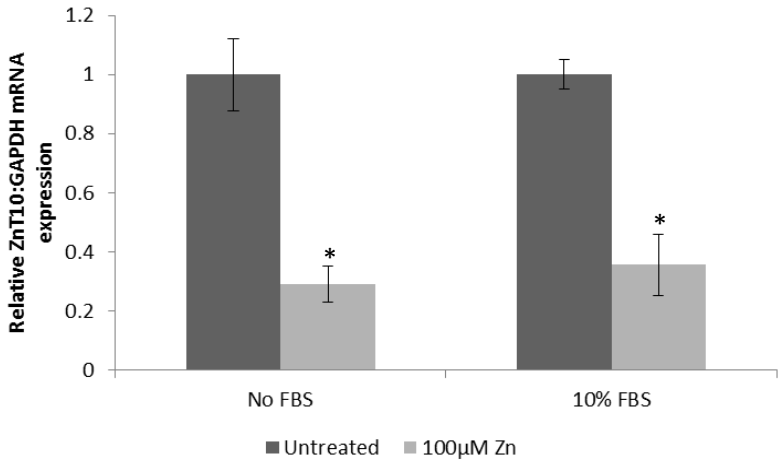

Figure 4.5 ZnT10 mRNA expression is affected by extracellular zinc (100 µM) but not by FBS concentration in SH-SY5Y cells. SH-SY5Y cells were cultured for 24 h with basal media (3 µM zinc) or with 100 µM extracellular zinc (added as $ZnCl_2$) in the presence or absence of 10 % FBS. Total RNA was extracted and levels of ZnT10 mRNA were measured by RT-qPCR. Data is expressed relative to GAPDH mRNA levels in the same samples. Values are shown as mean ± SEM, $n = 3$. *$p < 0.05$ bv Students *t*-test.

A

C-(A/C)-C-(T/A/G)-C-C-(C/T)-$(N)_n$-(G/A)-G-G-(A/T/C)-G-(T/G)-G

B

AACAACAACGAAACTCTGTCTCAAAAAAAAAAAAGAGTCTTTATTTGGAATAAACCTTCATGTAG
GTCAGTCGATTGTACTGCGTATCAGGTCATGCTGTCAGGGACACGTGGGGGTGAGTAGAATAT
TCTCTTCAATGAAGAATGAGACAAGTACACAGAGGAGGTCAGCCCTGGTTTCTTTGGCGGCCA
AGGGACTTGTGTCTACCACAAAGTAGACCAGCCTTCGAGTGCTAGGCAGGAGTGCATGCTTAC
AGAAGTGGGGTCTGCTCTCCTGAGGGCTGCCTGCGATTCACCCAGGGAAGGAAGCCTTGACA
GCGAAGATCCTGAAGGGGAACGGGGACGATCTTGTGCCATGAGTGGGTAATAGGAACGATCC
TGCACCGTTTATAATGGCTGTGAGGAACAAGAGAGGATTAAATAGCTTTATCCTGGGGTTAGTG
GAATGAGGGTGGAGGGCTGAGTGGCGGATGAGGTCACATTTCACGAAATGAAAAGCAGGAAG
CACCCTCAAGGGCAAGTTGCCCCAAGCCTGTGCTCCGGGGCCTTGCACCTGATTAATATGGAA
TCTGCACCGCAAGGTGCCTATGGGCACGTACGCGAAGGTGTCCCAGTCCACCGCAGCGAACA
CACCCCACAGCAGCCAAGGCCCTTATGACTGAGTCAACAGGACACTGGCGACCCTGAGGGCC
AGGAGAAGCGGGGTGTCTGGGTGAATCCCACCTCTGCATGGGGAGGGAGTCTGTGAAGATTG
ACGTCCAGACACGCCCCCTCTCCTCCGCAGCGCCCCTCTCTGCACAGTCCTGTCCCACAAAG
AGAGACATCGGCTCGTGGCCACCTGCCAAGTCAGGCCCAGGCCGCGAGGGAGGGGAAAAGG
GCCGCGGGAGGCGGTGCACGGGCTGTTCAGATACTGCCCCCGCCACTCCTTTAGACTCTGGA
CGTGCGGGGACTGGTGGCGCTCGGCCTCGCGTTATAAAAAGCGGTGGGGCAGGGCCGGCGA
GACAATCTGGGAGGCGGGTACCGGGCCTCACGGATCCGCGCCGCGCCCCCCACCTGTGGCT
GCGCGCGGGGTGGGCTGCGCTCCCCTGGGCGGCGCCGGGCGCCCGGGGCTGGTGGCGAG
ATGGGCCGCTACTCTGGCAAGACGTGCCGGCTGCTCTTCATGCTGGTGCTC

NNN Forward Primer

NNN Reverse Primer including predicted ZRE (942 bp)

NNN Predicted ZTRE sequence (*NNN CpG island*)

NNN Transcribed but untranslated region

ATG Start Codon

NNN MRE consensus sequence

NNN CuRE consensus sequence

Figure 4.6 Analysis of the ZnT10 promoter region A. The ZTRE sequence **B.** The ZnT10 promoter region annotated to show the putative ZTRE region (+58 to +84) (yellow); the primers used for generation of the promoter-reporter construct (forward; brown, reverse; green). The ATG start site is shown in red and the transcribed but untranslated region is highlighted in blue. The predicted metal responsive element (MRE) consensus sequences (Karin at al., 1984, Koizumi et al., 1999) are highlighted in brown. The predicted copper responsive element (CuRE) (Quinn and Merchant 1995) is highlighted in green.

Name/ Accession Number	Primer Sequences	Amplicon Length (bp)	Annealing Temp (°C)
Generate promoter-reporter construct	AGTGCTAGGCAGGAGTGCAT GAGCACCAGCATGAAGAGC	942	58
Substitute ZTRE (generate 5′ segment[1,2])	GATCCGATGGCTAGATCGAGTGCTAGGCAGGAGTGCATGC ***TCAGGATCGCGCGCAGCCACCATTCAA***GGGCGCGGCGCGGA TCCG	N/A	65-50[3]
Substitute ZTRE (generate 3′ segment[1,2])	***TTGAATGGTGGCTGCGCGCGCGATCCTGA***CTGCGCTCCCCTG GGCGG CTGCCGCCGTCGCCGGCTGAGCACCAGCATGAAGAGC	N/A	65-50[3]
Substitute ZTRE (join 5′ and 3′ products)	GATCCGATGGCTAGATCG CTGCCGCCGTCGCCGGCT	N/A	55

Table 4.2 Primer sequences to generate pBlueSLC30A10prom and pBlueSLC30A10prom$_{MUT}$ from genomic DNA. [1]Underlined sequence is additional unique random sequence to avoid re-amplification of wild-type sequence in the PCR reaction that joins the 5' and 3' segments. [2]Bold, italic sequence shows the sequence used to substitute the ZTRE. [3]Annealing temperature reduced from 65 °C by 1 °C every alternate cycle until 50 °C.

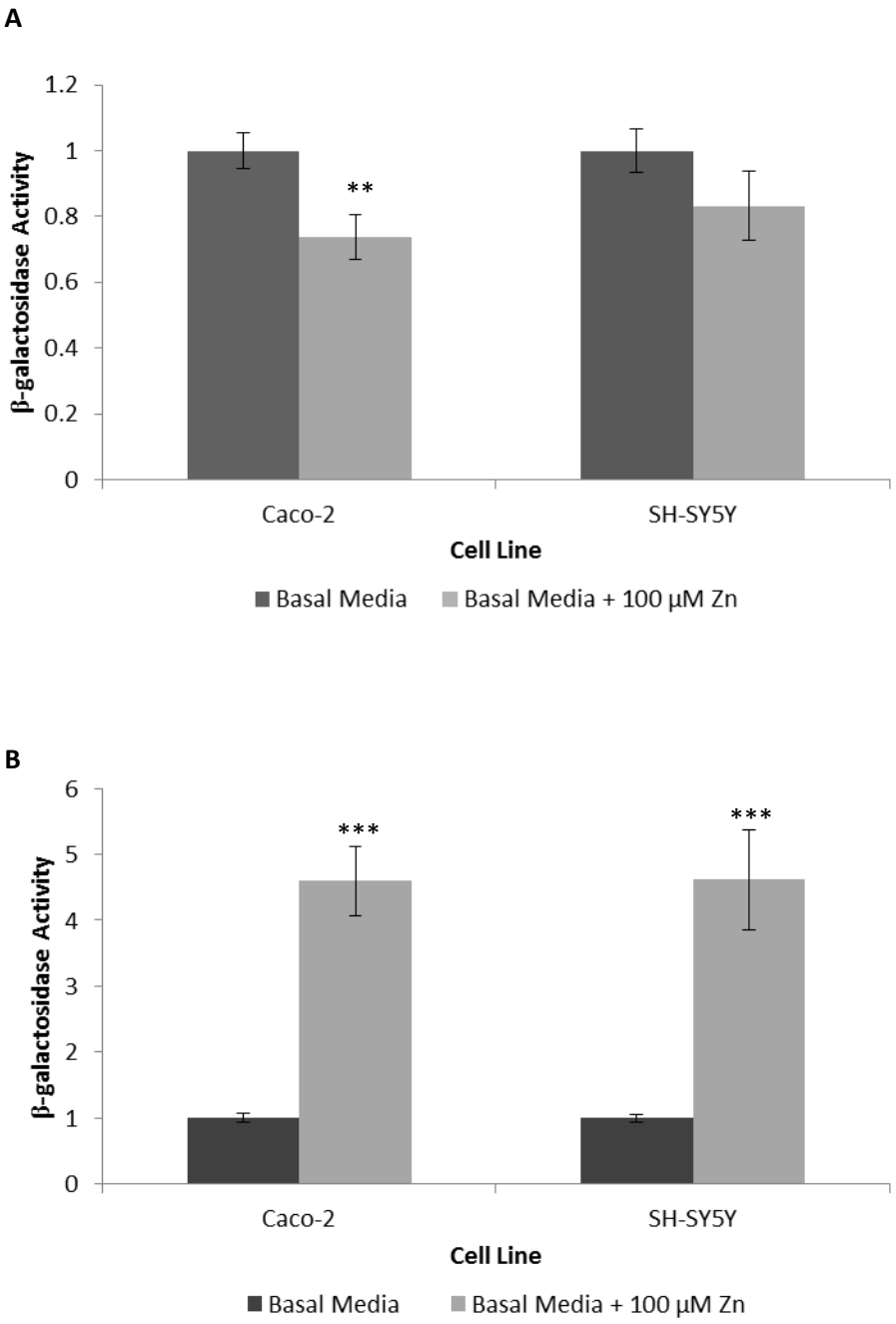

Figure 4.7 The response of the ZnT10 promoter to elevated extracellular zinc concentrations in Caco-2 and SH-SY5Y cells. Promoter activity was detected as activity in cell lysates of a β-galactosidase reporter gene immediately downstream of the genomic region in the vector pBlue-TOPO (Invitrogen) assayed using the substrate chlorophenol red-β-D-galactopyranoside. Negative controls included vector only. **A**. Relative levels of activity of the ZnT10 promoter region (-762 to +180) relative to start of transcription) at extracellular zinc concentrations (3 and 100 µM). **B**. Response of the human MT2a promoter (-358 to +40), assayed using the same reporter system, to manipulation of the extracellular zinc concentration (100 µM) in Caco-2 and SH-SY5Y cells. Values are means ± SEM (n = 3-6). *** $p < 0.001$, ** $p < 0.01$ compared with 3 µM zinc by Student's t-test.

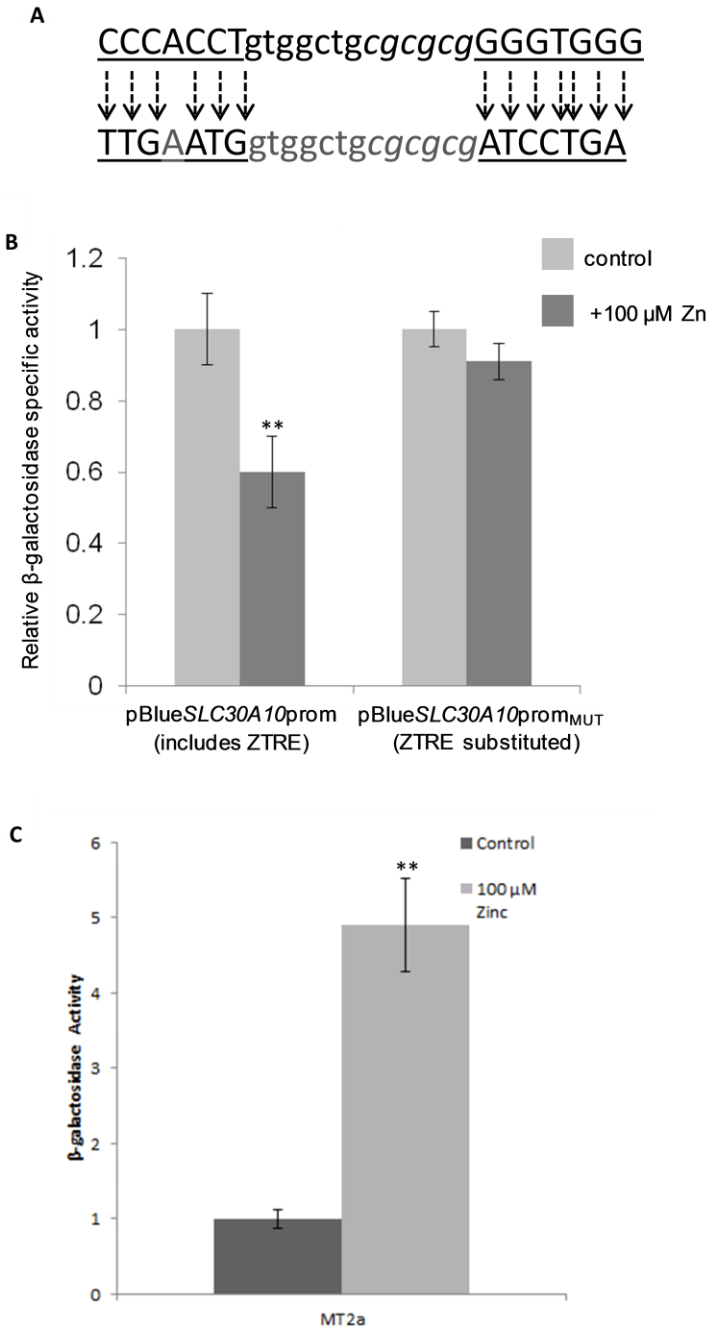

Figure 4.8 Analysis of ZTRE mutation in Caco-2 cells A. Schematic of ZTRE mutation in ZnT10 promoter region **B**. Relative levels of activity of the pBlueSLC30A10prom and pBlueSLC30A10prom$_{MUT}$ at extracellular zinc concentrations (3 and 100 µM). The response of the ZnT10 promoter and the mutant to elevated extracellular zinc concentrations in Caco-2 Promoter activity was detected as activity in cell lysates of a β-galactosidase reporter gene immediately downstream of the genomic region in the vector pBlue-TOPO (Invitrogen) assayed using the substrate chlorophenol red-β-D-galactopyranoside. Negative controls included vector only. **C**. Response of the human MT2a promoter (-358 to +40), assayed using the same reporter system, to manipulation of the extracellular zinc concentration in Caco-2 cells. Values are means ± SEM (n = 3). ** $p < 0.01$ compared with 3 µM zinc by Student's t test.

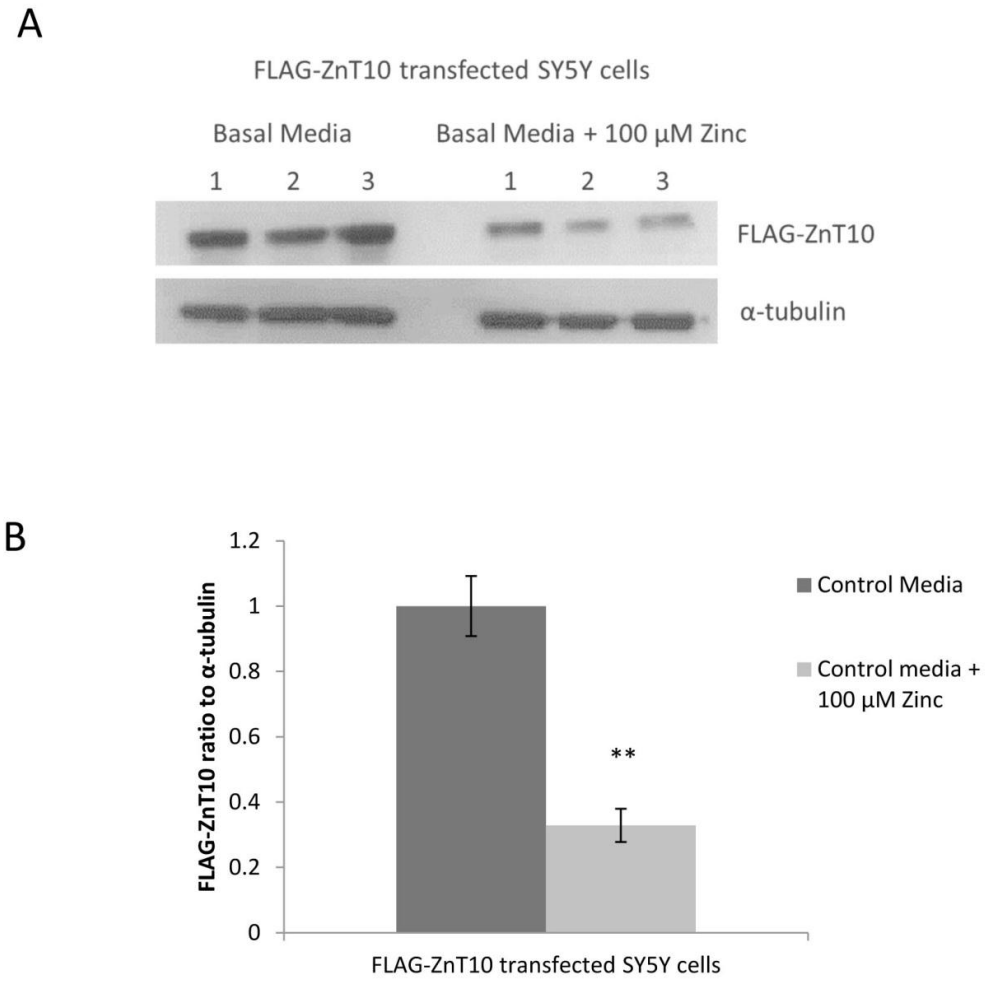

Figure 4.9 The effect of increased extracellular zinc on ZnT10 protein expression in SH-SY5Y cells. A. Expression in SH-SY5Y cells of ZnT10 protein fused with a FLAG epitope tag at the N- terminus visualized by immunoblotting at 100 µM of extracellular zinc. **B** Histograms were obtained by densitometric measurement of band intensities from the immunoblot shown above and are expressed relative to α-tubulin protein levels measured in the same samples. Values are means ± SEM, $n = 3$. ** $p < 0.01$ by Student's t test.

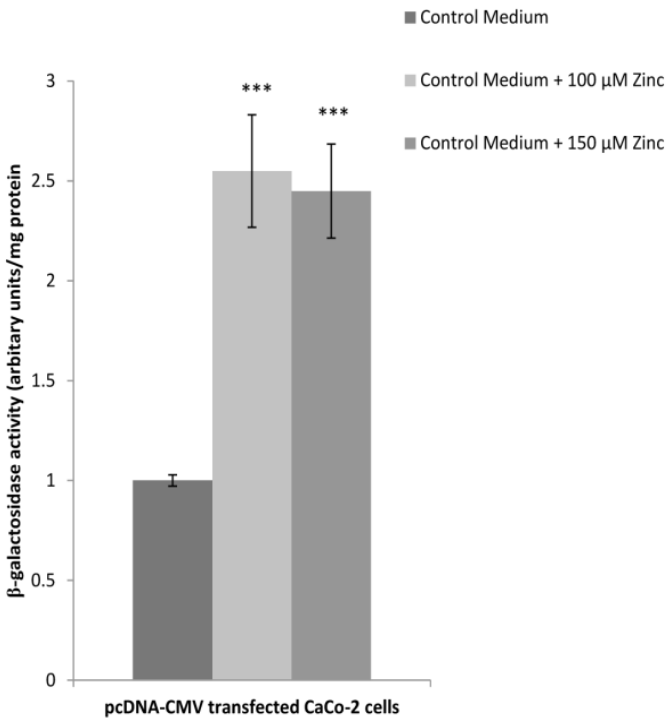

Figure 4.10 Response of the CMV promoter to an elevated concentration of extracellular zinc in Caco-2 cells. Caco-2 cells were transiently transfected with a pBlue-TOPO reporter construct containing the CMV promoter. Transfected cells were exposed to control serum-free medium or serum-free medium supplemented with either 100 µM or 150 µM $ZnCl_2$ for 24 hours and promoter activity was measured as β-galactosidase reporter gene activity. Values are means ± SEM (n = 3-9), and are expressed as a ratio of β-galactosidase reporter activity in control medium. *** $p < 0.001$ by Student's t test.

Name/ Accession Number	Primer Sequences	Amplicon Length (bp)	Annealing Temp (°C)
Mouse Znt8 NM_172816	5'-$_{397}$CTA GAC AGA GAA CTT CGA CAG$_{417}$-3' 5'-$_{532}$CTT GCT TGC TCG ACC TGT TC$_{513}$-3'	136 bp	60
Mouse Znt10 NM_001033286	5'-$_{826}$GTA GCA GGT GAT TCC CTG AAC$_{846}$-3' 5'-$_{965}$GTG ATG ACC ACA ACC ACG GAC$_{945}$-3'	140 bp	60

Table 4.3 Primer sequences used to generate mouse Znt8 and mouse Znt10 products. The numbering on each of the oligonucleotides represents its position on the gene.

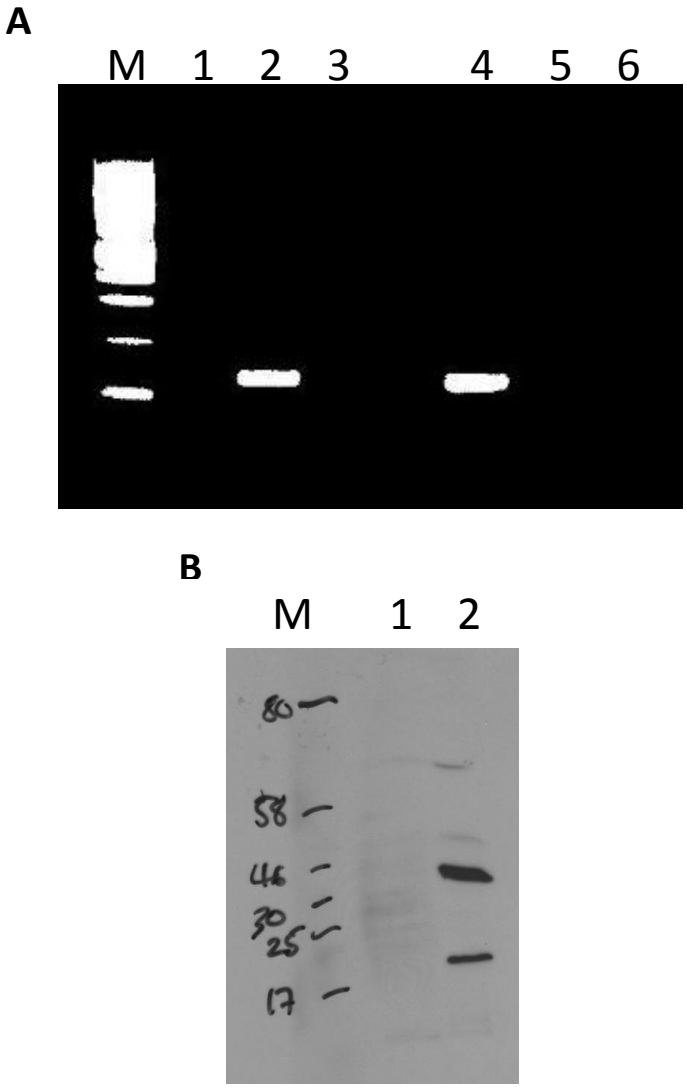

Figure 4.11.**Analysis of the specificity of commercial ZnT10 antibodies A.** RT-PCR using primers in Table 4.3; specific to mouse Znt10 (lane 1-3) and mouse Znt8 (lane 4-6) on RNA extracted from mouse brain (Lane 2 and 5) and pancreatic beta MIN6 cells (Lane 1 and 4). Lane 3 and Lane 6 are water controls. **B.** Immunoblotting using the ZnT10 (ZnT-10 (Q-14); Santa Cruz) primary antibody (1:1000) followed by a secondary donkey anti-goat IgG-HRP antibody (sc-2020; 1:10000; Santa Cruz) on SH-SY5Y neuroblastoma cells (brain derived lane 1) and Min6 (pancreas derived lane 2). Lane M - Approximate band sizes given using comparison to a pre-stained broad range protein marker (NEB).

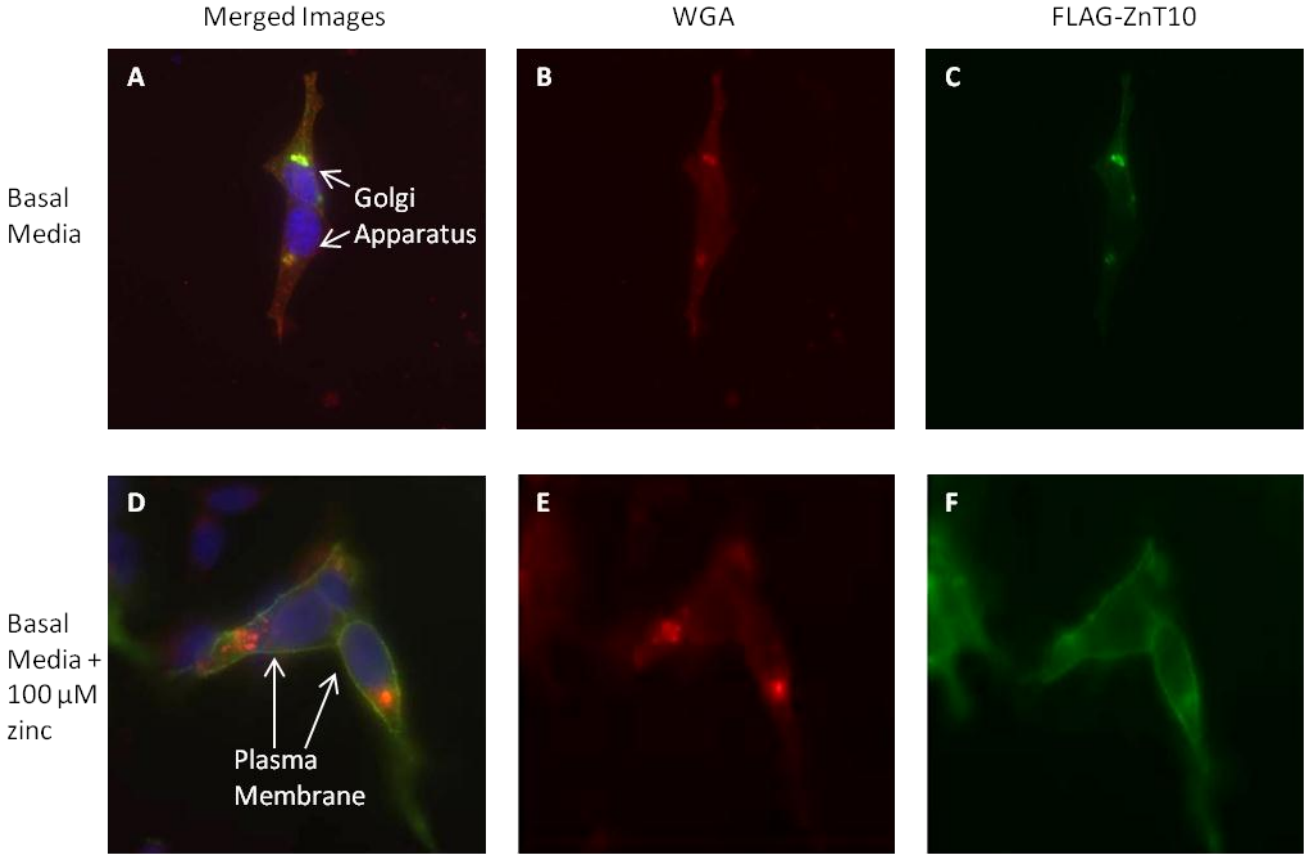

Figure 4.12 Subcellular localisation of ZnT10. Representative images of ZnT10 expressed with an N-terminal FLAG epitope tag in SH-SY5Y cells. ZnT10 localises to the Golgi apparatus under low extracellular zinc culture conditions (basal media; 3 µM), as revealed by co-localisation with Rh-labelled wheat germ agglutinin (WGA) in permeabilised cells (shown in panels **A, B** and **C**). ZnT10 translocates towards the plasma membrane with the addition of 100 µM extracellular $ZnCl_2$ for 24 h period immediately prior to viewing the cells shown by a reduction in a co-localisation with Rh-labelled WGA (shown in panels **D, E** and **F**). In merged images shown nuclei are stained with DAPI (blue, merged images in panels **A** and **D**). Cells were treated with anti-FLAG antibody (1:1000) (green, images in panels **C** and **F**) for 1 h, prior to permeabilisation with 0.1 % Triton X-100 and co-staining with Rh-labelled WGA (red, images in panels **B** and **E**). Experiments were carried out in triplicate and representative images shown.

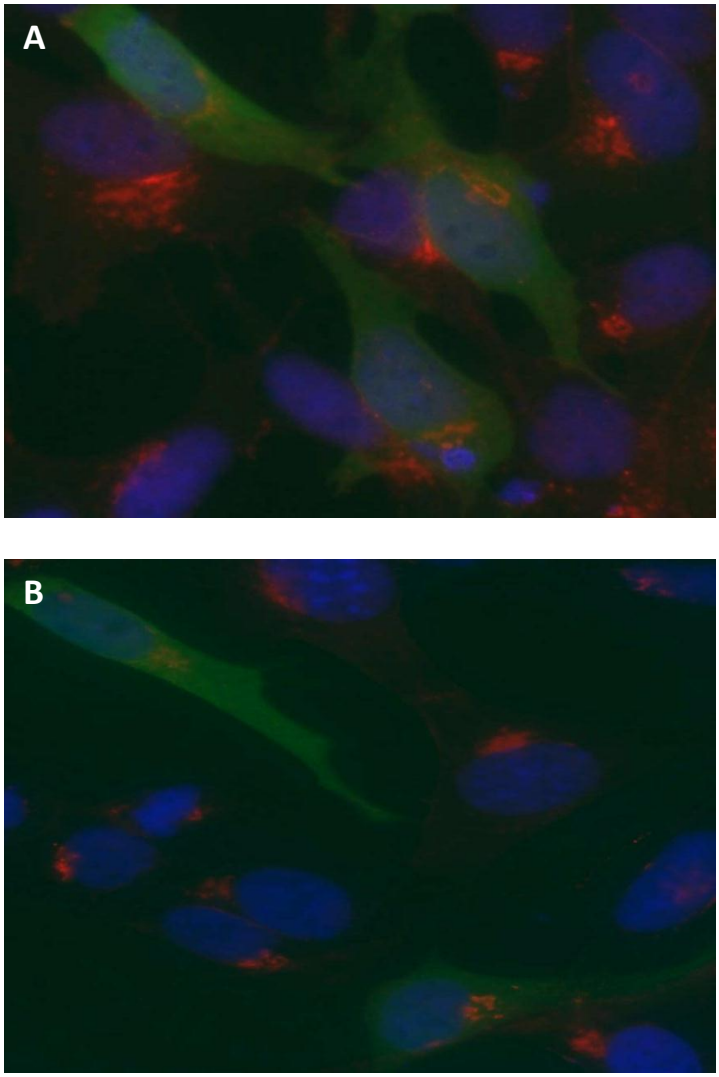

Figure 4.13 Subcellular localisation of ZnT10 vector only control. Representative images of an N-terminal FLAG epitope tag expressed with a BAP protein fusion (no ZnT10 insert, negative control) in SH-SY5Y cells. Cells were treated with anti-FLAG antibody (1:1000) (green) for 1 h, prior to permeabilisation with 0.1 % Triton X-100 and co-staining with Rh-labelled WGA (red). Nuclei are stained with DAPI (blue). **A.** No distinct localisation under low extracellular zinc culture conditions (basal media) **B.** No distinct localisation with the addition of 100 µM extracellular $ZnCl_2$ for 24 h period immediately prior to viewing the cells. Experiments were carried out in triplicate and representative images shown.

Chapter 5: The role of other divalent cations in ZnT10 regulation

5.1 Outline

The work outlined in this chapter is related to further characterisation of ZnT10, in response to the divalent cations copper, cobalt and nickel. The CDF family of ion transporters evolutionarily appear to be capable of transporting various divalent cations including cobalt, manganese, iron, cadmium and nickel (Anton et al., 1999, Delhaize et al., 2003, Grass et al., 2005, Munkelt et al., 2004). The mammalian ZnTs have not been fully characterised in relation to their response to these cations however there is a small body of research investigating interactions of the ZIP transporters and divalent cations. For example, ZIP8 and ZIP14 have been shown to be capable of cadmium transport, in addition to zinc with ZIP14 also able to transport manganese. However zinc is the preferred substrate for both ZIP8 and ZIP14 (Liu et al., 2008, Pinilla-Tenas et al., 2011). Interestingly, whilst ZIP4 has been shown to bind to copper, nickel and zinc it has only been shown to be able to transport copper and zinc (Antala and Dempski, 2012). This demonstrates that this family of proteins could have transport and indeed binding capabilities beyond zinc and these may in fact vary for each family member. Given that ZIPs are thought to interact with the divalent cations through their basic region, much like ZnTs, it is possible that ZnTs may also bind and be regulated by other metals. Of more relevance to this study is a very recent publication that reports ZnT10 can transport manganese. ZnT10 was able to restore growth in the manganese sensitive *Δpmr1* yeast strain (Tuschl et al., 2012). This indicates that ZnT10 will respond to cations in addition to zinc. Here I present results that show a regulatory response of ZnT10 at both the mRNA and protein level by cobalt and nickel. Subcellular localisation is also altered by metal treatments.

In the UK, in healthy individuals the RNI for copper is 1.2 mg/d for both men and women (age 19-50) (Henderson et al., 2003b). Copper is found in foods such as nuts, shellfish and offal. It is an essential nutrient that acts as a cofactor for many enzymes. Approximately 1 % of the eukaryotic genome is thought to contain copper binding proteins which, biochemically, are involved in processes such as respiration, free radical detoxification, iron transport and cross-linking of collagen and elastin (Andreini et al., 2008a). It is important for growth and development and is required to maintain a healthy immune system. Excess copper however can be toxic to cells. There is evidence for a synergistic relationship between zinc and copper within the human body, alluded to by the defects in copper homeostasis found in patients with Wilson's disease. This is an autosomal recessive condition characterised by a mutation in the copper ATPase (ATP7B) that results in an excessive hepatic copper accumulation manifesting as liver disease with neurological symptoms (Roberts and Schilsky, 2008). This can be fatal if the disease is not treated. High levels of zinc have been shown to be therapeutic in the condition, in that supplementation with zinc (up to 150 mg/d) stimulates intestinal MT, which in turn chelates copper in the intestine, reducing accumulation and increasing excretion in patient stools (Marcellini et al., 2005). Intriguingly, by both microarray and RT-qPCR ATP7B mRNA has been shown to decrease in response to zinc treatment in JAR cells (Jackson et al., 2009). A search in the putative promoter region has revealed a ZTRE sequence -610 bp to -383 bp, relative to the transcriptional start site, an interesting observation for future research. Furthermore, the ratio of copper to zinc (CZr) has been postulated to be a biomarker of ageing. Subsequent investigation into this hypothesis has yielded important initial results that suggest that the CZr showed both significant and stronger relationships to physical and functional measures of ageing than either copper or zinc alone (Mocchegiani et al., 2012a). In addition study

participants in the high CZr tertile had a significantly higher risk of death. Copper homeostasis is tightly maintained by a network of proteins. Primarily uptake of copper is attributed to the CTR proteins (SLC31A) with CTR1 mediating copper influx across the plasma membrane and into cells and CTR2 mediating copper transport within the cell (Zhou and Gitschier, 1997). Therefore the CTR proteins act much like the ZIP family of transporters for zinc. Conversely, ATP7A and ATP7B control export of copper, as the ZnTs do for zinc (Wang et al., 2011b). In addition, copper chaperones deliver copper to specific target enzymes. The interplay of zinc and copper and their similarities in mechanisms of homeostasis is intriguing. The data presented in this chapter shows that ZnT10 is not regulated by copper at the mRNA or the protein level and copper does not induce a change in subcellular localisation pattern in SH-SY5Y cells transiently expressing p3xFLAG-ZnT10. Moreover, despite the presence of a copper responsive element (CuRE), the ZnT10 promoter activity is not altered in response to copper.

Cobalt is an essential trace element that is present in lower levels than zinc and copper in metalloproteins, occurring in only 1 % of structurally characterised proteins compared with 9 % for zinc (Andreini et al., 2008b). The abundance of cobalt is relatively low in nature, but it is known to compete with iron in biological functions such as respiration. Cobalt in excess causes toxicity disease states, such as dermatitis, pneumonia, allergic asthma and lung cancer (Barceloux, 1999). As with zinc and copper, cobalt homeostasis is tightly regulated by uptake systems, efflux systems and metallochaperones (reviewed by Okamoto and Eltis, 2011). Cobalamin is a cobalt containing cofactor, acting as an electron sink by enabling the coordination of a cobalt ion, thereby stabilising the ion and facilitating its use in biochemical reactions. Our knowledge of cobalt homeostasis comes from bacterial systems. Interestingly, in these

systems regulation of efflux appears to be directly regulated by the cobalt ion, whereas uptake seems to be indirectly regulated by cofactors such as cobalamin. The regulation of cobalt effluxers identified in bacteria is thought to act at a transcriptional level (Koch et al., 2007, Liesegang et al., 1993). In contrast, uptake is thought to be regulated both at transcriptional and translation levels (Okamoto and Eltis, 2011). The data presented in this chapter reveals that mammalian ZnT10 is regulated by cobalt - decreasing expression at the mRNA level, without inducing a change in promoter activity in the wild-type ZnT10 promoter construct. Conversely, cobalt appears to up-regulate protein expression in cells expressing p3xFLAG-ZnT10 and induces a change the in subcellular localisation pattern in SH-SY5Y cells.

Nickel is an essential nutrient found in eubacteria, archaebacteria, fungi and plants. Similarly to zinc, copper and cobalt, nickel is a cofactor for many enzymes (reviewed by Li and Zamble, 2009). The only characterised nickel requiring enzyme found in eukaryotic systems is urease. This enzyme is absent in vertebrates and in fact nickel utilisation is restricted to plants and lower eukaryotes, such as fungi (Zhang et al., 2009). Most nickel requiring enzymes are limited to expression in microorganisms. Humans were thought to produce gastric urease however, discovery of *Helicobacter pylori* has led to the knowledge that the urease comes from this source. Moreover it has been hypothesised that gastritis is caused by this bacteria, in part, due to the ammonia produced by the urease enzyme thereby inducing toxicity in epithelial cells (Smoot, 1997). Thus nickel differs from the above metals, in that it is thought to be non-essential in the human body. Nickel exposure can however be toxic to humans via ingestion or absorption through the skin and comes from the use in manufacture of everyday items such as cooking utensils, coins and jewellery (Garrow et al., 2000) and in fact, in terms of humans, this toxicity has been the focus of research into nickel. The principle organs

effected by environmental exposure to nickel are the skin and the lungs causing conditions such as allergic contact dermatitis, lung fibrosis and lung cancer (reviewed by Cameron et al., 2011). Although the exact mechanisms of nickel induced carcinogenesis are not known, it is thought that it initiates pathogenesis by interfering with the metabolism of other essential metals e.g. iron, manganese, calcium, zinc and magnesium altering both genetic and epigenetic mechanisms (Kasprzak et al., 2003). Furthermore, the presence of nickel in tobacco smoke increases exposure to the metal and is thought to induce carcinogenesis in the head and neck in addition to in the lungs (Khlifi and Hamza-Chaffai, 2010). In those organisms that require nickel, systems exist to maintain homeostasis with importers, effluxers and metallochaperones protecting against toxicity. Whilst effluxers act to transport nickel few are specific to this ion. This implies that nickel accumulation is controlled primarily by tight regulation of uptake (Nies, 2003). Despite this an example of a nickel specific exporter is found in the *Thlaspi goesingense* plant; Metal Tolerance Protein 1 (TgMTP1) (Persans et al., 2001). This transporter has been studied due to the hyperaccumulation of nickel/zinc in *T. Goesingense*. The plant has the ability to accumulate up to 1.2 % of its shoot biomass as nickel (Kramer et al., 1997). Ordinarily this level of nickel would be toxic however *T. Goesingense* is protected from this effect by vacuole sequestration of nickel thought to be mediated partly by TgMTP1 (Kim et al., 2004). This transporter belongs to the CDF family and therefore it follows that other CDF family members may possess this same ability, even if such a characteristic is redundant. Based on this, the focus of my research, in part, was to assess the regulation of ZnT10 in response to nickel. Intriguingly the novel results presented in this chapter indicate that ZnT10 can be up-regulated in response to nickel at both the mRNA and protein level. In addition nickel

induces a change in p3xFLAG-ZnT10 protein subcellular localisation in transiently transfected SH-SY5Y cells in a manner similar to zinc.

5.2 Regulation of ZnT10 by extracellular cations at the mRNA level

The effect of extracellular metal cation availability on levels of expression of ZnT10 mRNA in SH-SY5Y cells and Caco-2 cells was determined by culturing cells at 100 µM of copper, 100 µM cobalt and 100 µM nickel for 24h. Confirmation of metal stock concentrations were obtained by inductively coupled plasma mass spectrometry (ICP-MS) (Table 5.1). Concentrations of metals in basal media are estimated as 0.124 µM cobalt, 0.002 µM of copper and 0.054 µM nickel (Versieck et al., 1980). Cell viability data as measured by the reduction of resazurin to resorufin (Alamar Blue, Invitrogen) for SH-SY5Y cells are shown in Figure 5.1. In addition these concentrations have been used previously in the literature with no reported effect on Caco-2 cell viability at this concentration. For concentrations of copper it has been determined that there is no significant difference in membrane permeability in this cell line at 100 µM copper (Tennant et al., 2002) and lactate dehydrogenase (a marker of oxidative stress) only gave a significant increase in Caco-2 cells at a copper concentration of 150 µM and above (Zodl et al., 2003). Cell viability assays, including Alamar blue assays, for Caco-2 cells treated with cobalt have demonstrated no significant difference compared with controls up to 48 hours, at a concentration as high as 200 µM (Horev-Azaria et al., 2011). For treatment with nickel, 200 µM of this ion did not affect the permeability of the cells (Tallkvist and Tjalve, 1998). Total RNA was extracted from cells and RT-qPCR carried out using GAPDH as the reference gene. Primers used for RT-qPCR analysis are shown in Table 3.4. Standard curves for all RT-qPCR passed acceptance criteria (Figure 5.2). All levels were assessed as a ratio to GAPDH and normalised to

untreated samples. Results are shown in Figure 5.3 and Figure 5.4A. Summarising the data compared with untreated samples, cobalt gives a significance decrease in ZnT10 transcript abundance relative to GAPDH in both cell types. For SH-SY5Y cells; p = 0.05 (Figure 5.3) and for Caco-2 cells; 100 µM cobalt p = 0.04 (Figure 5.4A). Conversely, nickel gives a significant increase in ZnT10 transcript abundance relative to GAPDH for both cell lines. For SH-SY5Y cells: 100 µM nickel; p = 0.002 (Figure 5.3) and for Caco-2 cells 100 µM nickel; p = 0.007 (Figure 5.4A). However there was no difference in ZnT10 transcript abundance in either cell line for treatment with copper. For SH-SY5Y cells: 100 µM copper; p = 0.63 (Figure 5.3) and for Caco-2 cells 100 µM copper; p = 0.12 (Figure 5.4A). In support of GAPDH as a reference gene for these experiments ZnT10 transcript abundance relative to TOPI as the reference gene in Caco-2 cells treated confirmed the above results with a significant decrease with 100 µM cobalt (p = 0.003), a significant increase with 100 µM nickel (p = 0.005) and no significant difference for 100 µM copper (p = 0.57) (Figure 5.4B). Zinc treatments were analysed as an additional control in all cases. Thus I can conclude that along with zinc, ZnT10 appears to be down-regulated at the mRNA in response to cobalt treatment, up-regulated in response to nickel with no change in response to copper.

5.3 Regulation of the ZnT10 promoter by metal treatments

Chapter 4 established the transcriptional regulation of ZnT10 in response to zinc is, at least in part, attributed to the ZTRE identified in the 5' UTR of ZnT10. Here the ZTRE was investigated to establish whether this response is specific to zinc or whether, as seen with mRNA, the promoter activity of this ZTRE region can be influenced by the other divalent cations studied. Again copper, cobalt and nickel were tested at a concentration of 100 µM. Interestingly, through analysis using the bioinformatic

programme, Fuzznuc (http://www.hpa-bioinfotools.org.uk/pise/fuzznuc.html), I identified a putative copper responsive element (CuRE) (Quinn and Merchant, 1995) in the promoter region of ZnT10; CTGCCA (-282 to 276 bp relative to the ATG start site) (Figure 4.6). To my knowledge, cobalt responsive sequences have not been elucidated however, I have identified two predicted MREs (Karin et al., 1984, Koizumi et al., 1999) in this promoter region; TGCGCGC (-60 to -54 bp relative to the ATG start site) and TGCGCTC (-44 to 38 bp relative to the ATG start site) (Figure 4.6).

5.3.1 *ZTRE response to extracellular metal treatments*

To study transcriptional regulation by copper, cobalt and nickel of the *ZnT10* gene, the response of the active promoter region to changes in the extracellular cation concentration in Caco-2 cells was measured. As previously described (section 4.3.2) a ZnT10 promoter-reporter construct (-762 bp to +180 bp, relative to the transcription start site, in pBlue-TOPO) was generated in which the candidate ZTRE (position +58 bp to +84 bp) was retained (pBlueSLC30A10prom). Cells were transfected transiently with the pBlueSLC30A10prom and maintained for 24 hour in both basal medium or medium supplemented with 100 µM zinc, 100 µM copper, 100 µM cobalt or 100 µM nickel. Excluding the response to zinc, reporter gene expression (β-galactosidase activity) was not changed significantly for any of the metals in Caco-2 cells (copper; $p = 0.37$, cobalt $p = 0.66$ and nickel; $p = 0.83$) (Figure 5.5).

5.3.2 *Response of the promoter region of ZnT10 to extracellular metal treatments after mutation of the ZTRE*

In order to ascertain whether mutation of this ZTRE region within the 942 bp promoter reporter construct pBlueSLC30A10prom had an effect at elevated extracellular copper, cobalt or nickel concentrations an additional promoter-reporter construct was made;

pBlueSLC30A10prom$_{MUT}$ (section 4.3.3). Within this construct, pBlueSLC30A10prom$_{MUT,}$ the primers shown in Table 4.2 were used to substitute the ZTRE present in ZnT10, retaining the inter-palindrome linker region but mutating the near palindromic sequences at either end as shown in Figure 4.8A. This gave an end-product of a 942 bp promoter reporter construct to compare with pBlueSLC30A10prom. In line with previous experiments, Caco-2 cells were transfected transiently with either the pBlueSLC30A10prom or pBlueSLC30A10prom$_{MUT}$ and maintained for 24 hour in both basal medium or medium supplemented with 100 µM zinc, 100 µM copper, 100 µM cobalt or 100 µM nickel. Reporter gene expression (β-galactosidase activity) was unchanged at the higher extracellular concentration for both copper and nickel for both promoter reporter constructs; pBlueSLC30A10prom and pBlueSLC30A10prom$_{MUT}$. Interestingly, pBlueSLC30A10prom showed no change at the higher concentration of cobalt however, the mutated promoter reporter construct, pBlueSLC30A10prom$_{MUT}$, showed a significant increase in activity with the addition of 100 µM cobalt (p = 0.002) (Figure 5.5).

5.4 ZnT10 expression in response to extracellular cations at the protein level

To examine the effect of metal treatment on ZnT10 protein expression, SH-SY5Y cells were transiently transfected with the plasmid p3xFLAG–ZnT10, a plasmid construct from which ZnT10 was expressed with an N-terminal FLAG epitope tag. Twenty-four hours post transfection cells were treated with basal medium or medium supplemented with either 100 µM zinc, 100 µM copper, 100 µM cobalt or 100 µM nickel for a further 24 hours. Subsequently the cells were lysed using a buffer containing 4 % SDS, 125 mM Tris and 5 % β-mercaptoethanol in order to extract the protein (section 2.4.2). The protein was electrophoresed on a denaturing 10 % acrylamide gel and blotted onto a

PVDF membrane (section 2.7.2). Equal quantities of protein prepared from cells treated under all conditions, as determined spectrophotometrically (Nanodrop) was loaded onto the gel. Equal loading of both samples was further confirmed by re-immunoprobing blots with an anti-α-tubulin antibody. Western blot analysis used an anti-FLAG antibody (Sigma; 1 in 1000 dilution) and subsequently an anti-mouse IgG-HRP secondary antibody (GE Healthcare; 1 in 20000 dilution). These were visualised by enhanced chemiluminescence (ECL) HRP substrate (Thermo Scientific). This revealed a protein band of approximately 56 kDa (the expected size for ZnT10 (53 kDa) plus 3 x FLAG (3 kDa)) in all samples, indicating that N-terminal cleavage had not taken place. Western blots were stripped and re-probed, using an anti-α-tubulin primary antibody (Abcam; 1 in 5000 dilution) and an anti-rabbit IgG -HRP secondary antibody (Abcam; 1 in 20000 dilution). Analysis of ZnT10 expression levels by densitometric quantification of band intensities, expressed as a ratio to α-tubulin and normalised to untreated samples, revealed a significant increase in p3xFLAG-ZnT10 protein expression at 100 µM cobalt (p = 0.006) and 100 µM nickel (p = 0.01) compared with the untreated cells. However there was no change in protein expression with 100 µM copper treatment (p = 0.5). Again we see the expected down-regulation at 100 µM zinc (p = 0.03) (Figure 5.6).

Attempts to investigate endogenous ZnT10 levels were unsuccessful due to the lack of antibody specificity. This work is summarised in Chapter 4.

5.5 Subcellular localisation of ZnT10 in response to extracellular cations

To examine the intracellular distribution of ZnT10, SH-SY5Y cells were transiently transfected with the plasmid p3xFLAG–ZnT10. Forty eight hours post transfection cells were fixed using 4 % PFA and stained with the anti-FLAG antibody (1:1000,

Sigma). Rhodamine conjugated WGA, a lectin that selectively binds N-acetylglucosamine and N-acetylneuraminic acid, was used to stain the Golgi apparatus in cells permeabilised with 0.1 % Triton X-100 following PFA fixation. Chapter 4 reports that ZnT10 co-localised with WGA in permeabilised cells, consistent with localisation to the Golgi apparatus (Figure 4.12). Alteration in the pattern of localisation was induced by changing the extracellular metal concentration in basal medium with the addition of 100 µM extracellular copper, 100 µM extracellular cobalt or 100 µM extracellular nickel for 24 hour period immediately prior to viewing the cells. Treatment with 100 µM extracellular cobalt showed a distinctly different localisation pattern to untreated cells (Figure 5.7) with no co-localisation with WGA and a more diffuse expression pattern. Extracellular nickel at a concentration of 100 µM showed a localisation pattern more consistent with zinc treatment (Figure 5.7) whereby there was a reduced co-localisation with the WGA in permeabilised cells and a more diffuse pattern of localisation including some expression towards the plasma membrane. With 100 µM extracellular copper, strong Golgi apparatus expression remained, similar to untreated cells (Figure 5.7). Transfection experiments were carried out in triplicate. All p3xFLAG-ZnT10 transfected cells revealed an identical pattern of localisation under the different treatments. p3xFLAG-BAP (used as a negative control) showed a diffuse pattern of expression throughout the cell in all experiments, which was not altered by extracellular cation treatment, confirming that localisation of the signal to specific subcellular regions was a function of the attached ZnT10 protein.

5.6 Discussion

In this chapter, using RT-qPCR, I have demonstrated a decrease in endogenous mRNA expression of ZnT10 in response to increased extracellular cobalt in both the Caco-2 and SH-SY5Y cell line models. This result is novel as regulation of the ZnT family of transporters by the divalent cation has not previously been shown. Up-regulation of ZnT10 at the mRNA level in response to extracellular nickel in both cell lines was also observed. This result was unexpected as nickel is not thought to be important in the human body and therefore the regulation of ZnT10 by nickel would not seem necessary. Conversely, due to the reported synergy between zinc and copper, and given the regulation at the mRNA level by both cobalt and nickel it is curious that copper has no effect on the mRNA expression levels of ZnT10. These observations are intriguing especially given the recent publication identifying frame-shift mutations in the *SLC30A10* gene in patients with the neurological conditions dystonia and Parkinsonism that lead to hypermanganesemia in brain regions (Quadri et al., 2012). Rescue experiments were performed in a yeast mutant demonstrating the ability of wild-type ZnT10 to restore growth in a manganese sensitive yeast mutant *Δpmr1* (Tuschl et al., 2012). Analysis of the zinc binding ability of ZnT5 has identified a region within this CDF that is known to be involved in selectivity of the transporter (Ohana et al., 2009). This region is conserved in ZnT10 (Figure 3.1). Mutational analysis of this region in ZnT10 would allow us to ascertain if these residues are involved in selectivity in this CDF member. Additionally, ZnT10 has a serine rich region opposed to the conventional histidine rich region found in most family members (Seve et al., 2004). It is possible that transporter ability may be attributed to this area. Interestingly ZnT6 also contains this serine rich region and it is known to act as a heterodimer with ZnT5 in order to transport zinc (Huang et al., 2002, Suzuki et al., 2005b). This knowledge could be used

in order to support ZnT10 studies if ZnT6 also has manganese transporting capabilities. It is difficult to make comparisons with other ZnTs, as this work has not been carried out however what should be noted is the universal order of preference of metal binding known as the Irving-Williams series. As the ionic radii decreases the normal periodic trend would dictate that the stability of which the ion can bind would increase and therefore the series gives weakest binding affinities for manganese < iron < cobalt < nickel < copper > zinc (Irving and Williams, 1948). It is of note that as the affinities increase there is a concurrent increase in how tightly the metal is buffered within the cytoplasm with copper being extremely tightly buffered and bound. Following this series, if all the metals tested here were present in the cytosol, all proteins would bind copper given that it is the divalent cation with the tightest affinity (reviewed by Waldron and Robinson, 2009). Interestingly, results indicate that of the metals tested, copper is the only one not to exhibit an effect on ZnT10 therefore suggesting that there is a mechanism developed to prevent the interaction. Investigation into the effects on regulation of both manganese and iron would add further insight into whether this order of preference is relevant in the cell line models. Moreover, it would be worthwhile assessing the roles of regulation the other ZnT family members in order to establish whether the seemingly specific nature, with respect to copper, is maintained throughout the mammalian family of transporters.

Chapter 4 describes mammalian zinc-responsive genomic elements responsible for transcriptional repression in response to elevated zinc concentration. Given the response of ZnT10 to the cations, nickel and cobalt, at the mRNA and protein level, the ZTRE identified was also investigated to establish whether these cations also have a response on the same promoter region.

The CuRE identified in the region cloned into the promoter-reporter construct; CTGCCA (-282 to 276 bp relative to the ATG start site), would lead to a prediction of a response to copper, however no copper response was detected in our system. The sequences for CuREs were first discovered in *Chlamydomonas reinhardtii,* where copper deficiency induces the expression of cytochrome c_6. These elements were identified in the promoter region of the gene thereby activating transcription of cytochrome c_6 in copper deficient cells (Quinn and Merchant, 1995). Here I assessed promoter activity of ZnT10 in response to increased extracellular copper. Quinn et al., (1995) assessed the CuRE in conditions of both copper deficiency and copper supplementation however they did so relative to a minimal promoter element derived from the β_2-tubulin gene and did not assess the CuRE construct at basal levels of copper. Activation appears to be evident but whether repression occurs, relative to wild-type has not been addressed. It is possible that the arrangement of the CuRE could be a factor in this as there is only a single copy of the CuRE. The data presented by Quinn et al., (1995) reveals two CuREs although, it is noted that one element seems to function independently of its counterpart. Perhaps more relevant are the studies into the yeast copper transport proteins FRE1, CTR1 and CTR3 all of which contain an alternative CuRE in their promoter; TTTGCTC. This sequence is not present in the upstream region of ZnT10 present in the pBlueSLC30A10prom. The CuRE identified here repressed transcription of FRE1, CTR1 and CTR3 in the presence of copper, a result attributed to this common element (Labbe et al., 1997) and therefore its absence from the promoter region of ZnT10 would indicate that it is not influenced by copper.

MREs have a core consensus sequence of TGCRGNC (Stuart et al., 1985, Culotta and Hamer, 1989). Using bioinformatics I have identified two MRE consensus sequences in the promoter region of ZnT10; TGCGCGC (-60 to -54 bp relative to the ATG start site)

and TGCGCTC (-44 to 38 bp relative to the ATG start site). MREs are *cis*-acting DNA sequences that are known to be required for heavy metal-induced transcriptional activation (Karin et al., 1984). Much research has been carried out into the involvement of zinc and MREs in mammalian MT genes and importantly the MT2a promoter, described in Chapter 4, contains seven MREs (Koizumi et al., 1999). Koizumi et al., (1999) reported that it is necessary to have multiple copies of these MREs in the promoter sequence and that MRE copies act synergistically. Thus, although research focuses on responses to cadmium and zinc (Karin et al., 1984), (Koizumi et al., 1999), the presence of two MREs in the promoter of ZnT10 would suggest the ability of a response to the divalent cations tested. However promoter activity was not altered by treatment with cobalt, copper or nickel. Therefore, for this arrangement neither the CuRE nor the MREs allow metal binding in this system. It is interesting that the MREs fall over the ZTRE identified in Chapter 4 and it is possible that the conformation necessary for an effective ZTRE does not allow for binding of the necessary elements to the MREs. In addition, since there are no effects on transcription for these other metals, then perhaps the changes in mRNA are in fact due to the stability of the transcripts rather than transcriptional control.

Subsequent experiments investigated the mutation of the ZTRE region in response to the other cations. The truncation in response to zinc highlighted the importance of the ZTRE sequence, however the lack of response of the wild-type ZTRE to the cations would imply that this is not the mode of regulation for these metals. Surprisingly, cobalt induced a significant increase in promoter reporter activity in the mutant ZTRE construct. It is a possibility that mutation causes a conformational change that works two-fold. In the first instance the structural change means that the zinc induced transcriptional repressor is unable to bind. Secondly, the restructured conformation

allows a cobalt induced transcriptional activator to bind to the now accessible MRE thereby increasing promoter activity. This response is restricted to cobalt as neither copper nor nickel showed an increase in promoter activity with the mutant construct. Future work would include mutation of the MRE within the mutant ZTRE construct to see whether this element is responsible for the increase in promoter activity seen.

Cells transfected transiently to over-express ZnT10 fused to the FLAG epitope tag at the N-terminus revealed an increase in ZnT10 expression at the protein level with both increased extracellular cobalt and nickel. This result for extracellular cobalt is in contrast to that seen at the mRNA level. In line with the mRNA levels however, extracellular copper gave no change in the protein level of p3xFLAG-ZnT10. This strategy to investigate the effects of metals on levels of ZnT10 protein expression was employed as the commercially available antibodies to ZnT10 (Santa Cruz) were not effective (see Chapter 4). Data investigating the effect of cobalt and nickel on the CMV promoter would strengthen this result. Intriguingly, cobalt has the opposing effect in the protein extracted from transfected cells to the effect at the endogenous mRNA level. This could be an effect on the CMV promoter of the vector. If it is a true response at the protein level perhaps this effect in part could be explained in term of mRNA stability. RT-qPCR allows measurement of the level of mRNA expression in the cells at that time point, however it is unable to establish whether this effect is seen at the level of transcription because the mRNA level is a balance between synthesis and degradation. Therefore the mRNA level quantified can be affected by mRNA stability. The time point will have an effect on the results. For example, if the response of ZnT10 to cobalt occurs earlier than 24 hours this would enable an increase in ZnT10 at the protein level to be observed, however if this mRNA is degraded at a high rate then at this time point the observed mRNA level would be less. Future experimentation would enable further

insight into the mechanisms at play. The stability of mRNA could also have an effect on the response to nickel. I would not expect a human ZnT to be regulated by nickel, however the role of certain CDFs to nickel is interesting. One example is TgMTP1 in the plant *T. goesingense*, which helps protect the plant from the ordinarily toxic levels of nickel by facilitating the sequestration of nickel in the vacuoles (Kim et al., 2004). Indeed, this is a requirement of CDFs further down the evolutionary tree than ZnTs and one explanation for the response to nickel in ZnT10 would be that this ability to respond has been evolutionarily conserved, despite being thought to be redundant in humans. Investigation with other ZnTs would help in elucidating these roles further. In addition, assessing endogenous ZnT10 would also accelerate this knowledge and ascertain the true protein response to nickel.

In Chapter 4 the subcellular localisation of ZnT10 in SH-SY5Y cells is reported to be at the Golgi apparatus in cells transfected transiently with an N-terminal FLAG-tagged construct of ZnT10 with an observed movement towards the plasma membrane with addition of 100 µM extracellular zinc. At extracellular concentrations of 100 µM nickel ZnT10 was observed to re-localise towards the plasma membrane a result that corresponds to the response seen with zinc. Intracellular trafficking of several zinc transporters in response to zinc has been observed, in particular for members of the ZIP family of zinc transporters, specifically ZIP1, 3, 4, 5 and 8 (Wang et al., 2004b, Desouki et al., 2007) as described in Chapter 4. Di-leucine motifs occur in ZnT10 between amino acid positions 242 and 243 as well as 286 and 287 and 298 and 299, which are found within the predicted C-terminal cytosolic region. It is a possibility that the re-distribution of ZnT10 from the Golgi apparatus to the plasma membrane is dependent on one or more of these di-leucine motifs. These are comparable with motifs that are thought to mediate trafficking of other metal transporters, such as the MNK copper

transporting protein and ZnT6 which are both translocated from the TGN (Petris and Mercer, 1999, Huang et al., 2002). Moreover, given the similar response of p3xFLAG-ZnT10 with extracellular nickel as compared to extracellular zinc observed in SH-SY5Y cells perhaps this motif is also involved in the trafficking seen with this metal. The importance of these motifs in the intracellular distribution and nickel-induced redistribution of ZnT10 should be addressed in future experiments in which they are deleted by site-directed mutagenesis. The translocation seen here in response to nickel acts to support further the hypothesis that this is due to sequences that are conserved from evolutionary counterparts that are ordinarily redundant in humans. There has been a relatively recent rise in use of the metal in the manufacture of everyday items (Garrow et al., 2000). Perhaps the conservation of the sequences that are nickel responsive can be interpreted in two ways. Firstly, it is a possibility that the sequences have not been selected against despite being redundant. Therefore, the recent rise in environmental nickel plays detrimental role in the human body by using these elements, causing subsequent toxicity. Alternatively, the nickel responsive sequences may have been retained due to the protective properties they offer the cell upon nickel exposure. In this instance, the rise in nickel exposure would lead to a saturation of these mechanisms.

The pattern of expression in response to cobalt is particularly intriguing. Fluorescent microscopy revealed a more diffuse pattern of expression throughout the cell as compared with all other treatments and with basal medium. Interestingly, for metalloproteins it has been shown that the localisation of folding within the protein influences the metal to be bound. In fact metal co-factors are important in the folding of many proteins and if the correct metal is present at the folding stage only the correct metal is able to bind subsequently, therefore, if there is an excess of competing metals there is the potential that this will interfere with protein structure. The importance of

these factors is evident for cyanobacterium proteins MncA and CucA. MncA is a substrate of twin-arginine translocase that is able to acquire manganese by folding in the cytoplasm where copper is tightly buffered or bound. The folding of MncA means that the site that binds manganese is buried. Conversely, CucA is a substrate of the general secretory pathway that acquires the more competitive metal copper by binding in the periplasm (Waldron and Robinson, 2009). This also highlights the importance of compartmentalising metals. Indeed with respect to the Irving-Williams series, cobalt is buffered to a lesser degree as compared with both zinc and nickel. Furthermore, I observed an increase in p3xFLAG-ZnT10 expression by Western blotting with extracellular cobalt treatment. It is therefore a possibility that the increase in the protein coupled and with influx of cobalt from the extracellular treatment enabled the interaction with p3xFLAG-ZnT10 and cobalt, when ordinarily the protein would bind to zinc, thus resulting in altered folding and therefore localisation. It would be interesting to establish whether ZnT10 retains its efflux ability, described in Chapter 3, when cobalt is present or whether the localisation pattern observed is indicative of a broader spectrum of changes in the protein resulting in lack of function. The reaction of ZnT10 to cobalt and nickel are novel and exciting results but they require further investigation to draw more accurate conclusions as to the relevance of the regulation and localisation changes.

Corresponding to both mRNA and protein expression again copper does not seem to have an effect on p3xFLAG-ZnT10. This would indicate that ZnT10 is not regulated by this metal and therefore is not involved in its transport. The lack of response of ZnT10 to copper is not unique in the ZnT family of transporters. ZnT1 has also been found not to alter protein expression in response to copper treatment (30 microg/ml) for 48 and 72 hours in the hepatoblastoma cell line; HepG2 (Urani et al., 2003).

	Dilution	Concentration (µM)
Cobalt	1	1.106
	10	11.79
	100	114.2
Stock Concentration (mM)		**114.2**
Copper	1	0.945
	10	9.75
	100	101.6
Stock Concentration (mM)		**97.9**
Nickel	1	1.08
	10	10.95
	100	111.1
Stock Concentration (mM)		**109.7**

Table 5.1 ICP-MS analysis of metal stocks to be diluted for cell treatments

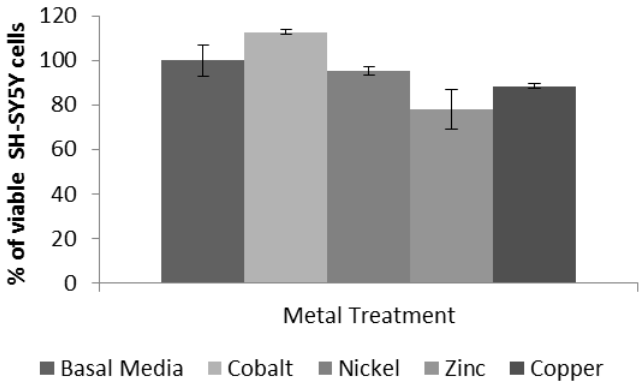

Figure 5.1 The effect of extracellular cation treatment on cell viability in SH-SY5Y cells measured by the conversion of resazurin to resorufin (Alamar Blue, Invitrogen) in the presence of 100 µM extracellular cation concentration (indicated). All values are shown as mean ± SEM, *n* = 3.

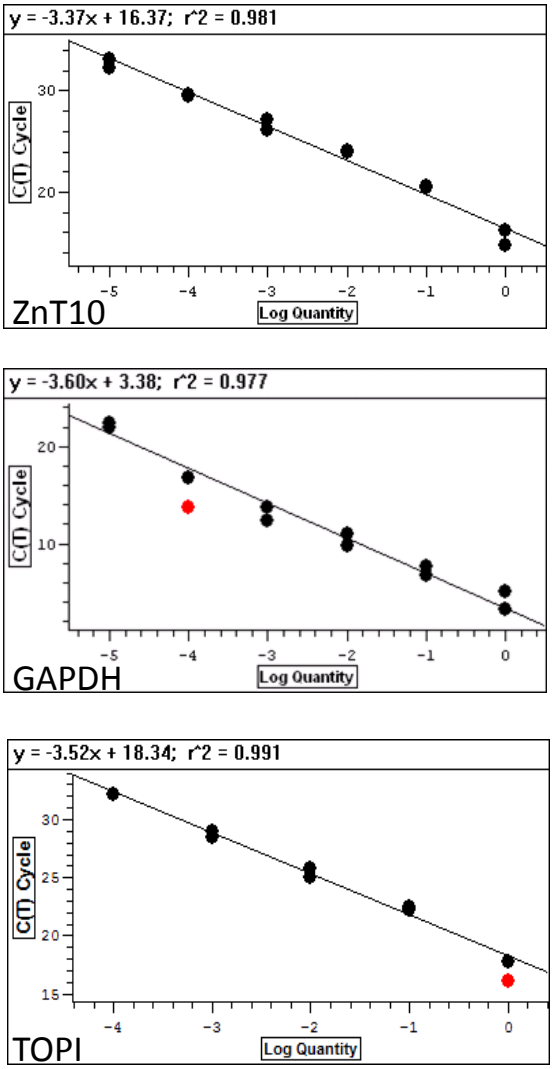

Figure 5.2 Standard curves generated to measure relative levels of ZnT10 by RT-qPCR, using SYBR green fluorescence and the DNA Engine Opticon 2 (MJ Research). Standards for GAPDH and ZnT10 products were generated by amplifying the region between the primers shown in Table 3.4, and subcloned into the vector pCR2.1-TOPO TA (Invitrogen). TOPI primers were purchased from PrimerDesign. A TOPI PCR product was produced and subcloned into the pGEM-T-easy vector to give the standard TOPI-pGEM (generated by Dr Alison Howard). The mean log concentration of each dilution was plotted against PCR cycle number at which the fluorescent threshold was crossed (C_T). Excluded data points are shown in red. These standard curves were used to calculate relative levels of ZnT10 transcripts.

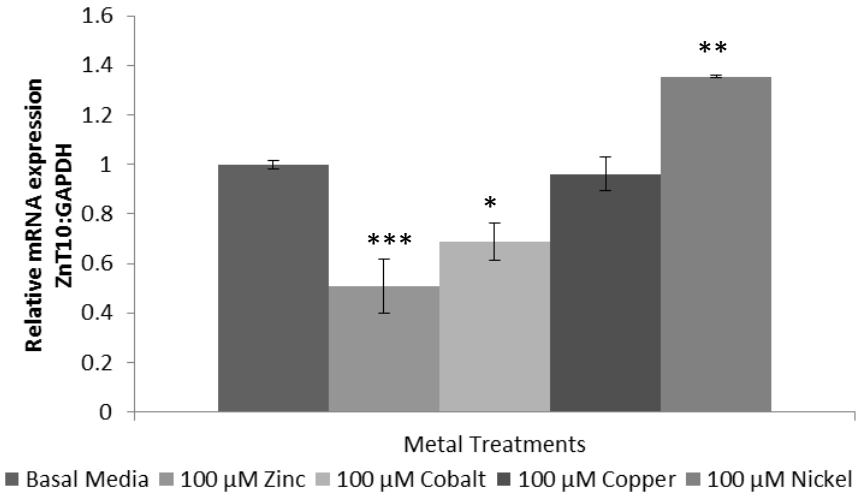

Figure 5.3 Response of SH-SY5Y cells to extracellular cation treatments. ZnT10 mRNA levels in the presence of 100 µM extracellular cation concentration (indicated), relative to GAPDH, normalised to levels with basal medium for each condition as determined by RT-qPCR using primers shown in table 3.4. All values are shown as mean ± SEM, $n = 3$. *** $p < 0.001$, ** $p < 0.01$, * $p < 0.05$ by Students *t*-test.

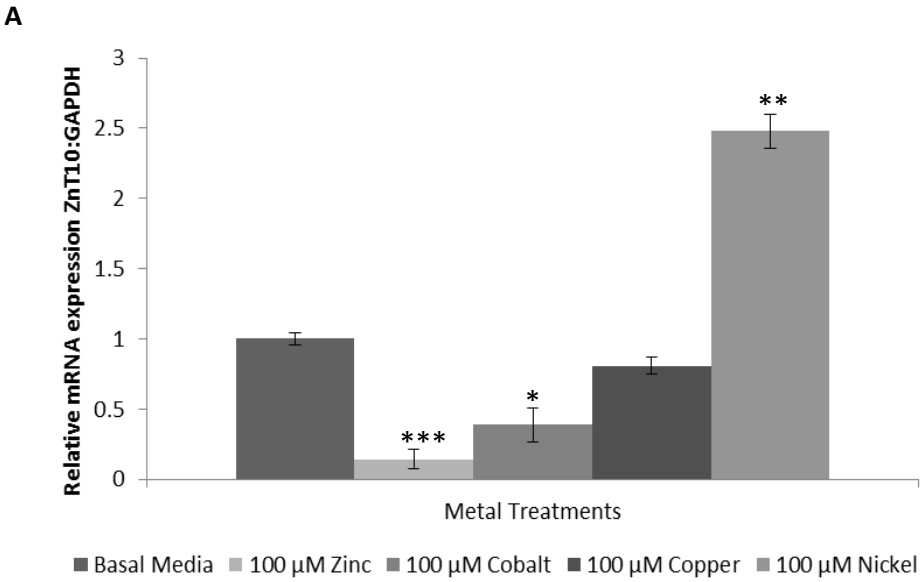

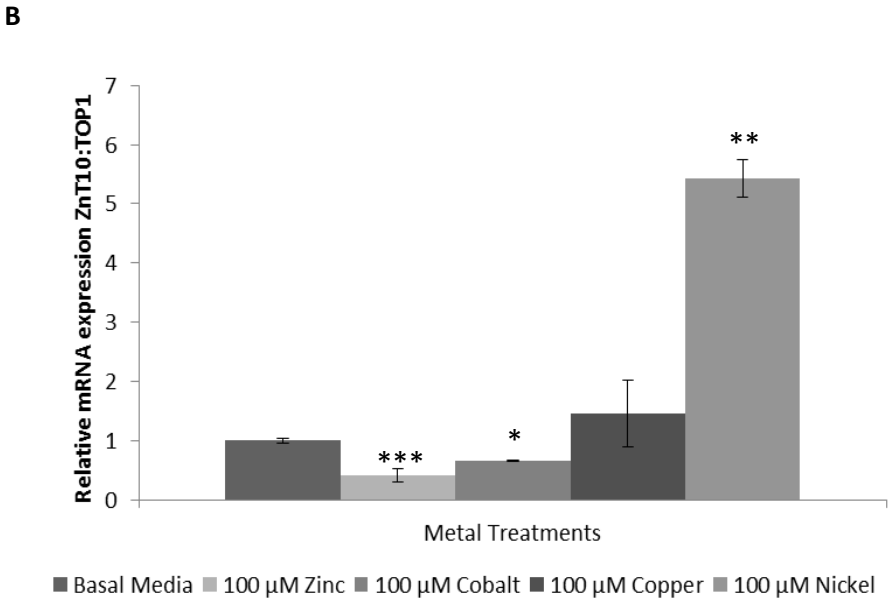

Figure 5.4 Response of Caco-2 cells to extracellular cation treatments. ZnT10 mRNA levels in the presence of 100 µM extracellular cation concentration (indicated), normalised to levels with basal medium for each condition as determined by RT-qPCR using primers shown in table 3.4. All values are shown as mean ± SEM, $n = 3$. *** $p < 0.001$, ** $p < 0.01$, * $p < 0.05$ by Students *t*-test. **A.** Relative to GAPDH **B.** Relative to TOPI.

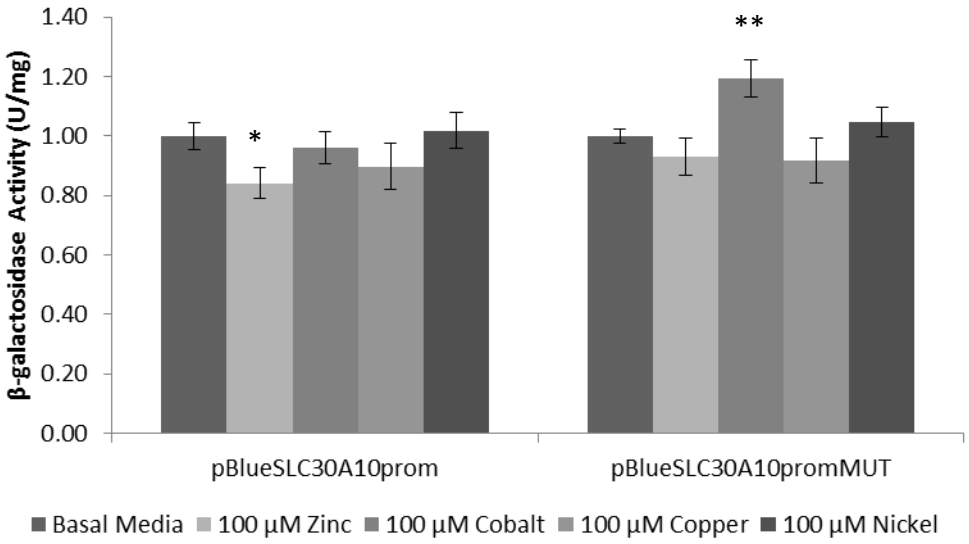

Figure 5.5 The response of the SLC30A10 promoter wild-type (pBlueSLC30A10prom) and mutant (pBlueSLC30A10prom$_{MUT}$) to elevated extracellular cation concentrations in Caco-2 cells. Promoter activity was detected as activity in cell lysates of a β-galactosidase reporter gene immediately downstream of the genomic region in the vector pBlue-TOPO (Invitrogen) assayed using the substrate chlorophenol red-β-D-galactopyranoside. Negative controls included vector only. Relative levels of activity of the SLC30A10 promoter region amplified (-762 to +180, relative to the transcription start site) at extracellular cation concentrations (100 µM). Values are means (n = 6), with standard errors represented by vertical bars. ** $p < 0.01$, $p < 0.05$ compared with basal medium by Student's t-test.

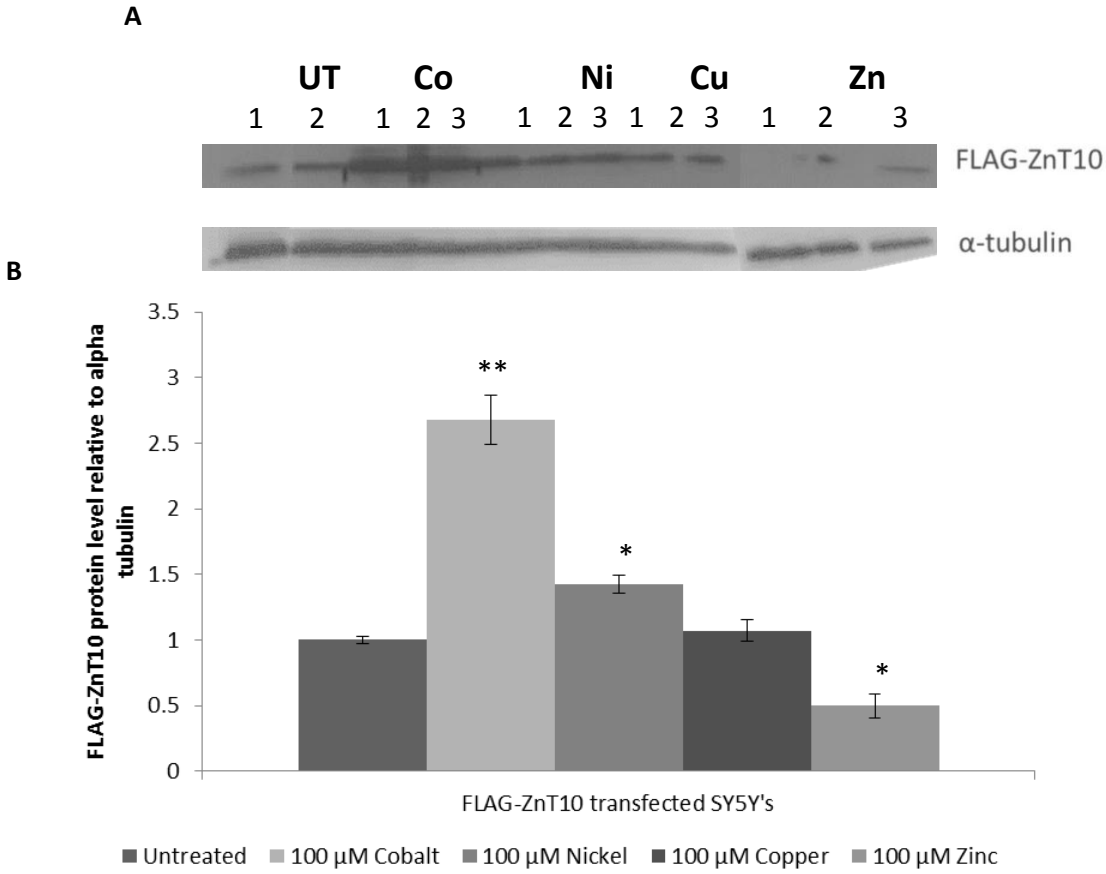

Figure 5.6 The effect of increased extracellular cation treatment on ZnT10 protein expression in SH-SY5Y cells. A. Expression in SH-SY5Y cells of ZnT10 protein fused with a FLAG epitope tag at the N- terminus visualised by immunoblotting at different concentrations of extracellular cations (as indicated; replicates shown, UT = untreated). **B.** Histograms were obtained by densitometric measurement of band intensities from the immunoblot shown above and are expressed relative to alpha tubulin protein levels measured in the same samples. Values are means (untreated; $n = 2$, treated; $n = 3$). All values are shown as mean ± SEM. $^{**}p < 0.01$, $^{*}p < 0.05$ by Student's *t*-test.

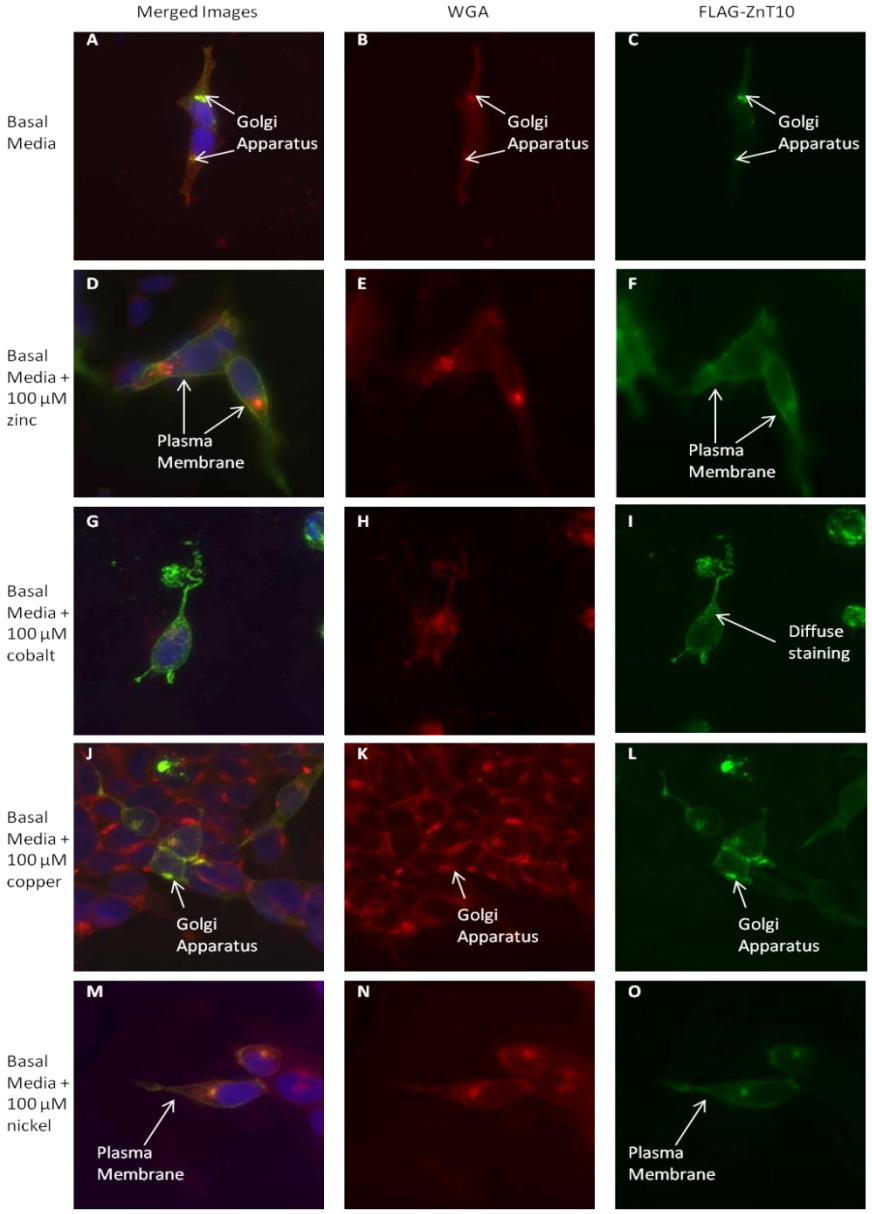

Figure 5.7 Subcellular localisation of ZnT10 in SH-SY5Y cells in response to 100 µM of extracellular cation treatment. ZnT10 localises to the Golgi apparatus under basal media conditions, as revealed by co-localisation with Rh-labelled wheat germ agglutinin (WGA) in permeabilised cells (shown in panels **A, B** and **C**). ZnT10 translocates towards the plasma membrane with the addition of 100 µM extracellular zinc for 24 h period immediately prior to viewing the cells shown by a reduction in a co-localisation with Rh-labelled WGA (shown in panels **D, E** and **F**). ZnT10 translocates shows a more diffuse pattern of staining with the addition of 100 µM extracellular cobalt for 24 h period immediately prior to viewing the cells (shown in panels **G, H** and **I**). ZnT10 localises to the Golgi apparatus with the addition of 100 µM copper, as revealed by co-localisation with Rh-labelled wheat germ agglutinin (WGA) in permeabilised cells (shown in panels **J, K** and **L**). ZnT10 translocates towards the plasma membrane with the addition of 100 µM extracellular nickel for 24 h period immediately prior to viewing the cells shown by a reduction in a co-localisation with Rh-labelled WGA (shown in panels **M, N** and **O**). In merged images shown nuclei are stained with DAPI (blue, merged images in panels **A, D, G, J** and **M**). Cells were treated with anti-FLAG antibody (1:1000) (green, images in panels **C, F, I, L** and **O**) for 1 h, prior to permeabilisation with 0.1 % Triton X-100 and co-staining with Rh-labelled WGA (red, images in panels **B**, **E, I, K** and **N**).

Chapter 6: ZnT10 in neurodegeneration

6.1 Outline

The results presented in this chapter are an outcome of an investigation into the expression of ZnT10 in Alzheimer's disease (AD) and explores the effect of oxidative stress and the inflammatory immune response, important factors that contribute to neurodegeneration. I show that ZnT10 mRNA levels are significantly reduced in AD post mortem tissue, a result which I confirmed in a transgenic (Tg) mouse model of AD. In addition, this apparent decrease in ZnT10 transporter expression is greater in human post-mortem tissue taken from females, an interesting finding given the greater prevalence of AD in women.

Zinc is thought to be involved in AD progression, however there are many questions that remain unanswered. It is evident that the transcription of amyloid precursor protein (APP) is regulated by the zinc-dependent transcription factors Sp1 and NF-κB (Cuajungco and Lees, 1997). In addition, zinc is able to promote formation of Aβ oligomers and aggregates at physiological concentrations available in the brain by binding Aβ at 3 N-terminal histidine residues (Bush et al., 1993). It follows that these mechanisms, that ordinarily act to maintain homeostasis within this tissue, may be dysregulated in disease states and indeed the involvement of ZnTs in AD has previously been investigated based on this knowledge. There are significant increases at the protein level of the transporters Znt1, Znt3, Znt4, Znt6 and Znt7 in the hippocampus and neocortex of APP/PS1 Tg mice (Zhang et al., 2008). These are areas of the brain important in AD progression. The largest increase in expression was observed for Znt3, which is particularly relevant due to its role in neurotransmission (Section 1.7.2). Znt5 also showed an increase, but this did not reach statistical significance. Furthermore,

Zhang et al., (2008) showed in addition to zinc being found and promoting senile plaque (SP) formation, immunoreactions of brain sections from these mouse models showed a distinct expression pattern of Znts, with Znt1 and Znt4 found throughout the SPs, whereas Znt3, Znt5 and Znt6 were localised in peripheral regions and Znt7 predominantly in the core.

Human studies of ZnT dysregulation in AD have on the whole corroborated the mouse model results. For example up-regulation of the ZnT1 protein is evident in the hippocampus in AD brain tissue (Lovell et al., 2005). It is thought that this increase in ZnT1 expression in the disease state causes an increase in zinc ions available in the extracellular space for initiation of Aβ deposition and SP formation (Lyubartseva et al., 2009). Interestingly, in terms of the nutritional status of the elderly, which is known to be deficient in zinc (Fairweather-Tait et al., 2008), it is perhaps note-worthy that mice fed a zinc deficient diet had a decrease in brain Znt1 expression (Dong et al., 2008). Lyubartseva et al., (2009) also showed that in the preclinical disease states; Mild Cognitive Impairment (MCI) and Pre-clinical AD (PCAD) an initial decrease in ZnT1 is observed before progression to AD. This highlights an important aspect of research that has not yet been fully explored.

It is of interest that, researchers have found that there is a positive correlation between Braak score (NFT pathology) and ZnT1 levels, such that ZnT1 increases with an increase in Braak score. A trend towards significance was also revealed for ZnT6 (Lovell et al., 2005, Lyubartseva et al., 2009). As described in Chapter 1, ZnT4 and ZnT6 have also been implicated in AD progression, with elevated protein levels of both transporters in the hippocampus of AD patients (Smith et al., 2006). ZnT6 is located in the Golgi apparatus and therefore it has been hypothesised that the increase in levels of

this transporter in AD results in an increase in zinc in this organelle. The importance of this is related to the localisation of both APP and the enzymes that metabolise APP, which are also found in the Golgi apparatus. Therefore, the accumulation of zinc could subsequently promote Aβ formation by binding to APP and inhibiting α-secretase (section 1.9) (Lyubartseva et al., 2009). ZnT4 is found in the lysosomal and endosomal compartments in hippocampal tissue and similarly an increase in ZnT4 transporter expression would be expected to enable the sequestration of zinc into these compartments. This is evident further by reports of Aβ accumulation in this system in the post-mortem AD brain (Takahashi et al., 2002).

ZnT3 is an important transporter to consider in the context of ZnT regulation in AD. It is known that ZnT3 is localised predominantly in the membranes of zinc-rich synaptic vesicles in the hippocampus (Palmiter et al., 1996b) and Znt3 knockout mice are devoid of zinc in these zinc-enriched terminals. Furthermore, increased amyloid deposition is related to the age-related increased activity of Znt3 found in female mice, a phenomenon that was abolished in Znt3 knockout mouse models (Lee et al., 2002). This result is particularly relevant with AD being more prevalent in the female population. In addition, in the AD Tg2576 mouse model, ablation of Znt3 inhibits the production of Aβ pathology. The translation of Znt3 mouse research into humans has come with a few discrepancies however. The level of mRNA and protein expression of ZnT3 appears to be lowered in the cortical regions of human AD patients (Beyer et al., 2009, Adlard et al., 2010) whereas the protein level in these mouse models was increased (Zhang et al., 2008).

Further understanding of the ZnT family and their interactions in the brain may elucidate a role for ZnTs and zinc in the progression and pathology of AD. Now that I

have identified ZnT10 expression in brain (Chapter 3) investigation is required to determine the role of ZnT10 in the development of AD.

A pathway implicated in the progression of AD is the Renin-Angiotensin System (RAS). This is a hormonal system that regulates blood pressure and fluid balance and it therefore has an important role in the development of hypertension (Taquini and Taquini, 1961). However, more recent research has revealed that the mammalian brain contains all components of the RAS (De Bundel et al., 2008, Speth and Karamyan, 2008) and in fact the brain has high concentrations of the angiotensin receptors (Gard and Rusted, 2004). In summary, angiotensins are synthesised from the conversion of angiotensinogen to angiotensin I (Ang I) which is catalysed by the enzyme renin (Figure 6.1). Ang I is further metabolised to Ang II, by angiotensin converting enzyme (ACE). Ang II has multiple fates, all of which are active, however with differing potencies; Ang III (Ang_{2-8}), Ang IV (Ang_{3-8}), Ang_{1-7} or Ang_{3-7}. These peptides act through G-protein coupled receptors; angiotensin type (AT) receptors, that are able to signal through phospholipase C and Ca^{2+}. Ang I is thought to be inactive but Ang II and Ang III are able to activate the AT_1 and AT_2 receptors (de Gasparo et al., 2000). Conversely, Ang IV and $Ang_{3–7}$ bind with low affinity at the AT_1 and AT_2 receptor subtypes but with high affinity to the AT_4 receptor (Swanson et al., 1992). Interestingly, Ang II is able to act as a neurotransmitter in the brain, mainly acting on osmoreceptors in the hypothalamus to influence thirst however it is also known to interact with other neurotransmitters such as acetylcholine, blocking its downstream effects (Gard, 2002). The cholinergic system is integral to the regulation of cognitive functions, in particular synaptic plasticity, specifically in learning and short-term memory therefore its inhibition is detrimental to these pathways.

Recent research has shown ZnT10 to be down-regulated after 3 days of treatment with Ang II thereby inducing senescence in vascular smooth muscle cells (VSMCs). This result is intriguing as conversely, the over-expression of ZnT10 in this system has been shown to decrease the production of reactive oxygen species (ROS) preventing senescence (Patrushev et al., 2012). Elucidation of the role ZnT10 within the brain RAS may improve our understanding of this transporter's role in oxidative stress and inflammation, given that these are downstream effects of this system. In the brain RAS, downstream of the AT_1 receptor is activation of NADPH oxidase; this pathway is poorly understood but it is known to require Rac1 and protein kinase C (PKC) (Zimmerman et al., 2004, Wang et al., 2006). The consequence of NADPH oxidase activation is the conversion of NADPH to NAD^+ and the by-products of such a reaction are ROS. An excess of ROS are known to cause oxidative stress and thus are an important consideration in the aetiology of AD. Furthermore, continuous activation of the brain RAS in hRN/hANG-Tg mice (human renin (hRN) and human angiotensinogen (hANG) transgenic mice), a hypertensive mouse model, enhances oxidative stress and causes a decline in cognitive function by excessive stimulation of the AT_1 receptor (Zhu et al., 2004). In addition ROS can induce a redox-dependent signal transduction pathway that leads to NF-κB activation and therefore stimulation of the inflammatory immune response. Inflammation also causes extensive damage in the brain of AD patients (Zimmerman et al., 2004). AT_1 receptor blockers (ARBs) have been suggested as a treatment for AD (Danielyan et al., 2010) by reducing cerebral blood flow, oxidative stress and inflammation (Horiuchi and Mogi, 2011). Moreover, blockage of AT_1 by ARBs allows unbound Ang II to stimulate the AT_2 receptor, which antagonises the effect of AT_1 thereby promoting cell differentiation and regeneration in neuronal tissue. This negates the oxidative stress and inflammation that results from Ang II

activation of AT_1 (Horiuchi and Mogi, 2011). Here I demonstrate that, over a short time period, ZnT10 mRNA expression increases with Ang II treatment but it is not altered under conditions of oxidative stress. As in the AD cases, ZnT10 decreases when the inflammatory immune response is induced by LPS.

6.2 ZnT10 expression in AD

As stated above, many ZnTs are dysregulated in AD. To date ZnT10 has not been studied in this context. Here I show a significant down-regulation in a small number of AD patients, which is supported by data in brain tissue from the APP/PS1 Tg mouse model in which there is also a significant decrease in Znt10 mRNA expression.

6.2.1 *ZnT10 expression in human AD tissues*

To investigate the effects of AD process, human brain tissue RNA was analysed from AD pathology cases (n = 13; female n = 8, male n = 5) and compared with age-matched controls (n = 10; female n = 3, male n = 7) (Appendix I). Frontal cortex RNA was obtained from the Newcastle Brain Tissue Resource (Newcastle, UK). Due to the pre-mortem decline in AD the RNA quality was not ideal as measured by RNA integrity number (RIN range 2.5-7.3), however RT-qPCR analysis was carried out in order to give an indication of expression levels of ZnT10 in AD patients. Primers used for RT-qPCR analysis are shown in Table 3.4. Standard curves for all RT-qPCR passed acceptance criteria (Figure 6.2). All data are expressed as a ratio to GAPDH. When AD patients are normalised to age-matched controls there is a significant decrease in ZnT10 levels in this small number of brain tissues (p = 0.006) (Figure 6.3A). Moreover, when the results are analysed based upon gender there is a gender specific decrease seen only in ZnT10 in female AD patients (p = 0.004) but not in males (p = 0.211) (Figure 6.3B). This is a particularly important result given the raised prevalence of AD in females.

6.2.2 *ZnT10 expression in Tg mouse tissues*

In line with the human samples, frontal cortex brain tissue samples were obtained from 12 month old female WT (n = 5) and APP/PS1 mice (n = 11) (supplied by Dr Paul Adlard, The University of Melbourne). APP/PS1 mice contain two transgenes inserted at a single locus. The first is the APP sequence that is modified to encode the human Swedish mutations K595N/M596L. Secondly, PS1 corresponds to the human presenilin 1 gene, in this case there is a deletion of exon 9 and is therefore known as the DeltaE9 mutation (http://jaxmice.jax.org/strain/005864.html). These mice have amyloid beta deposits and exhibit deficits in spatial learning (Gimbel et al., 2010). Brain samples were removed and snap frozen before being stored in RNA Later at -80°C. Samples were shipped in RNA later on dry ice and RNA was extracted using Trizol (section 2.4.1). Primers used for RT-qPCR analysis are shown in Table 6.1. Standard curves for all RT-qPCR passed acceptance criteria (Figure 6.4). RT-qPCR analysis was carried out as a ratio to 18S rRNA. These results support the human AD results, with a significant decrease in Znt10 mRNA levels in the Tg-hemizygotes compared with the non-carriers (p = 0.01) (Figure 6.5). It is note-worthy that all mouse samples were from female mice and therefore gender differences could not be explored in this instance.

6.3 The effect of RAS on expression of ZnT10 mRNA

Due to published data on the involvement of the RAS in the brain during neurodegenerative conditions and the recently published data that indicates a role for Ang II in ZnT10 regulation in VSMCs (Patrushev et al., 2012). I designed a system to investigate Ang II influence over ZnT10 in the neuroblastoma cell line, SH-SY5Y. In addition, the role of oxidative stress and the inflammatory immune response on ZnT10

expression was also investigated. A summary of the study design is shown in Figure 6.6.

6.3.1 *Effect of Ang II on ZnT10 mRNA expression*

Human neuroblastoma SH-SY5Y cells were treated with 0.1 µM Ang II for 24 hours in the absence of FBS. This level of Ang II has previously been used in assays investigating ZnT10 expression in VSMCs (Patrushev et al., 2012) in addition to $Na^{(+)}/H^{(+)}$ exchanger assays in SH-SY5Y cells (Reid et al., 2004). I have previously shown that removal of FBS does not influence ZnT10 expression levels (Chapter 4; Figure 4.5). Primers used for RT-qPCR analysis are shown in Table 3.4. Standard curves for all RT-qPCR passed acceptance criteria (Figure 6.2). Analysis of mRNA expression was carried out using RT-qPCR as a ratio to both GAPDH and TOPI. Results relative to both reference genes show a significant increase in ZnT10 expression at the mRNA level in response to extracellular Ang II treatment ($p = 0.03$ and $p = 0.04$, respectively) (Figure 6.7A and 6.7*i inset*).

6.3.2 *Effect of oxidative stress on ZnT10 mRNA expression*

Human neuroblastoma SH-SY5Y cells were treated with 0.025 mM *tert*-Butyl hydroperoxide (tBHP) for 40 min in the presence of 10 % FBS. This level of tBHP and length of treatment has previously been used to induce oxidative stress in assays in SH-SY5Y cells (Krishnamurthy et al., 2000). Medium was removed and replaced with basal medium plus 10 % FBS for a further 24 hour time period, before RNA was harvested. Primers used for RT-qPCR analysis are shown in Table 3.4. Standard curves for all RT-qPCR passed acceptance criteria (Figure 6.2). Analysis of mRNA expression was carried out using RT-qPCR as a ratio to GAPDH and TOPI. As a control experiment, to ensure oxidative stress had actually been induced by the treatment, levels of PKR

(double-stranded RNA dependant protein kinase) were assessed by semi-quantitative RT-PCR as a ratio to GAPDH. Primers used for RT-PCR analysis are shown in Table 6.2. PKR is a serine-threonine kinase and in response to oxidative stress, it is able to catalyse the phosphorylation of the α subunit of eukaryotic translation initiation factor-2 (eIF2) in order to inhibit protein synthesis (Der et al., 1997). Up-regulation of PKR has previously been reported to occur in SH-SY5Y cells in response to induced oxidative stress by H_2O_2 treatment (Mouton-Liger et al., 2012). Here I confirm a significant increase in PKR levels in the SH-SY5Y cells treated with tBHP for 40 minutes compared with controls ($p = 0.001$) (Figure 6.7B). Results did not show any significant difference in ZnT10 mRNA expression from control samples relative to either GAPDH or TOPI ($p = 0.66$ and $p = 0.45$ respectively) (Figure 6.7A and 6.7*i inset*). This indicates that although oxidative stress was induced in the cells tested, levels of ZnT10 were not altered indicating that ZnT10 is not regulated by this oxidative stress pathway.

6.3.3 *Role of the inflammatory immune response in ZnT10 mRNA expression*

Human neuroblastoma SH-SY5Y cells were treated with 100 ng/ mL Lipopolysaccharide (LPS) from *E. coli* for 24 hours in the absence of FBS. This level of LPS has previously been used to induce the inflammatory immune response in assays in SH-SY5Y cells (Pandey et al., 2009). Primers used for RT-qPCR analysis are shown in Table 3.4. Standard curves for all RT-qPCR passed acceptance criteria (Figure 6.2). Analysis of mRNA expression was carried out using RT-qPCR as a ratio to GAPDH and TOPI. To ensure that the inflammatory immune response had been induced, levels of Toll-like receptor 3 (TLR3) were assessed by semi-quantitative RT-PCR as a ratio to GAPDH. Primers used for RT-PCR analysis are shown in Table 6.2. Toll-like receptors are present on the cell surface and are able to respond to stimulants produced by microorganisms in order to initiate the host defence and to stimulate the release of

molecules involved in the inflammatory immune response, such as antimicrobial peptides and inflammatory cytokines. LPS from *E. coli* is known to stimulate TLR3 and causes up-regulation of the receptor in SH-SY5Y cells (Nessa B. N. et al., 2006). There was a significant increase in the TLR3 mRNA levels in cells treated with LPS compared with controls (p = 0.03) (Figure 6.7C). Results relative to both reference genes show a significant decrease in ZnT10 expression at the mRNA level in response to extracellular LPS treatment (p = 0.01 and p = 0.03 respectively) (Figure 6.7A and 6.7*i inset*). This indicates that the inflammatory immune response may regulate ZnT10 expression at the mRNA level and gives evidence for a role of ZnT10 in this pathway.

6.4 Discussion

The results presented here show a significant decrease in ZnT10 expression at the mRNA level in frontal cortex of brain tissue samples from AD patients compared with age-matched controls (p = 0.006) giving the first indication that ZnT10 expression at the mRNA level is affected in AD. Furthermore, when separated on the basis of gender there is a significant decrease in levels of ZnT10 in female AD cases compared with controls (p = 0.004) whereas no significant difference between control and AD cases was observed in the samples derived from males (p = 0.211). There is however, no significant difference in ZnT10 mRNA levels between the males and females (control males versus control females p = 0.66, AD males versus AD females p = 0.67). The dysregulation of ZnTs in AD is not without precedence. In fact, at the mRNA level ZnT3 has been found to be significantly reduced in AD (Beyer et al., 2009). In this study using RT-qPCR the authors found a 45-60 % reduction of ZnT3 mRNA levels in the AD patients compared with controls, in all four cortical regions tested (medial temporal gyrus, superior occipital gyrus, superior parietal gyrus, and superior frontal

gyrus) but there was no significant differences in the expression in the cerebellum. Furthermore, there is an age-dependent increased activity of the Znt3 protein in the Tg2576 mouse model which is abolished in the Znt3 knockout mouse (Lee et al., 2002). This is an intriguing observation, given the seemingly age and gender specific relationship associated with expression levels of ZnT10 in AD brain tissue.

Due to the valuable nature of the post-mortem brain tissue samples only one area of the brain, frontal cortex, was tested for ZnT10 and whilst this displays a decrease in transporter expression in AD patients, there is no data as yet as to whether this is region specific. This is an important factor as transporter dysregulation appears to be localised to the cortex and not found in the cerebellum. In addition to the data for ZnT3 mRNA levels (described above (Beyer et al., 2009)), mRNA expression for other zinc transporters; ZIP1, ZIP6, ZnT1 and ZnT6 in brain tissue has also been shown to increase in the four cortical regions (middle temporal gyrus, superior occipital gyrus, superior parietal gyrus, and superior frontal gyrus) but not in the cerebellum (Beyer et al., 2012). Further research is required to establish whether ZnT10 also follows this pattern.

Another factor that needs to be taken into consideration is the quality of these samples. A recognised problem for AD cases is that they usually have a long pre-mortem decline and therefore have acidosis and consequently poor RNA quality. Here the RIN (RIN range 2.5-7.3) were below what would be desirable in a RT-qPCR experiment (Bustin et al., 2009). In addition, the number of samples (AD = 13 cases; 8 female and 5 male, Control = 10 cases, 3 female and 7 male) was low due to the difficulty in obtaining samples. The inter-individual variation between human samples is high therefore the numbers involved in this study are not to the desirable statistical power. Furthermore, I

do not have any information on the medication taken prior to death of these patients. This is an important factor as this too could influence many pathways and the mRNA expression of ZnT10.

In order to help overcome these issues and to further strengthen the results, RNA was extracted from frontal cortex brain tissue samples obtained from 12 month old female WT (n = 5) and APP/PS1 mice (n = 11). APP/PS1 mice are a mouse model of Alzheimer's disease containing two transgenes inserted at a single locus. The first is the APP sequence that is modified to encode the human Swedish mutations K595N/M596L. Secondly, PS1 corresponds to the human presenilin 1 gene. In this case there is a deletion of exon 9 therefore known as DeltaE9 mutation (http://jaxmice.jax.org/strain/005864.html). As in AD, these mice have Aβ deposits and exhibit deficits in spatial learning (Gimbel et al., 2010). The use of this mouse model to study AD is widespread and in particular this model has been used to identify dysregulation of several Znts using Western Blot analysis. Researchers found there was an increase in the protein expression of transporters tested (Znt1, Znt3, Znt4, Znt5, Znt6 and Znt7) in the hippocampus and neocortex, with only levels for Znt5 failing to reach significance (Zhang et al., 2008). Further investigation into Znt expression in AD included analysing SPs obtained from these mouse models. These were tested by immunoreactions to ascertain whether there is expression of Znts within these aggregates. Intriguingly there was a distinct expression pattern evident with Znt1 and Znt4 found throughout the SPs whereas Znt3, Znt5 and Znt6 were in peripheral regions and Znt7 predominantly in the core (Zhang et al., 2008). The research into ZnT distribution in SP has not been translated to humans. This would be an interesting consideration but because I was unable to confirm the specificity of the commercial ZnT10 antibodies (see Chapter 4) ZnT10 staining of brain tissue sections were

unsuccessful as was assessing endogenous levels of protein expression by Western blotting for both the mouse and the human AD brain. The translation of results across species however must be viewed with caution as data using this mouse model revealed an increase in Znt3 protein levels, whereas human results gave a decrease in both mRNA and protein levels (Beyer et al., 2009, Adlard et al., 2010). Analysis of our RT-qPCR results from the female APP/PS1 Tg mouse frontal cortex samples were however in agreement with the human AD results, showing a significant decrease in Znt10 mRNA in the Tg mouse brain ($p = 0.01$).

Human studies of ZnT dysregulation in AD have highlighted the importance of specifying the stage of disease progression. For example, the decline in multiple cognitive functions in the progression of AD is thought to begin with an interim stage labelled MCI with only 5 % of these patients remaining stable i.e. not developing dementia. In addition, there is a condition which is described as PCAD, in this case the patient does not have any overt clinical manifestations of AD however does have significant AD pathology at post-mortem. There are differences in ZnT expression profiles between AD and the precursor states described in the literature. For example ZnT1 shows a significant decrease in the hippocampus of subjects with MCI and PCAD (Lovell et al., 2005, Lyubartseva et al., 2009). It is hypothesised that this would lead to an increase in intracellular zinc. It is evident that levels of zinc are elevated in the AD brain (Cornett et al., 1998) and therefore there is more available zinc to bind to APP and Aβ. Furthermore, the presence of zinc itself is able to up-regulate ZnT1 transporter expression, as a compensatory mechanism increasing zinc ion availability in the extracellular space thereby enabling initiation of Aβ deposition and SP formation and exacerbating disease progression. This up-regulation of ZnT1 is evident at the protein level in AD brain tissue (Lovell et al., 2005). Research focusing on ZnT4 and ZnT6 has

also emphasised the need for more understanding of ZnT regulation in disease states. Elevations of both these transporters are found in PCAD (Lyubartseva et al., 2009) however there is no significant difference in levels of either transporter between MCI and age-matched controls. In AD cases however, both ZnT4 and ZnT6 mRNA levels are found to significantly increase in the hippocampus (Smith et al., 2006). It follows that the increased levels of ZnT6 and ZnT4 are thought to act as a compensatory mechanism for the decrease in levels of ZnT1. Due to the subcellular localisation of ZnT6 at the Golgi apparatus (where the γ-secretase complex interacts with APP), it is thought that this induces an increase in zinc in this organelle subsequently promoting Aβ formation by binding to APP and inhibiting α-secretase. ZnT4 is found in the lysosomal and endosomal compartments and will sequester zinc into these compartments. Indeed Aβ accumulation has been reported in this system in the post-mortem AD brain (Takahashi et al., 2002). An area that is important to address, but is outside the scope of this research, is regulation of ZnT10 in both PCAD and MCI since this could elucidate a role for ZnT10 in the progression of AD. However results from my research allude to a mechanism for ZnT10 dysregulation in the final disease state of AD. Results presented in Chapter 4 reveal that under basal conditions ZnT10 is localised to the Golgi apparatus but undergoes translocation towards the plasma membrane with the addition of extracellular zinc. In addition I provided evidence of a down-regulation of both ZnT10 mRNA and protein, in response to increasing levels of extracellular zinc. Therefore I postulate that the increase in zinc ion levels in the AD brain (Cornett et al., 1998) induce a down-regulation of ZnT10 measured at the mRNA level in the AD brain tissue. Moreover, the localisation of ZnT10 would exacerbate AD disease progression two-fold. Initially, the localisation to the Golgi apparatus would allow promotion of Aβ formation by increasing zinc sequestration in this organelle

thereby enabling the binding of zinc to APP and the inhibition of α-secretase, in a similar manner to that hypothesised for ZnT6 (Lyubartseva et al., 2009). Secondly, elevated levels of zinc induce the translocation of ZnT10 towards the plasma membrane, allowing ZnT10 to act in the same way as ZnT1, effluxing zinc into the extracellular space, so possibly providing zinc ions for initiation of Aβ deposition and SP formation. The down-regulation at the mRNA level is intriguing, and further investigation is required to establish whether there is a parallel at the protein level and indeed in the activity of ZnT10.

A previous study, using RT-qPCR, has shown that Znt10 mRNA, and incidentally Znt3 mRNA, are down-regulated in response to 3 days treatment with Ang II. In addition, mRNA levels of both transcripts were analysed at both 24 and 48 hours but there was no significant difference found. Moreover, over-expression of Znt10 decreased production of ROS and prevented senescence. These experiments were carried out in rat VSMCs and implicate Znt10 and Znt3 in the RAS (Patrushev et al., 2012). Here I present data to suggest that ZnT10 is also involved in the brain RAS. Firstly, I show that after 24 hours of treatment with Ang II in SH-SY5Y cells, levels of ZnT10 are significantly increased by RT-qPCR (as a ratio to GAPDH $p = 0.03$, as a ratio to TOPI $p = 0.04$). It is note-worthy that, whilst the result after 24 hour is the opposite of that in published data, a down-regulatory response was only detected by the authors using RT-PCR after 3 days of treatment. RT-PCR is a semi-quantitative technique that is potentially not as sensitive as RT-qPCR and therefore these subtle differences may have been overlooked and could allow for the variation in results. Furthermore, analysis by Patrushev et al., (2012) was in rat VSMCs and, whilst VSMCs themselves were not analysed, results in Chapter 3 revealed no endogenous expression of ZnT10 in heart or skeletal muscle therefore direct comparisons cannot necessarily be drawn. Differences

reported could also be due to tissue and/ or species specific responses and indeed variations in the influence of RAS between tissue types.

Ang II binds to AT_1 receptors, the downstream effect of this is activation of NADPH oxidase allowing the conversion of NADPH to NAD^+ and producing ROS as the by-product. In addition to the above impact of over-expression on ROS, Patrushev et al., (2012) also show that knockdown of Znt10 using siRNA increase ROS. Here oxidative stress initiated by tBHP had no effect on expression of ZnT10 mRNA as shown by RT-qPCR (p = 0.66) suggesting that ZnT10 has an effect upstream of ROS production affecting the outcome, rather than being regulated by ROS *per se*. In my system, PKR levels confirmed the induction of oxidative stress in the SH-SY5Y cell line with a significant increase in treated cells (p = 0.001). Imitation of oxidative stress evidently has an effect on expression of certain ZnTs. When oxidative stress was induced in the rat cerebral cortex by nitric oxide there was an up-regulation of Znt1, Znt2, and Znt4 mRNAs, however levels of Znt3 RNA levels were unaffected (Aguilar-Alonso et al., 2008). This is puzzling as in the VSMC system Znt3 was shown to be effected in the same way as Znt10, in that over-expression of Znt3 decreased ROS and, conversely, siRNA knockdown of Znt3 increased ROS (Patrushev et al., 2012) supporting the hypothesis that both Znt10 and Znt3 are not regulated by oxidative stress itself but act to impact on ROS production upstream. These contradictory results to ours and others (Aguilar-Alonso et al., 2008) may be a quirk of the rat VSMCs used. Interspecies variation cannot account for differences in the results for Znt3 given Aguilar-Alonso et al., (2008) also carried out their experiments in rat.

Another pathway downstream of RAS is the inflammatory immune response initiated by NF-κB. Here LPS induction of this pathway successfully induces the immune

response in SH-SY5Y cells, as shown by a significant increase in mRNA expression of TLR3 ($p = 0.03$). Levels of ZnT10 however were significantly decreased in response to LPS treatment (as a ratio to GAPDH $p = 0.01$ and as a ratio to TOPI $p = 0.03$). Zinc has been implicated in the immune system, for instance there are many processes where NF-κB modulates transcriptional activity of genes such as immunoreceptors and cytokines highlighting one role for zinc in the immune system (Zabel et al., 1991). Despite this, little is known about the function of ZnTs in the inflammatory immune response. Research has revealed that induction of the inflammatory immune response using LPS initiates a decrease in intracellular zinc as a result of increased expression of effluxers Znt1, Znt4 and Znt6 coupled with decreased expression of importers Zip6 and Zip10 in dendritic cells derived from mice (Kitamura et al., 2006). This pathway is stimulated by the activation of TLR4 by LPS. Furthermore, the authors showed that both Zip6 over-expression and zinc supplementation was sufficient to inhibit the up-regulation of major histocompatibility complex (MHC) class II molecules ordinarily exhibited with LPS treatment. Moreover, investigation in immunologically relevant cell types has highlighted the importance of ZnTs in the immune system. In the different leukocyte subsets tested ZnT1 appeared to be the most regulated transporter with expression in all subsets. Interestingly, ZnT4 was localised to the plasma membrane in these cell types, a phenomenon restricted to cells of the immune system. In addition, ZnT8 revealed an inter-individual variability not seen for the other transporters. In response to zinc deficiency ZnT5, ZnT6 and ZnT7 were up-regulated in contrast to the down-regulation of ZnT1 (Overbeck et al., 2008). Combined these results imply a role for ZnTs in the homeostasis of zinc in the immune system, an area that requires further experimentation with the inclusion of ZnT10.

The results presented here further implicate ZnT10 in the aetiology of AD as there is a significant decrease in ZnT10 expression at the mRNA level in AD patients. Moreover, the inflammatory immune response plays a large role in the aetiology of AD (Akiyama, 1994). Furthermore, non-steroid anti-inflammatory drugs (NSAIDs) have been shown to reduce the cognitive impairment associated with AD (Cote et al., 2012). The down-regulation of ZnT10 also seen with induction of the inflammatory immune response in SH-SY5Y cells indicates that this pathway could be responsible for the overall reduction in ZnT10 levels in the AD brain.

Whilst this chapter establishes novel preliminary data for the role of ZnT10 in the progression and aetiology of AD, it also highlights the need for future research into this area.

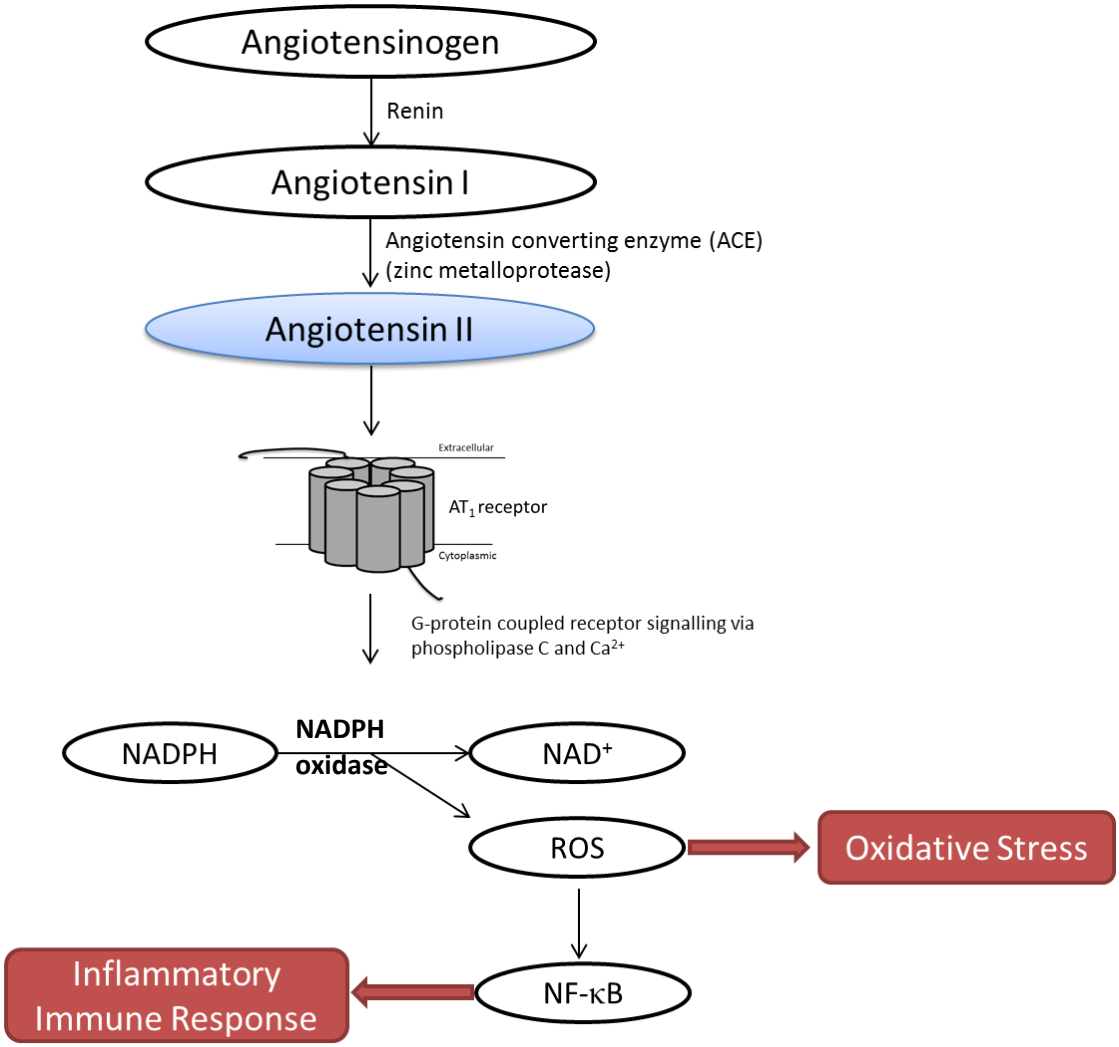

Figure 6.1 The Renin-Angiotensin System (RAS) in the brain. Angiotensins are synthesised from the conversion of angiotensinogen to angiotensin I (Ang I) catalysed by the enzyme renin. Ang I is further metabolised to Ang II, by angiotensin converting enzyme (ACE) (a zinc metalloprotease.). Ang II acts through the G-protein coupled receptor; angiotensin type (AT) receptor 1, that are able to signal through phospholipase C and Ca^{2+}. (de Gasparo et al., 2000). Downstream of the AT_1 receptor is activation of NADPH oxidase; converting NADPH to NAD^+. The by-products of such a reaction are reactive oxygen species (ROS) and ultimately oxidative stress. ROS can also induce a redox-dependent signal transduction pathway that leads to NF-κB activation and stimulation of the inflammatory immune response.

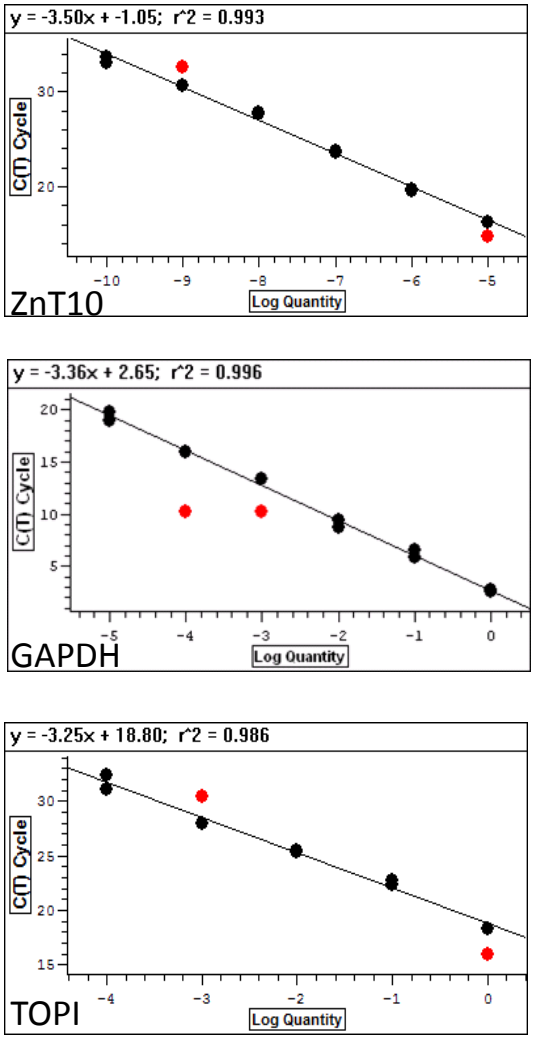

Figure 6.2 Standard curves generated to measure relative levels of ZnT10 by RT-qPCR, using SYBR green fluorescence and the DNA Engine Opticon 2 (MJ Research). Standards for GAPDH and ZnT10 products were generated by amplifying the region between the primers shown in Table 3.4, and subcloned into the vector pCR2.1-TOPO TA (Invitrogen). TOPI primers were purchased from PrimerDesign. A TOPI PCR product was produced and subcloned into the pGEM-T-easy vector to give the standard TOPI-pGEM (generated by Dr Alison Howard). The mean log concentration of each dilution was plotted against PCR cycle number at which the fluorescent threshold was crossed (C_T). Excluded data points are shown in red. These standard curves were used to calculate relative levels of ZnT10 transcripts.

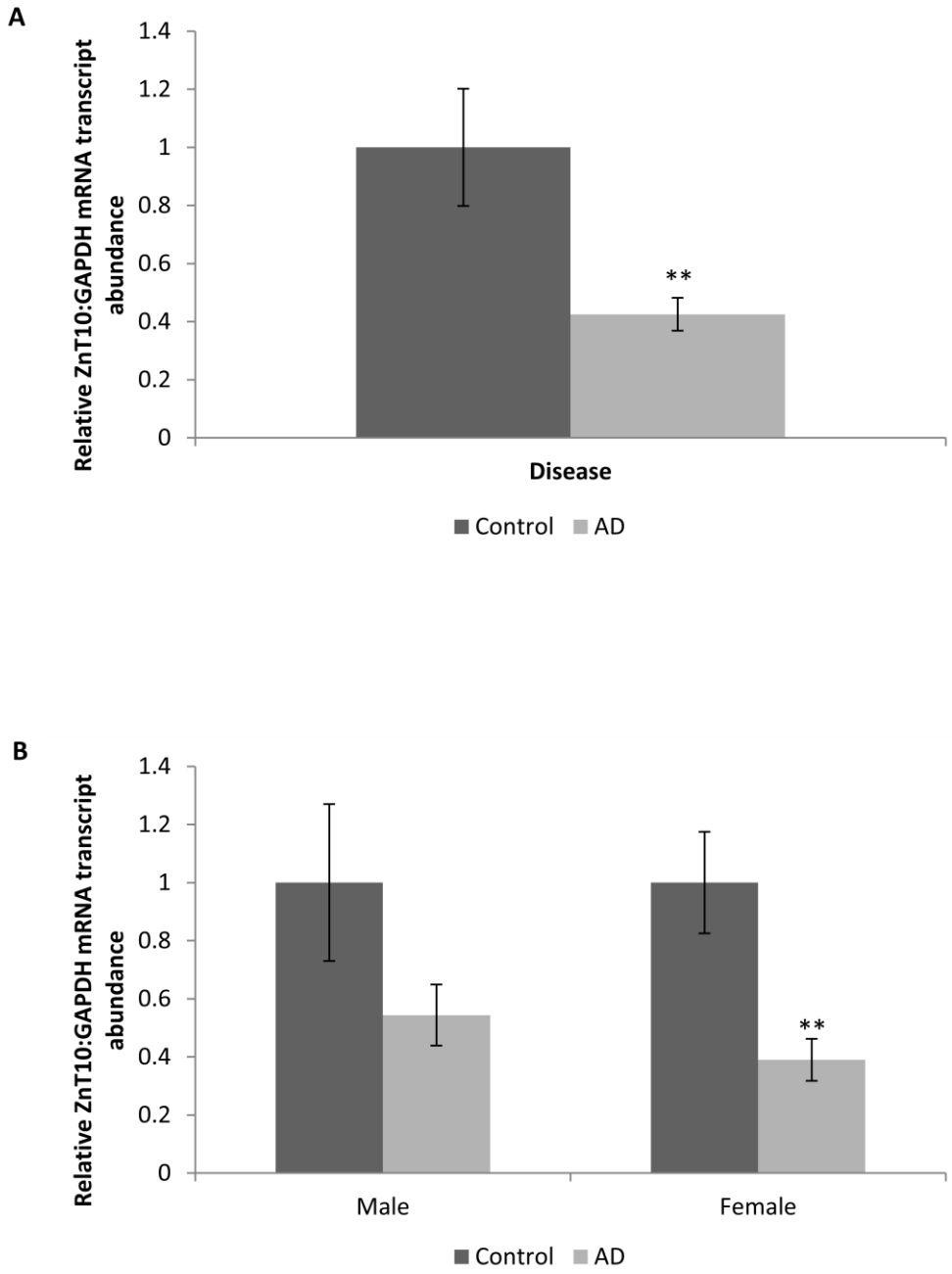

Figure 6.3 ZnT10 mRNA expression in human frontal cortex brain tissue. Relative levels of ZnT10 in brain tissue from AD brains (n = 13; female n = 8 male n = 5) and control brains (n = 10; female n = 3, male n = 7). Data are expressed relative to GAPDH mRNA levels measured in the same samples. Primers are given in Table 3.4. All values are shown as mean ± SEM **A.** Shows all data combined **B**. Results are stratified based on gender. ** $p < 0.01$ by Student's t test.

Name/ Accession Number	Primer Sequences	Amplicon Length (bp)	Annealing Temp (°C)
Znt10 NM_001033286	5'-$_{826}$GTA GCA GGT GAT TCC CTG AAC$_{846}$-3' 5'-$_{965}$GTG ATG ACC ACA ACC ACG GAC$_{945}$-3'	140 bp	60
18S rRNA NM_011296	5'-$_{117}$CAT TAA GGG CGT GGG GCG G$_{135}$-3' 5'-$_{247}$GTC GTG GGT TCT GCA TGA TG$_{228}$-3'	131 bp	60/56

Table 6.1 Primer sequences for mouse Znt10 analysis of brain tissue by RT-qPCR analysis. The numbering on each of the oligonucleotides represents its position on the gene.

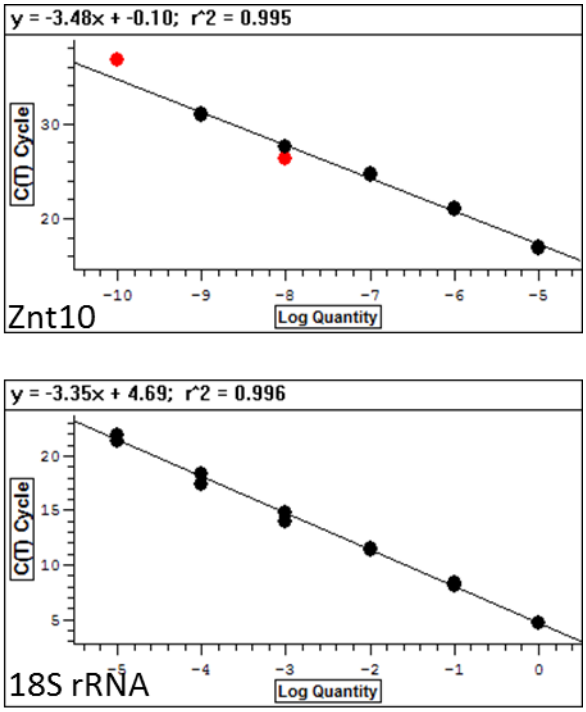

Figure 6.4 Standard curves generated to measure relative levels of Znt10 by RT-qPCR, using SYBR green fluorescence and the DNA Engine Opticon 2 (MJ Research). Standards for 18S rRNA and mouse Znt10 products were generated by amplifying the region between the primers shown in Table 6.1, and subcloned into the vector pCR2.1-TOPO TA (Invitrogen). The mean log concentration of each dilution was plotted against PCR cycle number at which the fluorescent threshold was crossed (C_T). Excluded data points are shown in red. These standard curves were used to calculate relative levels of mouse Znt10 transcripts.

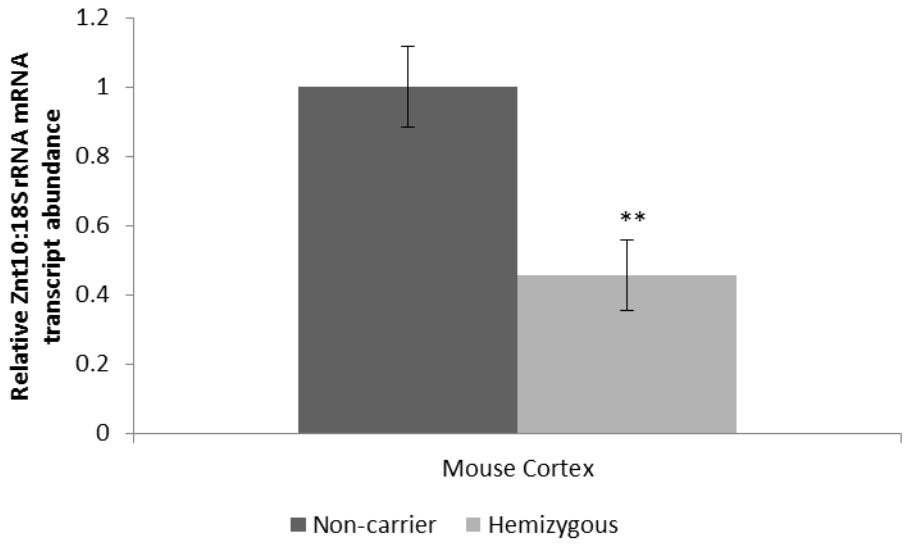

Figure 6.5 Znt10 mRNA expression in frontal cortex mouse brain tissue. Relative levels of Znt10 in brain tissue from APP/PS1 Tg mouse brains (n = 11) and control mouse brains (n = 5). Data are expressed relative to 18S rRNA mRNA levels measured in the same samples. Primers are given in table 6.1. All values are shown as mean ± SEM ** $p < 0.01$ by Student's t test.

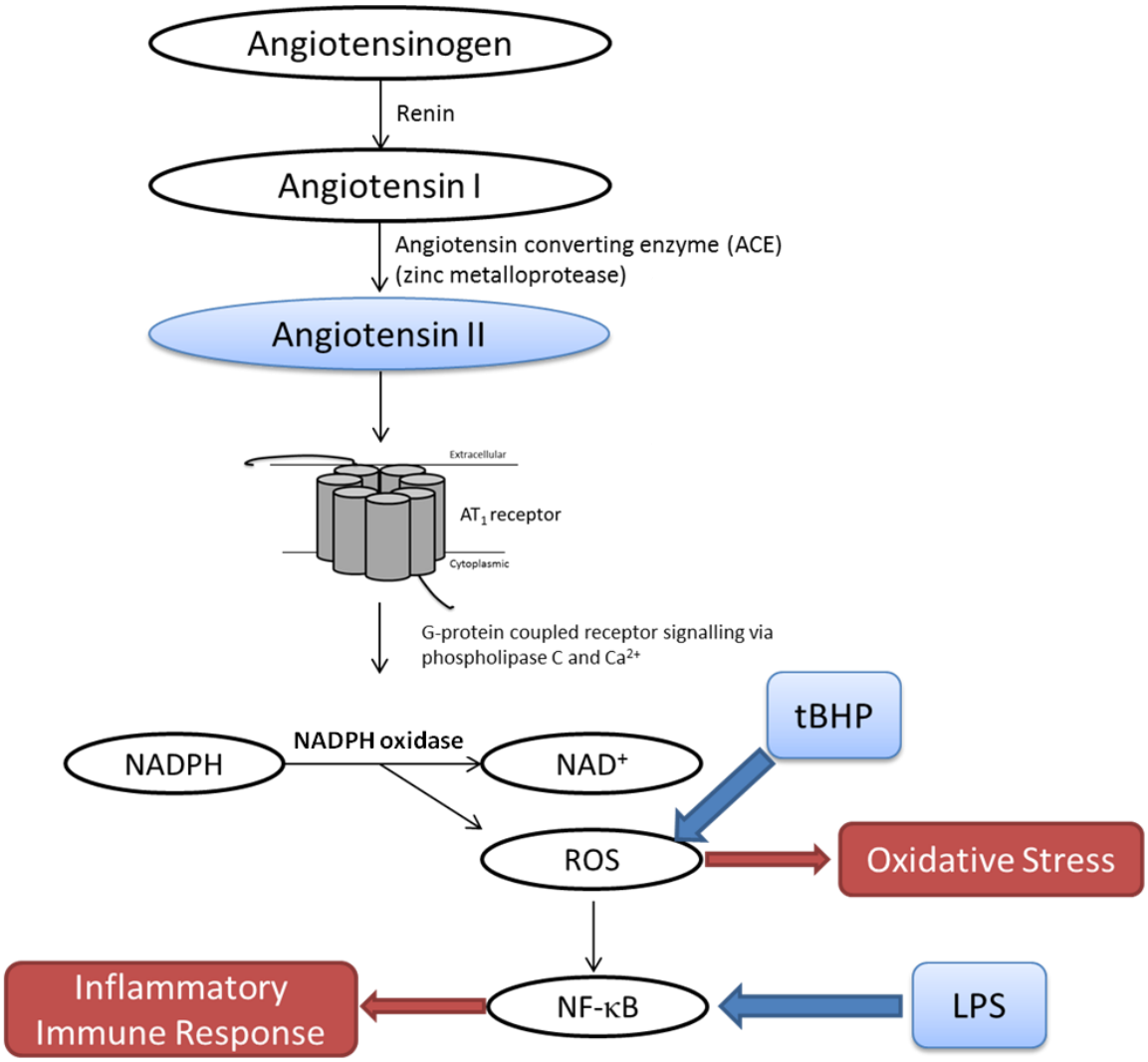

Figure 6.6 Schematic of the study design for studying the Renin-Angiotensin System (RAS) in SH-SY5Y cells. Treatments are shown in blue. Cells were treated with Angiotensin II at a concentration of 0.1 µM for 24 hours prior to RNA extraction. tBHP (0.025 mM; 40 minutes) was used to generate ROS and initiate oxidative stress. LPS from *E. coli* (100 ng/mL; 24 hours) was used to activate NF-κB activation and stimulate the inflammatory immune response.

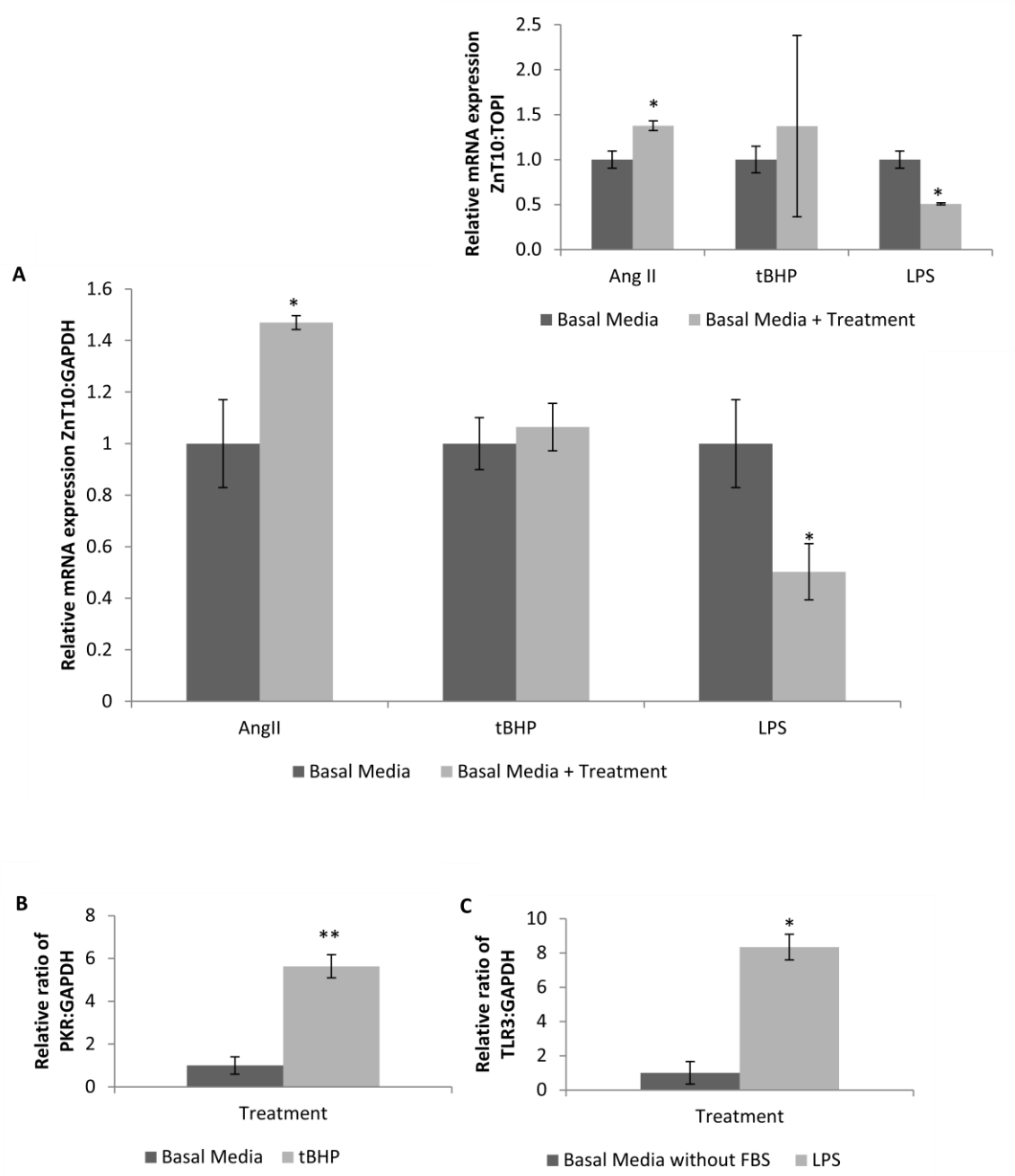

Figure 6.7 Does the RAS have an effect on ZnT10 mRNA expression in SH-SY5Y cells? SH-SY5Y cells were cultured for 24 h with Ang II or LPS orSH-SY5Y cells were cultured for 40 min with tBHP before culturing for a further 24 h in basal media (n = 3). RNA was extracted and levels of **A.** ZnT10 were measured by RT-qPCR. Data are expressed relative to GAPDH (or TOPI *inset* **(i)**) mRNA levels measured in the same samples. Primers are given in table 3.4. Levels of **B.** PKR and **C.** TLR3 were measured by RT-PCR. Primers are given in table 6.2. All values are shown as mean ± SEM ** $p < 0.01$, * $p < 0.05$ by Student's t test.

.

Name/ Accession Number	Primer Sequences	Amplicon Length (bp)	Annealing Temp (°C)
PKR*	5′-GGCACCCAGATTTGACCTTC-3′ 5′-TCCTTGTTCGCTTTCCATCA-3′	490 bp	60
TLR3**	5'-TCCGTTGAGAAGAAGGTTTTCGGG-3' 5'-ATATCCTCCAGCCCTCCAAGTGGA-3'	322 bp	60

Table 6.2 Primer sequences for PKR and TLR3 by RT-PCR analysis. *(Mouton-Liger et al., 2012) **(Nessa B. N. et al., 2006)

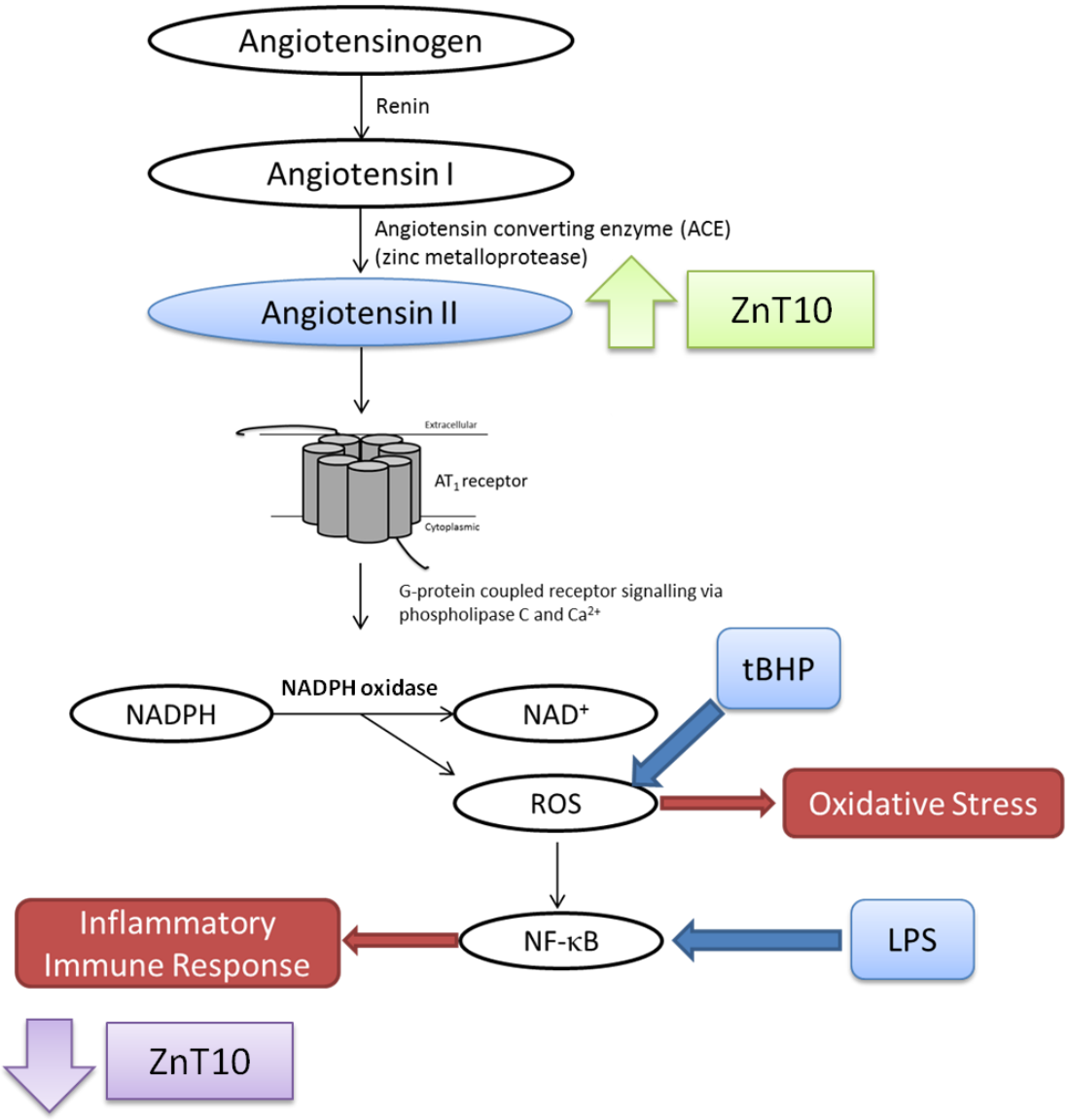

Figure 6.8 Schematic summarising the observations made based on experiments probing the effect of the Renin-Angiotensin System (RAS) in SH-SY5Y cells. Treatments are shown in blue. Cells were treated with Angiotensin II at a concentration of 0.1 µM for 24 hours prior to RNA extraction. tBHP (0.025 mM; 40 minutes) was used to generate ROS and initiate oxidative stress. LPS from *E. coli* (100 ng/mL; 24 hours) was used to activate NF-κB activation and stimulate the inflammatory immune response. Ang II caused a significant increase in ZnT10 mRNA expression ($p < 0.05$). tBHP was used to generate ROS and initiate oxidative stress this caused no significant change in ZnT10 mRNA expression levels. LPS was used to activate NF-κB activation and stimulate the inflammatory immune response, this caused a significant decrease in ZnT10 mRNA expression levels ($p < 0.05$).

Chapter 7: The effect of metals on BACE1 splicing events

7.1 Outline

In this chapter I continue to investigate the involvement of zinc in AD. Zinc transporter dysregulation plays a role in AD aetiology, as discussed in Chapter 6, and so it follows that alterations in levels of zinc transporters will ultimately result in differing levels of intracellular zinc. A broad overview of the involvement of zinc in AD was given in Chapter 1. Here I will focus on the role of zinc and other metal cations in the alternative splicing of the enzyme β-secretase 'BACE'. BACE1 is a type I transmembrane aspartic proteinase known to be involved in the amyloidogenic pathway described in Chapter 1 (Figure 1.5) where it is involved in the processing of APP thereby promoting the production of the neurotoxic peptide Aβ. The homolog BACE2 is only expressed at low levels in neurones and does not have the same cleavage activity as BACE1 with regards to APP (Vassar et al., 2009) and therefore is not discussed. This chapter reveals that the cations zinc, copper, cobalt and nickel are involved, to differing levels, in the BACE1 alternative splicing events at the mRNA level.

BACE1 has four known splice variants, each with a different enzymatic activity (Mowrer and Wolfe, 2008). Interestingly, levels of total BACE1 activity and protein expression correlate positively with Aβ production. This also has implications in the AD brain as BACE1 levels are increased in the frontal cortex of human post mortem AD brain tissue (Ahmed et al., 2010). In BACE1 knockout mice there is an absence of Aβ production and, although these mice appear healthy, there is evidence that there is a reduced myelination and some cognitive deficits (Willem et al., 2006).

There are nine exons in the BACE1 gene and normal processing results in the full-length active protein of 501 amino acids (BACE501). Transcription is initiated from the normal 5' splice site in exon 3 in combination with the normal 3' splice site in exon 4 (indicated on Figure 7.1A). There is an alternative 5' splice site within exon 3 as well as an alternative 3' splice site within exon 4 and, as stated in Chapter 1, combinations of the use of these yield the various isoforms (indicated on Figure 7.1). The next largest isoform is 476 amino acids (BACE476), which results from use of the normal 5' splice site in exon 3 but an alternative 3' splice site in exon 4 gives rise to the in-frame deletion of 75 base pairs giving a protein product 25 amino acids shorter (Figure 7.1B). A similar, an in-frame deletion of 132 base pairs is evident for the isoform BACE457 (457 amino acids). In this case the alternative splice site used is an alternative 5' splice site in exon 3 in combination with the normal 3' splice site in exon 4 (Figure 7.1C). It follows that the final splice variant results from the use of both alternative splice sites; 5' alternative splice site in exon 3 in combination with the 3' alternative splice site in exon 4 (Figure 7.1D) yielding the isoform that is an in-frame deletion of 207 base pairs, resulting in the smallest BACE1 isoform of 432 amino acids (BACE432) (Mowrer and Wolfe, 2008). The multiple sequence alignment of all four splice variants is shown in Appendix J.

Intriguingly, the level of expression of each isoform correlates with size such that BACE501 is expressed at the highest levels > BACE476 > BACE457 > BACE432 in pathologically normal brains. BACE501 has also been found to be the most active isoform with the difference in activity attributed to the conformational change caused by the alternative splicing between important active site, aspartates in exons 2 and 6. Researchers have predicted that these splicing events alter the final folding of the protein and presumably, the access of substrates to the catalytic site (Mowrer and

Wolfe, 2008). Investigations into these splicing events are of importance in the pathology of AD, due to the role of BACE1 in Aβ production. Influencing splicing events so as to decrease BACE501 levels and increase levels of the less active BACE476 and BACE457 forms could ultimately reduce Aβ production without having an overall effect on total BACE1 expression, thus supporting the argument that BACE501 is the main contributor to Aβ production (Mowrer and Wolfe, 2008). In the transgenic mouse model of AD, tg2576, there is an over-expression of the Swedish mutated human form of APP (APPsw). This is a double mis-sense mutation in exon 16 of the APP gene located on chromosome 21 that was originally identified due to its prevalence in a large Swedish pedigree. In fibroblast cell cultures, transfection of APPsw increases production of Aβ up to 7-fold compared with wild-type cells (Johnston et al., 1994). Intriguingly though, in the mouse model it has been shown that there is no change in the mRNA level of BACE1 within the brain. Despite this, there is increased enzymatic activity of BACE1 within these brains. The rise in activity is attributed to an increase in expression of the largest isoform BACE 501 (Zohar et al., 2005). This has led to the proposal that BACE1 protein expression and activity is increased in AD brains, despite mRNA levels remaining constant in both transgenic mice models (Zohar et al., 2005) and AD patients (Holsinger et al., 2002, Fukumoto et al., 2002).

Metals have been implicated in expression and activity of BACE1. In particular most research has focused on copper, due to a 24-residue peptide in the C-terminus of the BACE1 enzyme that contains cysteine residues that are able to bind a single copper atom with high affinity. Furthermore, in mammalian cells BACE1 has been shown to interact with the copper chaperone CCS. CCS is a copper delivery protein for the copper/zinc superoxide dismutase, SOD1. SOD1 binds both copper and zinc, the

cellular role of which is to destroy superoxide radicals that ultimately would result in oxidative stress. Over-expression of BACE1 in mammalian cells causes a reduction in the activity of SOD-1 due to an interaction of BACE1 with the CCS thus demonstrating a further role for BACE1 in metal homeostasis (Angeletti et al., 2005, Dingwall, 2007). Interestingly in previous research total BACE1 mRNA expression in rat adrenal medulla cells (PC12) increased with the addition of both copper and manganese but remained unchanged when extracellular zinc, iron and aluminium were added (Lin et al., 2008).

It is note worthy that there are discrepancies in the literature for BACE1 mRNA expression levels, with the majority of work focusing predominantly on total BACE1, rather than investigating the isoform differences. Knowledge into the splicing events of these isoforms is lacking and further studies of these and the potential role of metals in regulating these events could help to elucidate pathways implicated in AD pathogenesis. Results presented in this chapter are interpreted on the basis of the different BACE1 splice variants and here I report changes in the mRNA expression levels of the alternative splice variants in response to treatment of SH-SY5Y cells with extracellular zinc, copper, cobalt and nickel. These results could indicate a role for these cations in regulating these splicing events.

In line with my studies investigating the role of the brain RAS and mRNA expression I also investigated the role of RAS in splicing of BACE1. As summarised in Chapter 6 the RAS is a hormonal system well documented to control and regulate blood pressure and fluid balance and it has been extensively researched because of its importance in hypertension (Taquini and Taquini, 1961). The RAS is shown in Figure 6.1. Recent research has shown that the mammalian brain contains all components of the RAS (De

Bundel et al., 2008, Speth and Karamyan, 2008) and the brain has high concentrations of angiotensin receptors (Gard and Rusted, 2004). A metabolite of the system is Ang II which activates the AT_1 and AT_2 receptors (de Gasparo et al., 2000). Importantly, Ang II is able to act as a neurotransmitter in the brain, mainly acting to influence osmoreceptors in the hypothalamus to regulate the thirst response however it is also known to interact with other neurotransmitters such as acetylcholine, blocking its downstream effects (Gard, 2002). The cholinergic system is integral to the regulation of cognitive functions, in particular synaptic plasticity, specifically in learning and short-term memory therefore its inhibition is detrimental to these pathways. Here I show BACE1 splicing events are affected by levels of Ang II in the SH-SY5Y cell line model, with an increase in BACE501 and BACE457 mRNA being detected alongside a decrease in BACE476 mRNA manifesting as a non-significant overall change in total BACE1.

Downstream of the AT_1 receptor is activation of NADPH oxidase. As stated previously (see Chapter 6), a consequence of NADPH oxidase activation is the conversion of NADPH to NAD^+ and the by-products of such a reaction is ROS. An excess of ROS is known to cause oxidative stress and this is an important consideration in the aetiology of AD. Furthermore, continuous activation of the brain RAS in hRN/hANG-Tg mice (human renin (hRN) and human angiotensinogen (hANG) transgenic mice), a hypertensive mouse model, enhances oxidative stress and causes a decline in cognitive function by excessive stimulation of the AT_1 receptor (Zhu et al., 2004). Moreover, the Aβ complexes caused as a by-product of the amyloidogenic pathway, initiate altered neuronal ionic homeostasis resulting in the production of ROS and therefore oxidative stress. In addition to the usual side effects of oxidative stress, a further concern in AD is the alterations to protein kinase signalling pathways induced by this cellular state

causing kinases, such as GSK3, to be activated, thereby leading to tau hyperphosphorylation and subsequently exacerbating NFT burden, as classified by Braak staging at post-mortem. Oxidative stress has been previously shown to affect splicing events (Soliman et al., 2009). It is evident that oxidative stress increases total BACE1 protein levels in SH-SY5Y cells induced with H_2O_2 (Mouton-Liger et al., 2012). In this chapter I confirm an increase in BACE476, BACE457 and BACE432 isoforms with a decrease in the BACE501 isoform through induced oxidative stress in SH-SY5Y cells. Interestingly this is manifested as an overall significant increase in total BACE1 at the mRNA level.

ROS can also induce a redox-dependent signal transduction pathway that leads to NF-κB activation and therefore stimulation of the inflammatory immune response - inflammation can also cause extensive damage in the brain of AD patients (Zimmerman et al., 2004). Western blot analysis shows that LPS induced inflammatory response is able to increase levels of total BACE at the protein level, inducing neuroinflammation and an increase in Aβ and memory impairments in mouse models (Lee et al., 2008). The RT-qPCR data presented herein shows the converse to this with a significant decrease in total BACE1 mRNA expression, contributed to by significant reductions in both BACE501 and BACE476 splice variant expression.

Elucidation of the role of the brain RAS in activation of differential splicing events of BACE1, will further knowledge of this enzyme's role in oxidative stress and inflammation. Here I show novel results concerning the splice variants of BACE1.

7.2 The effect of zinc treatment on expression of different BACE1 splice variants

The effect of zinc availability on splicing events of BACE1 and therefore levels of expression of mRNA in SH-SY5Y cells was determined by culturing cells at 100 µM $ZnCl_2$ for 24 hour. Cell viability data for SH-SY5Y cells are presented in Chapter 4. Total RNA was extracted from cells (section 2.4.1) and standard curves were generated for each splice variant as described in section 2.5.5.1 before RT-qPCR was performed. Primer alignment used for RT-qPCR analysis of the splice variants is shown in Figure 7.1 and primer sequences are given in Table 7.1. Standard curves for all RT-qPCR passed acceptance criteria (Figure 7.2). GAPDH showed a consistent expression independent of the extracellular zinc treatment and in Chapter 5 I validated the use of GAPDH in these experiments by showing there is no difference in the results of extracellular zinc treatment relative to either reference gene GAPDH or TOPI and therefore GAPDH was chosen as the reference gene and normalisation control. GAPDH has also previously been used to normalise zinc response by RT-qPCR (Jackson et al., 2007, Hojyo et al., 2011). All levels of BACE1 were assessed as a ratio to the reference gene GAPDH.

Cells treated with an increased level of extracellular zinc manifested as a significant increase in total BACE1 mRNA expression when compared with untreated cells (p = 0.01) (Figure 7.3). Interestingly, when extrapolated for the individual variants, this was revealed as an increase in the splice variants BACE501 (p = 0.004) and BACE432 (p = 0.001), however a significant decrease in BACE476 was observed (p = 0.05). No change was observed in BACE457. In addition a standard curve was generated, as described in Section 2.5.5.1, for the MT1 control (Figure 7.2), in order to assess the increase in response to 100 µM extracellular zinc (Figure 7.3*i inset*). Thus I can

conclude that total BACE1 appears to be up-regulated at the mRNA level in response to extracellular zinc treatments, by altering levels in splicing such that BACE501 and BACE432 are significantly increased in treated cells. However, extracellular zinc treatment induces a significant decrease in BACE476. These results implicate zinc as a regulator of splicing events in BACE1. Alternatively to effects on splicing, it is note worthy that overall effects on total BACE1 may also reflect differences in mRNA stability of the alternative splice variants. Thus, if zinc has an effect on an individual variant mRNA stability that will be reflected as an increase in that variant manifested by an increase in total BACE1 mRNA levels.

7.3 The effect of other extracellular cations on expression of BACE1 splice variants

The effect of the extracellular cations (copper, cobalt and nickel) availability on splicing events of BACE1 and therefore levels of expression of mRNA in SH-SY5Y cells was determined by culturing cells at 100 µM copper (as $CuSO_4$), 100 µM cobalt (as $CoCl_2$) and 100 µM nickel (as $NiCl_2$) for 24 hour. Cell viability data for SH-SY5Y cells are presented in Chapter 5. Total RNA was extracted from cells (section 2.4.1), and standard curves were generated for each splice variant as described in section 2.5.5.1. Primers used for RT-qPCR analysis are shown in Table 7.1. Standard curves for all RT-qPCR passed acceptance criteria (Figure 7.2). GAPDH showed a consistent expression independent of the extracellular cation treatment and in Chapter 5 I validated the use of GAPDH in these experiments by showing there is no difference in the results of extracellular cation treatments relative to either reference gene GAPDH or TOPI and therefore GAPDH was chosen as the reference gene and normalisation control. All levels of BACE1 were assessed as a ratio to the reference gene GAPDH.

Cells treated with 100 µM extracellular copper manifested as a significant increase in total BACE1 mRNA expression when compared with untreated cells ($p = 0.01$) (Figure 7.4). Individually, this revealed a decrease in the most active splice variant form BACE501 ($p = 0.001$) with significant increases in all other variants; BACE476 ($p = 0.007$), BACE457 ($p = 0.03$) and BACE432 ($p = 0.005$) observed.

Cells treated with 100 µM extracellular cobalt showed a significant decrease in total BACE1 mRNA expression ($p = 0.02$) (Figure 7.4). This alteration was due to a decrease in splice variant BACE501 ($p = 0.03$) and BACE476 ($p = 0.07$) with a non-significant decrease in BACE457 ($p = 0.25$) and BACE432 ($p = 0.43$).

Cells treated with 100 µM extracellular nickel showed a significant decrease in total BACE1 mRNA expression when compared with untreated cells ($p = 0.02$) (Figure 7.4). This seems to be due to non-significant decreases in all of the splice variants; BACE501 ($p = 0.26$), BACE476 ($p = 0.24$), BACE457 ($p = 0.19$) and BACE432 ($p = 0.25$).

Thus I can conclude that total BACE1 appears to be regulated at the mRNA level in response to different extracellular cation treatment, by altering levels of the different splice variants expressed. Total BACE1 was up-regulated significantly with copper treatment, but down-regulated with both cobalt and nickel treatment. The individual splice variants, which contribute to these overall changes, also differ depending on treatments. BACE501 decreases significantly with both copper and cobalt treatment. BACE476 is up-regulated with copper treatment but conversely is down-regulated with cobalt treatment. BACE457 and BACE432 are both up-regulated with copper treatments and showed a non-significant decrease with cobalt treatments. All of the splice variants displayed a non-significant down-regulation with nickel treatments. The

combination of these data shows varying roles of cations in the transcriptional regulation and/ or mRNA stability of BACE1.

7.4 Levels of BACE1 splice variants in AD brain tissue

The amyloid cascade hypothesis has been prominent in AD research and despite findings to the contrary, it still remains dominant (reviewed by Pimplikar, 2009). Central to this hypothesis is the formation of Aβ by BACE1 which is able to cleave APP in the Golgi apparatus. Previously, only total BACE1 has been investigation in AD patients therefore, here I assess the levels of the BACE1 splice variants in AD patients relative to age-matched controls and compare human results to the APP/PS1 Tg mouse model.

7.4.1 *Levels of BACE1 splice variants in human brain tissue*

To investigate the effects of the disease process human brain tissue RNA was analysed from AD pathology cases (n = 13; female n = 8, male n = 5) and compared with age-matched controls (n = 10; female n = 3, male n = 7) (Appendix I). Frontal cortex RNA was obtained from the Newcastle Brain Tissue Resource (Newcastle, UK). Due to the pre-mortem decline in AD the RNA quality was not ideal as measured by RNA integrity number (RIN range 2.5-7.3), however RT-qPCR analysis was carried out in order to give an indication of expression levels of BACE1 splice variant expression levels in AD patients. Primers used for RT-qPCR analysis are shown in Table 7.1. Standard curves for all RT-qPCR passed acceptance criteria (Figure 7.2). All data are expressed as a ratio to GAPDH. When AD patients are compared with age-matched controls there was a non-significant decrease in total BACE1 levels when compared with controls (p = 0.08) (Figure 7.5). This reaches significance for BACE457 (p = 0.03) and BACE432 (p = 0.05) in this small number of brain tissues (Figure 7.5). Moreover, when the results

are analysed based upon gender, there is significant decrease total BACE1 expression in female AD patients compared with female controls (p = 0.02). This reaches significance for BACE457 (p = 0.008) and BACE432 compared with female controls (p = 0.00002) (Figure 7.6A). This is not observed in brain samples from males (Figure 7.6B). This is a particularly important result given the raised prevalence of AD in females.

7.4.2 *Expression levels of BACE1 splice variants in Tg mouse brain tissues*

In line with the human samples, frontal cortex brain tissue samples were obtained from 12 month old female WT (n = 5) and APP/PS1 mice (n = 11) (Dr Paul Adlard, University of Melbourne). APP/PS1 mice contain two transgenes inserted at a single locus. The first is the APP sequence that is modified to encode the human Swedish mutations K595N/M596L. Secondly, PS1 corresponds to the human presenilin 1 gene, in this case there is a deletion of exon 9 therefore known as DeltaE9 mutation (http://jaxmice.jax.org/strain/005864.html). These mice have Aβ deposits and exhibit deficits in spatial learning (Gimbel et al., 2010). Brain samples were removed and snap frozen before being stored in RNA Later at -80°C. Samples were shipped in RNA later on dry ice and RNA was extracted using Trizol (section 2.4.1). Primers used for RT-qPCR analysis are shown in Table 7.1. Standard curves for all RT-qPCR passed acceptance criteria (Figure 7.2). RT-qPCR analysis was carried out as a ratio to 18S rRNA. These results were not comparable to the human AD results and showed no change in total BACE1 (p = 0.88) and splice variant BACE501 (p = 0.93) and BACE432 mRNA expression (p = 0.23), compared with controls. In contrast BACE476 and BACE457 show significant increases in expression levels in the hemizygotes compared with the control non-carriers (p = 0.03 and p = 0.01 respectively) (Figure 7.7). This differs from results seen in human brain samples. It is note-worthy that all

mouse samples were from female mice and therefore gender differences could not be explored in this instance.

7.5 BACE1 splice variant mRNA expression in the RAS

As published data indicates an involvement of the brain RAS in neurodegenerative conditions experiments were derived to investigate the effect of Ang II on BACE1 splice variant mRNA expression in SH-SY5Y cells including experimentation into the role of oxidative stress and the inflammatory immune response on BACE1 splice variant expression. A summary of the study design is shown in Figure 7.8.

7.5.1 *Effect of Ang II on BACE1 splice variant mRNA expression*

Human neuroblastoma SH-SY5Y cells were treated with 0.1 μM Ang II for 24 hours in the absence of FBS. This level of Ang II has previously been used in $Na^{(+)}/H^{(+)}$ exchanger assays in SH-SY5Y cells (Reid et al., 2004). Primers used for RT-qPCR analysis are shown in Table 7.1. Standard curves for all RT-qPCR passed acceptance criteria (Figure 7.2). Analysis of mRNA expression was carried out using RT-qPCR as a ratio to GAPDH. In Chapter 6 I validated the use of GAPDH in these experiments by showing there is no difference in the results of Ang II treatments relative to either reference gene GAPDH or TOPI and therefore GAPDH was chosen as the reference gene and normalisation control. Results relative to GAPDH show no change in total BACE1 expression at the mRNA level in response to extracellular Ang II treatment (Figure 7.9A). However, when the splice variants were analysed, a significant increase in BACE501 (p = 0.001) compared with untreated cells was observed. This is not reflected in BACE457 (p = 0.22). Conversely, there were significant decreases in both BACE476 (p = 0.03) and BACE432 mRNA expression (p = 0.002) compared with

untreated cells. These results indicate that BACE1 splice variants are regulated within the brain by the RAS.

7.5.2 *Effect of oxidative stress on BACE1 splice variant mRNA expression*

Human neuroblastoma SH-SY5Y cells were treated with 0.025 mM tBHP for 40 min in the presence of 10 % FBS. This level of tBHP has previously been used to induce oxidative stress in assays in SH-SY5Y cells (Krishnamurthy et al., 2000). Medium was removed and replaced with basal medium plus 10 % FBS for a further 24 hour time period, before RNA was harvested. Primers used for RT-qPCR analysis are shown in Table 7.1. Standard curves for all RT-qPCR passed acceptance criteria (Figure 7.2). Analysis of mRNA expression was carried out using RT-qPCR as a ratio to GAPDH. In Chapter 6 I validate the use of GAPDH in these experiments by showing there is no difference in the results of tBHP treatments relative to either reference gene GAPDH or TOPI and therefore GAPDH was chosen as the reference gene and normalisation control. As a control experiment, to ensure that oxidative stress had actually been induced by the treatment, levels of PKR (double-stranded RNA dependant protein kinase) were assessed by semi-quantitative RT-PCR as a ratio to GAPDH. Primers used for RT-PCR analysis are shown in Table 6.2. PKR is a serine-threonine kinase and in response to oxidative stress signals it is able to catalyse the phosphorylation of the α subunit of eukaryotic translation initiation factor-2 (eIF2) in order to inhibit protein synthesis (Der et al., 1997). Up-regulation of PKR has been found to occur in SH-SY5Y cells in response to induced oxidative stress by H_2O_2 treatment (Mouton-Liger et al., 2012). Here I confirm a significant increase in PKR levels in the SH-SY5Y cells treated with tBHP as compared with controls (p = 0.001) (Figure 7.9B*i* *inset*). Results manifested as a non-significant increase in total BACE1 in tBHP treated samples compared with untreated samples (p = 0.07) (Figure 7.9B). This was a result of

significant increases in the mRNA expression of the individual splice variants BACE476 (p = 0.004), BACE457 (p = 0.03) and BACE432 (p = 0.005) when compared with untreated samples (Figure 7.9B). Interestingly however, BACE501 showed a significant decrease in the tBHP treated samples (p = 0.008) compared with untreated cells. This indicates that oxidative stress is implicated in the regulation of the splicing events seen in BACE1.

7.5.3 *Role of the inflammatory immune response in BACE1 splice variant mRNA expression*

Human neuroblastoma SH-SY5Y cells were treated with 100 ng/ mL LPS for 24 hours in the absence of FBS. This level of LPS has previously been used to induce the inflammatory immune response in assays in SH-SY5Y cells (Pandey et al., 2009). Primers used for RT-qPCR analysis are shown in Table 7.1. Standard curves for all RT-qPCR passed acceptance criteria (Figure 7.2). Analysis of mRNA expression was carried out using RT-qPCR as a ratio to GAPDH. In Chapter 6 I validated the use of GAPDH in these experiments by showing there is no difference in the results of LPS treatments relative to either reference gene GAPDH or TOPI and therefore GAPDH was chosen as the reference gene and normalisation control. To ensure that the inflammatory immune response had been induced, levels of Toll-like receptor 3 (TLR3) were assessed by semi-quantitative RT-PCR as a ratio to GAPDH. Primers used for RT-PCR analysis are shown in Table 6.2. Toll-like receptors are present on the cell surface and are able to respond to stimulants produced by microorganisms in order to initiate the host defence and to stimulate the release of molecules involved in the inflammatory immune response, such as antimicrobial peptides and inflammatory cytokines. LPS is known to stimulate TLR3 and causes up-regulation of the receptor in SH-SY5Y cells (Nessa B. N. et al., 2006). There was a significant increase in the TLR3 mRNA levels in cells treated

with LPS compared with untreated cells ($p = 0.03$) (Figure 7.9A*i inset*). Results show a non-significant decrease in total BACE1 expression at the mRNA level in response to extracellular LPS treatment compared with untreated cells ($p = 0.07$) (Figure 7.9). This was as a result of significant decreases in both BACE501 ($p = 0.04$) and BACE476 ($p = 0.04$) isoforms with a non-significant increase in BACE457 ($p = 0.09$) and no change in BACE432 ($p = 0.78$). This indicates that the inflammatory immune response may in part regulate splicing events in BACE1.

7.6 Discussion

There is much controversy in the literature about expression levels of BACE1 mRNA in AD and what this means for protein levels and enzyme activity. It is note worthy that the majority of work published focuses predominantly on total BACE1 rather than looking at the different isoforms. This is particularly important given the activity of splice variants BACE476, BACE457 and BACE432 are significantly reduced compared with BACE501 (Tanahashi and Tabira, 2001, Mowrer and Wolfe, 2008). This difference in activity of the variants should be taken into account when investigating BACE1 regulation. Moreover, in addition to transcriptional regulation, BACE1 appears to undergo translational modification at multiple levels (De Pietri Tonelli et al., 2004). Therefore these factors should be taken into consideration both in experimental design and interpretation of data. However translational regulation is outside the scope of this chapter. An additional consideration, not assessed in this work is mRNA stability of the individual variants. It is important to bear in mind that overall effects on total BACE1 may also reflect differences in mRNA stability of the alternative splice variants. Thus, if a treatment has an effect on an individual variant mRNA stability that will be shown as an increase in that variant manifested by an increase in total BACE1 mRNA levels.

Metals have been implicated in expression at the protein level and the activity of BACE1 previously. The focus of much research has been on copper due to the presence of a 24-residue peptide in the BACE1 C-terminal, which contains cysteine residues able to bind a single copper atom with high affinity. In mammalian cells BACE1 has been shown to interact with the copper chaperone CCS. CCS is a copper delivery protein for the copper/zinc superoxide dismutase, SOD1. SOD1 binds both copper and zinc, the cellular role of which is to destroy superoxide radicals that ultimately would result in oxidative stress. Over-expression of BACE1 in mammalian cells causes a reduction in the activity SOD-1 due to an interaction of BACE1 with the CCS thus elucidating a further role for BACE1 in metal homeostasis (Angeletti et al., 2005, Dingwall, 2007). Furthermore, copper and manganese increase the expression of BACE1 mRNA in rat adrenal medulla cells (PC12), with zinc, iron and aluminium not affecting expression in this model (Lin et al., 2008). Interestingly is has been established that BACE1 gene expression is regulated by the zinc dependent transcription factor Sp1 (Christensen et al., 2004). It should be noted that in these experiments total BACE1 levels were measured only and incorrect alignment of primers from published results means that the area of the BACE1 transcript tested cannot be ascertained.

Copper and zinc have been implicated in AD as both can bind APP competitively at physiological concentrations in the extracellular domain, inducing large conformational changes and, presumably, altering physiological function and processing of APP (Dahms et al., 2012). Additionally, both metals are found at high levels in SP of AD patients (Lovell et al., 1998). The first experiments presented here show that splicing events can be influenced by the metal cations zinc, copper, cobalt and nickel. The results presented here are in support of previous studies for copper, with a significant increase in total BACE1 at the mRNA level (p = 0.01) with the addition of 100 µM

extracellular copper but what is intriguing is that copper appears to down-regulate the most active splice variant form BACE501 (p = 0.001). In contrast, copper treatment increased expression of BACE476, BACE457 and BACE432 (p = 0.007, p = 0.03 and p = 0.005 respectively). In these experiments I also show that the addition of 100 µM of extracellular zinc causes a significant increase in total BACE1 levels (p = 0.01), with the most active variant (BACE501) showing an increase in expression along with BACE432 (p = 0.004 and p = 0.001 respectively), with a significant decrease in BACE476 (p = 0.05). This shows that although the overall effect of copper and zinc treatment is the same, (i.e. total BACE1 increases) it is imperative to measure individual splice variant expression, because their profile differs with treatment. This differs from reports in the literature, where zinc induced a decrease in BACE1 expression, however incorrect publication of the primer sequences meant that I was unable to establish where in the sequence the primers annealed and therefore whether it is actually total BACE1 that was measured, or one of the variants (Lin et al., 2008). To my knowledge there is no data on the direct influence of zinc or copper on BACE1 variant activity. This would be a very interesting avenue for further research.

There is a down-regulation of all BACE1 splice variants in response to 100 µM cobalt treatment resulting in a significant decrease in total BACE1 (p = 0.02). For the individual variants however the down-regulation only reaches significance for BACE501 (p = 0.03). The only research relating to cobalt and BACE1, measures levels of total BACE1 in retinol ganglion cells (RGCs) where 200 µM of cobalt acted to increase BACE1 levels (Zhu et al., 2009). BLAST searches were unable to establish the whereabouts of the primers in the sequence. The differences may be due to alterations in cell types or the possible measurement of alternative splice variants rather than total BACE1. In addition, the study described used 200 µM of cobalt as opposed to 100 µM

used here. There are no cell viability data in the paper therefore I am unable to determine whether the increased concentration is appropriate for the RGCs. There has been no experiments to establish whether the effect of cobalt is dose dependent and therefore this would also need to be ascertained.

The final cation to be tested for its effect on BACE1 mRNA expression was nickel. Nickel is not thought to be essential in the human body although, it is known to be toxic in high doses and cause conditions such as or allergic contact dermatitis. Nickel exposure comes from the use in manufacture of everyday items such as cooking utensils, coins and jewellery (Garrow et al., 2000). The expression of BACE1 mRNA levels to 100 μM nickel was comparable to the response to cobalt with a non-significant down-regulation observed for all splice variants in response to nickel treatment cumulating in a significant decrease in total BACE1 (p = 0.02). The similarity in response to cobalt is in itself intriguing, and further research into both cations would elucidate further roles in BACE1 regulation and/or activity.

In summary, these results indicate that both zinc and copper act to increase total BACE1 mRNA expression and in contrast cobalt and nickel appear to down-regulate total BACE1 mRNA expression levels. Intriguingly though, zinc seems to influence splicing events such that the most active isoform, BACE501 mRNA expression increases and BACE476 mRNA expression decreases whereas copper influences events so as to decrease BACE501 expression but increase expression of BACE476 mRNA. How these events translate into overall activity of BACE1, and ultimately Aβ production, would be an interesting avenue of research.

The analysis of human brain RNA from patients diagnosed with AD further emphasised the importance of measuring BACE1 splice variants individually, rather than total

levels. It is known that BACE1 protein expression and activity is increased in the human AD brain (Holsinger et al., 2002, Fukumoto et al., 2002) but this is the first time that BACE1 splice variants have been measured in tissues from AD patients. Frontal cortex RNA was analysed by RT-qPCR in order to establish a BACE1 splice variant expression profile. To summarise, the main findings of this experiment revealed an overall significant decrease in BACE457 and BACE432 (p = 0.03 and p = 0.05 respectively) in AD patients. Separation on the basis of gender strengthened this response in the female AD brain; BACE457 p = 0.008 and BACE432 p = 0.00002, with a gender specific significant decrease in total BACE1 expression (p = 0.02) observed in females. This response was not evident in males. Whether this response is truly gender specific or whether it can attributed to the small number of samples or the quality of the RNA samples is not known. Sample quality is an important consideration in any experiment and here the range of RIN values (2.5-7.3) is below what would be desirable for RT-qPCR.

In order to try and support the human AD samples, brain tissue from the APP/PS1 Tg mouse model was sought to investigate BACE1 splice variant expression levels in a model of AD. In the literature studies investigating BACE1 levels in the Tg2576 transgenic mouse model of AD have yielded some interesting results. In this Tg mouse there is an over-expression of the Swedish mutated human form of APP. Research in this model has shown that there is no change in the mRNA level of BACE1 within the Tg brain. Despite this, there is increase enzymatic activity of BACE1 within these brains. The rise in activity is attributed to an increase in expression of the largest isoform BACE501 (Zohar et al., 2005). This result was confirmed by RT-qPCR in the mouse brain for this splice variant. Zohar et al., (2005) concluded that the over-expression of APP in these mice induces a change in splicing events such that

BACE501 is increased. This being the most active isoform of BACE1 means that BACE1 activity subsequently increases despite the mRNA levels of total BACE1 remaining the same. In the APP/PS1 splice variant there is no overall change in total BACE1 mRNA levels in line with the Tg2576 findings. However, in contrast my results reveal there is also no alteration in BACE501 expression in the hemizygotes compared with non-carriers, however a significant increase in both BACE476 and BACE457 (p = 0.03 and p = 0.01 respectively) was measured. This may be due to the different Tg mice used. APPsw is a double missense mutation in exon 16 of the APP gene located on chromosome 21 that was originally identified due to its prevalence in a large Swedish pedigree. In fibroblast cell cultures, transfection of APPsw increases production of Aβ up to 7-fold compared with wild-type cells (Johnston et al., 1994). The APP/PS1 mouse contains two transgenes, the first is the APPsw, however additionally the PS1 corresponds to the human presenilin 1 gene, in this case there is a deletion of exon 9 therefore known as DeltaE9 mutation (http://jaxmice.jax.org/strain/005864.html). The effect of this second mutation and indeed the presence of two mutations instead of one could in itself have an effect on BACE1 splice variant expression. It is worth bearing in mind that all of the mouse tissues were from female mice and that comparison to the human female AD cases shows a contrasting pattern of expression, with only BACE501 giving an agreement of no change. This species difference is not without precedence, as researchers have shown differences in BACE1 splice variant levels between human and rat in non-diseased tissue. They established that BACE501 and BACE457 are found at high levels in the frontal cortex of both human and rat brain but that BACE432 was only expressed highly in rat (Zohar et al., 2003). The hypothesis that was proposed was that BACE1 transcripts may have different evolutionary conservation and therefore it follows that BACE1 transcripts could also differ between mouse and human. This

would be supported by the knowledge that rodents do not ordinarily form SP and therefore caution must be applied when translating the data both between mouse models and to humans. In addition, data was not available for the treatments of the patients with AD, not only could pharmaceuticals have an effect on the BACE1 splicing events and/ or expression this also presents an issue in terms of translation of studies from mice to humans.

There is a growing body of evidence that the brain RAS is involved in the development and progression of AD (Kehoe et al., 2009). Therefore, echoing studies used to investigate ZnT10, I investigated the role of the RAS on BACE1 splice variant mRNA expression in SH-SY5Y cells (summarised in Figure 7.10). The first step examined was treatment with 0.1 μM Ang II over a 24 hour time period. The result of this experiment was no change in total BACE1 mRNA in treated SH-SY5Y cells compared with controls. Interestingly however the ratio of splice variants did change, with a significant increase of BACE501 ($p = 0.001$) and significant decreases in BACE476 and BACE432 ($p = 0.03$ and 0.002 respectively). In a previous study the activity of BACE1 in HEK293 cells transfected with AT_1 and APP or PS1 and treated with Ang II at varying concentrations (10 nM to 1000 nM) was investigated. The conclusion of this study was that there is no change in BACE1 activity with Ang II treatment after 24 hours (Wang et al., 2011a). In combination with the results presented here, the implication would be that the increase in BACE501 is negated by the decrease observed in BACE476 and BACE432 to give no overall change in total BACE1 expression and ultimately activity of BACE1. These results do not prove this and the differences in experimental parameters must be taken into consideration.

Oxidative stress has been shown to be an important factor in the progression of AD (Zhu et al., 2004). Here, in line with previous experiments in SH-SY5Y cells (Krishnamurthy et al., 2000), 0.025 mM of tBHP was used to induce oxidative stress in these cells. This was confirmed by a significant increase in PKR in the treated cells. For the BACE1 splice variants total BACE1 displayed a near significant increase in the treated cells (p = 0.07) with significant increases observed for the variants BACE476, BACE457 and BACE432 (p = 0.004, p = 0.03 and p = 0.005 respectively) but a significant decrease in BACE501 (p = 0.008). It has been reported that oxidative stress acts to increase protein expression of BACE1 in SH-SY5Y cells, where oxidative stress was induced by treatment with 0.2 mM and 0.5 mM H_2O_2 for up to 16 hours. Additionally, RT-qPCR analysis showed an increase of BACE1 mRNA expression after 1 hour treatment with 0.5 mM H_2O_2 (Mouton-Liger et al., 2012). This is in accordance with the results presented here but again caution should be employed as there are differences in experimental parameters. Our experiments also show the importance of measuring the BACE1 splice variants.

The final implication of the RAS is inducing the inflammatory immune response with ROS stimulating NF-κB production. The inflammatory immune response plays a large role in the aetiology of AD (Akiyama, 1994) and in fact non-steroid anti-inflammatory drugs (NSAIDs) have been shown to reduce the cognitive impairment associated with AD (Cote et al., 2012). Explored here is the effect of the inflammatory immune response on BACE1 splice variant expression at the mRNA level. The inflammatory immune response was induced in SH-SY5Y cells using 100 ng/ mL LPS for 24 hours. Induction of the response was confirmed using RT-PCR to show a significant increase in TLR3 levels in the treated cells. Total BACE1 expression levels did not reach significance for LPS treated cells but did display a down-regulatory trend in response to

LPS treatment (p = 0.07). In the individual variants both BACE501 and BACE476 decreased significantly in the treated cells (p = 0.04 and p = 0.04 respectively) but no significant changes in BACE457 and BACE432 were observed (p = 0.09 and p = 0.78 respectively). The role of LPS on BACE1 splice variants at the mRNA level has not been investigated previously in SH-SY5Y cells. Memory impairment induced by LPS in mouse models has been attributed to the accumulation of Aβ as a result of neuroinflammation (Lee et al., 2008). A subsequent study demonstrated that this accumulation was due to an increase in BACE1 protein levels induced by the NF-κB pathway (Choi et al., 2012). Regulation at the transcriptional level and subsequent activity of BACE1 protein requires further investigation in order to unravel the complicated process to control BACE1 and its isoforms, however I present a number of novel findings to add to this growing body of data.

This chapter highlights the importance of measuring the individual splice variants opposed to only total BACE1. Differences in splice variant mRNA expression may not manifest as overall changes in total BACE1 mRNA expression, but may correspond to important alterations in activity of the enzyme ultimately having a down-stream effect on the production of the neurotoxic Aβ.

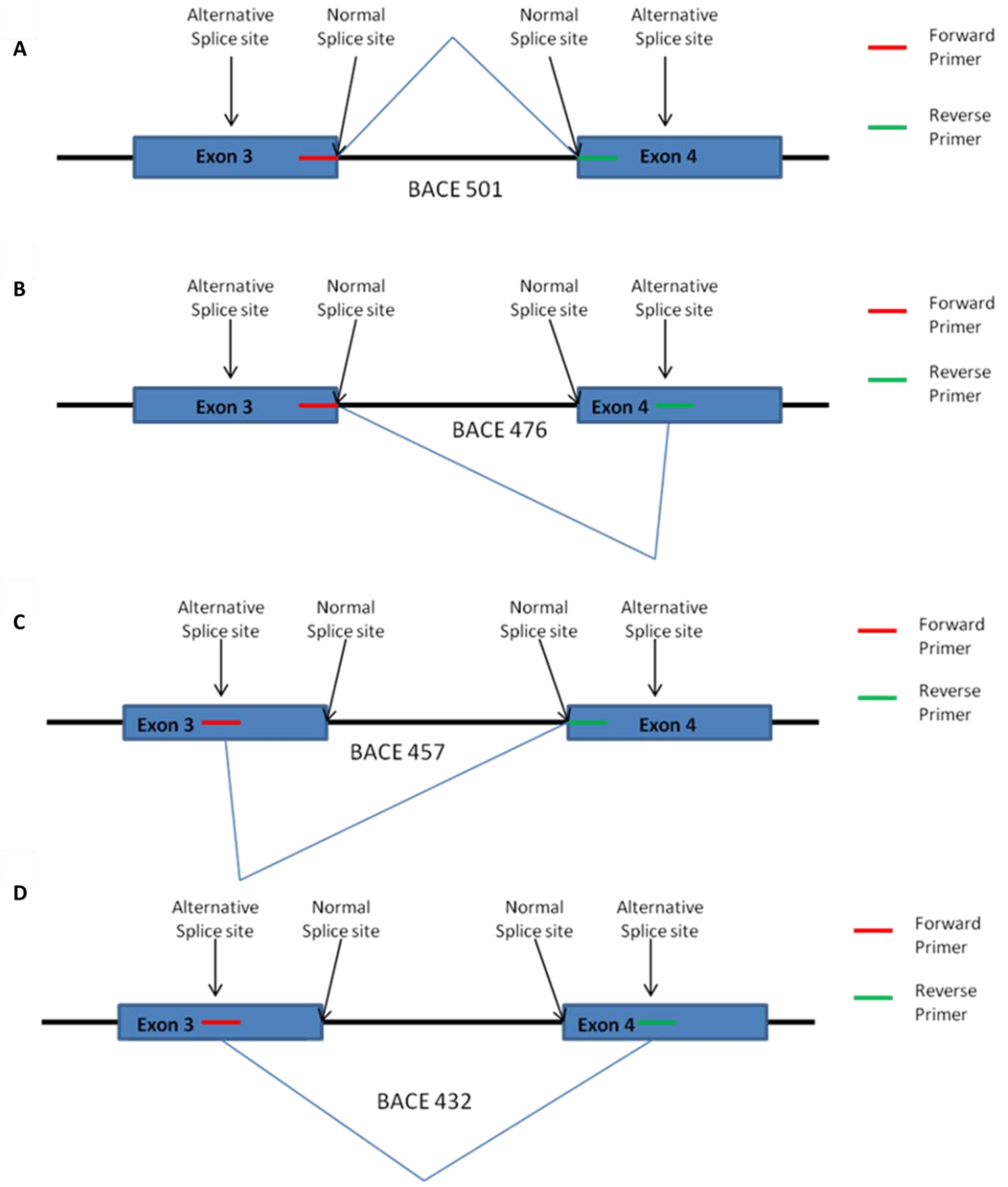

Figure 7.1 Schematic of the BACE1 splice variants. **A.** BACE 501. Transcription is initiated from the normal 5' splice site in exon 3 in combination with the normal 3' splice site in exon 4. **B.** BACE 476. Transcription is initiated from the normal 5' splice site in exon 3 in combination with the alternative 3' splice site in exon 4. **C.** BACE 457. Transcription is initiated from the alternative 5' splice site in exon 3 in combination with the normal 3' splice site in exon 4. **D.** BACE 432. Transcription is initiated from the alternative 5' splice site in exon 3 in combination with the alternative 3' splice site in exon 4. Schematic of primer design for each BACE1 splice variants are indicated (adapted from Mowrer and Wolfe, 2008).

Name/ Accession Number	Primer Sequences	Amplicon Length (bp)	Annealing Temp (°C)
BACE501* NM_012104.4	5′-$_{1005}$CTGGCCTATGCTGAGATTGC$_{1024}$-3′ 5′-$_{1083}$GAACGTGGGTCTGCTTTACC$_{1064}$-3′	79 bp	60
BACE476* NM_138972.3	5′-$_{968}$CTTCATCAACGGCTCCAACT$_{987}$-3′ 5′-$_{1037}$ACCACAAAGCCTGGCAATC$_{1018}$-3′	70 bp	60
BACE457* NM_138971.3	5′-$_{887}$ACCGACCTGCCTGACGAC$_{905}$-3′ 5′-$_{951}$GAACGTGGGTCTGCTTTACC$_{932}$-3′	65 bp	60
BACE432* NM_138973.3	5′-$_{887}$ACCGACCTGCTTTGTGGT$_{905}$-3′ 5′-$_{938}$CAGCACTTCAGACTGGTTGAG$_{917}$-3′	52 bp	60
Total BACE (exon5)* NM_012104.4	5′-$_{1175}$AGGTATCGACCACTCGCTGT$_{1194}$-3′ 5′-$_{1226}$CCGGATGGGTGTATACCAGA$_{1210}$ -3′	52 bp	60
ZnT10 NM_018713.2	5′-$_{844}$CGT AGC AGGTGA TTC CTT CAA C$_{865}$-3′ 5′-$_{956}$CAT CTC CCA TCA CAT GCA AAA G$_{935}$-3′	113 bp	60
GAPDH** NM_002046.3	5′-$_{113}$TGAAGGTCGGAGTCAACGGCTTTG$_{136}$-3′ 5′-$_{240}$CATGTAAACCATGTAGTTGAGGTC$_{217}$-3′	128 bp	60
MT1*** NM_005946	5′-$_{71}$ATGGACCCCAACTGCTCC$_{88}$-3′ 5′-$_{256}$TCAGGCACAGCAGCTGCAC$_{238}$-3′	186 bp	60
18S rRNA NM_011296	5′-$_{117}$CATTAAGGGCGTGGGGCGG$_{135}$-3′ 5′-$_{247}$GTCGTGGGTTCTGCATGATG$_{228}$-3′	131 bp	60

Table 7.1 Primer sequences for analysis of BACE1 splice variants using RT-qPCR analysis. The numbering on each of the oligonucleotides represents its position on the gene. *(Mowrer and Wolfe, 2008), **(Valentine et al., 2007), ***(Cragg et al., 2005).

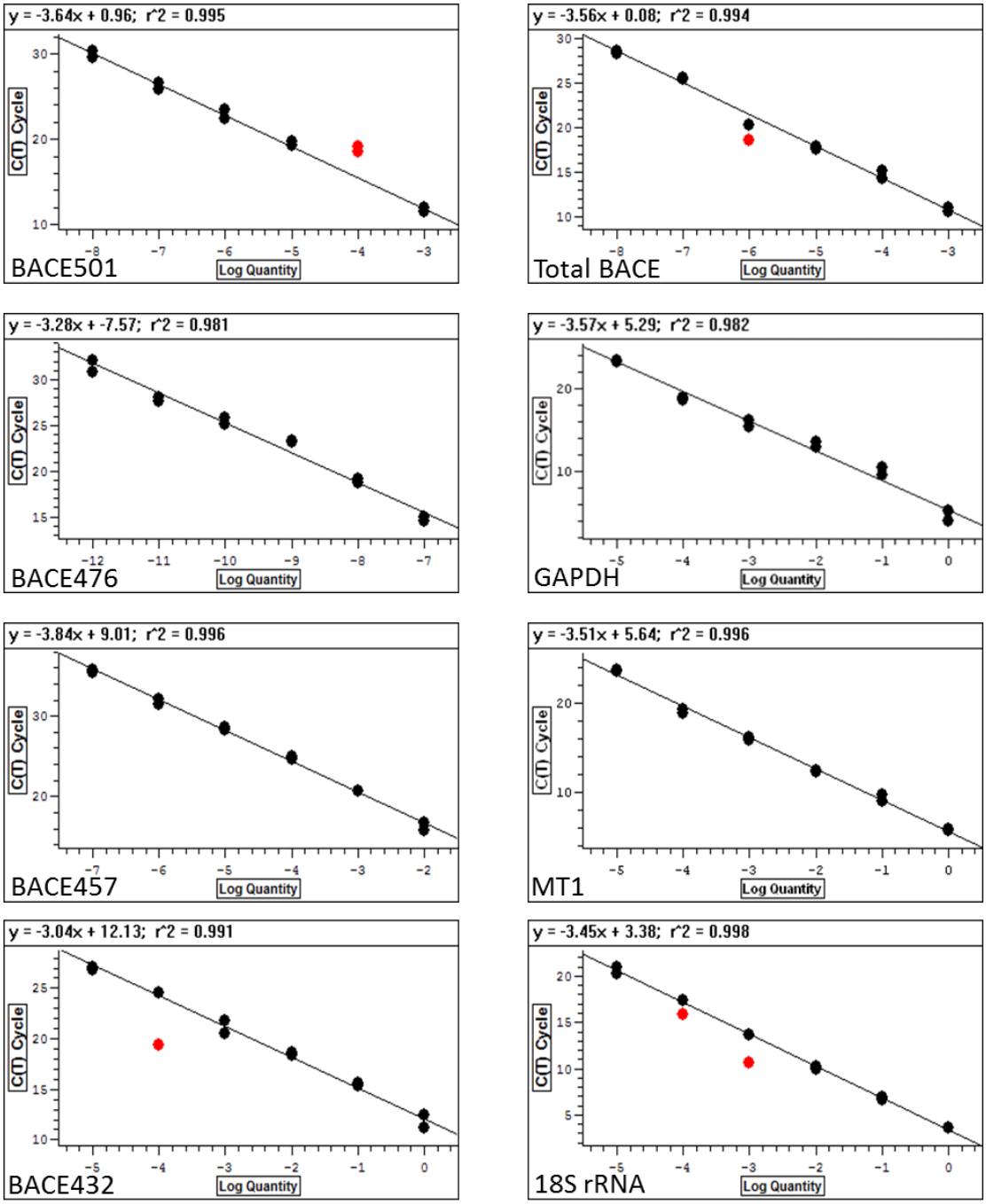

Figure 7.2 Standard curves generated to measure relative levels of BACE1 splice variants by RT-qPCR, using SYBR green fluorescence and the DNA Engine Opticon 2 (MJ Research). Standards for GAPDH, BACE1 splice variants and MT1 products were generated by amplifying the region between the primers shown in Table 7.1, and subcloned into the vector pCR2.1-TOPO TA (Invitrogen). The mean log concentration of each dilution was plotted against PCR cycle number at which the fluorescent threshold was crossed (C_T). Excluded data points are shown in red. These standard curves were used to calculate relative levels of BACE1 splice variant transcripts.

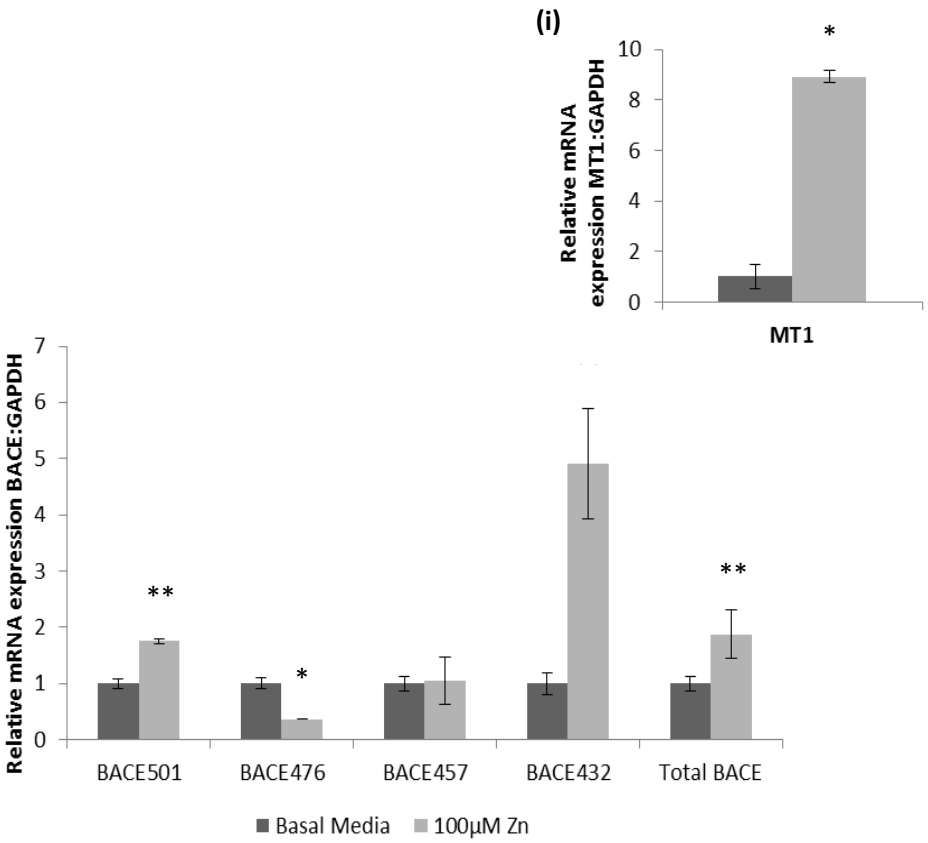

Figure 7.3 The effect of increased extracellular zinc on BACE1 splice variant mRNA expression in SH-SY5Y cells. Cells were cultured for 24 h in basal media (3 µM Zn) or at 100 µM extracellular zinc (added as $ZnCl_2$) then total RNA was extracted and levels of BACE1 splice variant and (i) MT1 mRNA were measured by RT-qPCR, using SYBR green fluorescence and the DNA Engine Opticon 2 (MJ Research). Primers are given in Table 7.1. Data are expressed relative to GAPDH mRNA levels measured in the same samples. All values are shown as mean ± SEM, $n = 6$. *** $p < 0.001$, ** $p < 0.01$, significantly different from 3 µM zinc (untreated) by Students *t*-test.

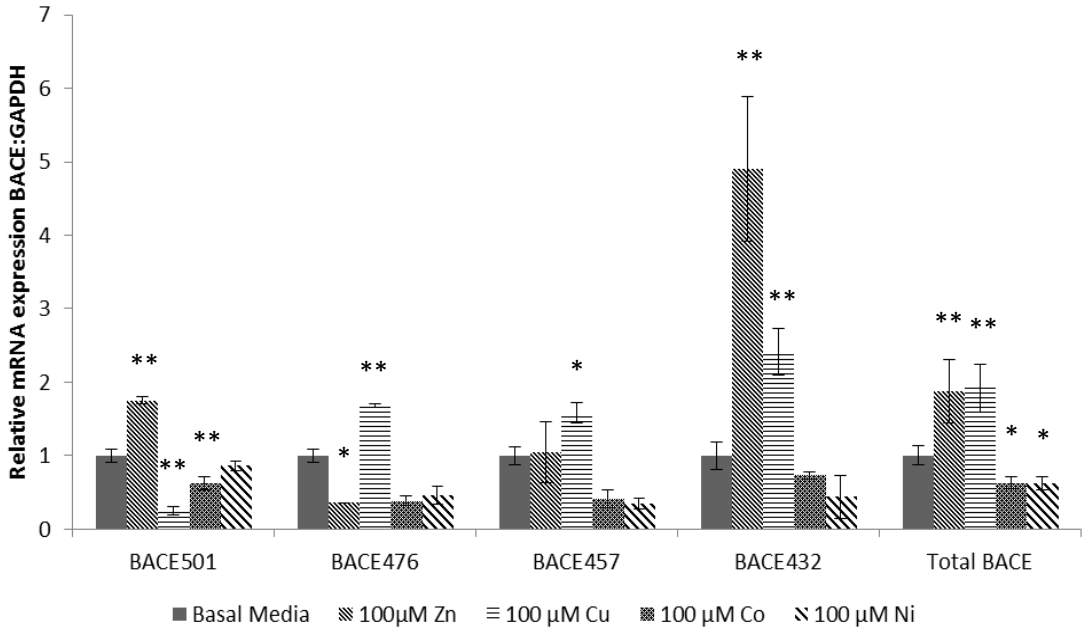

Figure 7.4 The effect of extracellular cation treatment on BACE1 splice variant mRNA expression in SH-SY5Y cells. Cells were cultured for 24 h at 100 µM copper (as $CuSO_4$), 100 µM cobalt (as $CoCl_2$) or 100 µM nickel (as $NiCl_2$) as indicated. Total RNA was extracted and levels of BACE1 splice variant mRNA were measured by RT-qPCR, using SYBR green fluorescence and the DNA Engine Opticon 2 (MJ Research). Primers are given in table 7.1. Data are expressed relative to GAPDH mRNA levels measured in the same samples. All values are shown as mean ± SEM, $n = 6$. *** $p < 0.001$, ** $p < 0.01$, significantly different from 3 µM zinc (untreated) by Students *t*-test.

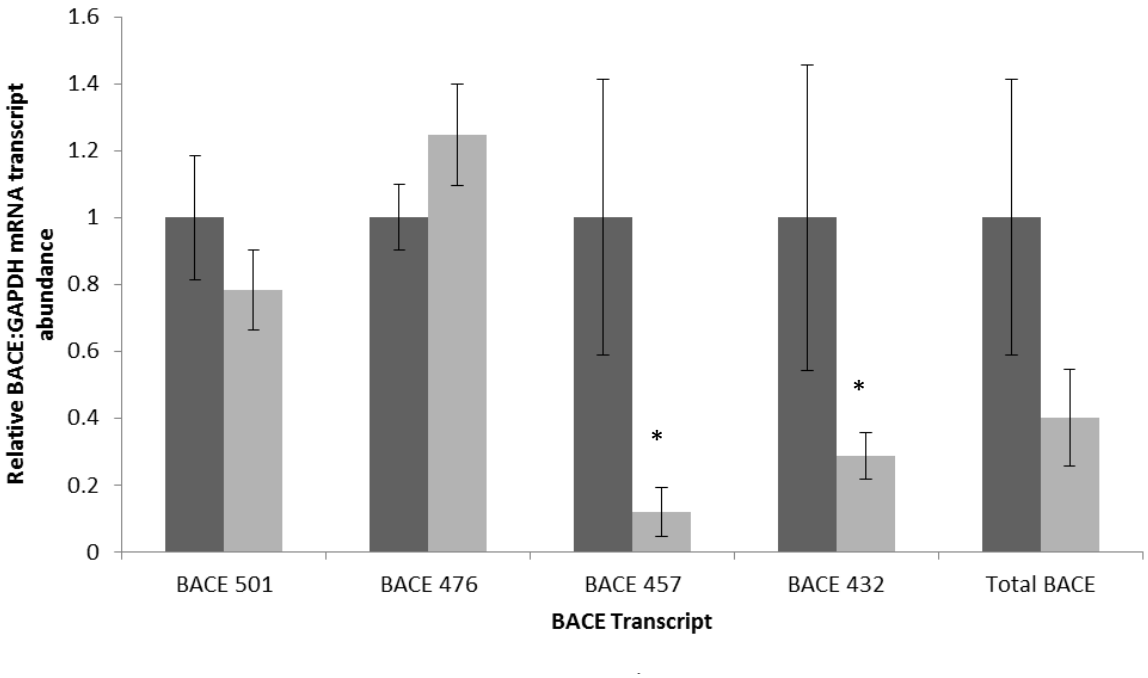

Figure 7.5 BACE1 splice variant mRNA expression in human brain frontal cortex tissue. Relative levels of BACE1 splice variants in brain tissue from control brains (n = 10) and AD brains (n = 13). Data are expressed relative to GAPDH mRNA levels measured in the same samples. Primers are given in Table 7.1. All values are shown as mean ± SEM * $p < 0.05$ significantly different from controls by Students t-test.

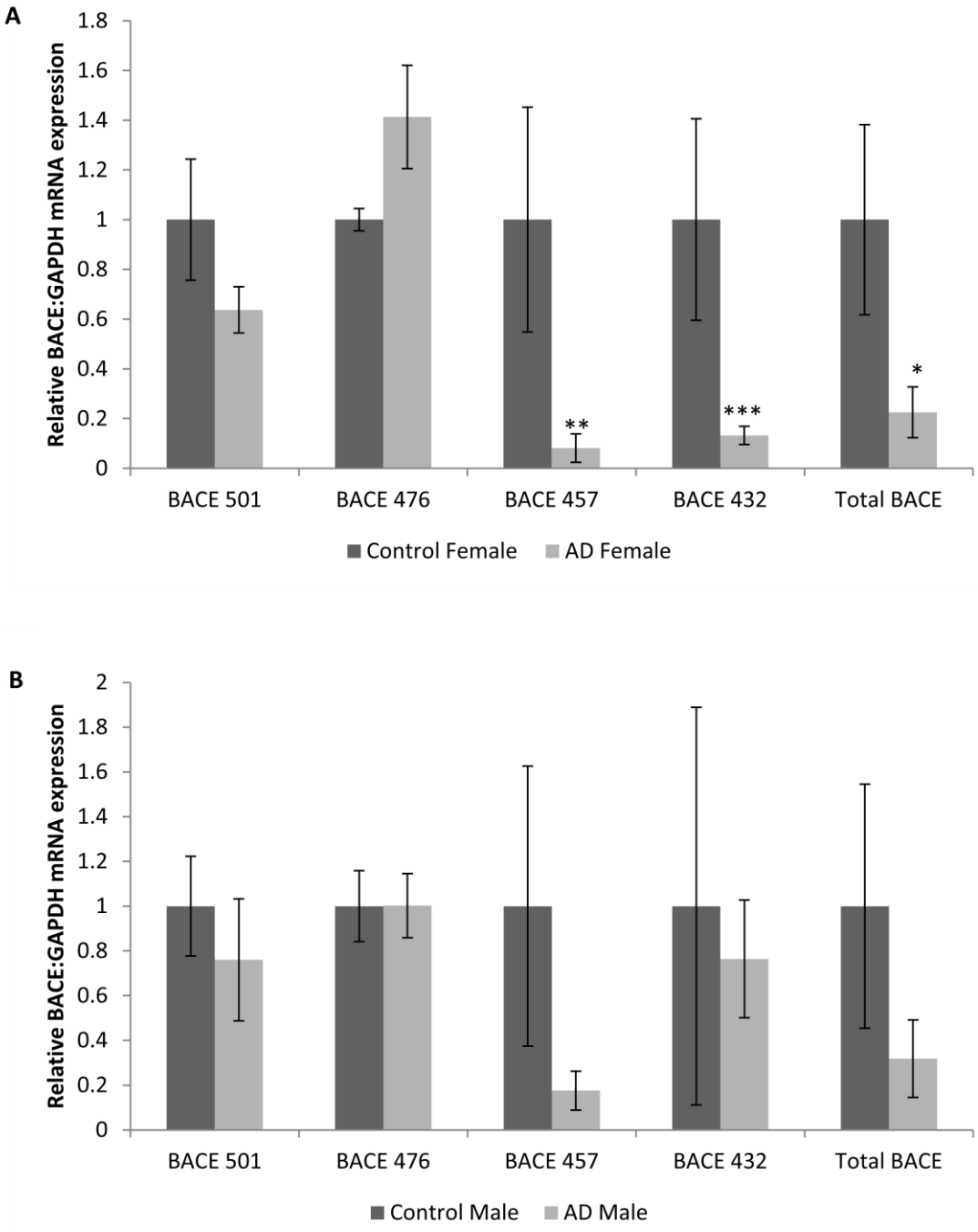

Figure 7.6 BACE1 splice variant mRNA expression in human brain frontal cortex tissue stratified for gender. Relative levels of BACE1 splice variants in brain tissue from **A.** Female control brains (n = 3) and female AD brains (n = 8) and **B.** Male control brains (n = 5) and male AD brains (n = 7). Data are expressed relative to GAPDH mRNA levels measured in the same samples. Primers are given in table 7.1. All values are shown as mean ± SEM * $p < 0.05$, ** $p < 0.01$, *** $p < 0.001$ significantly different from controls by Students t-test.

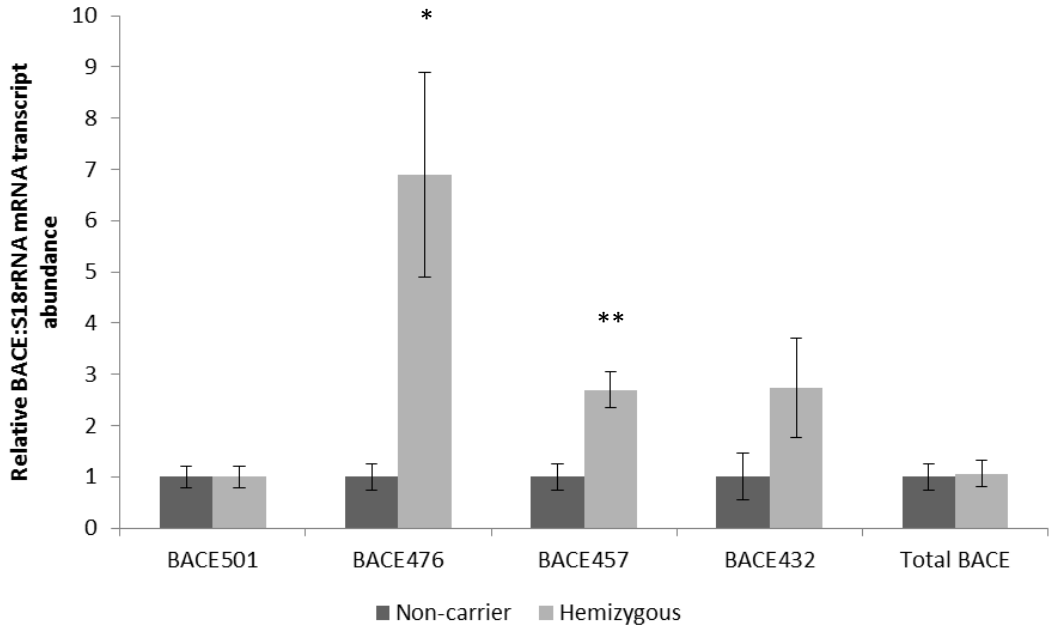

Figure 7.7 BACE1 splice variant mRNA expression in mouse brain frontal cortex tissue. Relative levels of BACE1 splice variants in brain tissue from APP/PS1 control mouse brains (n = 5) and Tg mouse brains (n = 11). Data are expressed relative to 18S rRNA mRNA levels measured in the same samples. Primers are given in Table 7.1. All values are shown as mean ± SEM * $p < 0.05$, ** $p < 0.01$ significantly different from controls by Students t-test.

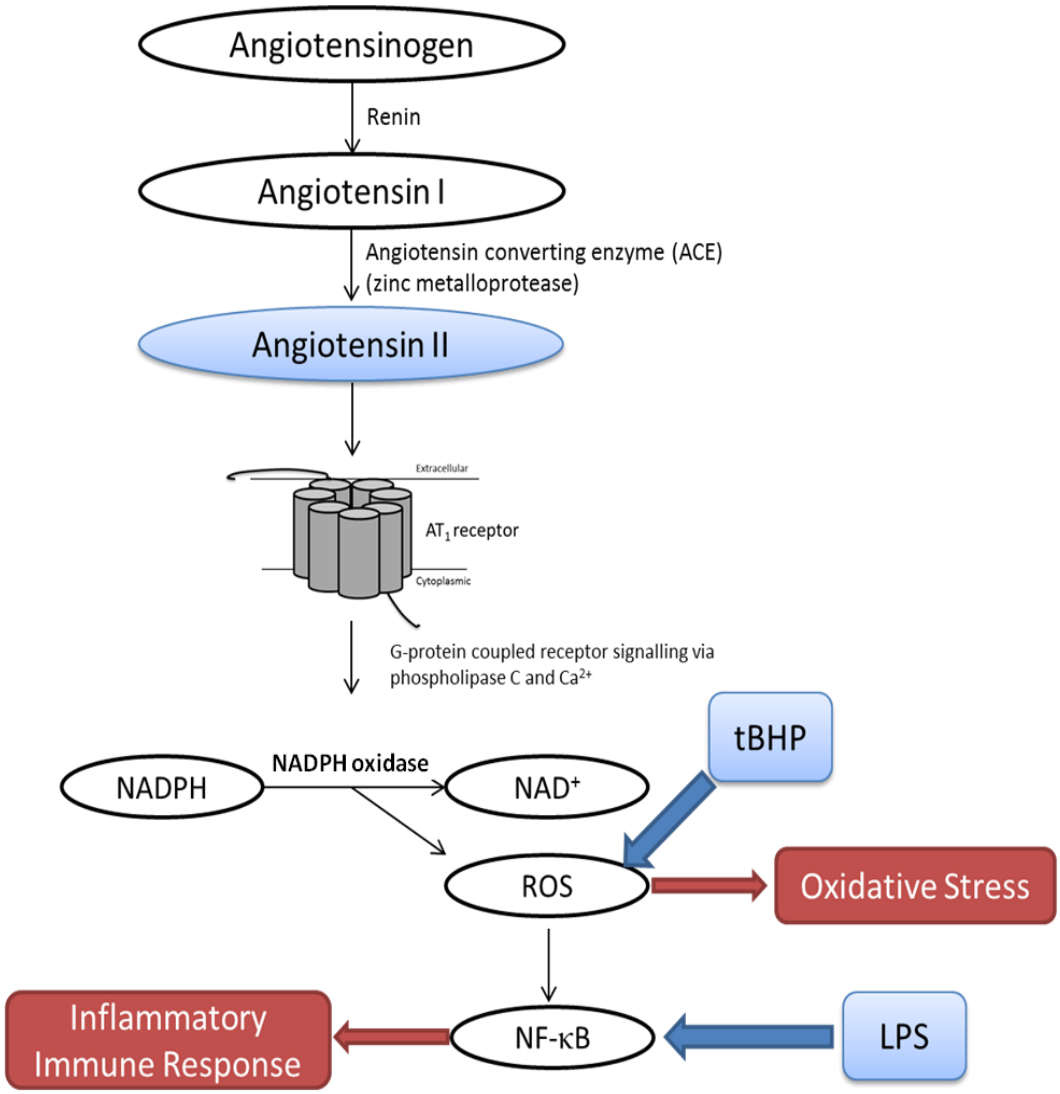

Figure 7.8 Schematic of the study design for studying the Renin-Angiotensin System (RAS) in SH-SY5Y cells. The RAS in the brain. Treatments are shown in blue. Cells were treated with Angiotensin II at a concentration of 0.1 µM for 24 hours prior to RNA extraction. Ang II acts through the G-protein coupled receptor; angiotensin type (AT) receptor 1, that is able to signal through phospholipase C and Ca^{2+}. (de Gasparo et al., 2000). Downstream of the AT_1 receptor is activation of NADPH oxidase; converting NADPH to NAD^+. The by-products of such a reaction is reactive oxygen species (ROS) and ultimately oxidative stress. tBHP (0.025 mM; 40 minutes) was used to generate ROS and initiate oxidative stress. ROS can also induce a redox-dependent signal transduction pathway that leads to NF-κB activation and stimulation of the inflammatory immune response. LPS from *E. coli* (100 ng/mL; 24 hours) was used to activate NF-κB activation and stimulate the inflammatory immune response

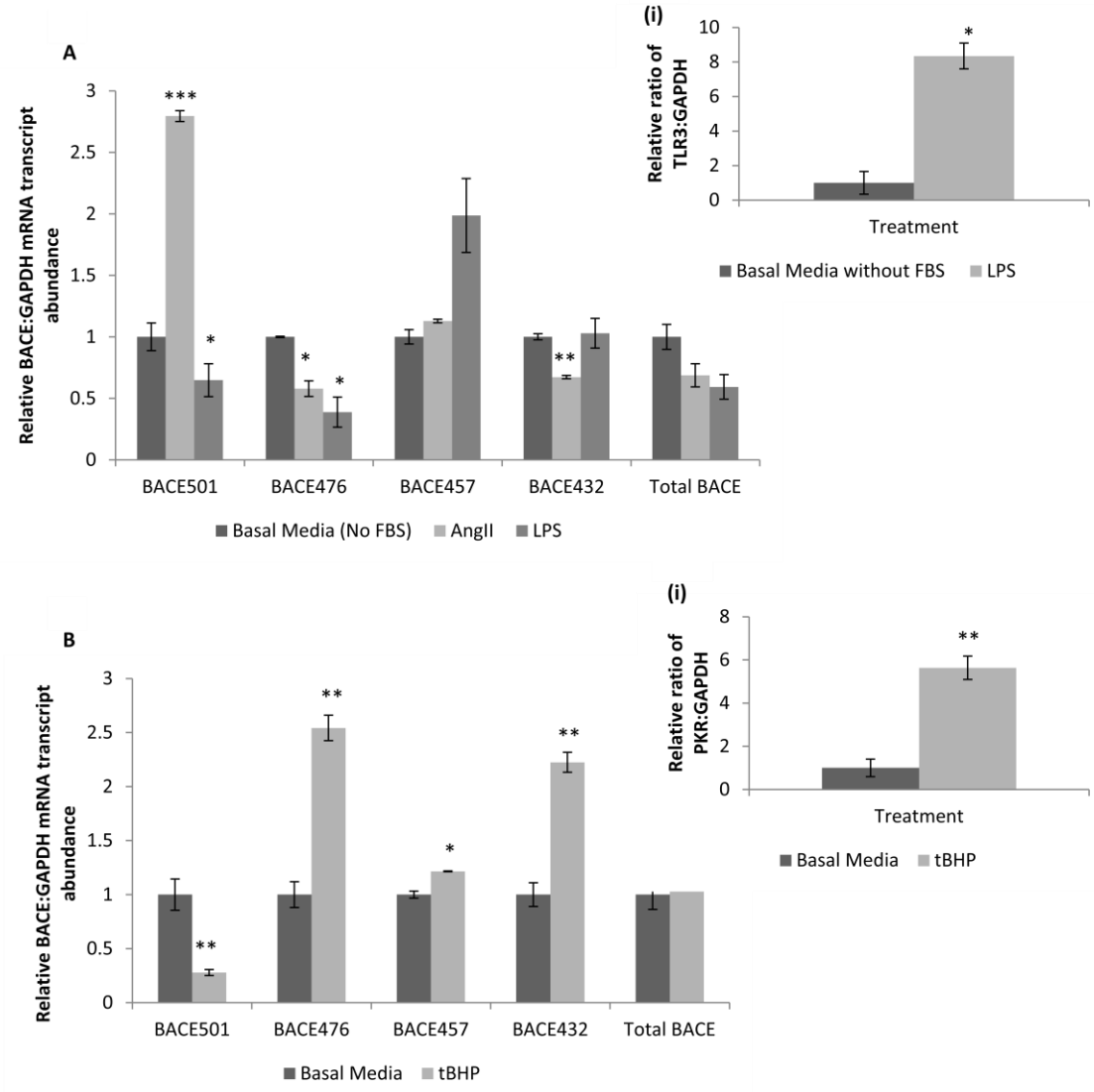

Figure 7.9 Does the RAS have an effect on BACE1 splice variant mRNA expression in SH-SY5Y cells? SH-SY5Y cells were cultured for 24 h with Ang II or LPS (shown in **A.)** or SH-SY5Y cells were cultured for 40 min with tBHP before culturing for a further 24 h in basal media (shown in **B.**). n = 3 for all treatments. RNA was extracted and levels of BACE1 splice variants were measured by RT-qPCR. Primers are given in table 7.1. Levels of **B.(i)** PKR and **A.(i)** TLR3 were measured by RT-PCR. Data are expressed relative to GAPDH mRNA levels measured in the same samples. Primers are given in table 6.3. All values are shown as mean ± SEM ** $p < 0.01$, * $p < 0.05$ significantly different from controls by Students *t*-test.

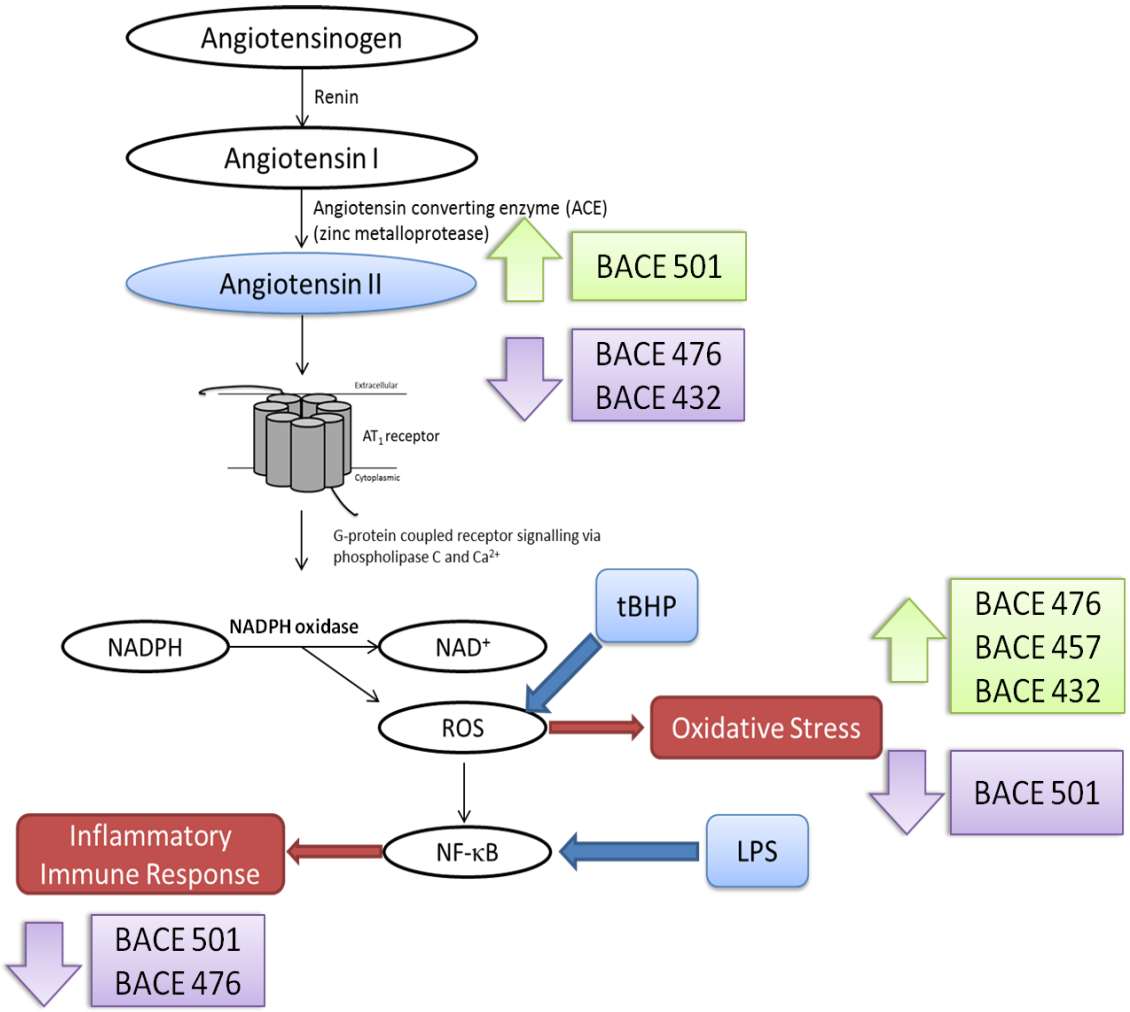

Figure 7.10 Schematic summarising the observations made based on experiments probing the effect of the Renin-Angiotensin System (RAS) in SH-SY5Y cells. Treatments are shown in blue. Cells were treated with Angiotensin II at a concentration of 0.1 µM for 24 hours prior to RNA extraction. tBHP (0.025 mM; 40 minutes) was used to generate ROS and initiate oxidative stress. LPS from *E. coli* (100 ng/mL; 24 hours) was used to activate NF-κB activation and stimulate the inflammatory immune response. Ang II caused a significant increase in BACE501 mRNA expression and significant decreases in BACE476 and BACE432 isoforms. tBHP was used to generate ROS and initiate oxidative stress this caused significant increases in BACE476, BACE457 and BACE432 mRNA expression levels and a significant decrease in BACE501 mRNA expression. LPS was used to activate NF-κB activation and stimulate the inflammatory immune response, this caused significant decreases in BACE501 and BACE476 mRNA expression levels.

Chapter 8: Summary and Final Discussion

Prior to 2012 the knowledge relating to ZnT10 was limited to a single article. Here bioinformatic data found that the human *SLC30A10* gene is localised to human chromosome 1 at the position q41. The gene spanned 15 kb with an arrangement of 4 exons, and was predicted to code for a 52.7 kDa protein. When compared to other family members it was predicted that ZnT10 had the conserved 6 TMDs and a basic region between TMD IV and V. An *in silico* method was used to assess the tissue expression pattern. This was performed by using an expressed sequence tag (EST) data mining strategy whereby the programme BLASTN was used to run the predicted ZnT10 transcript (ORF, 5' and 3' UTRs) against the human EST database, this gave a predicted ZnT10 expression profile. Interestingly, using this method ZnT10 was predicted to be restricted to foetal tissue and more specifically foetal liver and brain (Seve et al., 2004). The overall aim of my study was to confirm and extend the findings of Seve et al., (2004) in order to further characterise ZnT10 and investigate the role of this predicted transporter in neurodegeneration.

In Chapter 3 I confirm the bioinformatic findings of Seve et al., (2004), predicting 6 TMDs. The programmes used (TMPred, TMHMM) both predicted the conserved intracellular N- and C- termini. Further novel bioinformatic investigation demonstrated the presence of a CDF motif and identification of multiple sites for modification (3 *N*-glycosylation sites, 1 *O*-glycosylation site and 15 possible phosphorylation sites). It was important to establish the expression profile of ZnT10 and this has led to the novel discovery that ZnT10 is expressed in both adult mouse and adult human tissue. The expression profile in humans was elucidated by RT-qPCR with relatively high levels of expression in the liver, brain, small intestines and testes with lower levels of expression

in the ovary, colon, cervix, placenta and prostate. Simultaneously, support for the presence of ZnT10 in adult human tissues has been provided by identification and characterisation of mutations in the *SLC30A10* gene in dystonia with brain manganese accumulation (Stamelou et al., 2012, Tuschl et al., 2012) and its dysregulation in response to angiotensin II treatment (Patrushev et al., 2012). In addition to the expression profile, it was important to establish the function of ZnT10 and determine whether it has the ability to transport zinc. An in-direct functional assay was used, and this implied transport of zinc in the efflux direction, as would be expected from a member of the CDF family of transporters.

The homeostasis of zinc is very tightly regulated and therefore it follows that the zinc transporters are under strict regulation. In Chapter 4 I assessed the regulation of ZnT10 at both the mRNA and protein level in Caco-2 and SH-SY5Y cell line models, highlighting a down-regulation in response to increased extracellular zinc concentration. Furthermore, localisation was established which revealed ZnT10 to translocate in response to extracellular zinc treatment demonstrating a pattern of localisation to the Golgi apparatus under basal zinc conditions with movement towards the plasma membrane with the addition of 100 μM extracellular zinc, when assessed using SH-SY5Y cells transiently expressing a ZnT10 construct tagged with the FLAG epitope at the N-terminus. Additionally, identification of a putative zinc responsive element (ZTRE) in the 5'UTR of the ZnT10 promoter led to investigation of the transcriptional regulation of ZnT10, which revealed that the ZTRE region is important for promoter repression in response to increased extracellular zinc.

Given the regulation displayed for zinc and in the context of the evolution of CDF family members transporting various cations, ZnT10 regulation was assessed with

increased extracellular copper, cobalt and nickel. Interestingly, ZnT10 has very recently been shown to transport manganese therefore that the role for ZnT10 is broader than zinc transport (Tuschl et al., 2012). In Chapter 5 I demonstrate that ZnT10 is regulated by both extracellular nickel and cobalt at the mRNA and protein level. ZnT10 mRNA levels are decreased in response to extracellular cobalt. Conversely, extracellular nickel increases ZnT10 mRNA levels. At the protein level an increase in the p3xFLAG-ZnT10 construct is evident with both extracellular cobalt and extracellular nickel treatments. Copper was not shown to elicit an effect on ZnT10 indicating that the Irving-Williams series may be implicated in its regulation (manganese < iron < cobalt < nickel < copper > zinc) (Irving and Williams, 1948). Furthermore, immunofluorescent analysis of p3xFLAG-ZnT10 transiently transfected SH-SY5Y demonstrated a translocation of ZnT10 by extracellular nickel treatment that is similar to that seen with extracellular zinc treatment. Treatment with extracellular cobalt displayed a more diffuse pattern of localisation compared with untreated basal cells, whereas extracellular copper treatment showed a pattern consistent with basal media. Transcriptional regulation by these cations was also investigated however no change in promoter activity was observed for the wild-type promoter in response to extracellular cobalt, nickel or copper indicating alternative mechanisms of regulation must be involved. Intriguingly, mutation of the promoter displayed an increase in promoter activity in response to extracellular cobalt perhaps mediated by a conformational change allowing other response elements (e.g. MRE) in this region to become accessible. These observations are intriguing especially given the recent publication identifying frame-shift mutations in the *SLC30A10* gene in patients with the neurological conditions dystonia and Parkinsonism that lead to hypermanganesemia in brain regions (Quadri et al., 2012). Rescue experiments were performed in a yeast mutant demonstrating the ability of wild-type ZnT10 to restore

growth in a manganese sensitive yeast mutant *Δpmr1* (Tuschl et al., 2012). Analysis of the zinc binding ability of ZnT5 has identified a region within this CDF that is known to be involved in selectivity of the transporter (Ohana et al., 2009). This region is conserved in ZnT10 (Figure 3.1). Mutational analysis of this region in ZnT10 would allow us to ascertain if these residues are involved in selectivity in this CDF member. Additionally, ZnT10 has a serine rich region opposed to the conventional histidine rich region found in most family members (Seve et al., 2004). It is possible that transporter ability may be attributed to this area. Interestingly ZnT6 also contains this serine rich region and it is known to act as a heterodimer with ZnT5 in order to transport zinc (Huang et al., 2002, Suzuki et al., 2005b). This knowledge could be used in order to support ZnT10 studies if ZnT6 also has manganese transporting capabilities. Further analysis of these findings and investigations into the role of manganese plus additional characterisation of the transport ability of ZnT10 would enable more conclusions to be drawn.

Zinc dyshomeostasis has been implicated in the aetiology of AD but as yet its role has not been fully elucidated. ZnTs have been shown to be dysregulated in AD post-mortem brain tissue. For example up-regulation of the ZnT1 protein is evident in the hippocampus in AD brain tissue (Lovell et al., 2005). It is thought that this increase in ZnT1 expression in the disease state causes an increase in zinc ions available in the extracellular space for initiation of Aβ deposition and SP formation (Lyubartseva et al., 2009). Therefore, I assessed ZnT10 levels in human AD and APP/PS1 Tg mouse brain frontal cortex, results of which are reported in Chapter 6. A significant decrease in ZnT10 levels at the mRNA level was observed in both human AD brain tissue and brain tissue from APP/PS1 Tg mice compared with controls. Development and use of specific ZnT10 antibodies would allow further investigation at the protein level into the role of

ZnT10 in disease progression. Furthermore, RAS pathways involved in AD progression were investigated to further characterise the response of ZnT10. This identified an increase in ZnT10 mRNA in response to extracellular Ang II treatment. Conversely, LPS induced inflammatory immune response conferred a decrease in ZnT10 mRNA levels. Oxidative stress initiated by tBHP did not elicit a change in ZnT10 mRNA levels. These data highlights that ZnT10 may be implicated in AD pathology, however further research is required to elucidate its role further.

Finally the role of zinc and other cations in the splicing of the BACE1 enzyme were investigated. In Chapter 7 I demonstrate that extracellular zinc treatment induces an increase in total BACE1, with significant increases contributed by BACE501 and BACE432 splice variants, however a significant decrease in BACE476 was also evident. The cations copper, cobalt and nickel also seem to be involved in these splicing events, with an overall increase in total BACE1 elicited by extracellular copper treatment; however a significant decrease in total BACE1 for both extracellular cobalt and nickel treatments was seen. Interestingly, a different profile of splice variant expression was revealed with each cation. This phenomenon highlights the importance of examining BACE1 at an individual variants level. Levels of BACE1 splice variants were investigated in order to establish a profile in human AD and APP/PS1 Tg mouse model post-mortem frontal cortex tissue. Intriguingly there was an inter-species variation with significant decreases in BACE457 and BACE432 in human AD compared with controls, whereas in the Tg mouse models BACE476 and BACE457 displayed significant increases in expression. BACE1 splice variants were also investigated in response to the RAS. In summary, Ang II produced an increase in BACE501 levels, with decreased levels of BACE476 and BACE432. Initiation of oxidative stress using tBHP indicated an increase in BACE476, BACE457 and

BACE432 with a decrease in BACE501. Induction of the inflammatory immune response using LPS demonstrated decreases in BACE501 and BACE476.

The dysregulation of ZnT10 that I have demonstrated in the AD brain may contribute to disease aetiology given that ZnT10 acts to efflux zinc. It is possible that these effects may be mediated through alteration in splicing events of BACE1 in response to alterations in zinc availability in the brain. Here I show that an increase in zinc gives an increase in the most active isoform; BACE501. Therefore, it follows that any dyshomeostasis of zinc within the brain may have the potential to increase Aβ production thereby exacerbating AD progression. Clearly the interactions of these proteins and cations are complex and, whilst this body of data is important, these processes require further experimentation. The novel observations presented here, of ZnT10 and BACE1 splice variant alterations in AD and SH-SY5Y cell models, may guide research that is hypothesis based. For example, future experiments could include investigation into the effect of over-expression and/ or siRNA knockdown of ZnT10 on BACE1 splice variants. This would establish whether the differing transporter levels have a direct effect on alteration of BACE1 splicing events. However, I feel that future research would benefit from a systems biology perspective, to try and confirm the interactions that are taking place between and within the whole body. This work has generated a lot of data that are difficult to piece together in the larger biological sense. I believe the only way to accelerate this challenging research is to map these findings together and develop a model which uses a computational systems based approach, supported by laboratory based experiments. This would allow further insight into a complex, interacting network that is currently largely unknown by elucidating a general network of zinc metabolism and enable insight into networks and pathways that are regulated by zinc and its transporters in the brain.

To conclude, the work presented in this thesis has made novel contributions to the characterisation of ZnT10 and its role in cellular homeostasis in adult humans. This study has also implicated ZnT10 dysregulation in AD. Zinc is an important factor in the aetiology of AD and the role of ZnT family members needs to be investigated further. In addition, zinc alone seems to play a role in AD progression and work presented here shows that splicing events can be influenced by extracellular cations (zinc, copper, cobalt and nickel). These interactions may play an important role in unravelling the complex processes involved in AD.

Appendix A

Vector map of pCR2.1 TOPO TA

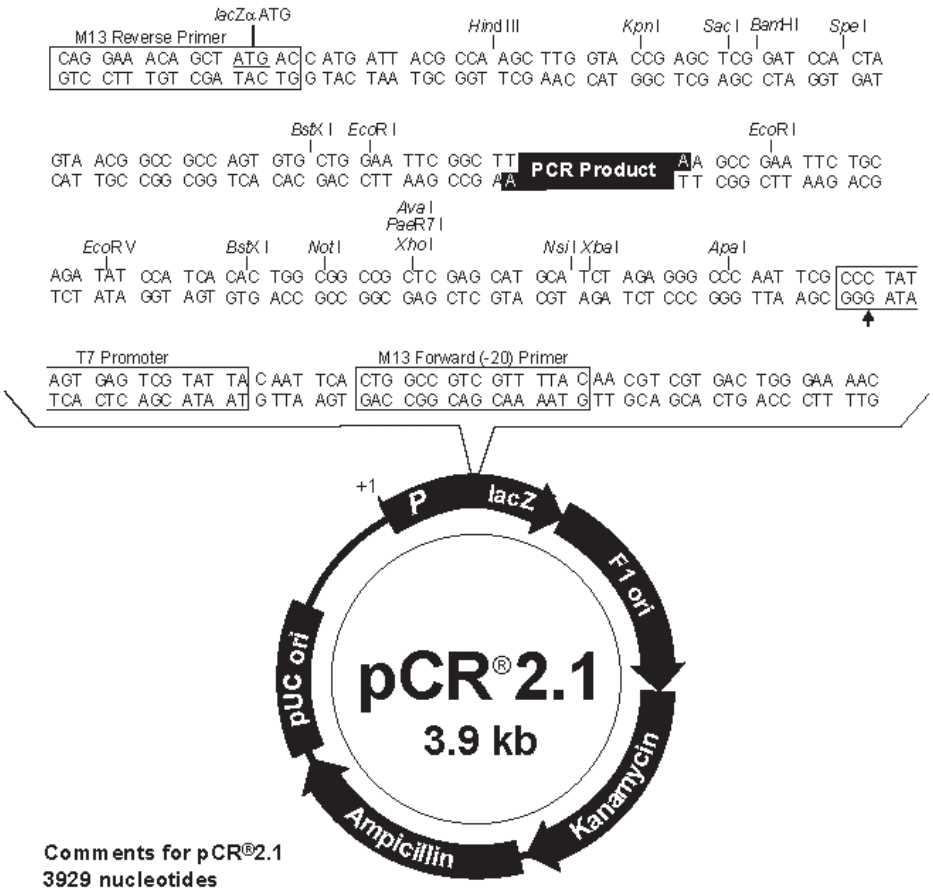

Comments for pCR®2.1
3929 nucleotides

LacZα gene: bases 1-545
M13 Reverse priming site: bases 205-221
T7 promoter: bases 362-381
M13 (-20) Forward priming site: bases 389-404
f1 origin: bases 546-983
Kanamycin resistance ORF: bases 1317-2111
Ampicillin resistance ORF: bases 2129-2989
pUC origin: bases 3134-3807

Invitrogen™
life technologies

Appendix B

Vector map of pBlue TOPO

pBlue-TOPO® Map

Map

The figure below summarizes the features of the pBlue-TOPO® vector. The vector is supplied linearized between base pairs 116 and 117. This is the TOPO® Cloning site. **The complete nucleotide sequence is available for downloading from our Web site (www.invitrogen.com)** or from Technical Service (see page 27.).

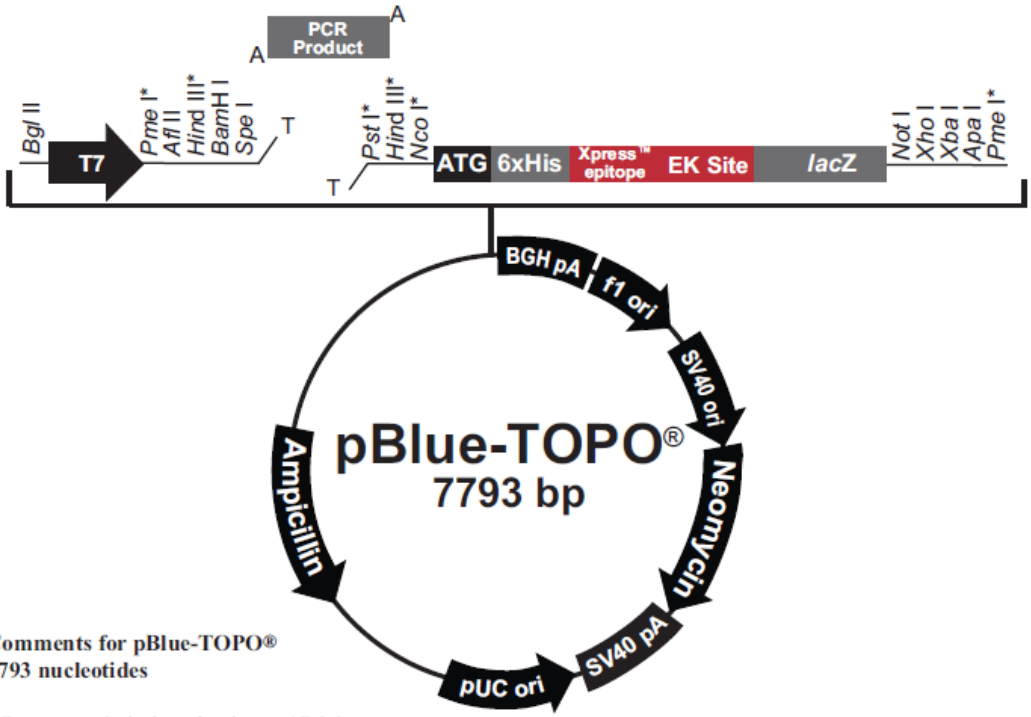

Comments for pBlue-TOPO®
7793 nucleotides

T7 promoter/priming site: bases 17-36
TOPO® Cloning site: bases 116-117
ATG initiation codon: bases 143-145
Polyhistidine region: bases 155-172
LacZ Reverse priming site: bases 173-191
Xpress™ epitope: bases 212-235
Enterokinase recognition site: bases 221-235
LacZ ORF: bases 264-3313
BGH polyadenylation sequence: bases 3386-3613
f1 origin: bases 3659-4087
SV40 promoter and origin: bases 4141-4423
Neomycin resistance gene: bases 4498-5292
SV40 polyadenylation sequence: bases 5466-5596
pUC origin: bases 5979-6652 (complementary strand)
Ampicillin resistance gene: bases 6797-7657 (complementary strand)

* These sites are not unique but may be used to excise the PCR product. The *Pme* I sites may be used to excise the reporter cassette, providing there are no *Pme* I sites in the PCR product.

Appendix C

pEGFP-C1 vector map

pEGFP-C1 Vector Information PT3028-5

GenBank Accession #: U55763 Catalog #6084-1

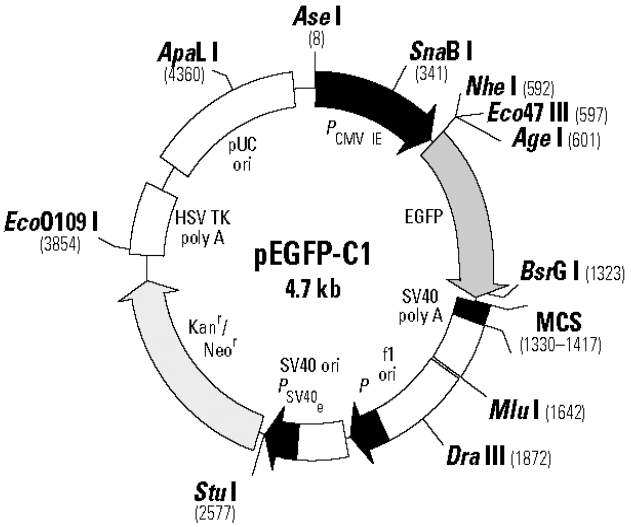

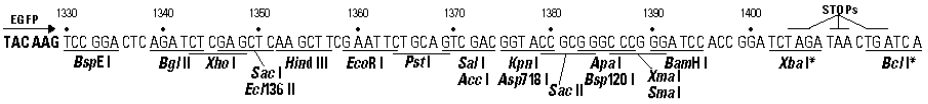

Restriction Map and Multiple Cloning Site (MCS) of pEGFP-C1. All restriction sites shown are unique. The *Xba* I and *Bcl* I sites (*) are methylated in the DNA provided by BD Biosciences Clontech. If you wish to digest the vector with these enzymes, you will need to transform the vector into a *dam*- host and make fresh DNA.

Description

pEGFP-C1 encodes a red-shifted variant of wild-type GFP (1–3) which has been optimized for brighter fluorescence and higher expression in mammalian cells. (Excitation maximum = 488 nm; emission maximum = 507 nm.) pEGFP-C1 encodes the GFPmut1 variant (4) which contains the double-amino-acid substitution of Phe-64 to Leu and Ser-65 to Thr. The coding sequence of the EGFP gene contains more than 190 silent base changes which correspond to human codon-usage preferences (5). Sequences flanking EGFP have been converted to a Kozak consensus translation initiation site (6) to further increase the translation efficiency in eukaryotic cells. The MCS in pEGFP-C1 is between the EGFP coding sequences and the SV40 poly A. Genes cloned into the MCS will be expressed as fusions to the C-terminus of EGFP if they are in the same reading frame as EGFP and there are no intervening stop codons. SV40 polyadenylation signals downstream of the EGFP gene direct proper processing of the 3' end of the EGFP mRNA. The vector backbone also contains an SV40 origin for replication in mammalian cells expressing the SV40 T-antigen. A neomycin resistance cassette (Neo^r), consisting of the SV40 early promoter, the neomycin/kanamycin resistance gene of Tn5, and polyadenylation signals from the Herpes simplex virus thymidine kinase (HSV TK) gene, allows stably transfected eukaryotic cells to be selected using G418. A bacterial promoter upstream of this cassette expresses kanamycin resistance in *E. coli*. The pEGFP-C1 backbone also provides a pUC origin of replication for propagation in *E. coli* and an f1 origin for single-stranded DNA production.

(PR29971; published 03 October 2002)

Appendix D

p3xFLAG-10 vector map

3050 Spruce Street
Saint Louis, Missouri 63103 USA
Telephone 800-325-5832 • (314) 771-5765
Fax (314) 286-7828
email: techserv@sial.com
sigma-aldrich.com

ProductInformation

p3XFLAG-CMV™-10 EXPRESSION VECTOR

Product No. **E 4401**
Store at 0 to –20 °C

Product Description
p3XFLAG-CMV™-10 expression vector is a 6.3 kb derivative of pCMV5[1] used to establish transient or stable intracellular expression of N-terminal 3XFLAG fusion proteins in mammalian cells. The vector encodes three adjacent FLAG® epitopes (Asp-Tyr-Lys-Xaa-Xaa-Asp) upstream of the multiple cloning region. This results in increased detection sensitivity using ANTI-FLAG® M2 antibody.[2] The third FLAG epitope includes the enterokinase recognition sequence, allowing cleavage of the 3XFLAG peptide from the purified fusion protein.

The promoter-regulatory region of the human cytomegalovirus[3] drives transcription of FLAG-fusion constructs. The aminoglycoside phosphotransferase II gene (Neo) confers resistance to aminoglycosides such as G 418,[4] allowing for selection of stable transfectants.

p3XFLAG-CMV-10 expression vector is a shuttle vector for *E. coli* and mammalian cells. Efficiency of replication is optimal when using an SV40 T antigen-expressing host, such as COS cells.

p3XFLAG-CMV-10 expression vector is supplied in 10 mM Tris, 1 mM EDTA, pH 8.0.

References
1. Andersson, S., *et al.*, J. Biol. Chem., **264**, 8222-8229 (1989)
2. Hernan, R., *et al.*, Biotechniques, **20**, 789-793 (2000)
3. Thomsen, D.R., *et al.*, Proc. Natl. Acad. Sci. USA, **81**, 659-663 (1984)
4. Jimenez, A. and Davies, J., Nature, **287**, 869-871 (1980)

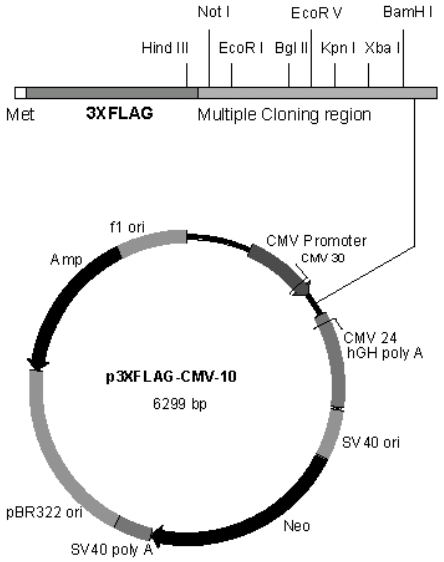

p3XFLAG-CMV-10 Features

Feature	Map Position
CMV promoter	166-916
CMV 30 sequencing primer	825-854
Translational initiation	928-930
3XFLAG sequence	931-996
Multiple cloning region	994–1056
hGH poly A	1061-1680
CMV 24 sequencing primer	1118-1141
SV40 ori	1699-2037
Neo	2073-2864
SV40 poly A	3511-3609
pBR322 ori	4528-4647
Ampicillin resistance	4824-5684
f_1 ori	5847-6299

Nucleotide Sequence of the Multiple Cloning Region of the p3XFLAG-CMV-10 Expression Vector

Sequence range: 925 to 1061

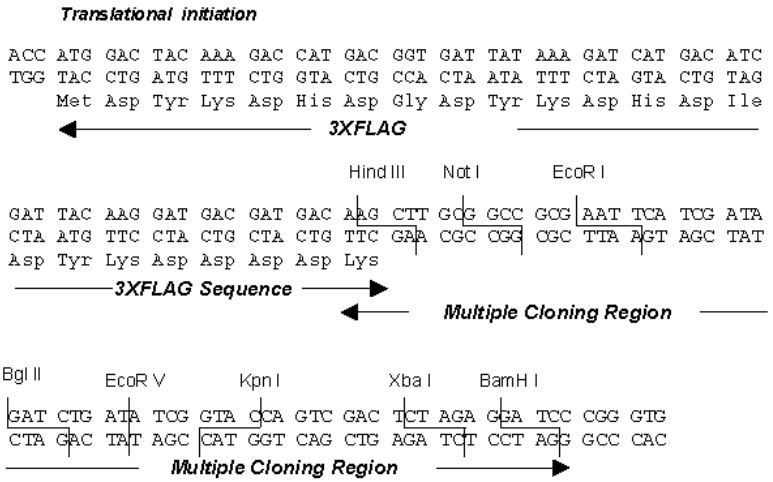

07/03

Appendix E

FLAG-BAP vector information

SIGMA-ALDRICH®

sigma-aldrich.com

3050 Spruce Street, St. Louis, MO 63103 USA
Tel: (800) 521-8956 (314) 771-5765 Fax: (800) 325-5052 (314) 771-5757
email: techservice@sial.com sigma-aldrich.com

Product Information

Amino-terminal FLAG-BAP™ Fusion Protein

Catalog Number **P7582**
Storage Temperature –20 °C

Product Description
Amino-terminal FLAG-BAP™ Fusion Protein is a 467 amino acid N-terminal FLAG® fusion protein of *E. coli* bacterial alkaline phosphatase (BAP) with a calculated molecular mass of 49.3 kDa.

The N-terminal FLAG-BAP Fusion Protein migrates as a 45–55 kDa band by SDS-PAGE depending on electrophoresis conditions.

Amino-terminal FLAG-BAP Fusion Protein has been found to be useful for assurance of the functional integrity of anti-FLAG M1 and M2 monoclonal antibodies in immunological procedures such as Western blotting, ELISA, immunoprecipitation, fluorescence microscopy, light microscopy, and FACS.

The product is supplied in 10 mM Tris, 120 mM NaCl, 0.05 mM $ZnCl_2$ in 50% glycerol, pH 8.0.

Reagents Required but Not Provided

- Tris buffered saline (TBS), 0.05 M Tris, 0.015 M NaCl, pH 7.4
- Non-fat dry milk
- Anti-FLAG M1 monoclonal antibody (Catalog No. F3040) or anti-FLAG M2 monoclonal antibody (Catalog No. F3165)
- Anti-mouse IgG peroxidase conjugate
- Luminol (5-amino-2,3-dihydro-1,4-phthalazine-dione, Catalog No. A4685) or other peroxidase substrate

Precautions and Disclaimer
This product is for R&D use only, not for drug, household, or other uses. Please consult the Material Safety Data Sheet for information regarding hazards and safe handling practices.

Preparation Instructions
Dilute the anti-FLAG M1 or anti-FLAG M2 antibody solution to 10 µg/ml in TBS. Adjust the antibody concentration to maximize detection sensitivity and to minimize background.

Storage/Stability
The product ships on dry ice and storage at –20 °C is recommended.

Procedure
Procedure for Western Blot

1. Transfer the N-terminal FLAG-BAP Fusion Protein to a nitrocellulose membrane.
2. Block the membrane using a solution of 5% non-fat dry milk in TBS at 37 °C for 1 hour.
3. Wash the membrane twice for 1–2 minutes each in TBS at room temperature.
4. Incubate the membrane with anti-FLAG M1 or anti-FLAG M2 antibody as the primary antibody at room temperature for 30 minutes.
5. Wash the membrane three times for 1–2 minutes each in TBS at room temperature.
6. Incubate the membrane with anti-mouse IgG peroxidase conjugate as the secondary antibody at the manufacturer's recommended concentration in TBS. Incubate at room temperature for 30 minutes. Adjust the antibody concentration to maximize detection sensitivity and to minimize background.
7. Wash the membrane three times for 15 minutes each in TBS at room temperature.
8. Treat the membrane with luminol or other peroxidase substrate.

KR,MAM 03/11-1

Appendix F

p3xFLAG-ZnT10 sequences

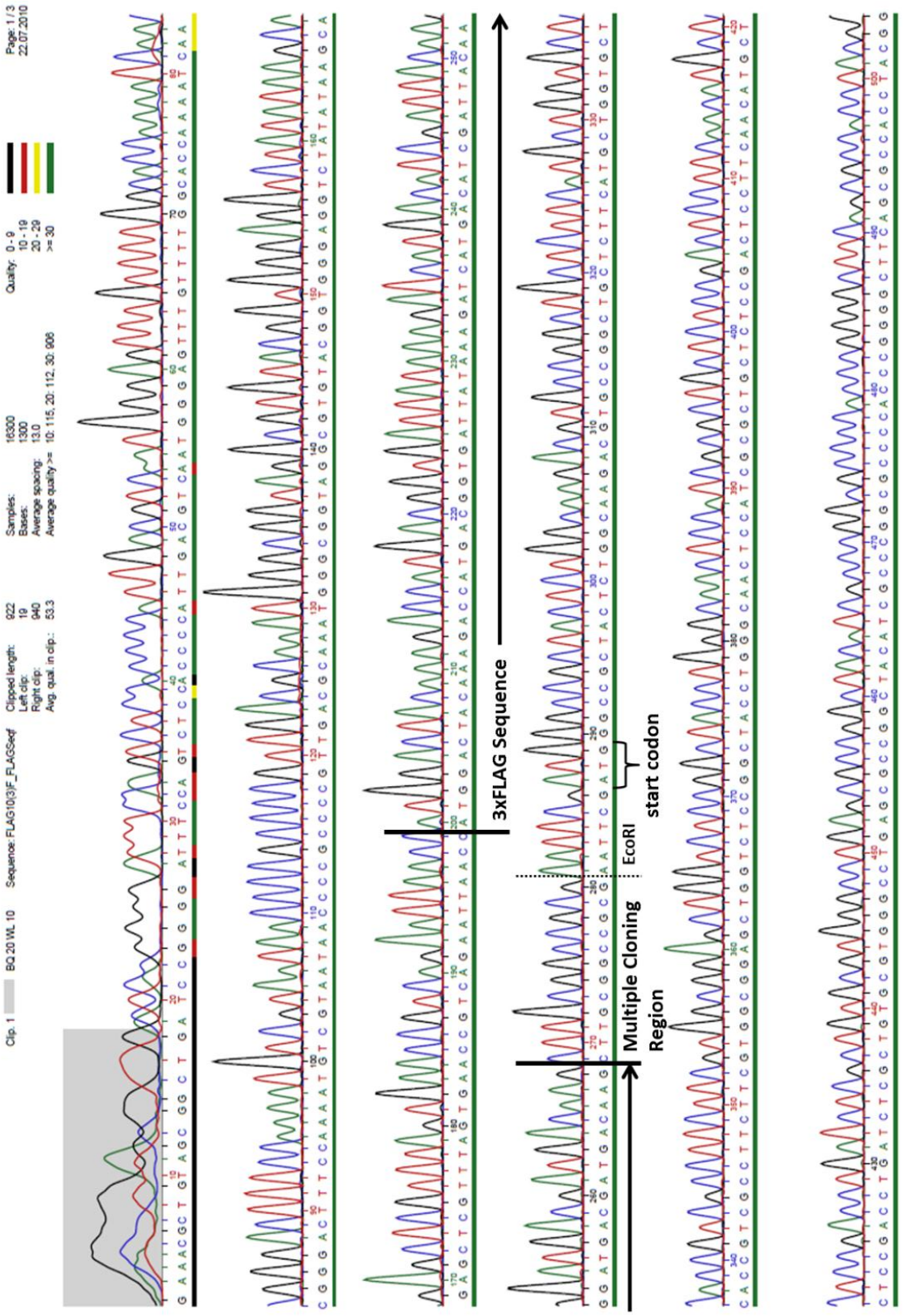

Appendix G

ZTRE sequence

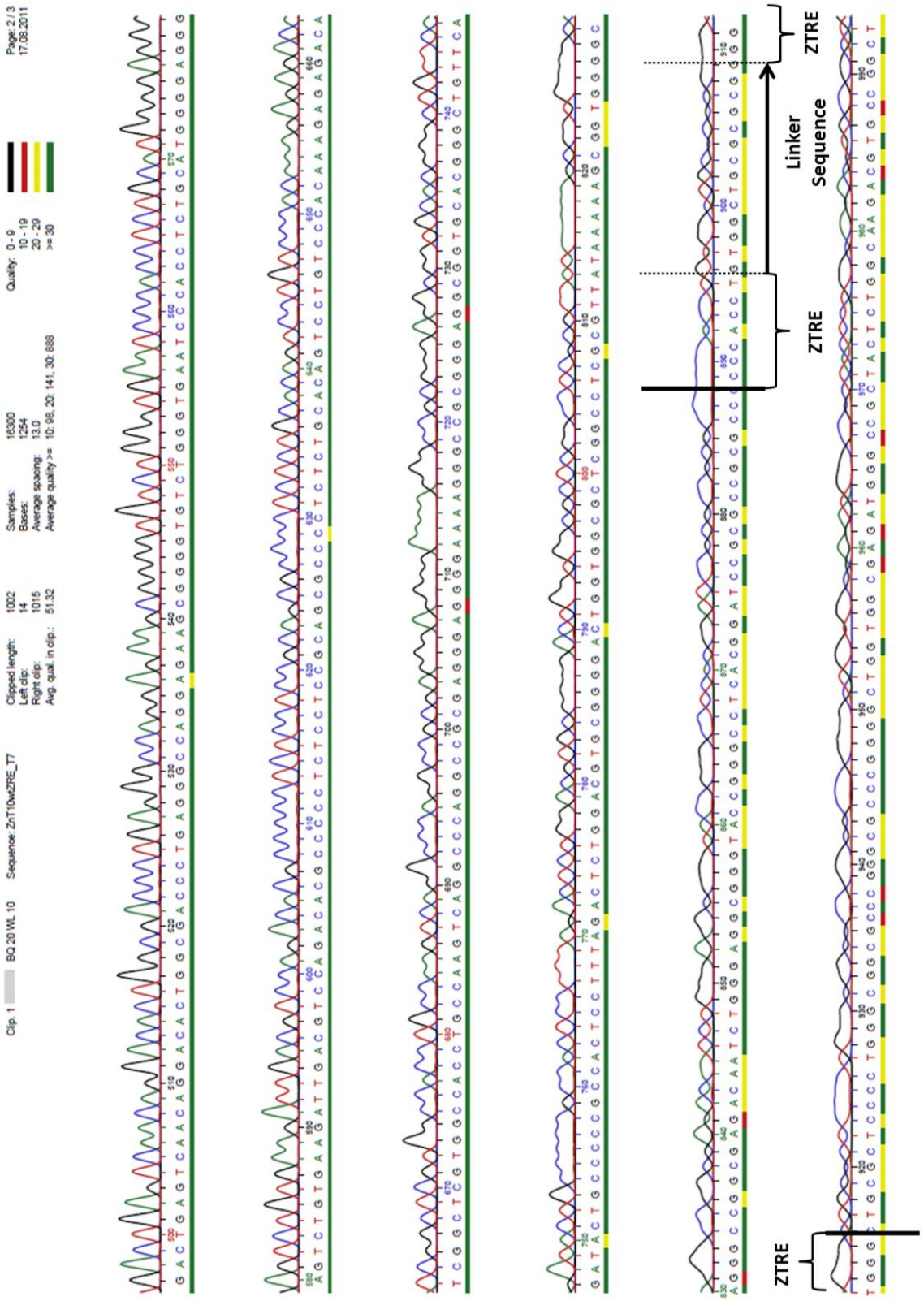

Appendix H

Mutated ZTRE sequence

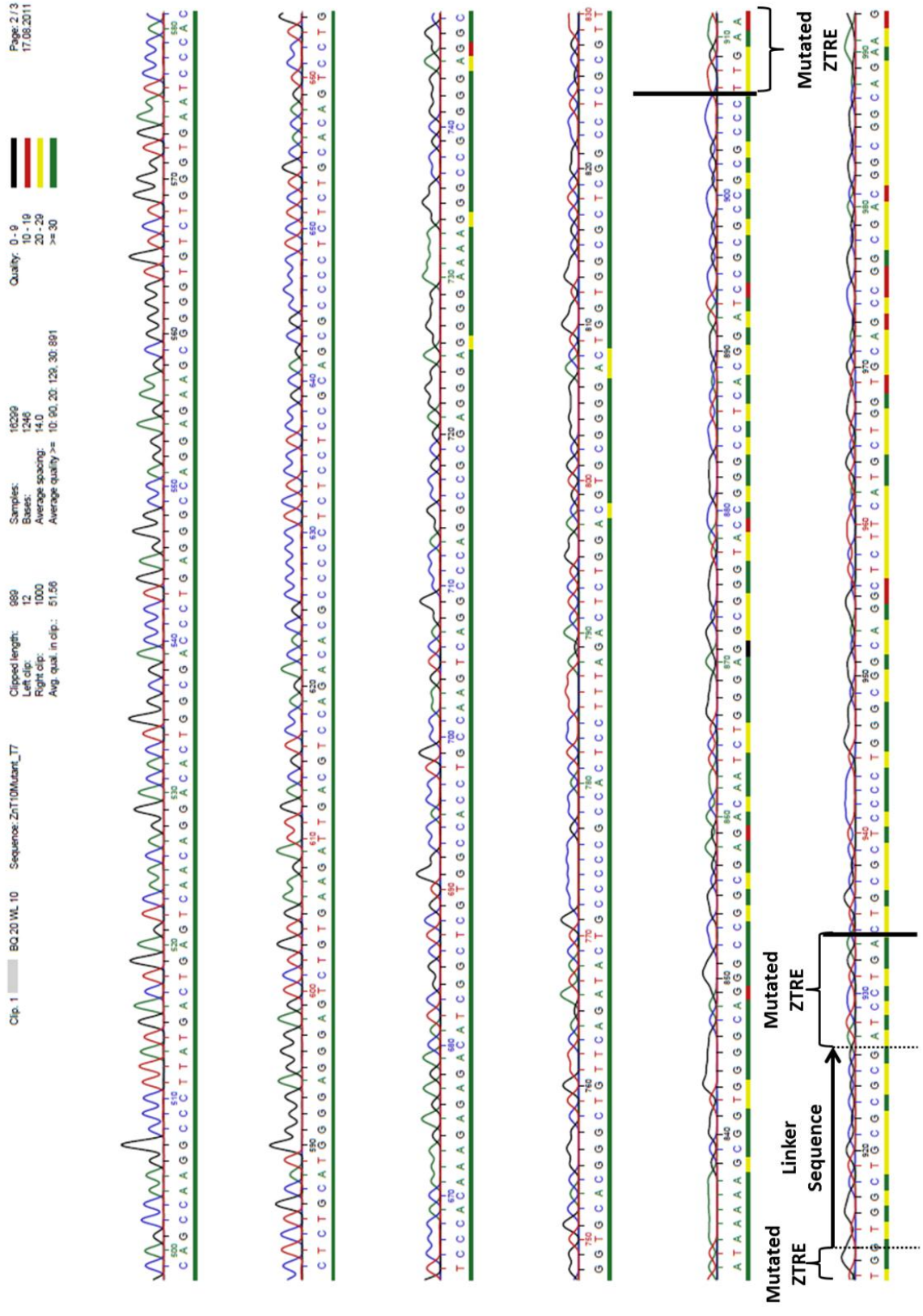

Appendix I

Brain Bank Sample Information

Number	Reference	Diagnosis	Braak	PMD	pH	Age	Gender
1	315	AD	5	6	6.5	76	f
2	06/97	AD	n/a	29	6.1	84	f
3	142/96	AD	5	24	5.9	71	m
5	291/99	AD	4	20	5.97	78	m
8	163/97	AD	n/a	4	6.1	80	f
10	07/03	AD	3	16	5.92	88	f
11	134	AD	5	15	6.58	79	f
12	135/93	AD	4	12	7.3	79	f
14	56/98	AD	5	16	6	68	m
18	998	AD	n/a	15	5.78	74	m
20	279/99	AD	4	17	5.76	91	f
22	08/95	AD	n/a	8	6.16	77	f
23	20/00	AD	5	6	5.78	74	m
24	36/93	AD	6	19	6.14	71	m
25	131/98	AD	2	16	n/a	83	f
26	119/94	AD	n/a	24	6.04	72	f
4	240/91	Con	4	30	6.23	80	m
6	97/97	Con	1	31	6.25	72	m
7	51/93	Con	n/a	21	6.57	57	m
9	27/93	Con	4	7	6.55	84	f
13	293/91	Con	0	17	n/a	65	m
15	95/96	Con	2	12	n/a	80	f
16	878	Con	n/a	32	6.23	81	f
17	307/83	Con	3	10	6.27	93	m
19	309/90	Con	n/a	36	n/a	82	m
21	82/93	Con	0	17	6.9	19	m
27	71/92	Con	4	16	5.57	75	f

Appendix J

BACE1 ClustalW 2.1 multiple alignment

```
BACE501 is variantA
BACE476 is variantB
BACE457 is variantC
BACE432 is variantD
Sequence variations are highlighted in yellow


>BACE1variantB      GTGTGTATGTGCCCTACACCCAGGGCAAGTGGGAAGGGGAGCTGGGCACCGACCTGGTAA 900
BACE1variantA      GTGTGTATGTGCCCTACACCCAGGGCAAGTGGGAAGGGGAGCTGGGCACCGACCTGGTAA 900
BACE1variantD      GTGTGTATGTGCCCTACACCCAGGGCAAGTGGGAAGGGGAGCTGGGCACCGACCTG---- 896
BACE1variantC      GTGTGTATGTGCCCTACACCCAGGGCAAGTGGGAAGGGGAGCTGGGCACCGACCTG---- 896
                   ************************************************************

>BACE1variantB      GCATCCCCCATGGCCCCAACGTCACTGTGCGTGCCAACATTGCTGCCATCACTGAATCAG 960
BACE1variantA      GCATCCCCCATGGCCCCAACGTCACTGTGCGTGCCAACATTGCTGCCATCACTGAATCAG 960
BACE1variantD      ------------------------------------------------------------
BACE1variantC      --------------CCTGACGACTCCCTGGAGCCTTTCTTTGACTCTCTGGTAAAGCAGA 942

>BACE1variantB      ACAAGTTCTTCATCAACGGCTCCAACTGGGAAGGCATCCTGGGGCTGGCCTATGCTGAGA 1020
BACE1variantA      ACAAGTTCTTCATCAACGGCTCCAACTGGGAAGGCATCCTGGGGCTGGCCTATGCTGAGA 1020
BACE1variantD      ------------------------------------------------------------
BACE1variantC      CCCACGTTCCCAACCTCTTCTCCCTGCAG------------------------------ 971

>BACE1variantB      TTGCCAG--------------------------------------------------- 1027
BACE1variantA      TTGCCAGGCCTGACGACTCCCTGGAGCCTTTCTTTGACTCTCTGGTAAAGCAGACCCACG 1080
BACE1variantD      ------------------------------------------------------------
BACE1variantC      ------------------------------------------------------------

>BACE1variantB      ----------------------GCTTTGTGGTGCTGGCTTCCCCCTCAACCAGTCTGAAG 1065
BACE1variantA      TTCCCAACCTCTTCTCCCTGCAGCTTTGTGGTGCTGGCTTCCCCCTCAACCAGTCTGAAG 1140
BACE1variantD      ----------------------CTTTGTGGTGCTGGCTTCCCCCTCAACCAGTCTGAAG 933
BACE1variantC      ----------------------CTTTGTGGTGCTGGCTTCCCCCTCAACCAGTCTGAAG 1008
                                          ************************************

>BACE1variantB      TGCTGGCCTCTGTCGGAGGGAGCATGATCATTGGAGGTATCGACCACTCGCTGTACACAG 1125
BACE1variantA      TGCTGGCCTCTGTCGGAGGGAGCATGATCATTGGAGGTATCGACCACTCGCTGTACACAG 1200
BACE1variantD      TGCTGGCCTCTGTCGGAGGGAGCATGATCATTGGAGGTATCGACCACTCGCTGTACACAG 993
BACE1variantC      TGCTGGCCTCTGTCGGAGGGAGCATGATCATTGGAGGTATCGACCACTCGCTGTACACAG 1068
                   ************************************************************
```

References

ACKLAND, M. L., ZOU, L., FREESTONE, D., VAN DE WAASENBURG, S. & MICHALCZYK, A. A. 2007. Diesel exhaust particulate matter induces multinucleate cells and zinc transporter-dependent apoptosis in human airway cells. *Immunology and cell biology,* 85**,** 617-22.

ADLARD, P. A., PARNCUTT, J. M., FINKELSTEIN, D. I. & BUSH, A. I. 2010. Cognitive loss in zinc transporter-3 knock-out mice: a phenocopy for the synaptic and memory deficits of Alzheimer's disease? *The Journal of neuroscience : the official journal of the Society for Neuroscience,* 30**,** 1631-6.

AGHOLME, L., LINDSTROM, T., KAGEDAL, K., MARCUSSON, J. & HALLBECK, M. 2010. An in vitro model for neuroscience: differentiation of SH-SY5Y cells into cells with morphological and biochemical characteristics of mature neurons. *Journal of Alzheimer's disease : JAD,* 20**,** 1069-82.

AGUILAR-ALONSO, P., MARTINEZ-FONG, D., PAZOS-SALAZAR, N. G., BRAMBILA, E., GONZALEZ-BARRIOS, J. A., MEJORADA, A., FLORES, G., MILLAN-PEREZPENA, L., RUBIO, H. & LEON-CHAVEZ, B. A. 2008. The increase in zinc levels and upregulation of zinc transporters are mediated by nitric oxide in the cerebral cortex after transient ischemia in the rat. *Brain research,* 1200**,** 89-98.

AHMED, R. R., HOLLER, C. J., WEBB, R. L., LI, F., BECKETT, T. L. & MURPHY, M. P. 2010. BACE1 and BACE2 enzymatic activities in Alzheimer's disease. *Journal of neurochemistry,* 112**,** 1045-53.

AKIYAMA, H. 1994. Inflammatory response in Alzheimer's disease. *The Tohoku journal of experimental medicine,* 174**,** 295-303.

ALONSO, A. D., ZAIDI, T., NOVAK, M., BARRA, H. S., GRUNDKE-IQBAL, I. & IQBAL, K. 2001. Interaction of tau isoforms with Alzheimer's disease abnormally hyperphosphorylated tau and in vitro phosphorylation into the disease-like protein. *The Journal of biological chemistry,* 276**,** 37967-73.

ANDREINI, C., BANCI, L., BERTINI, I. & ROSATO, A. 2006. Counting the zinc-proteins encoded in the human genome. *Journal of proteome research,* 5**,** 196-201.

ANDREINI, C., BANCI, L., BERTINI, I. & ROSATO, A. 2008a. Occurrence of copper proteins through the three domains of life: a bioinformatic approach. *Journal of proteome research,* 7**,** 209-16.

ANDREINI, C., BERTINI, I., CAVALLARO, G., HOLLIDAY, G. L. & THORNTON, J. M. 2008b. Metal ions in biological catalysis: from enzyme databases to

general principles. *Journal of biological inorganic chemistry : JBIC : a publication of the Society of Biological Inorganic Chemistry,* 13**,** 1205-18.

ANDREINI, C., BERTINI, I. & ROSATO, A. 2009. Metalloproteomes: a bioinformatic approach. *Accounts of chemical research,* 42**,** 1471-9.

ANDREWS, G. K. 2000. Regulation of metallothionein gene expression by oxidative stress and metal ions. *Biochemical pharmacology,* 59**,** 95-104.

ANDREWS, G. K. 2008. Regulation and function of Zip4, the acrodermatitis enteropathica gene. *Biochemical Society transactions,* 36**,** 1242-6.

ANGELETTI, B., WALDRON, K. J., FREEMAN, K. B., BAWAGAN, H., HUSSAIN, I., MILLER, C. C., LAU, K. F., TENNANT, M. E., DENNISON, C., ROBINSON, N. J. & DINGWALL, C. 2005. BACE1 cytoplasmic domain interacts with the copper chaperone for superoxide dismutase-1 and binds copper. *The Journal of biological chemistry,* 280**,** 17930-7.

ANTALA, S. & DEMPSKI, R. E. 2012. The human ZIP4 transporter has two distinct binding affinities and mediates transport of multiple transition metals. *Biochemistry,* 51**,** 963-73.

ANTON, A., GROSSE, C., REISSMANN, J., PRIBYL, T. & NIES, D. H. 1999. CzcD is a heavy metal ion transporter involved in regulation of heavy metal resistance in Ralstonia sp. strain CH34. *Journal of bacteriology,* 181**,** 6876-81.

ASSUNCAO, A. G., HERRERO, E., LIN, Y. F., HUETTEL, B., TALUKDAR, S., SMACZNIAK, C., IMMINK, R. G., VAN ELDIK, M., FIERS, M., SCHAT, H. & AARTS, M. G. 2010. Arabidopsis thaliana transcription factors bZIP19 and bZIP23 regulate the adaptation to zinc deficiency. *Proceedings of the National Academy of Sciences of the United States of America,* 107**,** 10296-301.

BANNISTER, J. V., BANNISTER, W. H. & ROTILIO, G. 1987. Aspects of the structure, function, and applications of superoxide dismutase. *CRC critical reviews in biochemistry,* 22**,** 111-80.

BAO, B., PRASAD, A. S., BECK, F. W. & SARKAR, F. H. 2007. Zinc up-regulates NF-kappaB activation via phosphorylation of IkappaB in HUT-78 (Th0) cells. *FEBS letters,* 581**,** 4507-11.

BARAMOVA, E. & FOIDART, J. M. 1995. Matrix metalloproteinase family. *Cell biology international,* 19**,** 239-42.

BARBER, R. D., HARMER, D. W., COLEMAN, R. A. & CLARK, B. J. 2005. GAPDH as a housekeeping gene: analysis of GAPDH mRNA expression in a panel of 72 human tissues. *Physiological genomics,* 21**,** 389-95.

BARCELOUX, D. G. 1999. Cobalt. *Journal of toxicology. Clinical toxicology,* 37**,** 201-6.

BEGUM, N. A., KOBAYASHI, M., MORIWAKI, Y., MATSUMOTO, M., TOYOSHIMA, K. & SEYA, T. 2002. Mycobacterium bovis BCG cell wall and lipopolysaccharide induce a novel gene, BIGM103, encoding a 7-TM protein: identification of a new protein family having Zn-transporter and Zn-metalloprotease signatures. *Genomics,* 80**,** 630-45.

BEIGHTON, P., DE PAEPE, A., STEINMANN, B., TSIPOURAS, P. & WENSTRUP, R. J. 1998. Ehlers-Danlos syndromes: revised nosology, Villefranche, 1997. Ehlers-Danlos National Foundation (USA) and Ehlers-Danlos Support Group (UK). *American journal of medical genetics,* 77**,** 31-7.

BELL, S. G. & VALLEE, B. L. 2009. The metallothionein/thionein system: an oxidoreductive metabolic zinc link. *Chembiochem : a European journal of chemical biology,* 10**,** 55-62.

BELLONI-OLIVI, L., MARSHALL, C., LAAL, B., ANDREWS, G. K. & BRESSLER, J. 2009. Localization of zip1 and zip4 mRNA in the adult rat brain. *Journal of neuroscience research,* 87**,** 3221-30.

BEREZOVSKA, O., LLEO, A., HERL, L. D., FROSCH, M. P., STERN, E. A., BACSKAI, B. J. & HYMAN, B. T. 2005. Familial Alzheimer's disease presenilin 1 mutations cause alterations in the conformation of presenilin and interactions with amyloid precursor protein. *The Journal of neuroscience : the official journal of the Society for Neuroscience,* 25**,** 3009-17.

BERTONI-FREDDARI, C., FATTORETTI, P., CASOLI, T. & DI STEFANO, G. 2006. *Neurobiology of the aging brain,* San Diego, CA, Elsevier.

BERTONI-FREDDARI, C., FATTORETTI, P., CASOLI, T., DI STEFANO, G., GIORGETTI, B. & BALIETTI, M. 2008. Brain aging: The zinc connection. *Exp Gerontol,* 43**,** 389-93.

BERTONI-FREDDARI, C., FATTORETTI, P., CASOLI, T., SPAGNA, C., MEIER-RUGE, W. & ULRICH, J. 1993. Morphological plasticity of synaptic mitochondria during aging. *Brain research,* 628**,** 193-200.

BERTONI-FREDDARI, C., FATTORETTI, P., PAOLONI, R., CASELLI, U., GIORGETTI, B. & SOLAZZI, M. 2003. Inverse correlation between mitochondrial size and metabolic competence: a quantitative cytochemical study of cytochrome oxidase activity. *Die Naturwissenschaften,* 90**,** 68-71.

BESECKER, B., BAO, S., BOHACOVA, B., PAPP, A., SADEE, W. & KNOELL, D. L. 2008. The human zinc transporter SLC39A8 (Zip8) is critical in zinc-

mediated cytoprotection in lung epithelia. *American journal of physiology. Lung cellular and molecular physiology,* 294**,** L1127-36.

BEYER, N., COULSON, D. T., HEGGARTY, S., RAVID, R., HELLEMANS, J., IRVINE, G. B. & JOHNSTON, J. A. 2012. Zinc transporter mRNA levels in Alzheimer's disease postmortem brain. *Journal of Alzheimer's disease : JAD,* 29**,** 863-73.

BEYER, N., COULSON, D. T., HEGGARTY, S., RAVID, R., IRVINE, G. B., HELLEMANS, J. & JOHNSTON, J. A. 2009. ZnT3 mRNA levels are reduced in Alzheimer's disease post-mortem brain. *Molecular neurodegeneration,* 4**,** 53.

BIEDLER, J. L., HELSON, L. & SPENGLER, B. A. 1973. Morphology and growth, tumorigenicity, and cytogenetics of human neuroblastoma cells in continuous culture. *Cancer research,* 33**,** 2643-52.

BIRD, A. J., BLANKMAN, E., STILLMAN, D. J., EIDE, D. J. & WINGE, D. R. 2004. The Zap1 transcriptional activator also acts as a repressor by binding downstream of the TATA box in ZRT2. *The EMBO journal,* 23**,** 1123-32.

BIRD, A. J., GORDON, M., EIDE, D. J. & WINGE, D. R. 2006. Repression of ADH1 and ADH3 during zinc deficiency by Zap1-induced intergenic RNA transcripts. *The EMBO journal,* 25**,** 5726-34.

BLENNOW, K., DE LEON, M. J. & ZETTERBERG, H. 2006. Alzheimer's disease. *Lancet,* 368**,** 387-403.

BLY, M. 2006. Examination of the zinc transporter gene, SLC39A12. *Schizophrenia research,* 81**,** 321-2.

BRAAK, H. & BRAAK, E. 1991. Neuropathological stageing of Alzheimer-related changes. *Acta neuropathologica,* 82**,** 239-59.

BRADFORD, M. M. 1976. A rapid and sensitive method for the quantitation of microgram quantities of protein utilizing the principle of protein-dye binding. *Analytical biochemistry,* 72**,** 248-54.

BROWN, K. D., WUEHLER, S. & PEERSON, J. M. 2001. The importance of zinc in human nutrition and estimation of the global prevalence of zinc deficiency. *Food and Nutrition Bulletin.*

BROWN, M. S., YE, J., RAWSON, R. B. & GOLDSTEIN, J. L. 2000. Regulated intramembrane proteolysis: a control mechanism conserved from bacteria to humans. *Cell,* 100**,** 391-8.

BUSENLEHNER, L. S., PENNELLA, M. A. & GIEDROC, D. P. 2003. The SmtB/ArsR family of metalloregulatory transcriptional repressors: Structural insights into prokaryotic metal resistance. *FEMS microbiology reviews,* 27**,** 131-43.

BUSH, A. I., MULTHAUP, G., MOIR, R. D., WILLIAMSON, T. G., SMALL, D. H., RUMBLE, B., POLLWEIN, P., BEYREUTHER, K. & MASTERS, C. L. 1993. A novel zinc(II) binding site modulates the function of the beta A4 amyloid protein precursor of Alzheimer's disease. *The Journal of biological chemistry,* 268**,** 16109-12.

BUSH, A. I., PETTINGELL, W. H., MULTHAUP, G., D PARADIS, M., VONSATTEL, J. P., GUSELLA, J. F., BEYREUTHER, K., MASTERS, C. L. & TANZI, R. E. 1994. Rapid induction of Alzheimer A beta amyloid formation by zinc. *Science,* 265**,** 1464-7.

BUSTIN, S. A., BENES, V., GARSON, J. A., HELLEMANS, J., HUGGETT, J., KUBISTA, M., MUELLER, R., NOLAN, T., PFAFFL, M. W., SHIPLEY, G. L., VANDESOMPELE, J. & WITTWER, C. T. 2009. The MIQE guidelines: minimum information for publication of quantitative real-time PCR experiments. *Clinical chemistry,* 55**,** 611-22.

CAMERON, K. S., BUCHNER, V. & TCHOUNWOU, P. B. 2011. Exploring the molecular mechanisms of nickel-induced genotoxicity and carcinogenicity: a literature review. *Rev Environ Health,* 26**,** 81-92.

CAO, J., BOBO, J. A., LIUZZI, J. P. & COUSINS, R. J. 2001. Effects of intracellular zinc depletion on metallothionein and ZIP2 transporter expression and apoptosis. *Journal of leukocyte biology,* 70**,** 559-66.

CERNAIANU, G., BRANDMAIER, P., SCHOLZ, G., ACKERMANN, O. P., ALT, R., ROTHE, K., CROSS, M., WITZIGMANN, H. & TROBS, R. B. 2008. All-trans retinoic acid arrests neuroblastoma cells in a dormant state. Subsequent nerve growth factor/brain-derived neurotrophic factor treatment adds modest benefit. *Journal of pediatric surgery,* 43**,** 1284-94.

CHERNY, R. A., ATWOOD, C. S., XILINAS, M. E., GRAY, D. N., JONES, W. D., MCLEAN, C. A., BARNHAM, K. J., VOLITAKIS, I., FRASER, F. W., KIM, Y., HUANG, X., GOLDSTEIN, L. E., MOIR, R. D., LIM, J. T., BEYREUTHER, K., ZHENG, H., TANZI, R. E., MASTERS, C. L. & BUSH, A. I. 2001. Treatment with a copper-zinc chelator markedly and rapidly inhibits beta-amyloid accumulation in Alzheimer's disease transgenic mice. *Neuron,* 30**,** 665-76.

CHIMIENTI, F., DEVERGNAS, S., FAVIER, A. & SEVE, M. 2004. Identification and cloning of a beta-cell-specific zinc transporter, ZnT-8, localized into insulin secretory granules. *Diabetes,* 53**,** 2330-7.

CHOI, D. Y., LEE, J. W., LIN, G., LEE, Y. K., LEE, Y. H., CHOI, I. S., HAN, S. B., JUNG, J. K., KIM, Y. H., KIM, K. H., OH, K. W., HONG, J. T. & LEE, M. S. 2012. Obovatol attenuates LPS-induced memory impairments in mice via inhibition of NF-kappaB signaling pathway. *Neurochemistry international,* 60**,** 68-77.

CHOWANADISAI, W., LONNERDAL, B. & KELLEHER, S. L. 2006. Identification of a mutation in SLC30A2 (ZnT-2) in women with low milk zinc concentration that results in transient neonatal zinc deficiency. *The Journal of biological chemistry,* 281**,** 39699-707.

CHRISTENSEN, M. A., ZHOU, W., QING, H., LEHMAN, A., PHILIPSEN, S. & SONG, W. 2004. Transcriptional regulation of BACE1, the beta-amyloid precursor protein beta-secretase, by Sp1. *Molecular and cellular biology,* 24**,** 865-74.

CHUNG, H. Y., SUNG, B., JUNG, K. J., ZOU, Y. & YU, B. P. 2006. The molecular inflammatory process in aging. *Antioxidants & redox signaling,* 8**,** 572-81.

CICCARONE, V., SPENGLER, B. A., MEYERS, M. B., BIEDLER, J. L. & ROSS, R. A. 1989. Phenotypic diversification in human neuroblastoma cells: expression of distinct neural crest lineages. *Cancer research,* 49**,** 219-25.

CITRON, M., OLTERSDORF, T., HAASS, C., MCCONLOGUE, L., HUNG, A. Y., SEUBERT, P., VIGO-PELFREY, C., LIEBERBURG, I. & SELKOE, D. J. 1992. Mutation of the beta-amyloid precursor protein in familial Alzheimer's disease increases beta-protein production. *Nature,* 360**,** 672-4.

CITRON, M., WESTAWAY, D., XIA, W., CARLSON, G., DIEHL, T., LEVESQUE, G., JOHNSON-WOOD, K., LEE, M., SEUBERT, P., DAVIS, A., KHOLODENKO, D., MOTTER, R., SHERRINGTON, R., PERRY, B., YAO, H., STROME, R., LIEBERBURG, I., ROMMENS, J., KIM, S., SCHENK, D., FRASER, P., ST GEORGE HYSLOP, P. & SELKOE, D. J. 1997. Mutant presenilins of Alzheimer's disease increase production of 42-residue amyloid beta-protein in both transfected cells and transgenic mice. *Nature medicine,* 3**,** 67-72.

CLIFFORD, K. S. & MACDONALD, M. J. 2000. Survey of mRNAs encoding zinc transporters and other metal complexing proteins in pancreatic islets of rats from birth to adulthood: similar patterns in the Sprague-Dawley and Wistar BB strains. *Diabetes research and clinical practice,* 49**,** 77-85.

COLE, T. B., WENZEL, H. J., KAFER, K. E., SCHWARTZKROIN, P. A. & PALMITER, R. D. 1999. Elimination of zinc from synaptic vesicles in the intact mouse brain by disruption of the ZnT3 gene. *Proceedings of the National Academy of Sciences of the United States of America,* 96**,** 1716-21.

CONEYWORTH, L. J., JACKSON, K. A., TYSON, J., BOSOMWORTH, H. J., VAN DER HAGEN, E., HANN, G. M., OGO, O. A., SWANN, D. C., MATHERS, J. C., VALENTINE, R. A. & FORD, D. 2012. Identification of the human ZTRE (zinc transcriptional regulatory element) - a palindromic protein-binding DNA sequence responsible for zinc-induced transcriptional repression. *The Journal of biological chemistry*.

CORDER, E. H., SAUNDERS, A. M., STRITTMATTER, W. J., SCHMECHEL, D. E., GASKELL, P. C., SMALL, G. W., ROSES, A. D., HAINES, J. L. & PERICAK-VANCE, M. A. 1993. Gene dose of apolipoprotein E type 4 allele and the risk of Alzheimer's disease in late onset families. *Science,* 261**,** 921-3.

CORNETT, C. R., MARKESBERY, W. R. & EHMANN, W. D. 1998. Imbalances of trace elements related to oxidative damage in Alzheimer's disease brain. *Neurotoxicology,* 19**,** 339-45.

COSTELLO, L. C. & FRANKLIN, R. B. 2006. The clinical relevance of the metabolism of prostate cancer; zinc and tumor suppression: connecting the dots. *Molecular cancer,* 5**,** 17.

COTE, S., CARMICHAEL, P. H., VERREAULT, R., LINDSAY, J., LEFEBVRE, J. & LAURIN, D. 2012. Nonsteroidal anti-inflammatory drug use and the risk of cognitive impairment and Alzheimer's disease. *Alzheimer's & dementia : the journal of the Alzheimer's Association,* 8**,** 219-26.

COUSINS, R. J. & MCMAHON, R. J. 2000. Integrative aspects of zinc transporters. *The Journal of nutrition,* 130**,** 1384S-7S.

COYLE, P., PHILCOX, J. C., CAREY, L. C. & ROFE, A. M. 2002. Metallothionein: the multipurpose protein. *Cellular and molecular life sciences : CMLS,* 59**,** 627-47.

CRAGG, R. A., CHRISTIE, G. R., PHILLIPS, S. R., RUSSI, R. M., KURY, S., MATHERS, J. C., TAYLOR, P. M. & FORD, D. 2002. A novel zinc-regulated human zinc transporter, hZTL1, is localized to the enterocyte apical membrane. *J Biol Chem,* 277**,** 22789-97.

CROUCH, P. J., HARDING, S. M., WHITE, A. R., CAMAKARIS, J., BUSH, A. I. & MASTERS, C. L. 2008. Mechanisms of A beta mediated neurodegeneration in Alzheimer's disease. *The international journal of biochemistry & cell biology,* 40**,** 181-98.

CUAJUNGCO, M. P. & LEES, G. J. 1997. Zinc metabolism in the brain: relevance to human neurodegenerative disorders. *Neurobiology of disease,* 4**,** 137-69.

CULOTTA, V. C. & HAMER, D. H. 1989. Fine mapping of a mouse metallothionein gene metal response element. *Molecular and cellular biology,* 9**,** 1376-80.

DAHMS, S. O., KONNIG, I., ROESER, D., GUHRS, K. H., MAYER, M. C., KADEN, D., MULTHAUP, G. & THAN, M. E. 2012. Metal binding dictates conformation and function of the amyloid precursor protein (APP) E2 domain. *Journal of molecular biology,* 416**,** 438-52.

DALTON, T. P., HE, L., WANG, B., MILLER, M. L., JIN, L., STRINGER, K. F., CHANG, X., BAXTER, C. S. & NEBERT, D. W. 2005. Identification of mouse SLC39A8 as the transporter responsible for cadmium-induced toxicity in the testis. *Proceedings of the National Academy of Sciences of the United States of America,* 102**,** 3401-6.

DANIELYAN, L., KLEIN, R., HANSON, L. R., BUADZE, M., SCHWAB, M., GLEITER, C. H. & FREY, W. H. 2010. Protective effects of intranasal losartan in the APP/PS1 transgenic mouse model of Alzheimer disease. *Rejuvenation Res,* 13**,** 195-201.

DE BUNDEL, D., SMOLDERS, I., VANDERHEYDEN, P. & MICHOTTE, Y. 2008. Ang II and Ang IV: unraveling the mechanism of action on synaptic plasticity, memory, and epilepsy. *CNS Neurosci Ther,* 14**,** 315-39.

DE GASPARO, M., CATT, K. J., INAGAMI, T., WRIGHT, J. W. & UNGER, T. 2000. International union of pharmacology. XXIII. The angiotensin II receptors. *Pharmacol Rev,* 52**,** 415-72.

DE PIETRI TONELLI, D., MIHAILOVICH, M., DI CESARE, A., CODAZZI, F., GROHOVAZ, F. & ZACCHETTI, D. 2004. Translational regulation of BACE-1 expression in neuronal and non-neuronal cells. *Nucleic acids research,* 32**,** 1808-17.

DELHAIZE, E., KATAOKA, T., HEBB, D. M., WHITE, R. G. & RYAN, P. R. 2003. Genes encoding proteins of the cation diffusion facilitator family that confer manganese tolerance. *Plant Cell,* 15**,** 1131-42.

DENING, T. & BARAPATRE, C. 2004. Mental health and the ageing population. *The journal of the British Menopause Society,* 10**,** 49-53, 64.

DER, S. D., YANG, Y. L., WEISSMANN, C. & WILLIAMS, B. R. 1997. A double-stranded RNA-activated protein kinase-dependent pathway mediating stress-induced apoptosis. *Proceedings of the National Academy of Sciences of the United States of America,* 94**,** 3279-83.

DESOUKI, M. M., GERADTS, J., MILON, B., FRANKLIN, R. B. & COSTELLO, L. C. 2007. hZip2 and hZip3 zinc transporters are down regulated in human prostate adenocarcinomatous glands. *Molecular cancer,* 6**,** 37.

DINELEY, K. E., VOTYAKOVA, T. V. & REYNOLDS, I. J. 2003. Zinc inhibition of cellular energy production: implications for mitochondria and neurodegeneration. *Journal of neurochemistry,* 85**,** 563-70.

DINGWALL, C. 2007. A copper-binding site in the cytoplasmic domain of BACE1 identifies a possible link to metal homoeostasis and oxidative stress in Alzheimer's disease. *Biochemical Society transactions,* 35**,** 571-3.

DONANGELO, C. M., ZAPATA, C. L., WOODHOUSE, L. R., SHAMES, D. M., MUKHERJEA, R. & KING, J. C. 2005. Zinc absorption and kinetics during pregnancy and lactation in Brazilian women. *The American journal of clinical nutrition,* 82**,** 118-24.

DONG, J., ROBERTSON, J. D., MARKESBERY, W. R. & LOVELL, M. A. 2008. Serum zinc in the progression of Alzheimer's disease. *J Alzheimers Dis,* 15**,** 443-50.

DUFNER-BEATTIE, J., KUO, Y. M., GITSCHIER, J. & ANDREWS, G. K. 2004. The adaptive response to dietary zinc in mice involves the differential cellular localization and zinc regulation of the zinc transporters ZIP4 and ZIP5. *The Journal of biological chemistry,* 279**,** 49082-90.

DUFNER-BEATTIE, J., LANGMADE, S. J., WANG, F., EIDE, D. & ANDREWS, G. K. 2003a. Structure, function, and regulation of a subfamily of mouse zinc transporter genes. *The Journal of biological chemistry,* 278**,** 50142-50.

DUFNER-BEATTIE, J., WANG, F., KUO, Y. M., GITSCHIER, J., EIDE, D. & ANDREWS, G. K. 2003b. The acrodermatitis enteropathica gene ZIP4 encodes a tissue-specific, zinc-regulated zinc transporter in mice. *The Journal of biological chemistry,* 278**,** 33474-81.

EIDE, D. J. 2004. The SLC39 family of metal ion transporters. *Pflugers Archiv : European journal of physiology,* 447**,** 796-800.

EIDE, D. J. 2006. Zinc transporters and the cellular trafficking of zinc. *Biochimica et biophysica acta,* 1763**,** 711-22.

EL-TAWIL, A. M. 2003. Zinc deficiency in men with Crohn's disease may contribute to poor sperm function and male infertility. *Andrologia,* 35**,** 337-41.

ELLIS, C. D., MACDIARMID, C. W. & EIDE, D. J. 2005. Heteromeric protein complexes mediate zinc transport into the secretory pathway of eukaryotic cells. *The Journal of biological chemistry,* 280**,** 28811-8.

FAIRWEATHER-TAIT, S. J., HARVEY, L. J. & FORD, D. 2008. Does ageing affect zinc homeostasis and dietary requirements? *Exp Gerontol,* 43**,** 382-8.

FALLER, P. 2009. Copper and zinc binding to amyloid-beta: coordination, dynamics, aggregation, reactivity and metal-ion transfer. *Chembiochem : a European journal of chemical biology,* 10**,** 2837-45.

FERRER, I., BARRACHINA, M. & PUIG, B. 2002. Glycogen synthase kinase-3 is associated with neuronal and glial hyperphosphorylated tau deposits in Alzheimer's disease, Pick's disease, progressive supranuclear palsy and corticobasal degeneration. *Acta neuropathologica,* 104**,** 583-91.

FINAMORE, A., MASSIMI, M., CONTI DEVIRGILIIS, L. & MENGHERI, E. 2008. Zinc deficiency induces membrane barrier damage and increases neutrophil transmigration in Caco-2 cells. *The Journal of nutrition,* 138**,** 1664-70.

FRANKLIN, R. B. & COSTELLO, L. C. 2007. Zinc as an anti-tumor agent in prostate cancer and in other cancers. *Archives of biochemistry and biophysics,* 463**,** 211-7.

FRANKLIN, R. B., FENG, P., MILON, B., DESOUKI, M. M., SINGH, K. K., KAJDACSY-BALLA, A., BAGASRA, O. & COSTELLO, L. C. 2005. hZIP1 zinc uptake transporter down regulation and zinc depletion in prostate cancer. *Molecular cancer,* 4**,** 32.

FRAZZINI, V., ROCKABRAND, E., MOCCHEGIANI, E. & SENSI, S. L. 2006. Oxidative stress and brain aging: is zinc the link? *Biogerontology,* 7**,** 307-14.

FREDERICKSON, C. J. 1989. Neurobiology of zinc and zinc-containing neurons. *International Review Neurobiology* 31**,** 145-238.

FREDERICKSON, C. J. & BUSH, A. I. 2001. Synaptically released zinc: physiological functions and pathological effects. *Biometals,* 14**,** 353-66.

FREDERICKSON, C. J., GIBLIN, L. J., KREZEL, A., MCADOO, D. J., MUELLER, R. N., ZENG, Y., BALAJI, R. V., MASALHA, R., THOMPSON, R. B., FIERKE, C. A., SARVEY, J. M., DE VALDENEBRO, M., PROUGH, D. S. & ZORNOW, M. H. 2006. Concentrations of extracellular free zinc (pZn)e in the central nervous system during simple anesthetization, ischemia and reperfusion. *Experimental neurology,* 198**,** 285-93.

FREDERICKSON, C. J., KLITENICK, M. A., MANTON, W. I. & KIRKPATRICK, J. B. 1983. Cytoarchitectonic distribution of zinc in the hippocampus of man and the rat. *Brain research,* 273**,** 335-9.

FREDERICKSON, C. J., KOH, J. Y. & BUSH, A. I. 2005. The neurobiology of zinc in health and disease. *Nature reviews. Neuroscience,* 6**,** 449-62.

FUKADA, T., CIVIC, N., FURUICHI, T., SHIMODA, S., MISHIMA, K., HIGASHIYAMA, H., IDAIRA, Y., ASADA, Y., KITAMURA, H.,

YAMASAKI, S., HOJYO, S., NAKAYAMA, M., OHARA, O., KOSEKI, H., DOS SANTOS, H. G., BONAFE, L., HA-VINH, R., ZANKL, A., UNGER, S., KRAENZLIN, M. E., BECKMANN, J. S., SAITO, I., RIVOLTA, C., IKEGAWA, S., SUPERTI-FURGA, A. & HIRANO, T. 2008. The zinc transporter SLC39A13/ZIP13 is required for connective tissue development; its involvement in BMP/TGF-beta signaling pathways. *PloS one,* 3**,** e3642.

FUKUMOTO, H., CHEUNG, B. S., HYMAN, B. T. & IRIZARRY, M. C. 2002. Beta-secretase protein and activity are increased in the neocortex in Alzheimer disease. *Arch Neurol,* 59**,** 1381-9.

GAITHER, L. A. & EIDE, D. J. 2000. Functional expression of the human hZIP2 zinc transporter. *The Journal of biological chemistry,* 275**,** 5560-4.

GAITHER, L. A. & EIDE, D. J. 2001a. Eukaryotic zinc transporters and their regulation. *Biometals : an international journal on the role of metal ions in biology, biochemistry, and medicine,* 14**,** 251-70.

GAITHER, L. A. & EIDE, D. J. 2001b. The human ZIP1 transporter mediates zinc uptake in human K562 erythroleukemia cells. *The Journal of biological chemistry,* 276**,** 22258-64.

GALVIN, J. E., POWLISHTA, K. K., WILKINS, K., MCKEEL, D. W., JR., XIONG, C., GRANT, E., STORANDT, M. & MORRIS, J. C. 2005. Predictors of preclinical Alzheimer disease and dementia: a clinicopathologic study. *Archives of neurology,* 62**,** 758-65.

GARD, P. R. 2002. The role of angiotensin II in cognition and behaviour. *Eur J Pharmacol,* 438**,** 1-14.

GARD, P. R. & RUSTED, J. M. 2004. Angiotensin and Alzheimer's disease: therapeutic prospects. *Expert Rev Neurother,* 4**,** 87-96.

GARROW, J. S., JAMES, W. P. T. & RALPH, A. 2000. *Human Nutrition and Dietetics,* London, Churchill Livingstone.

GEMMELL, E., BOSOMWORTH, H., ALLAN, L., HALL, R., KHUNDAKAR, A., OAKLEY, A. E., DERAMECOURT, V., POLVIKOSKI, T. M., O'BRIEN, J. T. & KALARIA, R. N. 2012. Hippocampal neuronal atrophy and cognitive function in delayed poststroke and aging-related dementias. *Stroke; a journal of cerebral circulation,* 43**,** 808-14.

GIBSON, R. S., HESS, S. Y., HOTZ, C. & BROWN, K. H. 2008. Indicators of zinc status at the population level: a review of the evidence. *The British journal of nutrition,* 99 Suppl 3**,** S14-23.

GIMBEL, D. A., NYGAARD, H. B., COFFEY, E. E., GUNTHER, E. C., LAUREN, J., GIMBEL, Z. A. & STRITTMATTER, S. M. 2010. Memory impairment in transgenic Alzheimer mice requires cellular prion protein. *The Journal of neuroscience : the official journal of the Society for Neuroscience,* 30**,** 6367-74.

GIRIJASHANKER, K., HE, L., SOLEIMANI, M., REED, J. M., LI, H., LIU, Z., WANG, B., DALTON, T. P. & NEBERT, D. W. 2008. Slc39a14 gene encodes ZIP14, a metal/bicarbonate symporter: similarities to the ZIP8 transporter. *Molecular pharmacology,* 73**,** 1413-23.

GITAN, R. S., SHABABI, M., KRAMER, M. & EIDE, D. J. 2003. A cytosolic domain of the yeast Zrt1 zinc transporter is required for its post-translational inactivation in response to zinc and cadmium. *The Journal of biological chemistry,* 278**,** 39558-64.

GIUNTA, C., ELCIOGLU, N. H., ALBRECHT, B., EICH, G., CHAMBAZ, C., JANECKE, A. R., YEOWELL, H., WEIS, M., EYRE, D. R., KRAENZLIN, M. & STEINMANN, B. 2008. Spondylocheiro dysplastic form of the Ehlers-Danlos syndrome--an autosomal-recessive entity caused by mutations in the zinc transporter gene SLC39A13. *American journal of human genetics,* 82**,** 1290-305.

GLOVER, C. N., BURY, N. R. & HOGSTRAND, C. 2003. Zinc uptake across the apical membrane of freshwater rainbow trout intestine is mediated by high affinity, low affinity, and histidine-facilitated pathways. *Biochimica et biophysica acta,* 1614**,** 211-9.

GOLDGABER, D., LERMAN, M. I., MCBRIDE, W. O., SAFFIOTTI, U. & GAJDUSEK, D. C. 1987. Isolation, characterization, and chromosomal localization of human brain cDNA clones coding for the precursor of the amyloid of brain in Alzheimer's disease, Down's syndrome and aging. *Journal of neural transmission. Supplementum,* 24**,** 23-8.

GRASS, G., OTTO, M., FRICKE, B., HANEY, C. J., RENSING, C., NIES, D. H. & MUNKELT, D. 2005. FieF (YiiP) from Escherichia coli mediates decreased cellular accumulation of iron and relieves iron stress. *Arch Microbiol,* 183**,** 9-18.

GRILLI, M., RIBOLA, M., ALBERICI, A., VALERIO, A., MEMO, M. & SPANO, P. 1995. Identification and characterization of a kappa B/Rel binding site in the regulatory region of the amyloid precursor protein gene. *The Journal of biological chemistry,* 270**,** 26774-7.

GROBER, E., HALL, C. B., LIPTON, R. B., ZONDERMAN, A. B., RESNICK, S. M. & KAWAS, C. 2008. Memory impairment, executive dysfunction, and intellectual decline in preclinical Alzheimer's disease. *Journal of the International Neuropsychological Society : JINS,* 14**,** 266-78.

GUFFANTI, A. A., WEI, Y., ROOD, S. V. & KRULWICH, T. A. 2002. An antiport mechanism for a member of the cation diffusion facilitator family: divalent cations efflux in exchange for K+ and H+. *Molecular microbiology,* 45**,** 145-53.

HAASE, H. & RINK, L. 2009. The immune system and the impact of zinc during aging. *Immunity & ageing : I & A,* 6**,** 9.

HAASS, C., HUNG, A. Y. & SELKOE, D. J. 1991. Processing of beta-amyloid precursor protein in microglia and astrocytes favors an internal localization over constitutive secretion. *The Journal of neuroscience : the official journal of the Society for Neuroscience,* 11**,** 3783-93.

HARA, H., KONISHI, A. & KASAI, T. 2000. Contribution of the cecum and colon to zinc absorption in rats. *The Journal of nutrition,* 130**,** 83-9.

HELSTON, R. M., PHILLIPS, S. R., MCKAY, J. A., JACKSON, K. A., MATHERS, J. C. & FORD, D. 2007. Zinc transporters in the mouse placenta show a coordinated regulatory response to changes in dietary zinc intake. *Placenta,* 28**,** 437-44.

HENDERSON, L., IRVING, K., GREGORY, J., BATES, C., PRENTICE, A., PERKS, J., SWAN, G. & FARRON, M. 2003a. *The National Diet and Nutrition Survey: Adults Aged 19 to 64 years*.

HENDERSON, L., IRVING, K., GREGORY, J., BATES, C. J., PRENTICE, A., PERKS, J., SWAN, G. & FARRON, M. 2003b. The National Diet and Nutrition Survey: Adults Aged 19 to 64 Years. Vitamin and Mineral Intake and Urinary Analytes. London.

HERZBERG, M., FOLDES, J., STEINBERG, R. & MENCZEL, J. 1990. Zinc excretion in osteoporotic women. *Journal of bone and mineral research : the official journal of the American Society for Bone and Mineral Research,* 5**,** 251-7.

HEUCHEL, R., RADTKE, F., GEORGIEV, O., STARK, G., AGUET, M. & SCHAFFNER, W. 1994. The transcription factor MTF-1 is essential for basal and heavy metal-induced metallothionein gene expression. *The EMBO journal,* 13**,** 2870-5.

HICKE, L. 1997. Ubiquitin-dependent internalization and down-regulation of plasma membrane proteins. *FASEB journal : official publication of the Federation of American Societies for Experimental Biology,* 11**,** 1215-26.

HIDALGO, I. J., RAUB, T. J. & BORCHARDT, R. T. 1989. Characterization of the human colon carcinoma cell line (Caco-2) as a model system for intestinal epithelial permeability. *Gastroenterology,* 96**,** 736-49.

HO, S. Y., DELGADO, L. & STORCH, J. 2002. Monoacylglycerol metabolism in human intestinal Caco-2 cells: evidence for metabolic compartmentation and hydrolysis. *The Journal of biological chemistry,* 277**,** 1816-23.

HOFMANN, K. & STOFFEL, W. 1993. TMbase - A database of membrane spanning proteins segments. *Biological chemistry,* 374.

HOGSTRAND, C., KILLE, P., NICHOLSON, R. I. & TAYLOR, K. M. 2009. Zinc transporters and cancer: a potential role for ZIP7 as a hub for tyrosine kinase activation. *Trends Mol Med,* 15**,** 101-11.

HOGSTRAND, C., VERBOST, P. M. & WENDELAAR BONGA, S. E. 1999. Inhibition of human erythrocyte Ca2+-ATPase by Zn2+. *Toxicology,* 133**,** 139-45.

HOJYO, S., FUKADA, T., SHIMODA, S., OHASHI, W., BIN, B. H., KOSEKI, H. & HIRANO, T. 2011. The zinc transporter SLC39A14/ZIP14 controls G-protein coupled receptor-mediated signaling required for systemic growth. *PloS one,* 6**,** e18059.

HOLSINGER, R. M., MCLEAN, C. A., BEYREUTHER, K., MASTERS, C. L. & EVIN, G. 2002. Increased expression of the amyloid precursor beta-secretase in Alzheimer's disease. *Ann Neurol,* 51**,** 783-6.

HOREV-AZARIA, L., KIRKPATRICK, C. J., KORENSTEIN, R., MARCHE, P. N., MAIMON, O., PONTI, J., ROMANO, R., ROSSI, F., GOLLA-SCHINDLER, U., SOMMER, D., UBOLDI, C., UNGER, R. E. & VILLIERS, C. 2011. Predictive toxicology of cobalt nanoparticles and ions: comparative in vitro study of different cellular models using methods of knowledge discovery from data. *Toxicol Sci,* 122**,** 489-501.

HORIUCHI, M. & MOGI, M. 2011. Role of angiotensin II receptor subtype activation in cognitive function and ischaemic brain damage. *Br J Pharmacol,* 163**,** 1122-30.

HOYER-HANSEN, M. & JAATTELA, M. 2007. Connecting endoplasmic reticulum stress to autophagy by unfolded protein response and calcium. *Cell death and differentiation,* 14**,** 1576-82.

HUANG, L. & GITSCHIER, J. 1997. A novel gene involved in zinc transport is deficient in the lethal milk mouse. *Nature genetics,* 17**,** 292-7.

HUANG, L., KIRSCHKE, C. P. & GITSCHIER, J. 2002. Functional characterization of a novel mammalian zinc transporter, ZnT6. *The Journal of biological chemistry,* 277**,** 26389-95.

HUANG, L., KIRSCHKE, C. P., ZHANG, Y. & YU, Y. Y. 2005. The ZIP7 gene (Slc39a7) encodes a zinc transporter involved in zinc homeostasis of the Golgi apparatus. *The Journal of biological chemistry,* 280**,** 15456-63.

HUANG, L., YU, Y. Y., KIRSCHKE, C. P., GERTZ, E. R. & LLOYD, K. K. 2007. Znt7 (Slc30a7)-deficient mice display reduced body zinc status and body fat accumulation. *The Journal of biological chemistry,* 282**,** 37053-63.

HUANG, Z. L., DUFNER-BEATTIE, J. & ANDREWS, G. K. 2006. Expression and regulation of SLC39A family zinc transporters in the developing mouse intestine. *Developmental biology,* 295**,** 571-9.

IGUCHI, K., OTSUKA, T., USUI, S., ISHII, K., ONISHI, T., SUGIMURA, Y. & HIRANO, K. 2004. Zinc and metallothionein levels and expression of zinc transporters in androgen-independent subline of LNCaP cells. *Journal of andrology,* 25**,** 154-61.

IGUCHI, K., USUI, S., INOUE, T., SUGIMURA, Y., TATEMATSU, M. & HIRANO, K. 2002. High-level expression of zinc transporter-2 in the rat lateral and dorsal prostate. *Journal of andrology,* 23**,** 819-24.

IRVING, H. & WILLIAMS, R. J. P. 1948. Order of stability of metal complexes. *Nature,* 162**,** 746–747.

IZUMI, R., YAMADA, T., YOSHIKAI, S., SASAKI, H., HATTORI, M. & SAKAKI, Y. 1992. Positive and negative regulatory elements for the expression of the Alzheimer's disease amyloid precursor-encoding gene in mouse. *Gene,* 112**,** 189-95.

JACKSON, K. A., HELSTON, R. M., MCKAY, J. A., O'NEILL, E. D., MATHERS, J. C. & FORD, D. 2007. Splice variants of the human zinc transporter ZnT5 (SLC30A5) are differentially localized and regulated by zinc through transcription and mRNA stability. *J Biol Chem,* 282**,** 10423-31.

JACKSON, K. A., VALENTINE, R. A., MCKAY, J. A., SWAN, D. C., MATHERS, J. C. & FORD, D. 2009. Analysis of differential gene-regulatory responses to zinc in human intestinal and placental cell lines. *The British journal of nutrition,* 101**,** 1474-83.

JACKSON, M. J. 1989. *Physiology of zinc: general aspects. In: Zinc in Human Biology,* London, Springer-Verlag.

JOHNSTON, J., O'NEILL, C., LANNFELT, L., WINBLAD, B. & COWBURN, R. F. 1994. The significance of the Swedish APP670/671 mutation for the development of Alzheimer's disease amyloidosis. *Neurochemistry international,* 25**,** 73-80.

JOU, M. Y., PHILIPPS, A. F., KELLEHER, S. L. & LONNERDAL, B. 2010. Effects of zinc exposure on zinc transporter expression in human intestinal cells of varying maturity. *Journal of pediatric gastroenterology and nutrition,* 50**,** 587-95.

KAGARA, N., TANAKA, N., NOGUCHI, S. & HIRANO, T. 2007. Zinc and its transporter ZIP10 are involved in invasive behavior of breast cancer cells. *Cancer science,* 98**,** 692-7.

KALTSCHMIDT, B., UHEREK, M., VOLK, B., BAEUERLE, P. A. & KALTSCHMIDT, C. 1997. Transcription factor NF-kappaB is activated in primary neurons by amyloid beta peptides and in neurons surrounding early plaques from patients with Alzheimer disease. *Proceedings of the National Academy of Sciences of the United States of America,* 94**,** 2642-7.

KAMBE, T., NARITA, H., YAMAGUCHI-IWAI, Y., HIROSE, J., AMANO, T., SUGIURA, N., SASAKI, R., MORI, K., IWANAGA, T. & NAGAO, M. 2002. Cloning and characterization of a novel mammalian zinc transporter, zinc transporter 5, abundantly expressed in pancreatic beta cells. *The Journal of biological chemistry,* 277**,** 19049-55.

KAMBE, T., YAMAGUCHI-IWAI, Y., SASAKI, R. & NAGAO, M. 2004. Overview of mammalian zinc transporters. *Cell Mol Life Sci,* 61**,** 49-68.

KANDEL, E. R., SCHWARTZ, J. H. & JESSELL, T. M. 2000. *Principles of Neural Science,* United States of America, McGraw-Hill.

KARIN, M., HASLINGER, A., HOLTGREVE, H., RICHARDS, R. I., KRAUTER, P., WESTPHAL, H. M. & BEATO, M. 1984. Characterization of DNA sequences through which cadmium and glucocorticoid hormones induce human metallothionein-IIA gene. *Nature,* 308**,** 513-9.

KASPRZAK, K. S., SUNDERMAN, F. W., JR. & SALNIKOW, K. 2003. Nickel carcinogenesis. *Mutation research,* 533**,** 67-97.

KATSETOS, C. D., HERMAN, M. M. & MORK, S. J. 2003. Class III beta-tubulin in human development and cancer. *Cell motility and the cytoskeleton,* 55**,** 77-96.

KAY, A. R. 2003. Evidence for chelatable zinc in the extracellular space of the hippocampus, but little evidence for synaptic release of Zn. *The Journal of neuroscience : the official journal of the Society for Neuroscience,* 23**,** 6847-55.

KEHOE, P. G., MINERS, S. & LOVE, S. 2009. Angiotensins in Alzheimer's disease - friend or foe? *Trends Neurosci,* 32**,** 619-28.

KELLEHER, S. L. & LONNERDAL, B. 2002. Zinc transporters in the rat mammary gland respond to marginal zinc and vitamin A intakes during lactation. *The Journal of nutrition,* 132**,** 3280-5.

KELLEHER, S. L. & LONNERDAL, B. 2003. Zn transporter levels and localization change throughout lactation in rat mammary gland and are regulated by Zn in mammary cells. *The Journal of nutrition,* 133**,** 3378-85.

KELLEHER, S. L. & LONNERDAL, B. 2005. Molecular regulation of milk trace mineral homeostasis. *Molecular aspects of medicine,* 26**,** 328-39.

KELLEHER, S. L., MCCORMICK, N. H., VELASQUEZ, V. & LOPEZ, V. 2011. Zinc in specialized secretory tissues: roles in the pancreas, prostate, and mammary gland. *Advances in nutrition,* 2**,** 101-11.

KELLEHER, S. L., VELASQUEZ, V., CROXFORD, T. P., MCCORMICK, N. H., LOPEZ, V. & MACDAVID, J. 2012. Mapping the zinc-transporting system in mammary cells: molecular analysis reveals a phenotype-dependent zinc-transporting network during lactation. *Journal of cellular physiology,* 227**,** 1761-70.

KHLIFI, R. & HAMZA-CHAFFAI, A. 2010. Head and neck cancer due to heavy metal exposure via tobacco smoking and professional exposure: a review. *Toxicology and applied pharmacology,* 248**,** 71-88.

KIM, A. H., SHELINE, C. T., TIAN, M., HIGASHI, T., MCMAHON, R. J., COUSINS, R. J. & CHOI, D. W. 2000. L-type Ca(2+) channel-mediated Zn(2+) toxicity and modulation by ZnT-1 in PC12 cells. *Brain research,* 886**,** 99-107.

KIM, D., GUSTIN, J. L., LAHNER, B., PERSANS, M. W., BAEK, D., YUN, D. J. & SALT, D. E. 2004. The plant CDF family member TgMTP1 from the Ni/Zn hyperaccumulator Thlaspi goesingense acts to enhance efflux of Zn at the plasma membrane when expressed in Saccharomyces cerevisiae. *The Plant journal : for cell and molecular biology,* 39**,** 237-51.

KIMURA, K. & KUMURA, J. Preliminary report on the metabolism of trace elements in neuro-psychiatric diseases: I. Zinc in schizophrenics. Proceedings of the Japan Academy, 1965. 943-47.

KING, J. C. 2011. Zinc: an essential but elusive nutrient. *The American journal of clinical nutrition,* 94**,** 679S-84S.

KING, J. C., SHAMES, D. M. & WOODHOUSE, L. R. 2000. Zinc homeostasis in humans. *The Journal of nutrition,* 130**,** 1360S-6S.

KIRCHGESSNER, M. 1993. *Underwood Memorial Lecture: Homeostasis and homeorhesis in trace element metabolism. In: Trace Elements in Man and Animals–TEMA 8,* Dresden, Germany., Verlag Media Touristik.

KIRSCHKE, C. P. & HUANG, L. 2003. ZnT7, a novel mammalian zinc transporter, accumulates zinc in the Golgi apparatus. *The Journal of biological chemistry,* 278**,** 4096-102.

KISHI, S. & YAMAGUCHI, M. 1994. Inhibitory effect of zinc compounds on osteoclast-like cell formation in mouse marrow cultures. *Biochemical pharmacology,* 48**,** 1225-30.

KITAMURA, H., MORIKAWA, H., KAMON, H., IGUCHI, M., HOJYO, S., FUKADA, T., YAMASHITA, S., KAISHO, T., AKIRA, S., MURAKAMI, M. & HIRANO, T. 2006. Toll-like receptor-mediated regulation of zinc homeostasis influences dendritic cell function. *Nature immunology,* 7**,** 971-7.

KOCH, D., NIES, D. H. & GRASS, G. 2007. The RcnRA (YohLM) system of Escherichia coli: a connection between nickel, cobalt and iron homeostasis. *Biometals : an international journal on the role of metal ions in biology, biochemistry, and medicine,* 20**,** 759-71.

KODIROV, S. A., TAKIZAWA, S., JOSEPH, J., KANDEL, E. R., SHUMYATSKY, G. P. & BOLSHAKOV, V. Y. 2006. Synaptically released zinc gates long-term potentiation in fear conditioning pathways. *Proceedings of the National Academy of Sciences of the United States of America,* 103**,** 15218-23.

KOIZUMI, S., SUZUKI, K., OGRA, Y., YAMADA, H. & OTSUKA, F. 1999. Transcriptional activity and regulatory protein binding of metal-responsive elements of the human metallothionein-IIA gene. *European journal of biochemistry / FEBS,* 259**,** 635-42.

KOSIK, K. S. 1990. Tau protein and neurodegeneration. *Molecular neurobiology,* 4**,** 171-9.

KRAMER, U., SMITH, R. D., WENZEL, W. W., RASKIN, I. & SALT, D. E. 1997. The Role of Metal Transport and Tolerance in Nickel Hyperaccumulation by Thlaspi goesingense Halacsy. *Plant physiology,* 115**,** 1641-1650.

KREBS, N. F. 2000. Overview of zinc absorption and excretion in the human gastrointestinal tract. *The Journal of nutrition,* 130**,** 1374S-7S.

KRISHNAMURTHY, P. K., MAYS, J. L., BIJUR, G. N. & JOHNSON, G. V. 2000. Transient oxidative stress in SH-SY5Y human neuroblastoma cells results in caspase dependent and independent cell death and tau proteolysis. *Journal of neuroscience research,* 61**,** 515-23.

LABBE, S., ZHU, Z. & THIELE, D. J. 1997. Copper-specific transcriptional repression of yeast genes encoding critical components in the copper transport pathway. *The Journal of biological chemistry,* 272**,** 15951-8.

LANGMADE, S. J., RAVINDRA, R., DANIELS, P. J. & ANDREWS, G. K. 2000. The transcription factor MTF-1 mediates metal regulation of the mouse ZnT1 gene. *The Journal of biological chemistry,* 275**,** 34803-9.

LANNFELT, L., BLENNOW, K., ZETTERBERG, H., BATSMAN, S., AMES, D., HARRISON, J., MASTERS, C. L., TARGUM, S., BUSH, A. I., MURDOCH, R., WILSON, J. & RITCHIE, C. W. 2008. Safety, efficacy, and biomarker findings of PBT2 in targeting Abeta as a modifying therapy for Alzheimer's disease: a phase IIa, double-blind, randomised, placebo-controlled trial. *Lancet neurology,* 7**,** 779-86.

LEE, J. W., LEE, Y. K., YUK, D. Y., CHOI, D. Y., BAN, S. B., OH, K. W. & HONG, J. T. 2008. Neuro-inflammation induced by lipopolysaccharide causes cognitive impairment through enhancement of beta-amyloid generation. *Journal of neuroinflammation,* 5**,** 37.

LEE, J. Y., COLE, T. B., PALMITER, R. D., SUH, S. W. & KOH, J. Y. 2002. Contribution by synaptic zinc to the gender-disparate plaque formation in human Swedish mutant APP transgenic mice. *Proceedings of the National Academy of Sciences of the United States of America,* 99**,** 7705-10.

LEE, J. Y., KIM, J. H., PALMITER, R. D. & KOH, J. Y. 2003. Zinc released from metallothionein-iii may contribute to hippocampal CA1 and thalamic neuronal death following acute brain injury. *Experimental neurology,* 184**,** 337-47.

LENGYEL, I., FLINN, J. M., PETO, T., LINKOUS, D. H., CANO, K., BIRD, A. C., LANZIROTTI, A., FREDERICKSON, C. J. & VAN KUIJK, F. J. 2007. High concentration of zinc in sub-retinal pigment epithelial deposits. *Experimental eye research,* 84**,** 772-80.

LI, L. & DAVIE, J. R. 2010. The role of Sp1 and Sp3 in normal and cancer cell biology. *Annals of anatomy = Anatomischer Anzeiger : official organ of the Anatomische Gesellschaft,* 192**,** 275-83.

LI, Y., HOUGH, C. J., SUH, S. W., SARVEY, J. M. & FREDERICKSON, C. J. 2001. Rapid translocation of Zn(2+) from presynaptic terminals into postsynaptic hippocampal neurons after physiological stimulation. *Journal of neurophysiology,* 86**,** 2597-604.

LI, Y., KIMURA, T., HUYCK, R. W., LAITY, J. H. & ANDREWS, G. K. 2008. Zinc-induced formation of a coactivator complex containing the zinc-sensing transcription factor MTF-1, p300/CBP, and Sp1. *Molecular and cellular biology,* 28**,** 4275-84.

LI, Y. & ZAMBLE, D. B. 2009. Nickel homeostasis and nickel regulation: an overview. *Chemical reviews,* 109**,** 4617-43.

LICHTEN, L. A. & COUSINS, R. J. 2009. Mammalian zinc transporters: nutritional and physiologic regulation. *Annu Rev Nutr,* 29**,** 153-76.

LICHTEN, L. A., RYU, M. S., GUO, L., EMBURY, J. & COUSINS, R. J. 2011. MTF-1-mediated repression of the zinc transporter Zip10 is alleviated by zinc restriction. *PloS one,* 6**,** e21526.

LICHTLEN, P., WANG, Y., BELSER, T., GEORGIEV, O., CERTA, U., SACK, R. & SCHAFFNER, W. 2001. Target gene search for the metal-responsive transcription factor MTF-1. *Nucleic acids research,* 29**,** 1514-23.

LIESEGANG, H., LEMKE, K., SIDDIQUI, R. A. & SCHLEGEL, H. G. 1993. Characterization of the inducible nickel and cobalt resistance determinant cnr from pMOL28 of Alcaligenes eutrophus CH34. *Journal of bacteriology,* 175**,** 767-78.

LILJAS, A., HAKANSSON, K., JONSSON, B. H. & XUE, Y. 1994. Inhibition and catalysis of carbonic anhydrase. Recent crystallographic analyses. *European journal of biochemistry / FEBS,* 219**,** 1-10.

LIN, R., CHEN, X., LI, W., HAN, Y., LIU, P. & PI, R. 2008. Exposure to metal ions regulates mRNA levels of APP and BACE1 in PC12 cells: blockage by curcumin. *Neuroscience letters,* 440**,** 344-7.

LIU, Z., LI, H., SOLEIMANI, M., GIRIJASHANKER, K., REED, J. M., HE, L., DALTON, T. P. & NEBERT, D. W. 2008. Cd2+ versus Zn2+ uptake by the ZIP8 HCO3--dependent symporter: kinetics, electrogenicity and trafficking. *Biochemical and biophysical research communications,* 365**,** 814-20.

LIUZZI, J. P., BLANCHARD, R. K. & COUSINS, R. J. 2001. Differential regulation of zinc transporter 1, 2, and 4 mRNA expression by dietary zinc in rats. *The Journal of nutrition,* 131**,** 46-52.

LIUZZI, J. P., BOBO, J. A., CUI, L., MCMAHON, R. J. & COUSINS, R. J. 2003. Zinc transporters 1, 2 and 4 are differentially expressed and localized in rats during pregnancy and lactation. *The Journal of nutrition,* 133**,** 342-51.

LIUZZI, J. P., GUO, L., CHANG, S. M. & COUSINS, R. J. 2009. Kruppel-like factor 4 regulates adaptive expression of the zinc transporter Zip4 in mouse small intestine. *American journal of physiology. Gastrointestinal and liver physiology,* 296**,** G517-23.

LIUZZI, J. P., LICHTEN, L. A., RIVERA, S., BLANCHARD, R. K., AYDEMIR, T. B., KNUTSON, M. D., GANZ, T. & COUSINS, R. J. 2005. Interleukin-6

regulates the zinc transporter Zip14 in liver and contributes to the hypozincemia of the acute-phase response. *Proceedings of the National Academy of Sciences of the United States of America,* 102**,** 6843-8.

LOVELL, M. A., ROBERTSON, J. D., TEESDALE, W. J., CAMPBELL, J. L. & MARKESBERY, W. R. 1998. Copper, iron and zinc in Alzheimer's disease senile plaques. *Journal of the neurological sciences,* 158**,** 47-52.

LOVELL, M. A., SMITH, J. L., XIONG, S. & MARKESBERY, W. R. 2005. Alterations in zinc transporter protein-1 (ZnT-1) in the brain of subjects with mild cognitive impairment, early, and late-stage Alzheimer's disease. *Neurotoxicity research,* 7**,** 265-71.

LOVELL, M. A., XIONG, S., XIE, C., DAVIES, P. & MARKESBERY, W. R. 2004. Induction of hyperphosphorylated tau in primary rat cortical neuron cultures mediated by oxidative stress and glycogen synthase kinase-3. *Journal of Alzheimer's disease : JAD,* 6**,** 659-71; discussion 673-81.

LYONS, T. J., GASCH, A. P., GAITHER, L. A., BOTSTEIN, D., BROWN, P. O. & EIDE, D. J. 2000. Genome-wide characterization of the Zap1p zinc-responsive regulon in yeast. *Proceedings of the National Academy of Sciences of the United States of America,* 97**,** 7957-62.

LYUBARTSEVA, G., SMITH, J. L., MARKESBERY, W. R. & LOVELL, M. A. 2009. Alterations of Zinc Transporter Proteins ZnT-1, ZnT-4 and ZnT-6 in Preclinical Alzheimer's Disease Brain. *Brain Pathol*.

MACDIARMID, C. W., GAITHER, L. A. & EIDE, D. 2000. Zinc transporters that regulate vacuolar zinc storage in Saccharomyces cerevisiae. *The EMBO journal,* 19**,** 2845-55.

MARCELLINI, M., DI CIOMMO, V., CALLEA, F., DEVITO, R., COMPARCOLA, D., SARTORELLI, M. R., CARELLI, G. & NOBILI, V. 2005. Treatment of Wilson's disease with zinc from the time of diagnosis in pediatric patients: a single-hospital, 10-year follow-up study. *The Journal of laboratory and clinical medicine,* 145**,** 139-43.

MARTEL, G., HEVI, C., KANE-GOLDSMITH, N. & SHUMYATSKY, G. P. 2011. Zinc transporter ZnT3 is involved in memory dependent on the hippocampus and perirhinal cortex. *Behavioural brain research,* 223**,** 233-8.

MATSUURA, W., YAMAZAKI, T., YAMAGUCHI-IWAI, Y., MASUDA, S., NAGAO, M., ANDREWS, G. K. & KAMBE, T. 2009. SLC39A9 (ZIP9) regulates zinc homeostasis in the secretory pathway: characterization of the ZIP subfamily I protein in vertebrate cells. *Bioscience, biotechnology, and biochemistry,* 73**,** 1142-8.

MATSUZAKI, S., MANABE, T., KATAYAMA, T., NISHIKAWA, A., YANAGITA, T., OKUDA, H., YASUDA, Y., MIYATA, S., MESHITSUKA, S. & TOHYAMA, M. 2004. Metals accelerate production of the aberrant splicing isoform of the presenilin-2. *Journal of neurochemistry,* 88**,** 1345-51.

MAYEUX, R. & STERN, Y. 2012. Epidemiology of Alzheimer disease. *Cold Spring Harbor perspectives in medicine,* 2.

MCCANCE, R. A. & WIDDOWSON, E. M. 1942. The absorption and excretion of zinc. *The Biochemical journal,* 36**,** 692-6.

MCMAHON, R. J. & COUSINS, R. J. 1998. Regulation of the zinc transporter ZnT-1 by dietary zinc. *Proceedings of the National Academy of Sciences of the United States of America,* 95**,** 4841-6.

MILNE, D. B., CANFIELD, W. K., GALLAGHER, S. K., HUNT, J. R. & KLEVAY, L. M. 1987. Ethanol metabolism in postmenopausal women fed a diet marginal in zinc. *The American journal of clinical nutrition,* 46**,** 688-93.

MILON, B., DHERMY, D., POUNTNEY, D., BOURGEOIS, M. & BEAUMONT, C. 2001. Differential subcellular localization of hZip1 in adherent and non-adherent cells. *FEBS letters,* 507**,** 241-6.

MILON, B., WU, Q., ZOU, J., COSTELLO, L. C. & FRANKLIN, R. B. 2006. Histidine residues in the region between transmembrane domains III and IV of hZip1 are required for zinc transport across the plasma membrane in PC-3 cells. *Biochimica et biophysica acta,* 1758**,** 1696-701.

MOCCHEGIANI, E., BERTONI-FREDDARI, C., MARCELLINI, F. & MALAVOLTA, M. 2005. Brain, aging and neurodegeneration: role of zinc ion availability. *Prog Neurobiol,* 75**,** 367-90.

MOCCHEGIANI, E., COSTARELLI, L., GIACCONI, R., CIPRIANO, C., MUTI, E., RINK, L. & MALAVOLTA, M. 2006a. Zinc homeostasis in aging: two elusive faces of the same "metal". *Rejuvenation research,* 9**,** 351-4.

MOCCHEGIANI, E., COSTARELLI, L., GIACCONI, R., CIPRIANO, C., MUTI, E., TESEI, S. & MALAVOLTA, M. 2006b. Nutrient-gene interaction in ageing and successful ageing. A single nutrient (zinc) and some target genes related to inflammatory/immune response. *Mechanisms of ageing and development,* 127**,** 517-25.

MOCCHEGIANI, E., MALAVOLTA, M., LATTANZIO, F., PIACENZA, F., BASSO, A., ABBATECOLA, A. M., RUSSO, A., GIOVANNINI, S., CAPOLUONGO, E., BUSTACCHINI, S., GUFFANTI, E. E., BERNABEI, R. & LANDI, F. 2012a. Cu to Zn ratio, physical function, disability, and mortality risk in older elderly (ilSIRENTE study). *Age (Dordr),* 34**,** 539-52.

MOCCHEGIANI, E., ROMEO, J., MALAVOLTA, M., COSTARELLI, L., GIACCONI, R., DIAZ, L. E. & MARCOS, A. 2012b. Zinc: dietary intake and impact of supplementation on immune function in elderly. *Age*.

MONTANINI, B., BLAUDEZ, D., JEANDROZ, S., SANDERS, D. & CHALOT, M. 2007. Phylogenetic and functional analysis of the Cation Diffusion Facilitator (CDF) family: improved signature and prediction of substrate specificity. *BMC genomics,* 8**,** 107.

MOUTON-LIGER, F., PAQUET, C., DUMURGIER, J., BOURAS, C., PRADIER, L., GRAY, F. & HUGON, J. 2012. Oxidative stress increases BACE1 protein levels through activation of the PKR-eIF2alpha pathway. *Biochimica et biophysica acta,* 1822**,** 885-96.

MOWRER, K. R. & WOLFE, M. S. 2008. Promotion of BACE1 mRNA alternative splicing reduces amyloid beta-peptide production. *J Biol Chem,* 283**,** 18694-701.

MUNKELT, D., GRASS, G. & NIES, D. H. 2004. The chromosomally encoded cation diffusion facilitator proteins DmeF and FieF from Wautersia metallidurans CH34 are transporters of broad metal specificity. *Journal of bacteriology,* 186**,** 8036-43.

MURGIA, C., VESPIGNANI, I., CERASE, J., NOBILI, F. & PEROZZI, G. 1999. Cloning, expression, and vesicular localization of zinc transporter Dri 27/ZnT4 in intestinal tissue and cells. *The American journal of physiology,* 277**,** G1231-9.

NELDNER, K. H. & HAMBIDGE, K. M. 1975. Zinc therapy of acrodermatitis enteropathica. *The New England journal of medicine,* 292**,** 879-82.

NESSA B. N., TANAKA T., KAMINO K., SADIK G., ANSAR A. B., KIMURA R., TANII H., OKOCHI M., MORIHARA T., TAGAMI S., KUDO T. & TAKEDA M. 2006. Toll-like receptor 3 mediated hyperphosphorylation of tau in human SH-SY5Y neuroblastoma cells. *Psychiatry and Clinical Neurosciences,* 60**,** S27-S33.

NICOLSON, T. J., BELLOMO, E. A., WIJESEKARA, N., LODER, M. K., BALDWIN, J. M., GYULKHANDANYAN, A. V., KOSHKIN, V., TARASOV, A. I., CARZANIGA, R., KRONENBERGER, K., TANEJA, T. K., DA SILVA XAVIER, G., LIBERT, S., FROGUEL, P., SCHARFMANN, R., STETSYUK, V., RAVASSARD, P., PARKER, H., GRIBBLE, F. M., REIMANN, F., SLADEK, R., HUGHES, S. J., JOHNSON, P. R., MASSEBOEUF, M., BURCELIN, R., BALDWIN, S. A., LIU, M., LARA-LEMUS, R., ARVAN, P., SCHUIT, F. C., WHEELER, M. B., CHIMIENTI, F. & RUTTER, G. A. 2009. Insulin storage and glucose homeostasis in mice null for the granule zinc transporter ZnT8 and studies of the type 2 diabetes-associated variants. *Diabetes,* 58**,** 2070-83.

NIES, D. H. 2003. Efflux-mediated heavy metal resistance in prokaryotes. *FEMS microbiology reviews,* 27**,** 313-39.

NISHIOKA, M., SHIMADA, M., KURITA, N., IWATA, T., MORIMOTO, S., YOSHIKAWA, K., HIGASHIJIMA, J. & MIYATANI, T. 2011. Gene expression profile can predict pathological response to preoperative chemoradiotherapy in rectal cancer. *Cancer genomics & proteomics,* 8**,** 87-92.

O'DELL, B. L. & REEVES, P. G. 1989. Zinc status and food intake. *In:* MILLS, C. F. (ed.) *Zinc in human biology.* London, United Kingdom: Springer-Verlag.

OHANA, E., HOCH, E., KEASAR, C., KAMBE, T., YIFRACH, O., HERSHFINKEL, M. & SEKLER, I. 2009. Identification of the Zn2+ binding site and mode of operation of a mammalian Zn2+ transporter. *The Journal of biological chemistry,* 284**,** 17677-86.

OKAMOTO, S. & ELTIS, L. D. 2011. The biological occurrence and trafficking of cobalt. *Metallomics : integrated biometal science,* 3**,** 963-70.

ONER, G., BHAUMICK, B. & BALA, R. M. 1984. Effect of zinc deficiency on serum somatomedin levels and skeletal growth in young rats. *Endocrinology,* 114**,** 1860-3.

OTEIZA, P. I., CLEGG, M. S., ZAGO, M. P. & KEEN, C. L. 2000. Zinc deficiency induces oxidative stress and AP-1 activation in 3T3 cells. *Free radical biology & medicine,* 28**,** 1091-9.

OTT, E. S. & SHAY, N. F. 2001. Zinc deficiency reduces leptin gene expression and leptin secretion in rat adipocytes. *Experimental biology and medicine,* 226**,** 841-6.

OUTTEN, C. E., OUTTEN, F. W. & O'HALLORAN, T. V. 1999. DNA distortion mechanism for transcriptional activation by ZntR, a Zn(II)-responsive MerR homologue in Escherichia coli. *The Journal of biological chemistry,* 274**,** 37517-24.

OVERBECK, S., UCIECHOWSKI, P., ACKLAND, M. L., FORD, D. & RINK, L. 2008. Intracellular zinc homeostasis in leukocyte subsets is regulated by different expression of zinc exporters ZnT-1 to ZnT-9. *Journal of leukocyte biology,* 83**,** 368-80.

PAL, S., HARTNETT, K. A., NERBONNE, J. M., LEVITAN, E. S. & AIZENMAN, E. 2003. Mediation of neuronal apoptosis by Kv2.1-encoded potassium channels. *The Journal of neuroscience : the official journal of the Society for Neuroscience,* 23**,** 4798-802.

PALMER, C. M. & GUERINOT, M. L. 2009. Facing the challenges of Cu, Fe and Zn homeostasis in plants. *Nature chemical biology,* 5**,** 333-40.

PALMITER, R. D. 1994. Regulation of metallothionein genes by heavy metals appears to be mediated by a zinc-sensitive inhibitor that interacts with a constitutively active transcription factor, MTF-1. *Proceedings of the National Academy of Sciences of the United States of America,* 91**,** 1219-23.

PALMITER, R. D. 1998. The elusive function of metallothioneins. *Proceedings of the National Academy of Sciences of the United States of America,* 95**,** 8428-30.

PALMITER, R. D., COLE, T. B. & FINDLEY, S. D. 1996a. ZnT-2, a mammalian protein that confers resistance to zinc by facilitating vesicular sequestration. *The EMBO journal,* 15**,** 1784-91.

PALMITER, R. D., COLE, T. B., QUAIFE, C. J. & FINDLEY, S. D. 1996b. ZnT-3, a putative transporter of zinc into synaptic vesicles. *Proceedings of the National Academy of Sciences of the United States of America,* 93**,** 14934-9.

PALMITER, R. D. & FINDLEY, S. D. 1995. Cloning and functional characterization of a mammalian zinc transporter that confers resistance to zinc. *The EMBO journal,* 14**,** 639-49.

PALMITER, R. D. & HUANG, L. 2004. Efflux and compartmentalization of zinc by members of the SLC30 family of solute carriers. *Pflugers Arch,* 447**,** 744-51.

PANDEY, N. R., SULTAN, K., TWOMEY, E. & SPARKS, D. L. 2009. Phospholipids block nuclear factor-kappa B and tau phosphorylation and inhibit amyloid-beta secretion in human neuroblastoma cells. *Neuroscience,* 164**,** 1744-53.

PAOLETTI, P., VERGNANO, A. M., BARBOUR, B. & CASADO, M. 2009. Zinc at glutamatergic synapses. *Neuroscience,* 158**,** 126-36.

PATRUSHEV, N., SEIDEL-ROGOL, B. & SALAZAR, G. 2012. Angiotensin II requires zinc and downregulation of the zinc transporters ZnT3 and ZnT10 to induce senescence of vascular smooth muscle cells. *PloS one,* 7**,** e33211.

PATZER, S. I. & HANTKE, K. 2000. The zinc-responsive regulator Zur and its control of the znu gene cluster encoding the ZnuABC zinc uptake system in Escherichia coli. *The Journal of biological chemistry,* 275**,** 24321-32.

PAULSEN, I. T. & SAIER, M. H., JR. 1997. A novel family of ubiquitous heavy metal ion transport proteins. *The Journal of membrane biology,* 156**,** 99-103.

PERRY, D. K., SMYTH, M. J., STENNICKE, H. R., SALVESEN, G. S., DURIEZ, P., POIRIER, G. G. & HANNUN, Y. A. 1997. Zinc is a potent inhibitor of the

apoptotic protease, caspase-3. A novel target for zinc in the inhibition of apoptosis. *The Journal of biological chemistry,* 272**,** 18530-3.

PERSANS, M. W., NIEMAN, K. & SALT, D. E. 2001. Functional activity and role of cation-efflux family members in Ni hyperaccumulation in Thlaspi goesingense. *Proceedings of the National Academy of Sciences of the United States of America,* 98**,** 9995-10000.

PETERSEN, A. B., SMIDT, K., MAGNUSSON, N. E., MOORE, F., EGEFJORD, L. & RUNGBY, J. 2011. siRNA-mediated knock-down of ZnT3 and ZnT8 affects production and secretion of insulin and apoptosis in INS-1E cells. *APMIS : acta pathologica, microbiologica, et immunologica Scandinavica,* 119**,** 93-102.

PETRIS, M. J. & MERCER, J. F. 1999. The Menkes protein (ATP7A; MNK) cycles via the plasma membrane both in basal and elevated extracellular copper using a C-terminal di-leucine endocytic signal. *Human molecular genetics,* 8**,** 2107-15.

PIMPLIKAR, S. W. 2009. Reassessing the amyloid cascade hypothesis of Alzheimer's disease. *The international journal of biochemistry & cell biology,* 41**,** 1261-8.

PINILLA-TENAS, J. J., SPARKMAN, B. K., SHAWKI, A., ILLING, A. C., MITCHELL, C. J., ZHAO, N., LIUZZI, J. P., COUSINS, R. J., KNUTSON, M. D. & MACKENZIE, B. 2011. Zip14 is a complex broad-scope metal-ion transporter whose functional properties support roles in the cellular uptake of zinc and nontransferrin-bound iron. *American journal of physiology. Cell physiology,* 301**,** C862-71.

POWELL, J. J., BURDEN, T. J., GREENFIELD, S. M., TAYLOR, P. D. & THOMPSON, R. P. 1999. Urinary excretion of essential metals following intravenous calcium disodium edetate: an estimate of free zinc and zinc status in man. *Journal of inorganic biochemistry,* 75**,** 159-65.

PRASAD, A. S. 2000. Effects of zinc deficiency on Th1 and Th2 cytokine shifts. *The Journal of infectious diseases,* 182 Suppl 1**,** S62-8.

PRASAD, A. S. 2008. Zinc in human health: effect of zinc on immune cells. *Molecular medicine,* 14**,** 353-7.

PRASAD, A. S., BAO, B., BECK, F. W. & SARKAR, F. H. 2001. Zinc activates NF-kappaB in HUT-78 cells. *The Journal of laboratory and clinical medicine,* 138**,** 250-6.

PRASAD, A. S., HALSTED, J. A. & NADIMI, M. 1961. Syndrome of iron deficiency anemia, hepatosplenomegaly, hypogonadism, dwarfism and geophagia. *The American journal of medicine,* 31**,** 532-46.

QIAN, J., XU, K., YOO, J., CHEN, T. T., ANDREWS, G. & NOEBELS, J. L. 2011. Knockout of Zn transporters Zip-1 and Zip-3 attenuates seizure-induced CA1 neurodegeneration. *The Journal of neuroscience : the official journal of the Society for Neuroscience,* 31**,** 97-104.

QUADRI, M., FEDERICO, A., ZHAO, T., BREEDVELD, G. J., BATTISTI, C., DELNOOZ, C., SEVERIJNEN, L. A., DI TORO MAMMARELLA, L., MIGNARRI, A., MONTI, L., SANNA, A., LU, P., PUNZO, F., COSSU, G., WILLEMSEN, R., RASI, F., OOSTRA, B. A., VAN DE WARRENBURG, B. P. & BONIFATI, V. 2012. Mutations in SLC30A10 cause parkinsonism and dystonia with hypermanganesemia, polycythemia, and chronic liver disease. *American journal of human genetics,* 90**,** 467-77.

QUINN, J. M. & MERCHANT, S. 1995. Two copper-responsive elements associated with the Chlamydomonas Cyc6 gene function as targets for transcriptional activators. *The Plant cell,* 7**,** 623-8.

QUITSCHKE, W. W. 1994. Two nuclear factor binding domains activate expression from the human amyloid beta-protein precursor promoter. *The Journal of biological chemistry,* 269**,** 21229-33.

RAFFANIELLO, R. D., LEE, S. Y., TEICHBERG, S. & WAPNIR, R. A. 1992. Distinct mechanisms of zinc uptake at the apical and basolateral membranes of caco-2 cells. *Journal of cellular physiology,* 152**,** 356-61.

REDENTI, S. & CHAPPELL, R. L. 2004. Localization of zinc transporter-3 (ZnT-3) in mouse retina. *Vision research,* 44**,** 3317-21.

REID, A. C., MACKINS, C. J., SEYEDI, N., LEVI, R. & SILVER, R. B. 2004. Coupling of angiotensin II AT1 receptors to neuronal NHE activity and carrier-mediated norepinephrine release in myocardial ischemia. *American journal of physiology. Heart and circulatory physiology,* 286**,** H1448-54.

RISHI, I., BAIDOURI, H., ABBASI, J. A., BULLARD-DILLARD, R., KAJDACSY-BALLA, A., PESTANER, J. P., SKACEL, M., TUBBS, R. & BAGASRA, O. 2003. Prostate cancer in African American men is associated with downregulation of zinc transporters. *Applied immunohistochemistry & molecular morphology : AIMM / official publication of the Society for Applied Immunohistochemistry,* 11**,** 253-60.

ROBERTS, E. A. & SCHILSKY, M. L. 2008. Diagnosis and treatment of Wilson disease: an update. *Hepatology,* 47**,** 2089-111.

ROMER, M. U., JENSEN, N. F., NIELSEN, S. L., MULLER, S., NIELSEN, K. V., NIELSEN, H. J. & BRUNNER, N. 2012. TOP1 gene copy numbers in colorectal cancer samples and cell lines and their association to in vitro drug sensitivity. *Scandinavian journal of gastroenterology,* 47**,** 68-79.

RYU, M. S., LICHTEN, L. A., LIUZZI, J. P. & COUSINS, R. J. 2008. Zinc transporters ZnT1 (Slc30a1), Zip8 (Slc39a8), and Zip10 (Slc39a10) in mouse red blood cells are differentially regulated during erythroid development and by dietary zinc deficiency. *The Journal of nutrition,* 138**,** 2076-83.

SARIS, N. E. & NIVA, K. 1994. Is Zn2+ transported by the mitochondrial calcium uniporter? *FEBS letters,* 356**,** 195-8.

SATO, N., HORI, O., YAMAGUCHI, A., LAMBERT, J. C., CHARTIER-HARLIN, M. C., ROBINSON, P. A., DELACOURTE, A., SCHMIDT, A. M., FURUYAMA, T., IMAIZUMI, K., TOHYAMA, M. & TAKAGI, T. 1999. A novel presenilin-2 splice variant in human Alzheimer's disease brain tissue. *Journal of neurochemistry,* 72**,** 2498-505.

SCHEPER, W., ZWART, R. & BAAS, F. 2004. Alternative splicing in the N-terminus of Alzheimer's presenilin 1. *Neurogenetics,* 5**,** 223-7.

SCHNEIDER, J., RUSCHHAUPT, M., BUNESS, A., ASSLABER, M., REGITNIG, P., ZATLOUKAL, K., SCHIPPINGER, W., PLONER, F., POUSTKA, A. & SULTMANN, H. 2006. Identification and meta-analysis of a small gene expression signature for the diagnosis of estrogen receptor status in invasive ductal breast cancer. *International journal of cancer. Journal international du cancer,* 119**,** 2974-9.

SEAL, C. J. & MATHERS, J. C. 1989. Intestinal zinc transfer by everted gut sacs from rats given diets containing different amounts and types of dietary fibre. *The British journal of nutrition,* 62**,** 151-63.

SEKLER, I., MORAN, A., HERSHFINKEL, M., DORI, A., MARGULIS, A., BIRENZWEIG, N., NITZAN, Y. & SILVERMAN, W. F. 2002. Distribution of the zinc transporter ZnT-1 in comparison with chelatable zinc in the mouse brain. *J Comp Neurol,* 447**,** 201-9.

SELKOE, D. J. 2001. Alzheimer's disease: genes, proteins, and therapy. *Physiological reviews,* 81**,** 741-66.

SENSI, S. L., PAOLETTI, P., BUSH, A. I. & SEKLER, I. 2009. Zinc in the physiology and pathology of the CNS. *Nature reviews. Neuroscience,* 10**,** 780-91.

SENSI, S. L., YIN, H. Z., CARRIEDO, S. G., RAO, S. S. & WEISS, J. H. 1999. Preferential Zn2+ influx through Ca2+-permeable AMPA/kainate channels triggers prolonged mitochondrial superoxide production. *Proceedings of the National Academy of Sciences of the United States of America,* 96**,** 2414-9.

SEVE, M., CHIMIENTI, F., DEVERGNAS, S. & FAVIER, A. 2004. In silico identification and expression of SLC30 family genes: an expressed sequence tag

data mining strategy for the characterization of zinc transporters' tissue expression. *BMC Genomics,* 5**,** 32.

SHAH, D. & SACHDEV, H. P. 2006. Zinc deficiency in pregnancy and fetal outcome. *Nutrition reviews,* 64**,** 15-30.

SHATZMAN, A. R. & HENKIN, R. I. 1981. Gustin concentration changes relative to salivary zinc and taste in humans. *Proceedings of the National Academy of Sciences of the United States of America,* 78**,** 3867-71.

SHERRINGTON, R., ROGAEV, E. I., LIANG, Y., ROGAEVA, E. A., LEVESQUE, G., IKEDA, M., CHI, H., LIN, C., LI, G., HOLMAN, K., TSUDA, T., MAR, L., FONCIN, J. F., BRUNI, A. C., MONTESI, M. P., SORBI, S., RAINERO, I., PINESSI, L., NEE, L., CHUMAKOV, I., POLLEN, D., BROOKES, A., SANSEAU, P., POLINSKY, R. J., WASCO, W., DA SILVA, H. A., HAINES, J. L., PERKICAK-VANCE, M. A., TANZI, R. E., ROSES, A. D., FRASER, P. E., ROMMENS, J. M. & ST GEORGE-HYSLOP, P. H. 1995. Cloning of a gene bearing missense mutations in early-onset familial Alzheimer's disease. *Nature,* 375**,** 754-60.

SIM, D. L. & CHOW, V. T. 1999. The novel human HUEL (C4orf1) gene maps to chromosome 4p12-p13 and encodes a nuclear protein containing the nuclear receptor interaction motif. *Genomics,* 59**,** 224-33.

SINCLAIR, S. A. & KRAMER, U. 2012. The zinc homeostasis network of land plants. *Biochimica et biophysica acta*.

SINDREU, C. & STORM, D. R. 2011. Modulation of neuronal signal transduction and memory formation by synaptic zinc. *Frontiers in behavioral neuroscience,* 5**,** 68.

SINGH, J. & KAUR, G. 2007. Transcriptional regulation of polysialylated neural cell adhesion molecule expression by NMDA receptor activation in retinoic acid-differentiated SH-SY5Y neuroblastoma cultures. *Brain research,* 1154**,** 8-21.

SMART, T. G., XIE, X. & KRISHEK, B. J. 1994. Modulation of inhibitory and excitatory amino acid receptor ion channels by zinc. *Prog Neurobiol,* 42**,** 393-441.

SMIDT, K., JESSEN, N., PETERSEN, A. B., LARSEN, A., MAGNUSSON, N., JEPPESEN, J. B., STOLTENBERG, M., CULVENOR, J. G., TSATSANIS, A., BROCK, B., SCHMITZ, O., WOGENSEN, L., BUSH, A. I. & RUNGBY, J. 2009. SLC30A3 responds to glucose- and zinc variations in beta-cells and is critical for insulin production and in vivo glucose-metabolism during beta-cell stress. *PloS one,* 4**,** e5684.

SMIDT, K., PEDERSEN, S. B., BROCK, B., SCHMITZ, O., FISKER, S., BENDIX, J., WOGENSEN, L. & RUNGBY, J. 2007. Zinc-transporter genes in human visceral and subcutaneous adipocytes: lean versus obese. *Molecular and cellular endocrinology,* 264**,** 68-73.

SMIDT, K. & RUNGBY, J. 2012. ZnT3: a zinc transporter active in several organs. *Biometals : an international journal on the role of metal ions in biology, biochemistry, and medicine,* 25**,** 1-8.

SMITH, J. L., XIONG, S., MARKESBERY, W. R. & LOVELL, M. A. 2006. Altered expression of zinc transporters-4 and -6 in mild cognitive impairment, early and late Alzheimer's disease brain. *Neuroscience,* 140**,** 879-88.

SMITH, M. J., SHARPLES, R. A., EVIN, G., MCLEAN, C. A., DEAN, B., PAVEY, G., FANTINO, E., COTTON, R. G., IMAIZUMI, K., MASTERS, C. L., CAPPAI, R. & CULVENOR, J. G. 2004. Expression of truncated presenilin 2 splice variant in Alzheimer's disease, bipolar disorder, and schizophrenia brain cortex. *Brain research. Molecular brain research,* 127**,** 128-35.

SMITH, R. M. 2009. NIST critically selected stability constants of metal complexes. 8 ed.: NIST Scientific and Technicial Databases [online].

SMOOT, D. T. 1997. How does Helicobacter pylori cause mucosal damage? Direct mechanisms. *Gastroenterology,* 113**,** S31-4; discussion S50.

SNYDER, E. M., NONG, Y., ALMEIDA, C. G., PAUL, S., MORAN, T., CHOI, E. Y., NAIRN, A. C., SALTER, M. W., LOMBROSO, P. J., GOURAS, G. K. & GREENGARD, P. 2005. Regulation of NMDA receptor trafficking by amyloid-beta. *Nature neuroscience,* 8**,** 1051-8.

SOLIMAN, D., HAMMING, K. S., MATEMISZ, L. C. & LIGHT, P. E. 2009. Reactive oxygen species directly modify sodium-calcium exchanger activity in a splice variant-dependent manner. *Journal of molecular and cellular cardiology,* 47**,** 595-602.

SPETH, R. C. & KARAMYAN, V. T. 2008. The significance of brain aminopeptidases in the regulation of the actions of angiotensin peptides in the brain. *Heart Fail Rev,* 13**,** 299-309.

STAIGER, H., MACHICAO, F., STEFAN, N., TSCHRITTER, O., THAMER, C., KANTARTZIS, K., SCHAFER, S. A., KIRCHHOFF, K., FRITSCHE, A. & HARING, H. U. 2007. Polymorphisms within novel risk loci for type 2 diabetes determine beta-cell function. *PloS one,* 2**,** e832.

STAMELOU, M., TUSCHL, K., CHONG, W. K., BURROUGHS, A. K., MILLS, P. B., BHATIA, K. P. & CLAYTON, P. T. 2012. Dystonia with brain manganese

accumulation resulting from SLC30A10 mutations: A new treatable disorder. *Movement disorders : official journal of the Movement Disorder Society*.

STEWART-KNOX, B. J., SIMPSON, E. E., PARR, H., RAE, G., POLITO, A., INTORRE, F., MEUNIER, N., ANDRIOLLO-SANCHEZ, M., O'CONNOR, J. M., COUDRAY, C. & STRAIN, J. J. 2005. Zinc status and taste acuity in older Europeans: the ZENITH study. *European journal of clinical nutrition,* 59 Suppl 2**,** S31-6.

STRITTMATTER, W. J., SAUNDERS, A. M., SCHMECHEL, D., PERICAK-VANCE, M., ENGHILD, J., SALVESEN, G. S. & ROSES, A. D. 1993. Apolipoprotein E: high-avidity binding to beta-amyloid and increased frequency of type 4 allele in late-onset familial Alzheimer disease. *Proceedings of the National Academy of Sciences of the United States of America,* 90**,** 1977-81.

STRYER, L., TYMOCZKO, J. L. & BERG, J. M. 2002. *Biochemistry,* New York, W H Freeman.

STUART, G. W., SEARLE, P. F. & PALMITER, R. D. 1985. Identification of multiple metal regulatory elements in mouse metallothionein-I promoter by assaying synthetic sequences. *Nature,* 317**,** 828-31.

SUZUKI, H., ASAKAWA, A., LI, J. B., TSAI, M., AMITANI, H., OHINATA, K., KOMAI, M. & INUI, A. 2011. Zinc as an appetite stimulator - the possible role of zinc in the progression of diseases such as cachexia and sarcopenia. *Recent patents on food, nutrition & agriculture,* 3**,** 226-31.

SUZUKI, T., ISHIHARA, K., MIGAKI, H., MATSUURA, W., KOHDA, A., OKUMURA, K., NAGAO, M., YAMAGUCHI-IWAI, Y. & KAMBE, T. 2005a. Zinc transporters, ZnT5 and ZnT7, are required for the activation of alkaline phosphatases, zinc-requiring enzymes that are glycosylphosphatidylinositol-anchored to the cytoplasmic membrane. *The Journal of biological chemistry,* 280**,** 637-43.

SUZUKI, T., ISHIHARA, K., MIGAKI, H., NAGAO, M., YAMAGUCHI-IWAI, Y. & KAMBE, T. 2005b. Two different zinc transport complexes of cation diffusion facilitator proteins localized in the secretory pathway operate to activate alkaline phosphatases in vertebrate cells. *The Journal of biological chemistry,* 280**,** 30956-62.

SWANSON, G. N., HANESWORTH, J. M., SARDINIA, M. F., COLEMAN, J. K., WRIGHT, J. W., HALL, K. L., MILLER-WING, A. V., STOBB, J. W., COOK, V. I., HARDING, E. C. & ET AL. 1992. Discovery of a distinct binding site for angiotensin II (3-8), a putative angiotensin IV receptor. *Regul Pept,* 40**,** 409-19.

TAKAHASHI, R. H., MILNER, T. A., LI, F., NAM, E. E., EDGAR, M. A., YAMAGUCHI, H., BEAL, M. F., XU, H., GREENGARD, P. & GOURAS, G.

K. 2002. Intraneuronal Alzheimer abeta42 accumulates in multivesicular bodies and is associated with synaptic pathology. *The American journal of pathology,* 161**,** 1869-79.

TAKEDA, A., TAKADA, S., ANDO, M., ITAGAKI, K., TAMANO, H., SUZUKI, M., IWAKI, H. & OKU, N. 2010. Impairment of recognition memory and hippocampal long-term potentiation after acute exposure to clioquinol. *Neuroscience,* 171**,** 443-50.

TAKEDA, A. & TAMANO, H. 2009. Insight into zinc signaling from dietary zinc deficiency. *Brain research reviews,* 62**,** 33-44.

TALLKVIST, J. & TJALVE, H. 1998. Transport of nickel across monolayers of human intestinal Caco-2 cells. *Toxicol Appl Pharmacol,* 151**,** 117-22.

TALMARD, C., LEUMA YONA, R. & FALLER, P. 2009. Mechanism of zinc(II)-promoted amyloid formation: zinc(II) binding facilitates the transition from the partially alpha-helical conformer to aggregates of amyloid beta protein(1-28). *Journal of biological inorganic chemistry : JBIC : a publication of the Society of Biological Inorganic Chemistry,* 14**,** 449-55.

TANAHASHI, H. & TABIRA, T. 2001. Three novel alternatively spliced isoforms of the human beta-site amyloid precursor protein cleaving enzyme (BACE) and their effect on amyloid beta-peptide production. *Neurosci Lett,* 307**,** 9-12.

TAQUINI, A. C., JR. & TAQUINI, A. C. 1961. The renin-angiotensin system in hypertension. *Am Heart J,* 62**,** 558-64.

TAYLOR, C. M., BACON, J. R., AGGETT, P. J. & BREMNER, I. 1991. Homeostatic regulation of zinc absorption and endogenous losses in zinc-deprived men. *The American journal of clinical nutrition,* 53**,** 755-63.

TAYLOR, K. M., HISCOX, S., NICHOLSON, R. I., HOGSTRAND, C. & KILLE, P. 2012. Protein kinase CK2 triggers cytosolic zinc signaling pathways by phosphorylation of zinc channel ZIP7. *Science signaling,* 5**,** ra11.

TAYLOR, K. M., MORGAN, H. E., JOHNSON, A., HADLEY, L. J. & NICHOLSON, R. I. 2003. Structure-function analysis of LIV-1, the breast cancer-associated protein that belongs to a new subfamily of zinc transporters. *The Biochemical journal,* 375**,** 51-9.

TAYLOR, K. M., MORGAN, H. E., JOHNSON, A. & NICHOLSON, R. I. 2004. Structure-function analysis of HKE4, a member of the new LIV-1 subfamily of zinc transporters. *The Biochemical journal,* 377**,** 131-9.

TAYLOR, K. M., MORGAN, H. E., JOHNSON, A. & NICHOLSON, R. I. 2005. Structure-function analysis of a novel member of the LIV-1 subfamily of zinc transporters, ZIP14. *FEBS letters,* 579**,** 427-32.

TAYLOR, K. M., MORGAN, H. E., SMART, K., ZAHARI, N. M., PUMFORD, S., ELLIS, I. O., ROBERTSON, J. F. & NICHOLSON, R. I. 2007. The emerging role of the LIV-1 subfamily of zinc transporters in breast cancer. *Molecular medicine,* 13**,** 396-406.

TAYLOR, K. M., VICHOVA, P., JORDAN, N., HISCOX, S., HENDLEY, R. & NICHOLSON, R. I. 2008. ZIP7-mediated intracellular zinc transport contributes to aberrant growth factor signaling in antihormone-resistant breast cancer Cells. *Endocrinology,* 149**,** 4912-20.

TENNANT, J., STANSFIELD, M., YAMAJI, S., SRAI, S. K. & SHARP, P. 2002. Effects of copper on the expression of metal transporters in human intestinal Caco-2 cells. *FEBS letters,* 527**,** 239-44.

THAL, D. R., GLAS, A., SCHNEIDER, W. & SCHOBER, R. 1997. Differential pattern of beta-amyloid, amyloid precursor protein and apolipoprotein E expression in cortical senile plaques. *Acta neuropathologica,* 94**,** 255-65.

THORNTON, J. K., TAYLOR, K. M., FORD, D. & VALENTINE, R. A. 2011. Differential subcellular localization of the splice variants of the zinc transporter ZnT5 is dictated by the different C-terminal regions. *PloS one,* 6**,** e23878.

TOKUDA, T., FUKUSHIMA, T., IKEDA, S., SEKIJIMA, Y., SHOJI, S., YANAGISAWA, N. & TAMAOKA, A. 1997. Plasma levels of amyloid beta proteins Abeta1-40 and Abeta1-42(43) are elevated in Down's syndrome. *Annals of neurology,* 41**,** 271-3.

TOMOBE, K., SHINOZUKA, T., KUROIWA, M. & NOMURA, Y. 2012. Age-related changes of Nrf2 and phosphorylated GSK-3beta in a mouse model of accelerated aging (SAMP8). *Archives of gerontology and geriatrics,* 54**,** e1-7.

TOZLU, S., GIRAULT, I., VACHER, S., VENDRELL, J., ANDRIEU, C., SPYRATOS, F., COHEN, P., LIDEREAU, R. & BIECHE, I. 2006. Identification of novel genes that co-cluster with estrogen receptor alpha in breast tumor biopsy specimens, using a large-scale real-time reverse transcription-PCR approach. *Endocrine-related cancer,* 13**,** 1109-20.

TRUONG-TRAN, A. Q., CARTER, J., RUFFIN, R. & ZALEWSKI, P. D. 2001a. New insights into the role of zinc in the respiratory epithelium. *Immunology and cell biology,* 79**,** 170-7.

TRUONG-TRAN, A. Q., CARTER, J., RUFFIN, R. E. & ZALEWSKI, P. D. 2001b. The role of zinc in caspase activation and apoptotic cell death. *Biometals : an*

international journal on the role of metal ions in biology, biochemistry, and medicine, 14**,** 315-30.

TSUDA, M., IMAIZUMI, K., KATAYAMA, T., KITAGAWA, K., WANAKA, A., TOHYAMA, M. & TAKAGI, T. 1997. Expression of zinc transporter gene, ZnT-1, is induced after transient forebrain ischemia in the gerbil. *The Journal of neuroscience : the official journal of the Society for Neuroscience,* 17**,** 6678-84.

TUSCHL, K., CLAYTON, P. T., GOSPE, S. M., JR., GULAB, S., IBRAHIM, S., SINGHI, P., AULAKH, R., RIBEIRO, R. T., BARSOTTINI, O. G., ZAKI, M. S., DEL ROSARIO, M. L., DYACK, S., PRICE, V., RIDEOUT, A., GORDON, K., WEVERS, R. A., CHONG, W. K. & MILLS, P. B. 2012. Syndrome of hepatic cirrhosis, dystonia, polycythemia, and hypermanganesemia caused by mutations in SLC30A10, a manganese transporter in man. *American journal of human genetics,* 90**,** 457-66.

UBERTI, D., RIZZINI, C., SPANO, P. F. & MEMO, M. 1997. Characterization of tau proteins in human neuroblastoma SH-SY5Y cell line. *Neuroscience letters,* 235**,** 149-53.

UENO, S., TSUKAMOTO, M., HIRANO, T., KIKUCHI, K., YAMADA, M. K., NISHIYAMA, N., NAGANO, T., MATSUKI, N. & IKEGAYA, Y. 2002. Mossy fiber Zn2+ spillover modulates heterosynaptic N-methyl-D-aspartate receptor activity in hippocampal CA3 circuits. *The Journal of cell biology,* 158**,** 215-20.

URANI, C., CALINI, V., MELCHIORETTO, P., MORAZZONI, F., CANEVALI, C. & CAMATINI, M. 2003. Different induction of metallothioneins and Hsp70 and presence of the membrane transporter ZnT-1 in HepG2 cells exposed to copper and zinc. *Toxicology in vitro : an international journal published in association with BIBRA,* 17**,** 553-9.

VALENTINE, R. A., JACKSON, K. A., CHRISTIE, G. R., MATHERS, J. C., TAYLOR, P. M. & FORD, D. 2007. ZnT5 variant B is a bidirectional zinc transporter and mediates zinc uptake in human intestinal Caco-2 cells. *J Biol Chem,* 282**,** 14389-93.

VALLEE, B. L. 1988. Zinc: biochemistry, physiology, toxicology and clinical pathology. *BioFactors,* 1**,** 31-6.

VALLEE, B. L. & FALCHUK, K. H. 1981. Zinc and gene expression. *Philosophical transactions of the Royal Society of London. Series B, Biological sciences,* 294**,** 185-97.

VALLEE, B. L. & FALCHUK, K. H. 1993. The biochemical basis of zinc physiology. *Physiological reviews,* 73**,** 79-118.

VASSAR, R., KOVACS, D. M., YAN, R. & WONG, P. C. 2009. The beta-secretase enzyme BACE in health and Alzheimer's disease: regulation, cell biology, function, and therapeutic potential. *J Neurosci,* 29**,** 12787-94.

VAUTRIN, J. 2009. SV2 frustrating exocytosis at the semi-diffusor synapse. *Synapse,* 63**,** 319-38.

VERSIECK, J., CORNELIS, R., LEMEY, G. & DE RUDDER, J. 1980. Determination of manganese in whole blood and serum. *Clinical chemistry,* 26**,** 531-2.

VOLKERT, D., SAEGLITZ, C., GUELDENZOPH, H., SIEBER, C. C. & STEHLE, P. 2010. Undiagnosed malnutrition and nutrition-related problems in geriatric patients. *The journal of nutrition, health & aging,* 14**,** 387-92.

WALDRON, K. J. & ROBINSON, N. J. 2009. How do bacterial cells ensure that metalloproteins get the correct metal? *Nature reviews. Microbiology,* 7**,** 25-35.

WANG, B., SCHNEIDER, S. N., DRAGIN, N., GIRIJASHANKER, K., DALTON, T. P., HE, L., MILLER, M. L., STRINGER, K. F., SOLEIMANI, M., RICHARDSON, D. D. & NEBERT, D. W. 2007. Enhanced cadmium-induced testicular necrosis and renal proximal tubule damage caused by gene-dose increase in a Slc39a8-transgenic mouse line. *American journal of physiology. Cell physiology,* 292**,** C1523-35.

WANG, B. R., SHI, J. Q., ZHANG, Y. D., ZHU, D. L. & SHI, J. P. 2011a. Angiotensin II does not directly affect Abeta secretion or beta-/gamma-secretase activity via activation of angiotensin II type 1 receptor. *Neuroscience letters,* 500**,** 103-7.

WANG, F., DUFNER-BEATTIE, J., KIM, B. E., PETRIS, M. J., ANDREWS, G. & EIDE, D. J. 2004a. Zinc-stimulated endocytosis controls activity of the mouse ZIP1 and ZIP3 zinc uptake transporters. *The Journal of biological chemistry,* 279**,** 24631-9.

WANG, F., KIM, B. E., DUFNER-BEATTIE, J., PETRIS, M. J., ANDREWS, G. & EIDE, D. J. 2004b. Acrodermatitis enteropathica mutations affect transport activity, localization and zinc-responsive trafficking of the mouse ZIP4 zinc transporter. *Human molecular genetics,* 13**,** 563-71.

WANG, G., ANRATHER, J., GLASS, M. J., TARSITANO, M. J., ZHOU, P., FRYS, K. A., PICKEL, V. M. & IADECOLA, C. 2006. Nox2, Ca2+, and protein kinase C play a role in angiotensin II-induced free radical production in nucleus tractus solitarius. *Hypertension,* 48**,** 482-9.

WANG, K., PUGH, E. W., GRIFFEN, S., DOHENY, K. F., MOSTAFA, W. Z., AL-ABOOSI, M. M., EL-SHANTI, H. & GITSCHIER, J. 2001. Homozygosity mapping places the acrodermatitis enteropathica gene on chromosomal region 8q24.3. *American journal of human genetics,* 68**,** 1055-60.

WANG, K., ZHOU, B., KUO, Y. M., ZEMANSKY, J. & GITSCHIER, J. 2002. A novel member of a zinc transporter family is defective in acrodermatitis enteropathica. *American journal of human genetics,* 71**,** 66-73.

WANG, X. & ZHOU, B. 2010. Dietary zinc absorption: A play of Zips and ZnTs in the gut. *IUBMB life,* 62**,** 176-82.

WANG, Y., HODGKINSON, V., ZHU, S., WEISMAN, G. A. & PETRIS, M. J. 2011b. Advances in the understanding of mammalian copper transporters. *Advances in nutrition,* 2**,** 129-37.

WANG, Y., WIMMER, U., LICHTLEN, P., INDERBITZIN, D., STIEGER, B., MEIER, P. J., HUNZIKER, L., STALLMACH, T., FORRER, R., RULICKE, T., GEORGIEV, O. & SCHAFFNER, W. 2004c. Metal-responsive transcription factor-1 (MTF-1) is essential for embryonic liver development and heavy metal detoxification in the adult liver. *FASEB journal : official publication of the Federation of American Societies for Experimental Biology,* 18**,** 1071-9.

WASTNEY, M. E., AAMODT, R. L., RUMBLE, W. F. & HENKIN, R. I. 1986. Kinetic analysis of zinc metabolism and its regulation in normal humans. *The American journal of physiology,* 251**,** R398-408.

WASTNEY, M. E., ANGELUS, P. A., BARNES, R. M. & SUBRAMANIAN, K. N. 1999. Zinc absorption, distribution, excretion, and retention by healthy preterm infants. *Pediatric research,* 45**,** 191-6.

WEAVER, B. P., DUFNER-BEATTIE, J., KAMBE, T. & ANDREWS, G. K. 2007. Novel zinc-responsive post-transcriptional mechanisms reciprocally regulate expression of the mouse Slc39a4 and Slc39a5 zinc transporters (Zip4 and Zip5). *Biological chemistry,* 388**,** 1301-12.

WEI, Y. & FU, D. 2005. Selective metal binding to a membrane-embedded aspartate in the Escherichia coli metal transporter YiiP (FieF). *The Journal of biological chemistry,* 280**,** 33716-24.

WHITE, A. R., DU, T., LAUGHTON, K. M., VOLITAKIS, I., SHARPLES, R. A., XILINAS, M. E., HOKE, D. E., HOLSINGER, R. M., EVIN, G., CHERNY, R. A., HILL, A. F., BARNHAM, K. J., LI, Q. X., BUSH, A. I. & MASTERS, C. L. 2006. Degradation of the Alzheimer disease amyloid beta-peptide by metal-dependent up-regulation of metalloprotease activity. *The Journal of biological chemistry,* 281**,** 17670-80.

WILLEM, M., GARRATT, A. N., NOVAK, B., CITRON, M., KAUFMANN, S., RITTGER, A., DESTROOPER, B., SAFTIG, P., BIRCHMEIER, C. & HAASS, C. 2006. Control of peripheral nerve myelination by the beta-secretase BACE1. *Science,* 314**,** 664-6.

WIMMER, U., WANG, Y., GEORGIEV, O. & SCHAFFNER, W. 2005. Two major branches of anti-cadmium defense in the mouse: MTF-1/metallothioneins and glutathione. *Nucleic acids research,* 33**,** 5715-27.

WONG-RILEY, M. T. 1989. Cytochrome oxidase: an endogenous metabolic marker for neuronal activity. *Trends Neurosci,* 12**,** 94-101.

WONG, C. P. & HO, E. 2012. Zinc and its role in age-related inflammation and immune dysfunction. *Molecular nutrition & food research,* 56**,** 77-87.

WONGDEE, K., TEERAPORNPUNTAKIT, J., RIENGROJPITAK, S., KRISHNAMRA, N. & CHAROENPHANDHU, N. 2009. Gene expression profile of duodenal epithelial cells in response to chronic metabolic acidosis. *Molecular and cellular biochemistry,* 321**,** 173-88.

WOOD, R. J. 2000. Assessment of marginal zinc status in humans. *The Journal of nutrition,* 130**,** 1350S-4S.

WU, C. Y., BIRD, A. J., CHUNG, L. M., NEWTON, M. A., WINGE, D. R. & EIDE, D. J. 2008. Differential control of Zap1-regulated genes in response to zinc deficiency in Saccharomyces cerevisiae. *BMC genomics,* 9**,** 370.

YAMAGUCHI, M. & HASHIZUME, M. 1994. Effect of beta-alanyl-L-histidinato zinc on protein components in osteoblastic MC3T3-El cells: increase in osteocalcin, insulin-like growth factor-I and transforming growth factor-beta. *Molecular and cellular biochemistry,* 136**,** 163-9.

YU, Y. Y., KIRSCHKE, C. P. & HUANG, L. 2007. Immunohistochemical analysis of ZnT1, 4, 5, 6, and 7 in the mouse gastrointestinal tract. *The journal of histochemistry and cytochemistry : official journal of the Histochemistry Society,* 55**,** 223-34.

ZABEL, U., SCHRECK, R. & BAEUERLE, P. A. 1991. DNA binding of purified transcription factor NF-kappa B. Affinity, specificity, Zn2+ dependence, and differential half-site recognition. *The Journal of biological chemistry,* 266**,** 252-60.

ZALEWSKI, P. D., FORBES, I. J., SEAMARK, R. F., BORLINGHAUS, R., BETTS, W. H., LINCOLN, S. F. & WARD, A. D. 1994. Flux of intracellular labile zinc during apoptosis (gene-directed cell death) revealed by a specific chemical probe, Zinquin. *Chemistry & biology,* 1**,** 153-61.

ZHAN, S. S., SANDBRINK, R., BEYREUTHER, K. & SCHMITT, H. P. 1995. APP with Kunitz type protease inhibitor domain (KPI) correlates with neuritic plaque density but not with cortical synaptophysin immunoreactivity in Alzheimer's disease and non-demented aged subjects: a multifactorial analysis. *Clinical neuropathology,* 14**,** 142-9.

ZHANG, L. H., WANG, X., ZHENG, Z. H., REN, H., STOLTENBERG, M., DANSCHER, G., HUANG, L., RONG, M. & WANG, Z. Y. 2008. Altered expression and distribution of zinc transporters in APP/PS1 transgenic mouse brain. *Neurobiol Aging*.

ZHANG, Y., RODIONOV, D. A., GELFAND, M. S. & GLADYSHEV, V. N. 2009. Comparative genomic analyses of nickel, cobalt and vitamin B12 utilization. *BMC genomics,* 10**,** 78.

ZHAO, H. & EIDE, D. J. 1997. Zap1p, a metalloregulatory protein involved in zinc-responsive transcriptional regulation in Saccharomyces cerevisiae. *Molecular and cellular biology,* 17**,** 5044-52.

ZHENG, D., FEENEY, G. P., KILLE, P. & HOGSTRAND, C. 2008. Regulation of ZIP and ZnT zinc transporters in zebrafish gill: zinc repression of ZIP10 transcription by an intronic MRE cluster. *Physiological genomics,* 34**,** 205-14.

ZHOU, B. & GITSCHIER, J. 1997. hCTR1: a human gene for copper uptake identified by complementation in yeast. *Proceedings of the National Academy of Sciences of the United States of America,* 94**,** 7481-6.

ZHU, X., RAINA, A. K., LEE, H. G., CASADESUS, G., SMITH, M. A. & PERRY, G. 2004. Oxidative stress signalling in Alzheimer's disease. *Brain research,* 1000**,** 32-9.

ZHU, X., ZHOU, W., CUI, Y., ZHU, L., LI, J., XIA, Z., SHAO, B., WANG, H. & CHEN, H. 2009. Muscarinic activation attenuates abnormal processing of beta-amyloid precursor protein induced by cobalt chloride-mimetic hypoxia in retinal ganglion cells. *Biochemical and biophysical research communications,* 384**,** 110-3.

ZIMMERMAN, M. C., DUNLAY, R. P., LAZARTIGUES, E., ZHANG, Y., SHARMA, R. V., ENGELHARDT, J. F. & DAVISSON, R. L. 2004. Requirement for Rac1-dependent NADPH oxidase in the cardiovascular and dipsogenic actions of angiotensin II in the brain. *Circulation research,* 95**,** 532-9.

ZODL, B., ZEINER, M., MARKTL, W., STEFFAN, I. & EKMEKCIOGLU, C. 2003. Pharmacological levels of copper exert toxic effects in Caco-2 cells. *Biological trace element research,* 96**,** 143-52.

ZOHAR, O., CAVALLARO, S., D'AGATA, V. & ALKON, D. L. 2003. Quantification and distribution of beta-secretase alternative splice variants in the rat and human brain. *Brain research. Molecular brain research,* 115**,** 63-8.

ZOHAR, O., PICK, C. G., CAVALLARO, S., CHAPMAN, J., KATZAV, A., MILMAN, A. & ALKON, D. L. 2005. Age-dependent differential expression of

BACE splice variants in brain regions of tg2576 mice. *Neurobiol Aging,* 26**,** 1167-75.